

ÉCOLE DE TECHNOLOGIE SUPÉRIEURE  
UNIVERSITÉ DU QUÉBEC

THESIS PRESENTED TO  
ÉCOLE DE TECHNOLOGIE SUPÉRIEURE

IN PARTIAL FULFILLMENT OF THE REQUIREMENTS FOR  
THE DEGREE OF DOCTOR OF PHILOSOPHY  
Ph. D.

BY  
Seyed Ali NIKNAM

BURRS UNDERSTANDING, MODELING AND OPTIMIZATION  
DURING SLOT MILLING OF ALUMINIUM ALLOYS

MONTREAL, MAY 27 2013

© Copyright 2013 reserved by Seyed Ali Niknam

© Copyright reserved

It is forbidden to reproduce, save or share the content of this document either in whole or in parts. The reader who wishes to print or save this document on any media must first get the permission of the author.

**BOARD OF EXAMINERS**

THIS THESIS HAS BEEN EVALUATED

BY THE FOLLOWING BOARD OF EXAMINERS

Professor Victor Songmene, Thesis Supervisor  
Department of Mechanical Engineering at École de technologie supérieure

Professor Ilian Bonev, President of the Board of Examiners  
Department of Automated Manufacturing Engineering at École de technologie supérieure

Professor Tan Pham, Member of the Board of Examiners  
Department of Mechanical Engineering at École de technologie supérieure

Dr Nejah Tounsi, External Examiner  
Research officer  
Aerospace Manufacturing Technology Centre (AMTC)  
National Research Council Canada (NRC), Montréal

Dr Ali Bonakdar, Independent External Examiner  
Manufacturing Engineering Specialist & Engineering Commodity Leader  
Rolls-Royce, Canada

THIS THESIS WAS PRESENTED AND DEFENDED

IN THE PRESENCE OF A BOARD OF EXAMINERS AND PUBLIC

IN APRIL 02 2013

AT ÉCOLE DE TECHNOLOGIE SUPÉRIEURE



## **DEDICATION**

*This thesis is dedicated to my loving parents and my beloved spouse  
for their love, endless supports  
and encouragements.*



## ACKNOWLEDGMENT

The last few years of my life have been the most challenging and rewarding because I truly had the opportunity to meet and understand people from many different countries who enriched my life by sharing a wide range of customs and cultural backgrounds. I am deeply grateful to all my advisors that opened my eyes and guided my steps in the long and winding road to the fantastic world of manufacturing science.

I would like to express my sincere gratitude to my advisor, Professor Victor Songmene, for the opportunity he has given me to work at the Laboratory of Products, Processes and Systems Engineering (LPPSE). Without his thrust, guidance, patience and supports, my research would not have been successful. Undoubtedly, he was the most influential person during my Ph.D and I hope the bond that we established will continue for many years to come.

My immense appreciation extends to Prof Tan Pham, Prof Ilian Bonev, Dr Nejah Tounsi and Dr Ali Bonakdar for serving as members of jury of my Ph.D defense committee and for providing valuable comments.

I appreciate National Sciences and Engineering Research Council of Canada (NSERC) and Consortium for Research and Innovation in Aerospace in Quebec (CRIAQ) for their financial support for this project. A partially financial support by Fonds Québécois de la Recherche sur la Nature et les Technologies (FQRNT) by the intermediary of the Aluminium Research Centre Canada– REGAL is gratefully acknowledged.

Sincere thanks are extended to my colleagues at LPPSE for their discussions and assistance in different parts of this research project. Special thanks go to Dr Yasser Zedan, Dr Jules Kouam, Dr Riad Khettabi, Dr Abdelhakim Djebara, Dr Imed Zaghbani, Dr Rene Kamguem, Mr Alireza Jalali, Mr Monzer Davoud, Mr Walid Joma and Mr Hossein Hamedanian.

## VIII

I wish to give my wholehearted thanks to my parents for their unwavering supports, kind words, well-wishing and patience for abiding by my absence.

Special thanks go to my beloved wife for her support, encouragement and patience and for lifting much of the burden of life during the final stages of this thesis.

Finally, I express my deep feelings to my God for giving me the will to do this work.

# **BURRS UNDERSTANDING, MODELING AND OPTIMIZATION DURING SLOT MILLING OF ALUMINIUM ALLOYS**

Seyed Ali NIKNAM

## **ABSTRACT**

Nowadays due to global competition, manufacturing industries must provide high quality products on time and within the cost constraints to remain competitive. High quality mechanical parts include those with better surface finish and texture, dimension and form accuracies, reduced tensile residual stress and burr-free. The burr formation is one of the most common and undesirable phenomenon occurring in machining operations, which reduces assembly and machined part quality. Therefore, it is desired to eliminate the burrs or reduce the effort required to remove them. Amongst machining operations, slot milling has a more complex burr formation mechanism with multiple burrs appear in machined part edges with non-uniform dimensions. The ultimate goal of this research work is burr minimization in slot milling operation. To this end, new strategies for understanding, modeling and optimizing burrs during slot milling of aluminum alloys are proposed for improving the part quality and ultimately reducing the non-value added expenses caused by deburring processes.

In order to have a better understanding of slot milling burr formation mechanism, multi-level experimental studies and statistical methods are used to determine the effects of machining conditions, tooling and workpiece materials on burrs size (height and thickness) when using dry high speed condition. It was found that optimum setting levels of process parameters to minimize each burr are dissimilar. The analysis of results shows that cutting tool, feed per tooth and depth of cut have certain level of influence on slot milling burrs. However most of the burrs are strongly affected by interaction effects between process parameters that consequently complicate developing burr size prediction models.

An analytical model is proposed to predict the thickness of the largest burr during slot milling of ductile materials. The model is based on the geometry of burr formation and continuity of work at the transition from chip formation to burr formation, which also takes into account the effect of the cutting force involved in the machining process. A computational model is also developed to predict the exit up milling side burr thickness based on the use of cutting parameters and material properties such as yield strength and specific cutting force coefficient, which are the only unknown variables in the model. Both analytical and computational models are validated using experimental results obtained during slot milling of 2024-T351 and 6061-T6 aluminium alloys.

Machining parameters optimization to minimize the burr size could have a negative impact on other machining performance characteristic, such as surface finish, tool life and material removal rate. Therefore, surface finish is also investigated with burr formation in this

research work. For simultaneous multiple responses optimization, a new modification to the application of Taguchi method is suggested by proposing fitness mapping function and desirability index. The proposed modification is validated by simultaneous minimization of surface roughness and thickness of five burrs during slot milling of 6061-T6 aluminium alloy. The optimization results demonstrate the potential and capability of the proposed approach.

**Key words:** slot milling, aluminium alloy, burr, analytical modeling, machining conditions, optimization.

# **BURRS UNDERSTANDING, MODELING AND OPTIMIZATION DURING SLOT MILLING OF ALUMINIUM ALLOYS**

Seyed Ali NIKNAM

## **RESUME**

De nos jours, en raison de la compétition mondiale, les industries manufacturières doivent produire des pièces de qualité élevée et à temps pour demeurer compétitives. Les pièces mécaniques de qualité incluent celles ayant un meilleur fini de surface et une meilleure texture, une bonne précision de forme et dimensionnelle, des contraintes résiduelles réduites et des pièces sans bavures. La formation de bavures, l'un des phénomènes indésirables courants rencontrés lors des opérations d'usinage, réduit la qualité des pièces usinées et celle des assemblages. Par conséquent, il est désiré d'éliminer les bavures ou de réduire l'effort requis pour les enlever.

Parmi les opérations d'usinage, le rainurage est une opération du fraisage provoquant des mécanismes de formation de bavures plus complexes. Ainsi de multiples bavures apparaissent dans une partie des bords usinés avec des dimensions non uniformes. Le but ultime de ce travail de recherche est la minimisation des bavures en opération de rainurage. À cette finalité, de nouvelles stratégies sont proposées pour la compréhension, la modélisation et l'optimisation des bavures pour le rainurage des alliages d'aluminium, afin d'améliorer la qualité des pièces et la réduction des coûts occasionnés par les processus d'ébavurage.

Afin de mieux comprendre les mécanismes de formation des bavures au rainurage, des études statistiques basées sur des plans d'expériences multi-niveaux sont utilisés pour déterminer les effets des conditions de coupe, de l'outil et des matériaux usinés sur la taille des bavures (hauteur et épaisseur) pendant le fraisage à haute vitesse des alliages d'aluminium. Il a été trouvé que les conditions optimales d'usinage permettant de minimiser chacune des bavures diffèrent d'une bavure à l'autre. L'analyse des résultats montre que l'outil de coupe, l'avance et la profondeur de coupe ont une influence variable sur la taille des bavures formées lors du rainurage. Cependant, la plupart des bavures sont fortement influencées par les interactions entre les paramètres des procédés, ce qui complique d'avantage le développement des modèles de prédiction des bavures. Ces résultats peuvent aider pour des travaux subséquents portant sur le fraisage de précision des alliages d'aluminium ou d'autres alliages légers.

Ensuite, un modèle analytique est proposé permettant de prédire l'épaisseur des bavures lors du fraisage des matériaux ductiles. Ce modèle est basé sur la géométrie de la bavure lors de la transition entre la formation des copeaux et la formation des bavures au cours de l'usinage et qui prend en compte l'effet de l'énergie de coupe impliquée dans le procédé. Un modèle numérique est aussi développé permettant de prédire l'épaisseur de la bavure de sortie en fraisage basé sur les paramètres de coupe et les propriétés du matériau telles que la limite

d'élasticité et les coefficients des forces spécifiques de coupe, qui sont les seuls inconnus dans le modèle. Les deux modèles (analytique et numérique) sont validés en utilisant les résultats expérimentaux obtenus lors du rainurage des alliages d'aluminium 2024-T351 et 6061-T6.

L'optimisation des paramètres d'usinage pour minimiser la taille des bavures peut avoir des effets négatifs sur d'autres caractéristiques de performance d'usinage tels que le fini de surface, la vie des outils de coupe et le taux d'enlèvement de métal. C'est la raison pour laquelle le fini de surface est aussi analysé en même temps que la formation des bavures dans cette étude. Pour sélectionner les meilleurs niveaux des paramètres du procédé d'usinage, une nouvelle méthode basée sur les surfaces de réponses et sur les fonctions de désirabilité est proposée et utilisée. La méthodologie proposée est validée sur la minimisation simultanée du fini de surface et de cinq types de bavures pendant le fraisage de l'alliage d'aluminium 6061-T6. Les résultats de cette optimisation démontrent le potentiel et la performance de la méthode proposée.

**Mot-clés:** rainurage, aluminium, bavure, modélisation, conditions d'usinage, optimisation.

## TABLE OF CONTENTS

	Page
INTRODUCTION .....	1
CHAPTER 1 LITERATURE REVIEW .....	7
1.1 Introduction.....	7
1.2 Definition and characterization of burr.....	7
1.2.1 Burr formation mechanism .....	10
1.2.2 Burr shapes.....	13
1.2.3 Burr size measurement and detection methods.....	16
1.2.4 Burr removal (deburring).....	17
1.2.5 Concerns on burr formation.....	22
1.3 Understanding and modeling of milling burr formation.....	23
1.3.1 Milling burrs shapes.....	23
1.3.2 Parameters governing milling burr formation.....	26
1.3.3 Milling burr formation modeling.....	32
1.4 Optimization methods.....	38
1.4.1 Taguchi method .....	38
1.4.2 Response surface methodology (RSM) .....	39
1.4.3 Desirability function .....	39
1.5 Conclusion of literature review and refining of problematic.....	40
CHAPTER 2 INVESTIGATION OF FACTORS GOVERNING SLOT MILLING BURR FORMATION.....	43
2.1 Introduction.....	43
2.2 Experimental procedure .....	44
2.2.1 Experimental plan .....	44
2.2.2 Experimental observations.....	46
2.2.3 Assumptions.....	48
2.3 Results and discussion .....	49
2.3.1 Method of analysis.....	49
2.3.2 Effects of process parameters on slot milling burrs.....	50
2.3.3 Response surface models .....	74
2.3.4 Controllable response.....	82
2.4 Conclusion .....	88
CHAPTER 3 MODELING OF BURR THICKNESS IN MILLING OF DUCTILE MATERIALS.....	91
3.1 Introduction.....	91
3.2 Theoretical modeling of milling burr thickness.....	92
3.3 Experimental results and discussion .....	99
3.4 Computational results and discussion.....	103
3.5 Conclusion .....	111

CHAPTER 4 SIMULTANEOUS OPTIMIZATION OF BURR SIZE AND SURFACE FINISH DURING SLOT MILLING OPERATION.....113

4.1 Introduction.....113

4.2 An overview of Taguchi Method.....115

4.3 Proposed methodology.....116

4.4 Experimental results.....123

    4.4.1 Experimental procedure.....123

    4.4.2 Analysis of responses.....124

4.5 Multiple responses optimization.....133

4.6 Experimental validation.....139

4.7 Conclusion.....142

CHAPTER 5 SUBSTANTIAL SUMMARY OF THE RESEARCH WORK .....143

5.1 Introduction.....143

5.2 Dominant process parameters on slot milling burrs size .....144

5.3 Controllable responses.....146

5.4 Milling burr size modeling of ductile materials.....147

5.5 Multiple responses optimization in slot milling.....151

5.6 Key contributions and outcomes of the thesis .....152

CONCLUSION.....157

RECOMMENDATIONS.....159

ANNEX I CONFERENCE ARTICLE 1:  
BURR FORMATION DURING DRY MILLING OF WROUGHT ALUMINUM ALLOYS .....161

ANNEX II JOURNAL ARTICLE 1:  
FACTORS GOVERNING BURR FORMATION DURING HIGH-SPEED SLOT MILLING OF WROUGHT ALUMINUM ALLOYS .....163

ANNEX III CONFERENCE ARTICLE 2:  
STATISTICAL INVESTIGATION ON BURR THICKNESS DURING MILLING OF 6061-T6 ALUMINIUM ALLOYS .....165

ANNEX IV JOURNAL ARTILCE 2:  
MODELING OF BURR THICKNESS IN MILLING OF DUCTILE MATERIALS.....167

ANNEX V CONFERENCE ARTICLE 3:  
EXPERIMENTAL INVESTIGATION AND MODELING OF MILLING BURRS.....169

ANNEX VI	JOURNAL ARTICLE 3: SIMULTANEOUS OPTIMIZATION OF BURRS SIZE AND SURFACE FINISH WHEN SLOT MILLING 6061-T6 ALUMINIUM ALLOYS .....	171
ANNEX VII	CONFERENCE ARTICLE 4: ANALYSIS AND OPTIMIZATION OF EXIT BURR SIZE AND SURFACE ROUGHNESS IN MILLING USING DESIRABILITY FUNCTION .....	173
BIBLIOGRAPHY .....		174



## LIST OF TABLES

		Page
Table 1.1	The most frequently used deburring processes .....	19
Table 2.1	Experimental process parameters and their levels .....	45
Table 2.2	Mechanical properties of studied aluminium alloys (Committee and Knovel, 2004)) .....	46
Table 2.3	Statistical summary of results .....	74
Table 2.4	Statistical summary of burr height models .....	81
Table 2.5	Statistical summary of burr thickness models .....	82
Table 2.6	Statistical summary of $F_t$ design models .....	86
Table 3.1	Cutting parameters and their levels.....	100
Table 3.2	Experimental and modeling results.....	101
Table 3.3	Statistical summary of regression models between experimental and modeled $B_t$ .....	103
Table 3.4	Experimental and simulated results when $Z=3$ ; $D=19.05$ mm; $\beta=30^\circ$ and $v_c=300$ m/min .....	109
Table 3.5	Statistical summary of the regression models between experimental and simulated results .....	109
Table 4.1	Cutting parameters and their levels.....	123
Table 4.2	Experimental responses .....	125
Table 4.3	Statistical results of responses .....	133
Table 4.4	Response characteristic terms ( $n = 6$ and $N = 54$ ) .....	134
Table 4.5	ANOVA table for $\eta_\psi$ .....	135
Table 4.6	Desirability of proposed setting levels of process parameters.....	137
Table 4.7	Process parameters used for verification tests .....	140

Table 4.8      Desirability of verified process parameters ( $A_2B_1C_1D_2$ ) .....141

## LIST OF FIGURES

		Page
Figure 1.1	Examples of burr definition (Gillespie, 1996) .....	8
Figure 1.2	Burr definition by ISO 13175 (Aurich <i>et al.</i> , 2009) .....	8
Figure 1.3	Measurement values of burr (Schäfer, 1975).....	9
Figure 1.4	Micrograph of the chip root showing the exit failure, negative shear and foot formation (Pekelharing, 1978).....	10
Figure 1.5	Burr/breakout formation model (Iwata, Osakada and Terasaka, 1984): (a) initiation, (b) development and (c) final burr formation .....	11
Figure 1.6	Burr formation mechanism in ductile and brittle materials (Hashimura, Hassamontr and Dornfeld, 1999).....	13
Figure 1.7	Schematic of Poisson, Tear and Rollover burr (Gillespie, 1996) .....	14
Figure 1.8	Types of machining burr (Aurich <i>et al.</i> , 2009) .....	15
Figure 1.9	Burr detection and measurement methods (Aurich <i>et al.</i> , 2009) .....	17
Figure 1.10	Example of machined part edges require deburring ( <i>adapted from</i> (Gillespie, 1999)) .....	18
Figure 1.11	Manual deburring (Tiabi, 2010).....	20
Figure 1.12	A robot arm combined with deburring brush (Means, 1986) .....	21
Figure 1.13	Milling burr formation classification-location ( <i>adapted from</i> (Hashimura, Hassamontr and Dornfeld, 1999)).....	24
Figure 1.14	Milling exit burr classification-shape .....	24
Figure 1.15	Face milling burrs (Lee, 2004).....	25
Figure 1.16	Slot milling burrs (Lee, 2004).....	26
Figure 1.17	Major process parameters for FEM simulation of metal cutting (Sartkulvanich, 2007).....	36
Figure 1.18	FEM simulation of burr formation in orthogonal cutting .....	37

Figure 2.1	Experimental devices: (a) 3-Axis CNC machine (b) Cutting tool used.....	45
Figure 2.2	Optical microscope used for burr size measurement .....	46
Figure 2.3	Profilometer used for surface roughness measurement .....	47
Figure 2.4	Cutting forces in normal, axial and feed directions .....	48
Figure 2.5	Slot milled machined parts with (a) burr formation with tiny scales; (b) large burr formation .....	51
Figure 2.6	Pareto chart of (a) $B_1$ height, (b) $B_1$ thickness.....	53
Figure 2.7	Pareto chart of (a) $B_2$ height, (b) $B_2$ thickness .....	54
Figure 2.8	Direct effect plot of (a) $B_1$ height, (b) $B_1$ thickness .....	55
Figure 2.9	Direct effect plot of (a) $B_2$ height, (b) $B_2$ thickness .....	56
Figure 2.10	Slot milling exit burrs .....	57
Figure 2.11	Interaction effect of tool - depth of cut (BC) on (a) $B_1$ height and (b) on $B_1$ thickness.....	61
Figure 2.12	Interaction effect of depth of cut-cutting speed (CE) on (a) $B_2$ height and (b) $B_2$ thickness .....	62
Figure 2.13	Pareto chart of (a) $B_5$ height, (b) $B_5$ thickness.....	64
Figure 2.14	Direct effect plot of (a) $B_5$ height, (b) $B_5$ thickness.....	65
Figure 2.15	Slot milling top burrs .....	66
Figure 2.16	Pareto chart of (a) $B_4$ height, (b) $B_4$ thickness.....	67
Figure 2.17	Pareto chart of (a) $B_8$ height, (b) $B_8$ thickness .....	68
Figure 2.18	Direct effect plot of (a) $B_4$ height, (b) $B_4$ thickness.....	69
Figure 2.19	Direct effect plot of (a) $B_8$ height, (b) $B_8$ thickness.....	71
Figure 2.20	Interaction effect of material- feed per tooth (AD) on (a) $B_4$ height and (b) $B_8$ height.....	72
Figure 2.21	Interaction effect of tool-cutting speed (BE) on (a) $B_4$ thickness and (b) $B_8$ thickness.....	73

Figure 2.22	3D contour plot of burr thickness studied at optimum cutting conditions.....	77
Figure 2.23	3D contour plot of burr height at optimum cutting conditions .....	80
Figure 2.24	(a) Pareto chart of $B_1$ thickness in linear design model, (b) Direct effect plot of $B_1$ thickness .....	83
Figure 2.25 2	D contour plot of $B_1$ thickness: (a) Tool 1, (b) Tool 2, (c) Tool 3.....	85
Figure 2.26	Pareto chart of $F_t$ in linear design model .....	86
Figure 2.27	Direct effect plot of $F_t$ .....	87
Figure 2.28	Exponential regression model between $F_t$ and $B_1$ thickness.....	87
Figure 3.1	Slot milling burrs .....	92
Figure 3.2	(a) Exit geometry in end milling; (b) geometry of burr initiation and formation ( <i>adapted from</i> (Ko and Dornfeld, 1991)).....	93
Figure 3.3	Slot milling under orthogonal cutting conditions ( <i>adapted from</i> (San-Juan, Martín and Santos, 2010)).....	96
Figure 3.4	Experimental and modeled $B_t$ for AA 2024-T351(using Eq(3.20)).....	102
Figure 3.5	Experimental and modeled $B_t$ for AA 6061-T6 (using (Eq(3.20)) .....	102
Figure 3.6	Scheme of the proposed theoretical model for $B_t$ prediction .....	108
Figure 3.7	Experimental and simulated $B_t$ for AA 2024-T351(using Eq(3.32)).....	110
Figure 3.8	Experimental and simulated $B_t$ for AA 6061-T6 (using Eq(3.32)).....	110
Figure 4.1	Procedure of multiple responses optimization using Taguchi method ....	122
Figure 4.2	Measurement overview of exit up milling side burr ( $B_1$ ) .....	124
Figure 4.3	(a) Pareto chart and (b) main effect plot of $B_1$ burr thickness .....	127
Figure 4.4	(a) Pareto chart and (b) main effect plot of $B_2$ burr thickness.....	128
Figure 4.5	(a) Pareto chart and (b) main effect plot of $B_4$ burr thickness.....	129
Figure 4.6	(a) Pareto chart and (b) main effect plot of $B_5$ burr thickness.....	130
Figure 4.7	(a) Pareto chart and (b) main effect plot of $B_8$ burr thickness.....	131

Figure 4.8	(a) Pareto chart and (b) main effect plot of surface roughness (Ra).....	132
Figure 4.9	Pareto chart of $\eta_{\psi}$ .....	135
Figure 4.10	Main effect plot of $\eta_{\psi}$ .....	136
Figure 4.11	3D contour plot of $\eta_{\psi}$ at cutting speed 300 m/min.....	138
Figure 4.12	3D contour plot of $\eta_{\psi}$ at cutting speed 750 m/min .....	138
Figure 4.13	3D contour plot of $\eta_{\psi}$ at cutting speed 1200 m/min .....	139
Figure 4.14	Main effect plot of optimized $\eta_{\psi}$ .....	141
Figure 5.1	The main and specific research objectives.....	144
Figure 5.2	Variation of resultant cutting force during slot milling of AA 2024-T351 .....	150
Figure 5.3	Variation of resultant cutting force during slot milling of AA 6061-T6 .....	150
Figure 5.4	The links between main objective and specific research objectives.....	155

## LIST OF SYMBOLS

Symbol	Units	Description
$B_t$	(mm or $\mu\text{m}$ )	Burr thickness
$B_h$	(mm or $\mu\text{m}$ )	Burr height
$a_p$	mm	Axial depth of cut
$v_c$	m/min	Cutting speed
$f_z$	mm/z	Feed per tooth
$n$	rev/s	Spindle speed
$Z$	-	Number of flutes/tooth
$D$	(mm or $\mu\text{m}$ )	Tool diameter
$\theta$	(deg)	Tool rotation angle
$\theta_p$	(deg)	Cutter pitch angle
$\varphi_j$	(deg)	Immersion angle for flute $j$
$h(\varphi)$	(mm or $\mu\text{m}$ )	Chip thickness
$h_m$	(mm or $\mu\text{m}$ )	Average chip thickness per revolution
$\gamma_0$	(deg)	Lag angle
$K_c$	( $\text{N}/\text{mm}^2$ )	Specific cutting force coefficient
$K_s$	( $\text{N}/\text{mm}^2$ )	Specific cutting force coefficient when $h_m = 0.2\text{mm}$
$K_{te}$	( $\text{N}/\text{mm}^2$ )	Tangential edge force coefficient
$K_{re}$	( $\text{N}/\text{mm}^2$ )	Radial edge force coefficient
$K_{ae}$	( $\text{N}/\text{mm}^2$ )	Axial edge force coefficient
$K_{tc}$	( $\text{N}/\text{mm}^2$ )	Tangential cutting force coefficient due to shearing action
$K_{rc}$	( $\text{N}/\text{mm}^2$ )	Radial cutting force coefficient due to shearing action
$K_{ac}$	( $\text{N}/\text{mm}^2$ )	Axial cutting force coefficient due to shearing action
$\Delta a_p$	mm	Elements of thickness
$dF_{t,j}$	N	Tangential force acting on a differential flute element $j$
$F_t$	N	Tangential force
$F_r$	N	Radial force
$F_a$	N	Axial force
$\Phi$	(deg)	Shear angle
$R\epsilon$	(mm or $\mu\text{m}$ )	Insert nose radius
$L$	(mm or $\mu\text{m}$ )	Tool chip contact length
$\lambda$	(deg)	Friction angle
$\mu$	-	Friction coefficient
$\beta$	(deg)	Helix angle
$\beta_0$	(deg)	Initial negative shear angle

$\theta_{ex}$	(deg)	Exit angle
$\theta_{st}$	(deg)	Entrance angle
$\Psi$	(deg)	In plane exit angle
$dx$	(mm or $\mu\text{m}$ )	Distance of the tool moved from onset of plastic hinging
$k_0$	( $\text{N}/\text{mm}^2$ )	Yield shear strength
$\sigma_e$	( $\text{N}/\text{mm}^2$ )	Yield strength
$\Delta W_b$	(Nm)	Work done for burr formation at the transition point
$\Delta W_c$	(Nm)	Work done for chip formation at the transition point
$M_p$	-	Mapping function
$\psi$	-	Fitness mapping function
$R$	-	Range of a response
$M_R$	-	Fitness mapping range
$M$	-	The Maximum of $M_R$
$\omega$	-	Weighting coefficient
$\mu$	-	Mapping coefficient
$Y_i$	-	Non-identical response
$m$	-	Mean value of responses
$\sigma$	-	Standard deviation of responses
$\eta$	-	Signal to noise ratio
$\eta_\psi$	-	Signal to noise ratio of fitness mapping function
$d_i$	-	Desirability of each response
$D_i$	-	Desirability of all transformed responses
$\kappa$	-	Optimization rate
$\varepsilon$	-	Prediction error
$t$	-	Weight exponent value
$F$	-	F-ratio
$P$	-	P-value
$DOF$	-	Degree of freedom
$MS$	-	Mean of square
$SS$	-	Sum of square

## INTRODUCTION

As manufacturing processes become advanced, precision components require more attention for both surface and edge generation. More precise and burr-free components with tight tolerances and better surface finish are being requested. This is especially true in aerospace and automobile industries. High quality products must be precisely manufactured according to design specifications and at low manufacturing costs. To fulfill these requirements, the manufacturing process should be well understood and its parameters optimized.

A phenomenon similar to chip generation is burr formation, which is a common problem that occurs in several industrial sectors, such as aerospace, ship construction, automobile, *etc.* It has also been among the most troublesome impediments to high productivity and automation, which largely affects the machined part quality. Therefore it is beneficial to limit the burr formation rather than deburring in subsequent finishing operations. In fact, deburring is expensive, time consuming and is considered as a non-productive operation. Throughout intensive research works during the last decades, the knowledge on the mechanisms of burr formation and deburring is understood to a good extent, followed by introduction of comprehensive and integrated strategies for burr prevention and minimization. Despite of all achievements, there are still many challenges on understanding, modeling and optimization of burr formation process and size, by means of burr size minimization and consequently production growth and cycle time reduction.

### **Defining the problem**

The burr formation process seems to be simple, but in fact, it is a highly complex phenomenon, involving many independent parameters that make the understanding of the burr formation mechanism more complicated. Most factors such as work part, tool, process and cutting conditions can have direct effects on burr formation. Other involved factors are machining instability due to vibrations, fluctuation of cutting forces and tool state (*e.g.* builds up edge formation, tool wear). Due to non-uniform chip thickness, tool runout and complex

interaction effects between cutting process parameters, the milling burr formation has a relatively complex mechanism than other machining modes, such as turning.

The main concerns when dealing with edge finishing are burr minimization and control and proper selection and automation of deburring operations. To avoid these undesirable expenses, burr size minimization and control are key factors. The burr size minimization or effectively burr prevention can be done through proper understanding of the basic mechanisms of burr formation and then studying the optimum cutting parameters. However it is a complicated task as burr formation is remarkably influenced by direct and interaction effects between process parameters.

One other approach for burr size minimization is to develop predictive models of burr size. To this end, the use of analytical and numerical methods is welcomed. Amongst numerical methods, finite element method (FEM) is a reasonable approach to model the metal cutting and burr formation processes (Toropov and Ko, 2006). Currently, the FEM is used to model the effects of cutting processes and process parameters on thermal and dynamic aspects of machining operations, computational assessment of tool and machined part geometry, residual stress, tools wear, chip and burr formation mechanism (Bansal, 2002). The main disadvantage of FE-burr formation models is that the obtained results are highly affected by the accuracy of input boundary conditions, which are not yet advanced and, therefore, are usually simplified. In addition, the results are dependent to software applied, time consuming and they usually require further experimental data for model (Niknam and Songmene, 2013).

Amongst machining operations, a few studies (Chern and Dornfeld, 1996; Ko and Dornfeld, 1996; Ko and Dornfeld, 1991) on analytical modeling of milling burr formation have been reported. Hence, most of the previous investigations have employed experimental approaches (Chern, 1993; Gillespie, 1976; Rangarajan and Dornfeld, 2004; San-Juan, Martín and Santos, 2010; Tsann-Rong, 2000). Amongst reported works on milling burr size modeling, none of them have dealt with slot milling burrs. Therefore, developing predictive models to simulate slot milling burrs size (mainly burr thickness) using material properties and cutting

parameters with no need to measure the burrs is certainly recommended. Special concentration should be paid to ductile materials such as aluminium alloys, which have a wide range of applications in automotive and aerospace industries.

As per author's knowledge, surprisingly except few works (Chen, Liu and Shen, 2006; Mian, Driver and Mativenga, 2011b; Tang *et al.*, 2011), very low volume of information is also available on factors governing slot milling burr formation. This is due to complex mechanism of slot milling burrs that involves three modes with various shapes and geometries as feed direction burrs (entrance and exit burrs), sideward and cutting direction burrs, which appear in eight edges of the machined part. Furthermore, most of the existing research works in literature characterize the burr height, while from deburring perspective, the burr thickness is more of interest, because it describes the time and method necessary for deburring a workpiece (Aurich *et al.*, 2009). Furthermore, only few studies (Lekkala *et al.*, 2011; Mian, Driver and Mativenga, 2011b) used statistical tools to determine the dominant process parameters on milling burr formation.

In most of the machining operations more than one type of burr occurs. Optimizing those factors leading to minimal burr size could have detrimental effects on other machining performance index, such as surface finish. Thus the use of appropriate techniques for simultaneous multiple responses optimization is certainly recommended. According to (Dhavamani and Alwarsamy, 2011), Fuzzy logic (FL), genetic algorithm (GA), Neural Network (NN), Taguchi method and response surface methodology (RSM) are the latest optimization techniques that are being applied successfully in industrial applications. Amongst, Taguchi-based optimization and desirability function have produced a unique and powerful optimization discipline that differs from traditional techniques (Phadke, 1989). The original Taguchi method is designed to optimize a single response (Gaitonde, Karnik and Davim, 2009), while most of the products have multiple performance characteristics. Optimization of multiple responses in Taguchi-style experiments has received little attention, because Taguchi design can not be applied directly, as each performance characteristic may not have the same measurement unit. Hence, it is essential to propose new modifications to

original Taguchi method for multiple responses optimization, as limited modifications have been suggested so far (Kilickap, 2010).

### **Research objectives**

The goal of this research project is to propose new strategies for understating, modeling and optimizing burrs during slot milling of aluminium alloys. The ultimate goal of this work is burr size minimization.

The specific research objectives can be summarized as follows:

1. To investigate the factors governing burr formation during slot milling of aluminium alloys.
2. To adapt and validate predictive models of burr size when milling ductile materials.
3. To suggest and validate new modifications to application of Taguchi method for simultaneous multiple responses optimization during milling operation.

### **Structure of thesis**

This thesis consists of five chapters. It starts with an introduction, followed by chapter one on literature review, three other chapters on various research tasks, and a chapter on substantial summary of the work presented, which links the outcomes of each chapter to proposed research objectives. Finally some conclusions, recommendations and future plans will be presented. The experimental conditions and parameters used in this research work are presented at the beginning of each chapter.

The thesis is organized as follows:

**Chapter 1** presents a comprehensive overview on burr formation mechanism, prediction, minimization and removal. Special focus is paid to milling burrs characterization, modeling and minimization. This chapter also includes a review of burr size measurements and

detection methods. An overview of optimization methods is presented, followed by a conclusion of the literature review.

**Chapter 2** presents a set of experimental works to understand the formation mechanism and dominant process parameters on five visible and large burrs during slot milling of 2024-T351 and 6061-T6 aluminium alloys (AAs). The factors investigated include the workpiece material, cutting tool coating and geometry, and machining parameters.

**Chapter 3** presents an analytical model of milling burr size (thickness) in ductile materials based on the geometry of burr formation and the theory of energy conservation. A computational model is also adopted and validated to predict the thickest milling burr along exit up milling side. This model only requires the use of material properties and cutting parameters to predict the burr thickness.

**Chapter 4** proposes new modifications and applications of Taguchi method for correct selection of optimum setting levels of process parameters for multiple responses optimization. The proposed approach is validated by simultaneous minimization of burrs size and surface finish in slot milling of AA 6061-T6.

**Chapter 5** presents a substantial summary of research work presented in chapters 2-4. It allows linking the outcomes of this work and the previous studies, and helps clarifying certain aspects and shortcomings that were identified in the problematic and research objectives. The discussion also shows the achievements of this research work on improving certain aspects of science related to burr size minimization during slot milling of aluminium alloys.

Finally, some concluding remarks and recommendations will be presented.



## CHAPTER 1

### LITERATURE REVIEW

#### 1.1 Introduction

Aluminium alloys are among the most machined metals. Machining of aluminium alloys features substantially higher cutting speeds and considerably lower cutting forces, as compared to that of steel (Zedan, 2011). The common alloying elements for aluminium are copper, silicon, manganese, zinc and tin. They are also classified as wrought or cast alloys depending on the processing used.

The major machinability assets related to aluminium alloys include tool life, chip characteristics, chip disposal, surface finish and burr formation. When proper conditions such as sharp cutting tools are used, aluminium alloys acquire a fine finish, thereby minimizing the necessity of protracted deburring and polishing operations. Burr formation is the main reason for tool change in milling of aluminium alloys (Rangarjan, 2005). Therefore, there is a growing need for minimizing burr formation that allows the use of cutting tools for a longer period of time and producing parts of higher quality. This led us to conduct research studies on understating, modelling and optimizing burrs size in slot milling of aluminium alloys.

#### 1.2 Definition and characterization of burr

In current industry, there are still many concerns on workpiece geometries generated by industrial instruments. One of the main concerns is known as ‘Burr’.

According to (Aurich *et al.*, 2009, p. 2):

“Burr is a body created in a workpiece surface during the manufacturing of a workpiece, which extends over the intended and actual workpiece surface and has slight volume in comparison with the workpiece, undesired, but to some extent, unavoidable”.

Gillespie's burr definition (Gillespie, 1996) is limited to cutting and shearing processes. In his definition, all the materials extending past the theoretical intersection of machined part surfaces correspond to burr (see Figure 1.1).

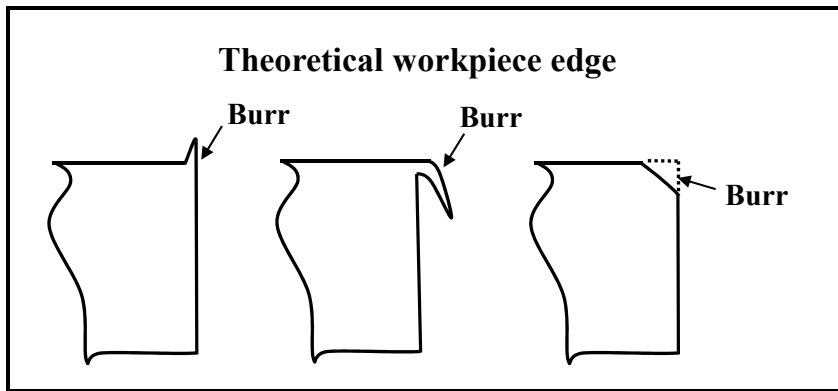


Figure 1.1 Examples of burr definition (Gillespie, 1996)

ISO 13715 defined the edges on a workpiece as burr (see Figure 1.2), if they have an overhang greater than zero (Aurich *et al.*, 2009).

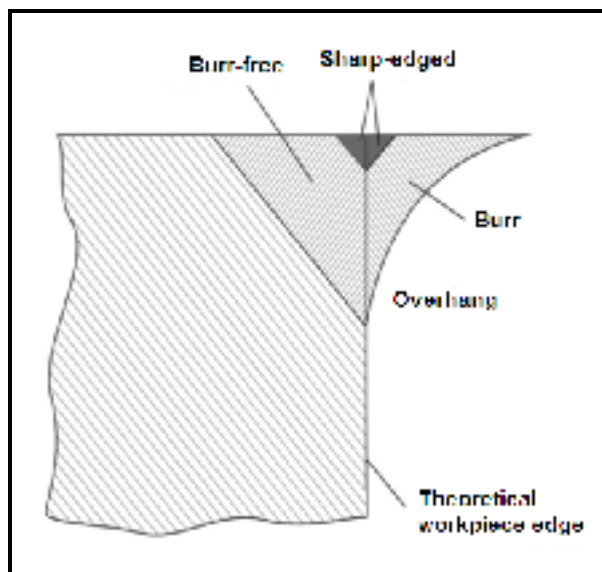


Figure 1.2 Burr definition by ISO 13715 (Aurich *et al.*, 2009)

As can be seen in Figure 1.3, to better describe the burr, a new term called as “burr value” was defined in (Schäfer, 1975). It contains the burr root thickness ( $b_f$ ), burr height ( $h_0$ ), burr thickness ( $b_g$ ) and burr root radius ( $r_f$ ). The burr root thickness ( $b_f$ ) is the thickness of the burr root area measured in the cross-section. The burr height ( $h_0$ ) is defined by the distance between the ideal edge of the workpiece and the highest point in the cross sectional area. The burr root radius ( $r_f$ ) is determined by positioning a circle to the burr root. The burr thickness ( $b_g$ ) describes the thickness parallel to the burr root area at a distance of ( $r_f$ ), as measured in the cross-section (Schäfer, 1975). The burr height and thickness are used to determine the tool replacement and schedule and also burr removal difficulties (Rangarjan, 2005). However the longitudinal profile of the burr is not highly informative in most cases, as it is rarely used to describe burrs. In addition it seems that the burr value can not be also used as an efficient parameter to better select the deburring method.

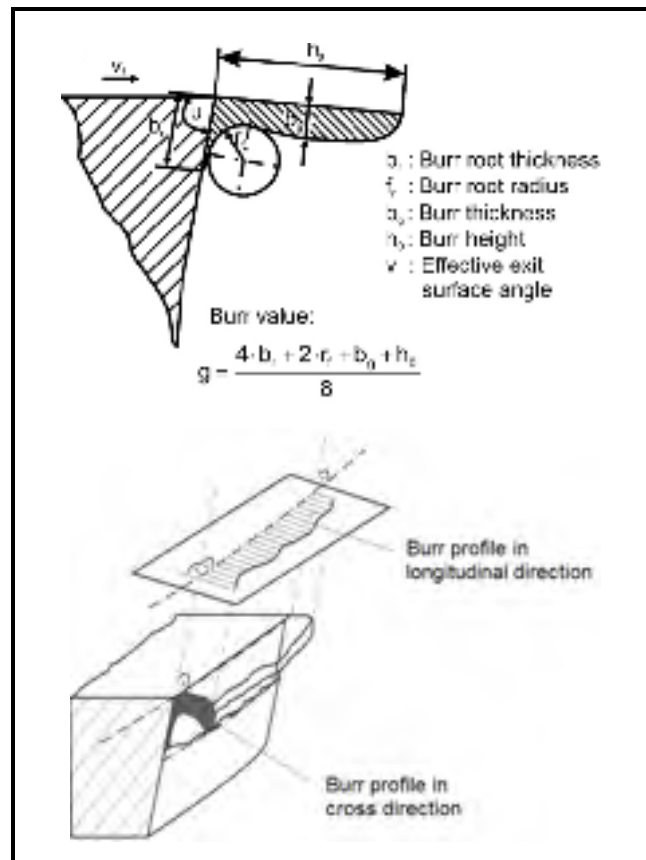


Figure 1.3 Measurement values of burr (Schäfer, 1975)

### 1.2.1 Burr formation mechanism

Pekelharing (1978) was the first person who described burr formation mechanism in metal cutting. He presented that negative shear is responsible for exit failure of cutting tools and root type burrs in milling (see Figure 1.4). The first fundamental work on burrs was published in (Gillespie, 1976). He developed an analytical model to illustrate burr formation mechanisms, which could predict burr properties.

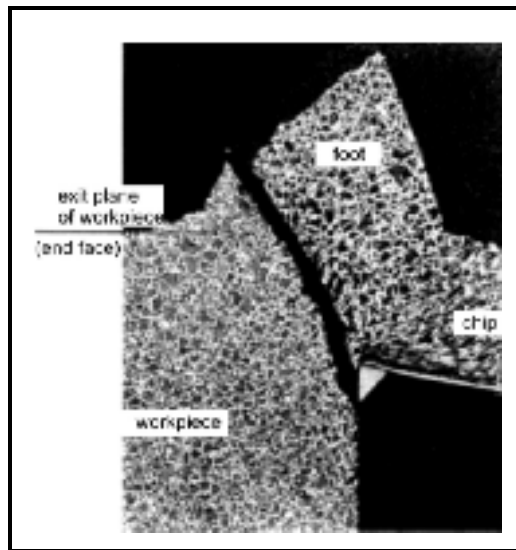


Figure 1.4 Micrograph of the chip root showing the exit failure, negative shear and foot formation (Pekelharing, 1978)

Sofronas (1975) was among the first researchers who studied the burr formation mechanism. He stated that burrs are in general a result of plastic deformation flow during cutting process. Gillespie introduced six physical processes leading to burr formation (Gillespie, 1999):

1. Lateral flow of material (it occurs whenever a solid is compressed);
2. Bending of material (e.g. chip rollover);
3. Tearing of chip;
4. Redeposition of material;
5. Incomplete cut-off ;
6. Flow of material into cracks;

According to (Gillespie, 1999), processes 1-3 involve plastic deformation of the machined part. Flow of material into crack in sixth process happens during burr formation in molding or primary shaping. Burr formation mechanism in orthogonal cutting can be divided into three stages: (1) initiation, (2) burr development and (3) final burr formation. Initiation of burr formation is characterized by the “negative deformation angle” denoted as  $\beta_o$ , and the initial tool distance of the tool tip  $A$  from the end of workpiece,  $\omega$  (see Figure 1.5(a)). Iwata *et al.* (1984) called  $AB$  as “negative deformation plane”. Nakayama and Arai (1987) have proposed a simple model of burr formation mechanism that includes the following three stages: (1) initiation, (2) transition and (3) push-out stage. Chern and Dornfeld (1996) proposed a model based on SEM observations of micro machining tests, which could perfectly predict the burr breakout.

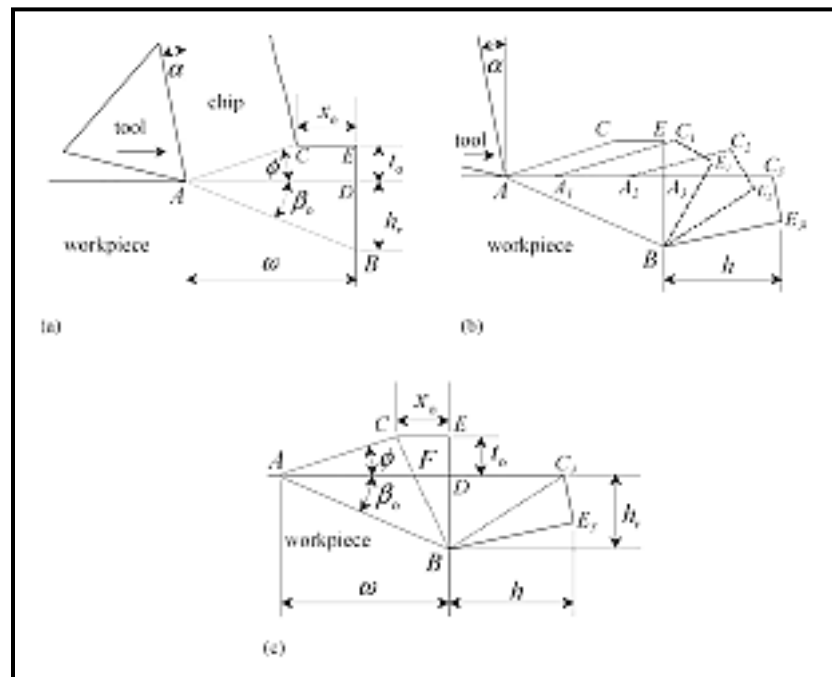


Figure 1.5 Burr/breakout formation model (Iwata, Osakada and Terasaka, 1984):  
 (a) initiation, (b) development and (c) final burr formation

According to (Hashimura, Hassamontr and Dornfeld, 1999), the burr formation mechanism is affected by mechanical properties of the workpiece, in addition to cutting conditions, such as

tool and workpiece geometry. This largely varies the burrs shape, locations and generation sources, especially when changing the workpiece. Therefore, the importance of burrs classification is evolved. Hashimura *et al.* (1999) classified the individual stages of burr formation for ductile and brittle materials (see Figure 1.6). From a certain stage of his model (stages 6-8), the burr formation is considered separately for ductile and brittle materials (see Figure 1.6). Stages 1–5 explain burr development without crack and stages 6–8 describe chip separation by crack propagation for ductile and brittle materials. In stage 6-I, crack initiates at the tool tip in the primary shear zone in a direction along the cutting line in ductile materials, which causes crack growth along primary shear zone (stage 7-I). The crack causes chip separation along the cutting line, therefore positive burr remains on the corner of the workpiece.

“The crack initiates at the tool tip in the negative shear zone and its propagation direction is towards the pivoting point (stage 6-II) in brittle materials. The induced crack in secondary shear zone causes chip separation from the workpiece. In stage 7-II, the crack grows along the negative shear zone. Moving along the cutting line, the tool induces crack growth and the crack mode may vary from shearing mode to opening mode. The workpiece edge also deforms slightly due to crack propagation. Stage 8-II indicates the end of burr formation in brittle materials. The crack separates the chip along with the part of the workpiece above the negative shear line. As a result, an area consisting of the fractured surface and a small amount of deformed material remains on the workpiece edge. In this case, the burr breaks out and is called a negative burr”(Aurich *et al.*, 2009, p. 7).

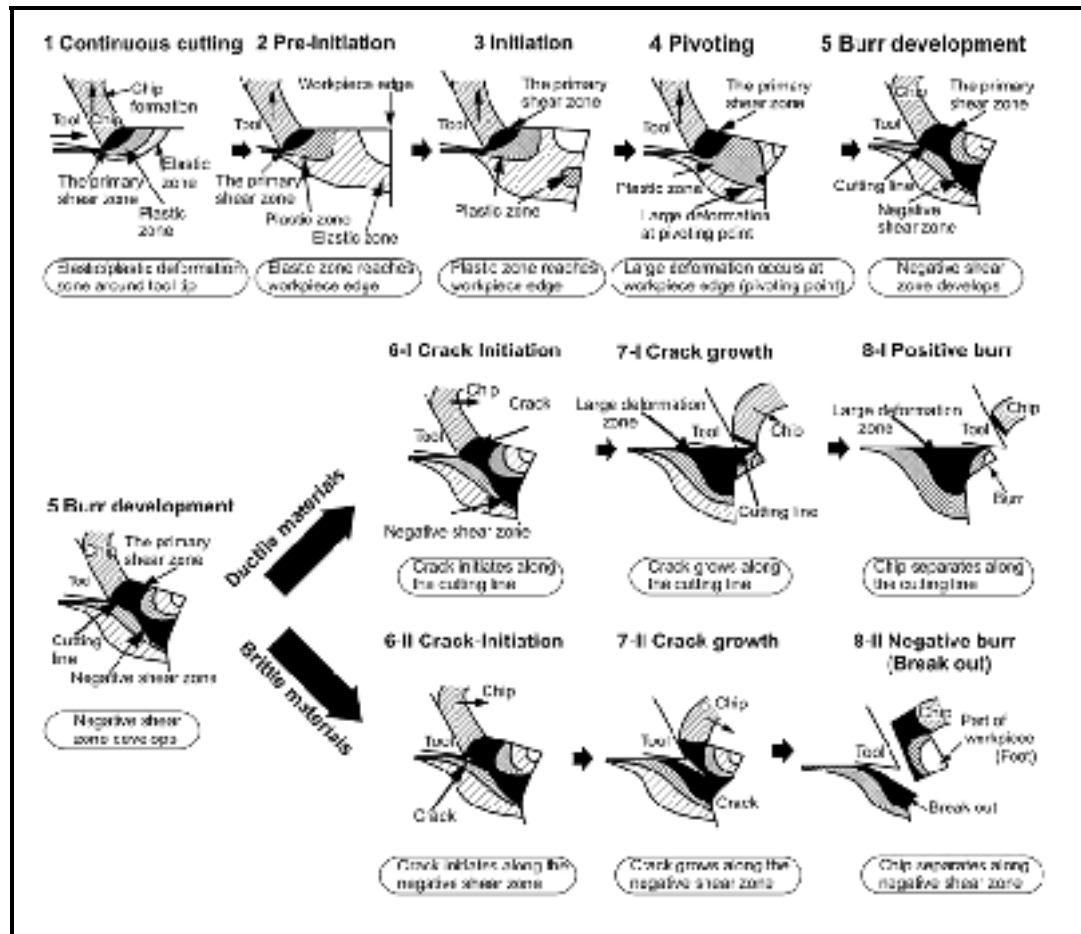


Figure 1.6 Burr formation mechanism in ductile and brittle materials (Hashimura, Hassamont and Dornfeld, 1999)

## 1.2.2 Burr shapes

Nowadays, there are several burr descriptions depending on application, manufacturing process, formation mechanism, shape and material properties (Aurich *et al.*, 2009). Gillespie (1996) defined four main types of machining burrs as follows: Poisson burr, Rollover burr, Tear burr and Cut-off burr (see Figure 1.7). The Poisson burr is a result of the material's tendency to bulge to the sides when it is compressed until the incidence of permanent plastic deformation (Nisbet and Mullet, 1978). Narayanaswami and Dornfeld (1994) called this phenomenon as side burr, because, according to engineering mechanics, "*Poisson effect*" is only present in the elastic range. The rollover burr is essentially a chip which is bent rather

than sheared resulting in a comparatively large burr. This type of burr is also known as an exit burr, because it is usually formed at the end of a cut. The tear burr is the result of material tearing loose from the workpiece rather than shearing cleanly. It is similar to the burr formed in punching operations. The cut-off burr is resulted by workpiece separation from the raw material before the separation cut is finished (Gillespie, 1976).

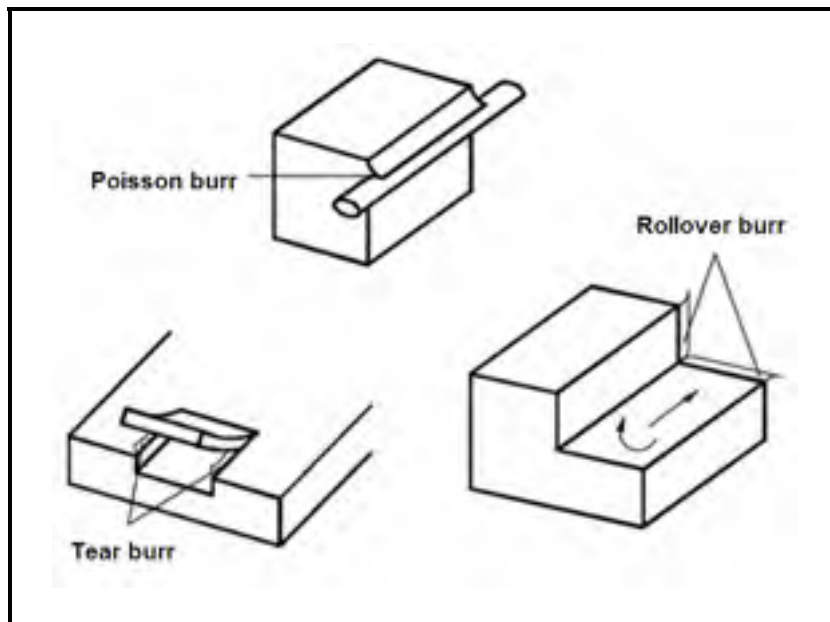


Figure 1.7 Schematic of Poisson, Tear and Rollover burr (Gillespie, 1996)

Two types of burrs known as primary and secondary burrs were introduced by Kishimoto *et al.*(1981).

“Through proper selection of cutting conditions and tool geometry, the rollover burr will be separated at its thinnest portion, and only a small burr will remain on the edge of the machined part”(Aurich *et al.*, 2009, p. 7).

According to (Aurich *et al.*, 2009), the former and latter burrs are known as primary and secondary burrs, respectively. Beier (1999) described a secondary burr as remaining material at the edge of a part after deburring process. From (Aurich *et al.*, 2009), secondary burrs formed after the breakage of the primary burrs. However, they are smaller than depth of cut,

while primary burrs are larger (Kishimoto *et al.*, 1981). Nakayama and Arai (1987) studied side burrs through experimental investigations. They described the burr formation in various machining processes by combining two classification systems as: (1) by direct concerning of cutting edge; (2) by mode and direction of burr formation. The various types of machining burrs are shown in Figure 1.8.

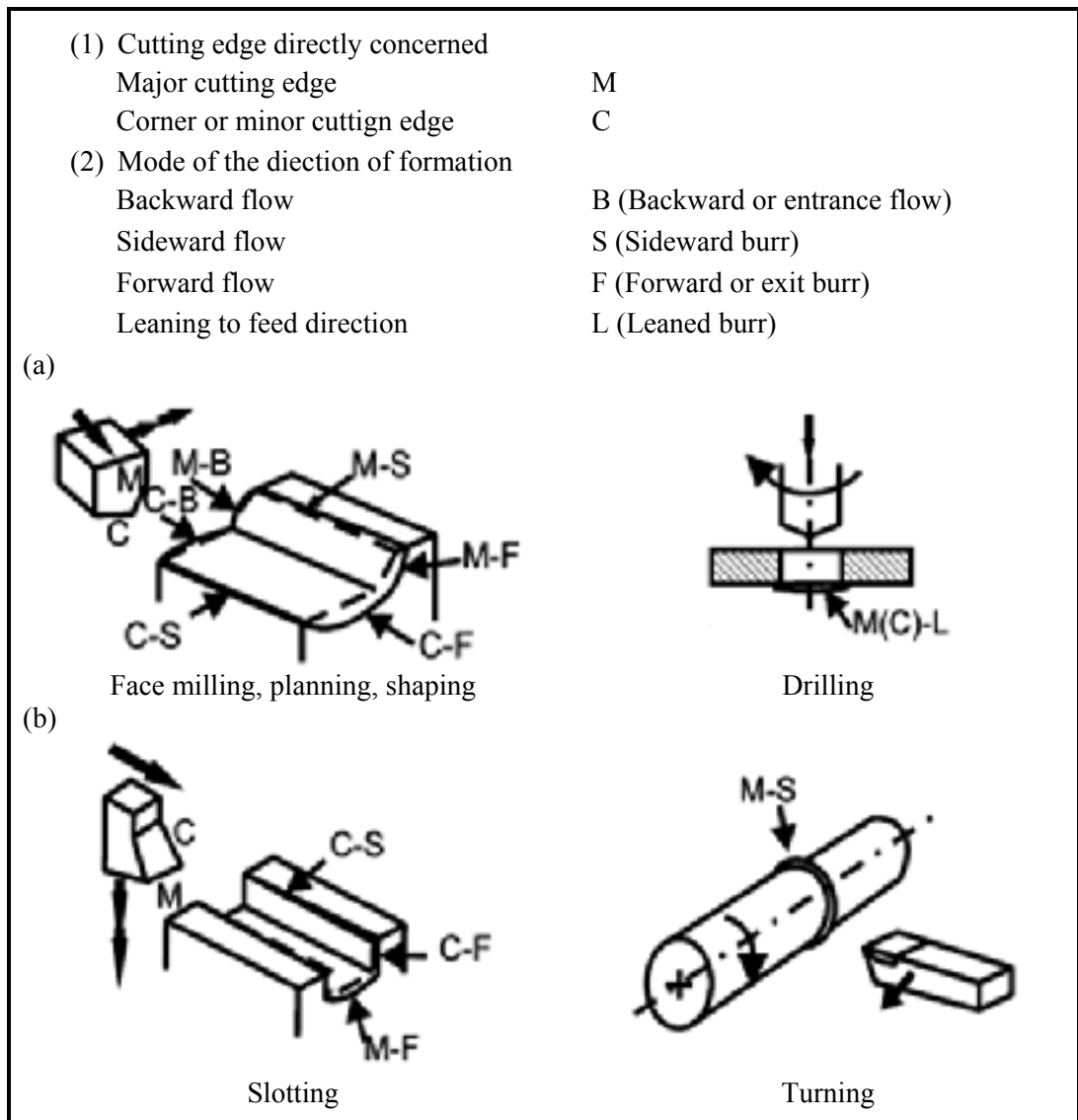


Figure 1.8 Types of machining burr  
(Aurich *et al.*, 2009)

### 1.2.3 Burr size measurement and detection methods

Due to the vital role of product quality, more attention has been paid to burr size measurement methods with particular attention on burrs geometrical characterization. The correct selection of burr size measurement methods depends on a number of factors such as the desired level of quality and requested measurement accuracy. However, according to (Aurich and Publica, 2006), over 71% of the interviewed companies still use the finger nail test for burr detection.

Three main burr size measurement systems are as follows:

- Mechanical systems
- Electrical systems
- Optical systems

According to Figure 1.9, burr detection and measurement methods can be classified into in-process and out-process techniques. The out-process techniques can be further grouped to with contact and contactless methods. Burr formation can be monitored by using indirect and direct methods. Direct methods consist of laser, optical and ultrasonic sensors. There are many optical systems for burr size measurement and detection with successful industrial implementations, such as camera systems, microscopes, laser and interferometer (Ko and Park, 2006; Lee, Huang and Lu, 1993; Tsai† and Lu, 1996; Wulf and Hayk, 2007). However these systems are expensive and difficult to use, while indirect methods are more cost effective. Amongst indirect methods, several studies used electrical systems for burr size measurement using capacitive sensor, capable of online monitoring of burrs and also inductive sensor systems for quantitative burr characterization and metal parts edges evaluation (Jagiella and Fericean, 2004; Lee, Park and Dornfeld, 1996; Olvera and Barrow, 1998). In addition, (Kishimoto *et al.*, 1981; Lee and Dornfeld, 2001) reported the use of silicon caoutchouc method to measure cross-sectional profiles of burrs using universal projector and AE as feedback sensing techniques in precision laser deburring process.

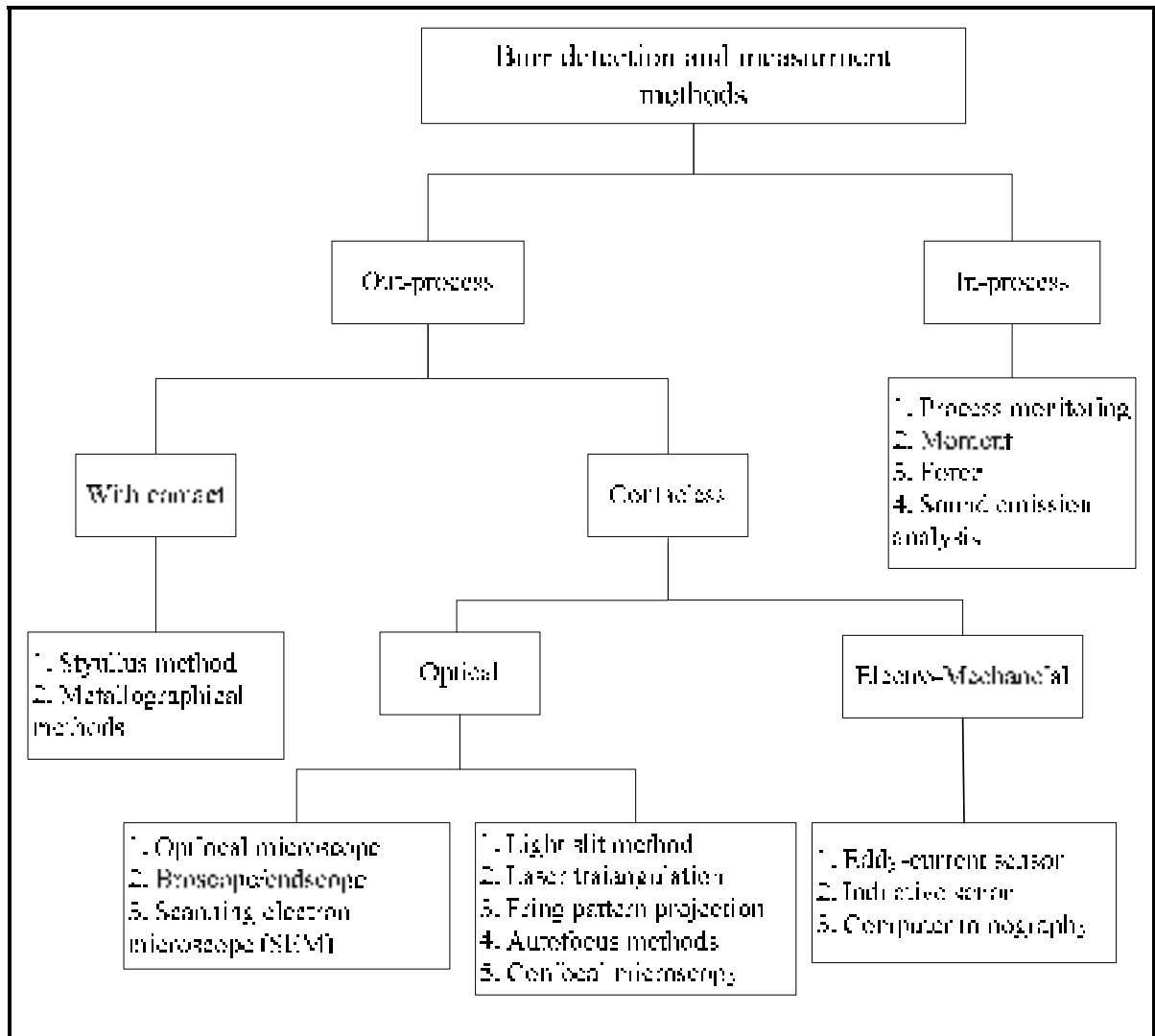


Figure 1.9 Burr detection and measurement methods  
(Aurich *et al.*, 2009)

#### 1.2.4 Burr removal (deburring)

Burrs have always been a serious concern in the surface and edge finishing of machined parts. According to (Gillespie, 1981), achieving an excellent edge quality when using deburring processes is often difficult. Even if the machined part is remarkably small, it may have several edges (see Figure 1.10), which require linear deburring, especially when machined part undergoes several operations.

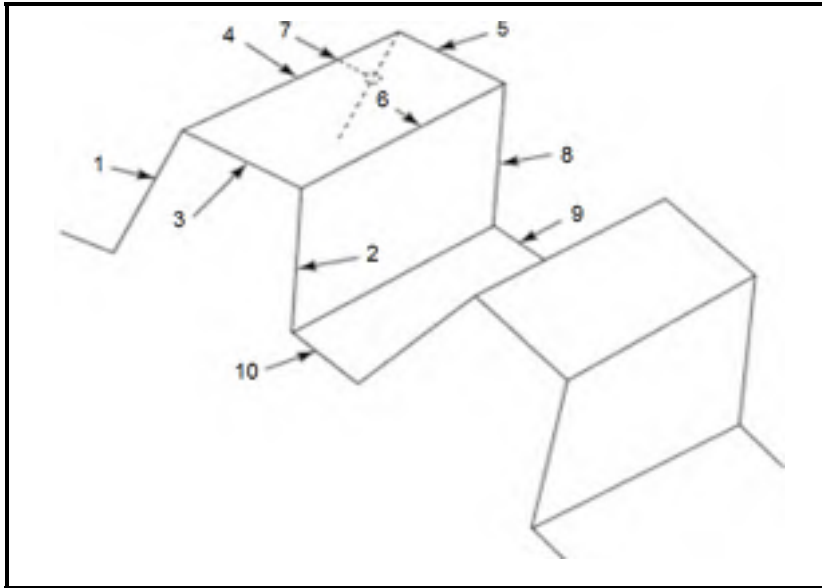


Figure 1.10 Example of machined part edges require deburring  
(*adapted from (Gillespie, 1999)*)

### Deburring process classification

Several classifications of deburring processes were proposed in (Gillespie, 1999; Przyklenk, 1986; Schäfer, 1975). The most complete one was made in (Gillespie, 1999). It encompasses all deburring methods, starting by manual deburring using hands to high technology finishing systems using CNC and industrial robots. He has identified 122 deburring and edge finishing processes which can be classified under following categories:

1. Mechanical deburring processes;
2. Thermal deburring processes;
3. Chemical deburring processes;
4. Electrical deburring processes;

In order to achieve the best surface and edge finishing quality, the appropriate selection of deburring processes is essential. Gillespie (1999) has identified the most frequently used deburring processes (see Table 1.1).

Table 1.1 The most frequently used deburring processes

No.	Deburring process	No.	Deburring process
1	Manual deburring	6	Barrel deburring
2	Brush deburring	7	Centrifugal barrel finishing
3	Bonded abrasive deburring	8	Robotic deburring
4	Abrasive jet deburring	9	Electro chemical deburring
5	Mass finishing	10	Vibratory finishing

### **Selection of deburring process**

Most of deburring tools and processes are developed for materials with specific geometries. Therefore, correct selection of deburring process is essential. The first approach for deburring process selection was proposed in (Schäfer, 1975). Later, a software tool was developed for the same purpose (Ioi, Matsunaga and Kobayashi, 1981). In this tool, burr shape, surface roughness, workpiece properties, weight and volume were used to create the database. Thilow (2008) also introduced an industrial system for similar purpose. The available deburring processes for burr removal in aluminium parts are introduced in (Przyklenk and Schlatter, 1987). According to (Narayanaswami and Dornfeld, 1994), factors governing deburring complexity are burr location, size, and number of edges to be deburred. Furthermore, a clear knowledge on how deburring process itself affects the workpiece dimensions and surface quality is a crucial factor for correct selection of deburring process (Gillespie, 1999). Unfortunately, all reported deburring processes have certain levels of side effects on machined part. This thesis does not, however, try to present the main advantages, disadvantages and restrictions related to each deburring process. The following passages present the basic information on some of the highly used deburring processes in today's industry.

### Manual deburring

Manual deburring is still known as the most widely used operation for many reasons, including extreme flexibility, low cost and lack of technology needed. According to (Gillespie, 1999), manual deburring is associated with wasting of time and asset, fatigue, frustration, etc. Moreover, in most of the industrial sectors, manual deburring is implemented in dry conditions by non-qualified operators (see Figure 1.11). This consequently increases the waste rate and delay in production lines.



Figure 1.11 Manual deburring  
(Tiabi, 2010)

### Mechanical deburring

During mechanical deburring processes, the burrs are reduced or removed by mechanical abrasion. The use of dry blasting for automatic deburring is examined in (Mchugh, 1988). Chen *et al.* (1991) presented a dynamic model for burr removal with a cooperative brushing tool. A deburring method for milled surfaces was proposed in (Anzai *et al.*, 1993). In this work, an inductor producing a co-current magnetic field is adapted to the milling spindle. Ultrasonic deburring was investigated in (Lee *et al.*, 2004). More mechanical deburring systems were also recently developed (Avila *et al.*, 2004; Beier and Nothnagel, 2004).

## Robotic deburring

Robotic deburring is used to reduce the work load and guarantee an adequate workpiece quality level. The use of robots for deburring operation was reported in (Asakawa, Toda and Takeuchi, 2002; Lee, Huang and Lu 2001). In (Asakawa, Toda and Takeuchi, 2002), automatic chamfering of a hole on a free-curved surface is presented on the basis of CAD model using an industrial robot. Different deburring processes are applied by robots with various difficulties in each case (Aurich *et al.*, 2009). Amongst, an overview of a robot arm combined with deburring brush is depicted in Figure 1.12. Hirabayashi *et al.* (1987) presented deburring robots equipped with force sensors for automatic deburring of elevator guide rails. A framework for robotic deburring applications in various industrial sectors was proposed in (Oliveira and Valente, 2004).



Figure 1.12 A robot arm combined with deburring brush  
(Means, 1986)

### 1.2.5 Concerns on burr formation

Recent studies have shown tremendous concerns on burr formation and deburring operations as follows:

1. Small finger injuries for assembly workers.
2. Source of debris (bits of burrs) during operation, thereby reducing the life time of the machined part.
3. Changing the parts resistance and reduce the tool life as well as efficiency (Ko and Dornfeld, 1991).
4. Presenting a hazard in handling of machined parts, which can interface with subsequent assembly operations.
5. The adhered burrs to the work part may become loose during operation and consequently cause difficulties and damages.

After a basic understanding of the mechanisms underlying the burr formation, the focus of research works has turned to deburring operations, which are in fact expensive, time consuming, non-productive and non-value added processes. As pointed out in (Gillespie, 1999), deburring and edge finishing of precision components may constitute as much as 30% of the cost of the finished parts. In practice, it is often necessary to combine several deburring and edges finishing processes to achieve the desired edge accuracy and surface finish requirements. In fact, the secondary finishing operations are difficult to automate, therefore may become a bottleneck in production lines (Gillespie, 1996).

In a recent study by Aurich *et al.* (2009) the costs are estimated up to €500 million per year only in Germany. According to (Gillespie, 1999), deburring concerns both the edges and surfaces of the workpiece. Furthermore, presence of burrs in manufactured components is a serious concern in terms of customer and supplier relations, as generally products are stamped as “*sharp edge free*” or “*free of burrs*”. Then, it is recommended to limit burr formation rather than deburring them in subsequent finishing operations. In many cases,

increasing the burr size is a key element of tool wear, leading to replacing of cutting tools that are otherwise still operating without problem (Aurich *et al.*, 2009).

Deburring side effects usually appear on the dimensions, surface finish, cleanliness, flatness, plating, soldering, welding, residual stress, surface imperfection, corrosion rate, fatigue resistance, electrical resistance, luster and color of the machined part. Proper understanding of the basic mechanisms of burr formation and then correct selection of optimal cutting parameters are strongly suggested for burr size minimization.

### **1.3 Understanding and modeling of milling burr formation**

#### **1.3.1 Milling burrs shapes**

Milling burrs are created when cutting tool enters and exits the machined parts. Hashimura *et al.*(1999) classified milling burrs according to their location and formation mechanism (see Figure 1.13). As can be seen in Figure 1.14, a nomenclature to classify exit burrs was proposed in (Chern, 1993; Hashimura, Hassamontr and Dornfeld, 1999). Under certain cutting conditions, large burrs are formed that pose difficulties for deburring operations. These large burrs are usually generated along the cutting direction and their height is consistent and approximately equal to depth of cut. In some cases, a burr is separated in its thinnest part, leaving only a small portion adhered to machined part surface. The burr height in this case is much smaller than the depth of cut.

According to Figure 1.15, the face milling burrs are considered as a two-dimensional (2D) problem, generated as cutting tool follows its path through the machined part. The main face milling burrs are exit burr, side burr, and top burr, which are created respectively along (1) the edge between the machined surface, (2) the edge between the transitional surface and the exit surface, and (3) the edge between the top surface and the transition surface (Lee, 2004).

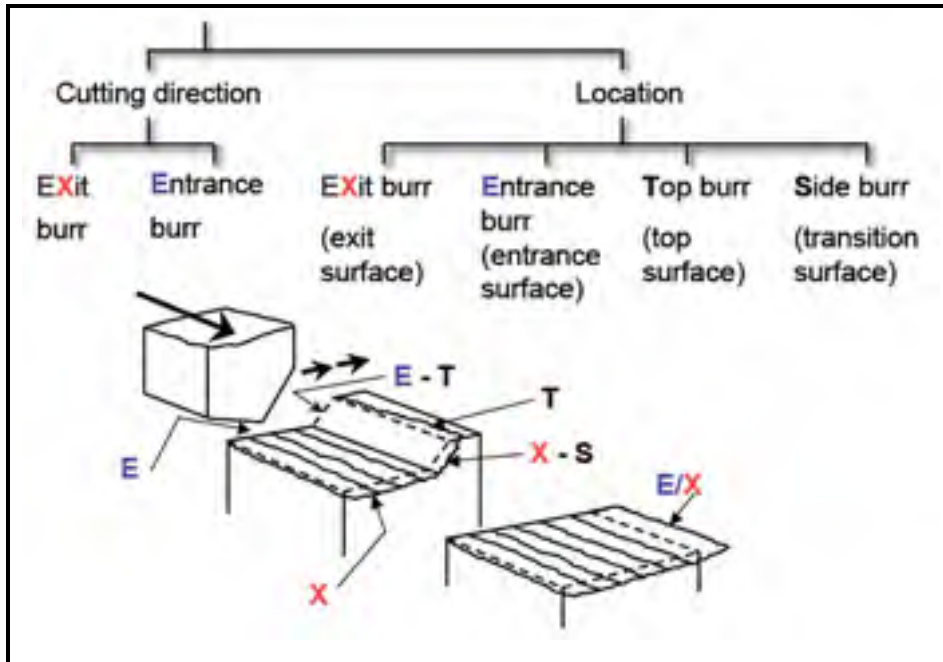


Figure 1.13 Milling burr formation classification-location (adapted from (Hashimura, Hassamontr and Dornfeld, 1999))

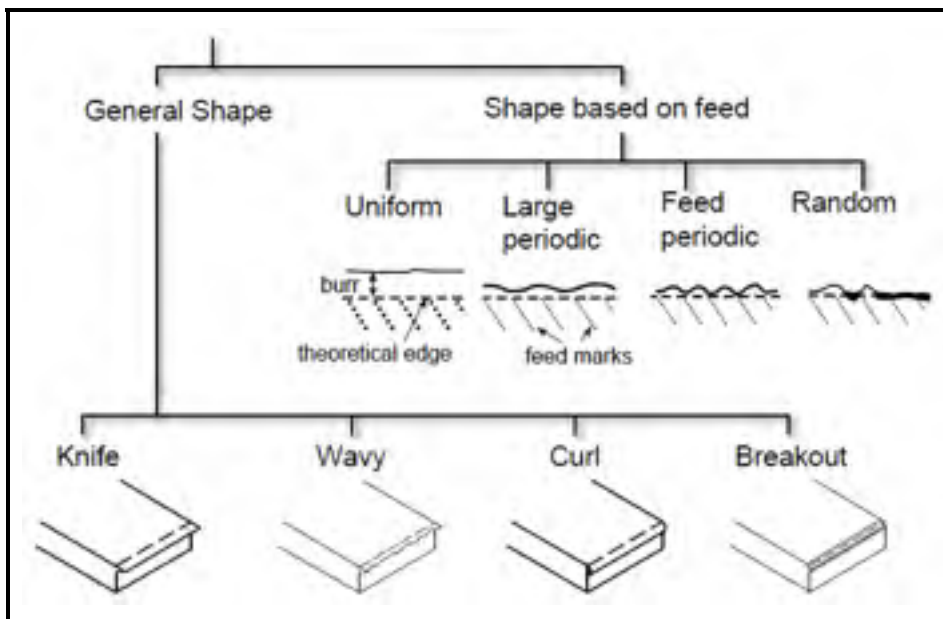


Figure 1.14 Milling exit burr classification-shape (adapted from (Chern, 1993; Hashimura, Hassamontr and Dornfeld, 1999))

Burr formation mechanism in end milling and slot milling operations are even more complex than the one in face milling. Unlike in face milling, subsequent tools passing through do not usually remove the burrs produced by previous tools in end milling. As a result, side burrs and top burrs are stocked on the part, possibly leading to several problems. In slot milling operation, entrance burrs along up milling side and entrance burrs are smallest in size. The top burrs along up/down milling sides and entrance and exit burrs along down milling side are on a medium-scale, comparatively.

As shown in Figure 1.16, the exit burr along up milling side and exit bottom side burr are the largest burrs (Chen, Liu and Shen, 2006). Considering the smaller size of entrance burrs as compared to exit burrs, more focus has been paid to understand the mechanism of burr formation at the exit zone of the milling process. Therefore, series of experiments were conducted by varying different factors in sequence to observe the variation of exit burrs (Gillespie, 1976; Shaw, 1984; Tang *et al.*, 2011; Tsann-Rong, 2000).

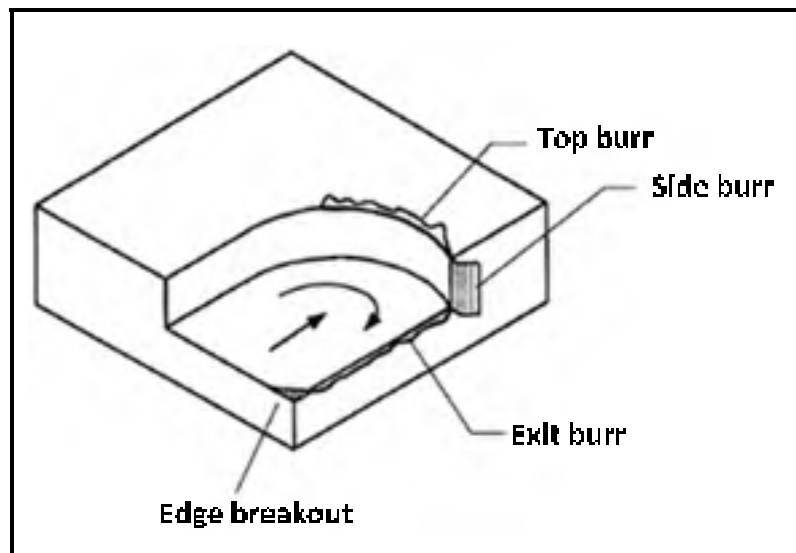


Figure 1.15 Face milling burrs  
(Lee, 2004)

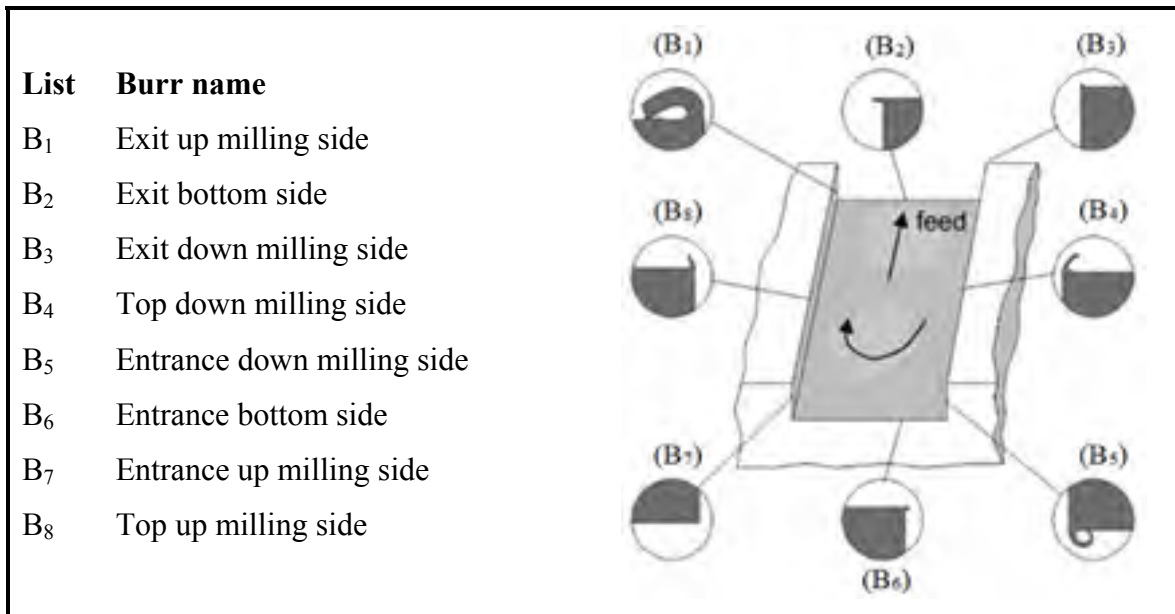


Figure 1.16 Slot milling burrs  
(Lee, 2004)

### 1.3.2 Parameters governing milling burr formation

Burr formation is considered as a crucial industrial concern. The previous studies have shown that it is almost impossible to avoid burr formation (Tiabi, 2010). Burr formation studies under following situations are much of interest:

1. Situations where burr size minimization is demanded;
2. Situations where regulation and standardizing the burrs are demanded;
3. Situations where burr removal (deburring) is demanded;

To examine these situations, it is necessary to monitor the burr formation behavior with respect to changes made in cutting conditions. Gillespie and blotter (1976) observed that burrs cannot be prevented by only changing the feed rate, cutting speed and tool geometry. According to (Aurich *et al.*, 2009; Sofronas, 1975; Tseng and Chiou, 2003), the principle factors governing milling burr formation are as follows:

1. Machined part (geometry, dimension, mechanical properties, *etc.*);
2. Cutting parameters (cutting speed, feed rate, depth of cut, *etc.*);

3. Cutting tool (material, shape, geometry, rake angle, lead angle, helix angle, *etc.*);
4. Machine tool (rotational speed, dynamic strength, *etc.*);
5. Manufacturing strategy (tool path, coolant, back cutting, lubrication, MQL, *etc.*);
6. Other parameters (e.g. cutting forces);

However, this summary is still inadequate due to complex interaction effects between process parameters, as their degree of influence on burr formation vary considerably by simple addition or removal of cutting parameters and/or changing the material. In other words, the dominant process parameters on burr formation cannot consistently be separated into direct and indirect factors (Aurich *et al.*, 2009). The following passages present the dominant process parameters on milling burr formation mechanism and size.

### **Machined part (workpiece)**

The machined part properties (e.g. chemical, mechanical) have significant effects on burr formation process. The dominant mechanical properties usually reported in the literature are hardness, ductility, yield strength and elongation (Leopold and Wohlgemuth, 2010). According to (Aurich *et al.*, 2009), a burr forms if the material escapes the cutting process and occurs at tool entry and exit. This has led to following outcomes:

- Larger burrs tend to be formed with increase in the material ductility.
- Burr formation reduces, if the material is restricted to deform in the force direction.

The most commonly used materials in aerospace industries are aluminium alloys, titanium alloys, nickel based alloys and composite materials. Some of these materials such as aluminium alloys are ductile. Ductility is one of the most important material property (Leopold and Wohlgemuth, 2010). According to (Kim and Dornfeld, 2002), machining of ductile materials tends to form larger burrs, particularly at higher levels of cutting speed and feed rate. However, when the material is brittle, fractured burrs are formed on the edge part. This phenomenon can be reinforced at higher cutting speed and feed rate, creating irregular burrs. The metallographic characteristics of machined part could influence the burr

formation, as the orientation of the machining direction could metallographically generate less distortion; consequently less burr formation is anticipated (Kim and Dornfeld, 2002).

### ***Workpiece geometry***

The workpiece edge angle is the most prominent geometrical element of the workpiece that highly affects the burr formation mechanism. According to (Przyklenk, 1986), cutting tests on the edge angle lower than  $90^\circ$  generate long and thin burrs, while short and thick burrs are formed on the parts with edge angle of  $90^\circ$  or larger.

### ***Surface treatment***

According to (Sofronas, 1975), the burr size increases with increase in the ratio of the chip and workpiece shear stress ( $\tau_c/\tau_w$ ). To reduce the burrs size, either, there should exist an increase in the shear stress of the part ( $\tau_w$ ), or decrease in shear stress of the chip ( $\tau_c$ ). The disadvantage of this method is that cracks may develop in hardened surface part, causing difficulties in controlling of the burr formation process. Increase the temperature hardens most of the materials and consequently affects the machining and deburring performance, even if the created burrs are small. According to (Gillespie, 1999), an attempt to prevent plastic deformation reduces the incidence of burr formation. His proposed methods include laser treatments, hard machining, localized mechanical processes, chemical and thermal treatments. In addition, chamfering on the external edges of the machined part before cutting operation is an excellent approach to prevent the material deformation at the part edge and consequently burr size reduction (Tiabi, 2010).

### **Cutting Conditions**

According to (Avila and Dornfeld, 2004), burr height irregularly varies when changing cutting conditions. Increase the cutting speed led to reduced burr size. In addition, milling operations at higher levels of feed rate reduces the burr size, while creating secondary burrs

that are easier to remove. From (Rangarajan, 2001), when the machined part surface is hardened in high speed machining, a transition from ductile to brittle behavior may occur. This phenomenon may lead to decreased burr height. Chern (1993) analyzed the burr formation during face milling of aluminium alloys. He found that secondary burr formation is dominated by depth of cut and feed rate. Nakayama and Arai (1987) revealed that the burr size can be reduced by limiting the undeformed chip thickness. The cutting conditions, tool and workpiece geometry may reduce the shear strain supported by the chip. Therefore, burr reduction may occur. Kim and Dornfeld (2002) showed that higher levels of depth of cut increases the burr size, subjected to other cutting parameters used.

According to (Tseng and Chiou, 2003), milling burrs are considered as Poisson burrs, which are not highly effected by cutting conditions. Wang and Zhan (2003b) stated that the burrs height in cutting direction are reduced with increase in the depth of cut, feed rate, cutting edge angle and back rake angle. Furthermore, the use of larger corner radius led to longer burr. According to (AM De Souza *et al.*, 2003; Schäfer, 1978), lower level of feed rate led to reduced burr size. Contrary, (Jones and Furness, 1997; Kishimoto *et al.*, 1981; Wang and Zhang, 2003b) found that higher level of feed rate reduces the burr size. This exhibits that the outcomes of experimental studies are not always similar. Olvera and Barrow (1998) found that exit angle and depth of cut influence the exit burr in the cutting direction, whereas depth of cut is the main factor affecting the exit burr in the feed direction. According to (Olvera and Barrow, 1996; Shefelbine and Dornfeld, 2004a), the use of high levels of axial depth of cut ( $a_p$ ) increases the possibility of burr size reduction, but, it may also cause inevitable damages to cutting tool, machine and machined part functionality. Therefore, the use of very high and/or low levels of cutting parameters is not suggested during milling operation. In order to reduce the costs and increase productivity, the use of optimization methods for correct selection of process parameters is strongly recommended.

### **Cutting tool geometry**

According to (Bansal, 2001), the use of larger axial rake angle and smaller lead angle led to smaller burrs. Larger nose radius increases the incidence of burr formation (Aurich *et al.*,

2009). Avila and Dornfeld (2004) showed that tool geometry and in-plane exit angle  $\Psi$  have significant effects on burr size and edge breakout during face milling of aluminium-silicon alloys (AlSi9Cu3 and AlSi7Mg). Tripathi and Dornfeld (2006) reported the possibility of burr free condition when using diamond end mill tools at high cutting speed. According to (Gillespie and Blotter, 1976), the use of sharp cutting edge tools with positive rake angle avoids built up edge (BUE) formation, thus reduces burr size. According to (Jones and Furness, 1997), milling tests with the exit angle of  $76^\circ$ - $118^\circ$  generate smaller burr, while Luo *et al.* (2008) showed that the largest burrs were created in exit angle of  $90^\circ$ . This exhibits that defining the optimum exit angle for burr size minimization in milling operations is a difficult task.

### **Machining strategy**

According to (Chu and Dornfeld, 2004; Wang and Zhang, 2003a), correct selection of machining strategy has positive effects on burr formation mechanism. The main machining strategies proposed until now include:

1. Optimization of the tool path planning, including machining direction and the tool engagement angle;
2. Using inserts and backup materials;
3. Using modified cutting parameters;
4. Using coolant and lubrication;

Tsann-Rong (2000) reported that the burr height is strongly dependent on the milling process. According to (Olvera and Barrow, 1998), the exit angle and tool nose geometry have significant influences on exit burrs characteristics. Bansal (2002) found that the use of milling inserts with positive axial rake and negative radial rake angles result in a good trade-off between small burr size and good surface quality. As to an improved tool path, this approach is also limited, as complex geometries would require optimized tool paths and higher cycle time (Aurich *et al.*, 2009). Luo *et al.* (2008) revealed that the friction angle becomes larger with increase in exit angle and oblique cutting angle. This led to longer exit

bottom and exit up milling side burrs, respectively. In order to predict the burr size in face milling, sets of algorithms were presented in (Chu, Dornfeld and Brennum, 2000; Rangarajan, Chu and Dornfeld, 2000) by means of avoiding tool exit. This has led to proposing tool path planning approaches for burr size minimization. The influence of back cutting on burr formation has been reported in (Rangarajan and Dornfeld, 2004). Przyklenk (1986) proposed a new strategy for burr reduction by using dry iced snow to cool down the machined part edge. Shefelbine and Dornfeld (Shefelbine and Dornfeld, 2004a; Shefelbine and Dornfeld, 2004b) stated that the use of coolant decreases the burr size, while larger burr is anticipated when using worn tools.

According to (Tiabi, 2010), proper lubrication reduces friction between the work part and tool, and it consequently reduces incidence of burr formation. However as stated by Aurich *et al.*(2005), in the case of certain materials, the use of lubricant hardens the burrs and complicates the deburring processes. Moreover, the use of cutting fluids seriously degrades the environmental air quality and increases machining costs 16-20%. One alternative approach with reduced cost and more environmental benefits is dry machining. Some works reported the use of dry milling (Dasch *et al.*, 2006; Kim and Kang, 1997; Shefelbine and Dornfeld, 2004b; Songmene V., Khettabi and Kouam, 2012). According to (Klocke and Eisenblätter, 1997), dry cutting is a suitable choice for machining of ductile materials, such as aluminium alloys.

When dealing with hard to cut materials, it is recommended to apply a new technique consisting only a few millimeters of fluid to the tool's cutting edge, known as minimum quantity lubricant (MQL). The MQL is atomized in a nozzle to form extensively fine droplets, which are then fed to machining point in the form of an aerosol spray at a rate not exceeding 100 ml/h (Weinert *et al.*, 2004). The great benefits of MQL on burrs size minimization were reported in (De Lacalle *et al.*, 2001; Rahman, Senthil Kumar and Salam, 2002). However further investigations are still required to select the suitable cutting conditions over a limited range of process parameters and materials studied.

## **Cutting forces**

Cutting forces are essentially affected by feed rate, depth of cut, tool and workpiece geometry. Milling burr formation is significantly influenced by the cutting forces (Tiabi, 2010). The direction and intensity of cutting forces affect the volume of the chip generated, and can also play an important role in material deformation. In case of milling operation, cutting forces can be theoretically and computationally calculated (Altintas, 1992; Altintas, 2000). A comprehensive investigation on influence of cutting forces on milling burr formation will be presented in the following chapters.

### **1.3.3 Milling burr formation modeling**

Burr formation modeling has been carried using various research methods such as experimental studies, analytical and numerical modeling. Considering the complexity of milling burr formation process, typically 2D models are more frequently used. Numerous burr expert systems were developed on the basis of experimental studies. These systems are database prediction tools (Leopold and Wohlgemuth, 2010) that involve comprehensive experiments by varying process parameters to monitor burr formation patterns. They have shown successful implementations in many cases, especially when varying only a few parameters is required (e.g. drilling process). However, providing a database for all elaborated parameters in milling operation is a time consuming and costly approach (Bansal, 2002). The major reported works on experimental studies, analytical and numerical models of milling burr formation are presented in following subsections:

#### **Analytical modeling**

Among machining operations, analytical modeling of milling burr formation is a challenging subject. This is due to complexity of milling burr formation mechanism, where burrs are created when cutting tool enters and exits the machined part. Therefore, the base model for studying the burr formation process has been the orthogonal cutting scheme (Toropov, Ko

and Lee, 2006). Analytical modeling of burr formation was studied as the plastic bending of non-cut parts of materials, using minimum energy principles and incompressibility assumption (Avila and Dornfeld, 2004; Chern and Dornfeld, 1996; Gillespie, 1976; Gillespie and Blotter, 1976; Hashimura, Hassamontr and Dornfeld, 1999; Ko and Dornfeld, 1996; Ko and Dornfeld, 1991; Kumar and Dornfeld, 2003; Narayanaswami and Dornfeld, 1994; Olvera and Barrow, 1998; Pekelharing, 1978). The first milling burr formation model was proposed in (Gillespie, 1976). Olvera and Barrow (1998) developed burr size prediction model for various exit angles and tool end nose geometries. Slip line method was also used to model exit burr formation in orthogonal cutting (Leopold and Wohlgemuth, 2010).

Analytical modeling of milling burr formation process was studied by “*Professor D. Dornfeld*” and his associates at “*University of California, Berkeley*”. Ko and Dornfeld (1991) proposed a model of burr formation in orthogonal cutting with three stages of burr formation process, including: burrs initiation, burr development and final burr formation. Later, Narayanaswami and Dornfeld (1994) presented a tool entrance/exit model. Chern and Dornfeld (1996) suggested burr formation/breakout model for orthogonal cutting, explaining that plastic bending and shearing of the negative deformation plane contribute to the burr formation while crack propagation along the plane causes the breakout.

An analytical model of material exhibiting fracture during burr formation was proposed in (Ko and Dornfeld, 1996), using the fracture strain from McClintock’s ductile fracture criterion. The burr size estimations were found accurate for less ductile materials, while the results of ductile materials (i.e. copper and aluminium alloy) were not consistent. A transition of primary to secondary burrs with respect to tool engagement was shown in (Hashimura, Hassamontr and Dornfeld, 1999). This has led to the development of a burr size prediction system, known as exit order sequence (EOS), which is mainly used for face milling process (Kumar and Dornfeld, 2003). Few other works recently focused on burr formation modeling in micro-end milling operations (Lekkala *et al.*, 2011; Zhang, Liu and Xu, 2013). However, very limited information is available on analytical modeling of slot milling burrs.

### **Experimental studying/modeling**

Kishimoto *et al.* (1981) studied face milling burr formation with special focus on primary and secondary burr formation. The effects of tool geometry, various workpiece materials, cutting parameters and tool path were investigated in (Gillespie, 1976). Milling burr formation was predicted and minimized for slot and face milling processes using tool path planning strategies and process parameter optimization, as well as workpiece rigidity strengthening (Chen, Liu and Shen, 2006). Burr formation during orthogonal cutting of aluminium alloy was studied in (Hashimura and Dornfeld, 1995). As feed rate increases, the tool position corresponding to the appearance of the pivot point increases. This led to increase in the burr thickness.

The influences of tool wear, cutting speed and coolant on burr size during face milling of cast iron and aluminium alloys were investigated in (Shefelbine and Dornfeld, 2004a; Shefelbine and Dornfeld, 2004b). Chern (2006) reported the influence of cutting conditions on burr formation when fly milling cutters were used in single-tooth face milling of aluminium alloys. He (Chern, 2006) reported that the burr geometry is strongly dependent to in-plane exit angle  $\Psi$ . According to (Avila and Dornfeld, 2004), burr height irregularly varies with changes in cutting conditions. Biermann and Heilmann (2010) investigated the principle coherences between burr formation and notch wear, separated into three steps. They also presented burr reduction strategies for turning, drilling and milling of different materials. In addition, a new promising strategy for milling burr reduction is proposed by cooling the component edge with dry ice snow (Biermann and Heilmann, 2010). According to (Wang and Zhang, 2003a), the dominant process parameters on cutting direction burrs are cutting parameters, shape of the workpiece end, cutting tool geometry and workpiece properties.

Tripathi and Dornfeld (2006) presented a review on several methodologies for burr prediction and minimization in face milling, with special attention on geometric solutions employed; understanding and modifying tool engagement conditions. The effects of cutting speed, feed rate, material hardness, tool wear and cutting tool exit angle on burr formation

during face milling of aluminium alloy were reported in (Jones and Furness, 1997). Milling tests with exit angles of  $76^{\circ}$ - $118^{\circ}$  led to smaller burrs, irrespective of tool wear condition. Furthermore, higher level of feed rate, lower level of cutting speed, new sharp cutting tools and harder materials have positive effects on burr size minimization. The effects of exit angle and tool nose geometry on exit burr formation for both finishing and roughing conditions (small and large depth of cut) were reported in (Olvera and Barrow, 1998). Four different types of burrs were observed on the exit edge, namely tear, curly, rubbing and wavy burrs. Luo *et al.* (2008) studied the mechanism of feed direction burrs in slot milling of aluminium alloys. According to (Rahman, Senthil Kumar and Salam, 2002), lower burr height was observed when using MQL. Additionally no chips stick to the tool unlike milling tests under flood cooling and dry condition. As stated by de Lacalle *et al.*(2001), MQL systems are very useful for chip evacuation and manufacturing cost reduction.

## **Numerical methods**

### ***Finite element method (FEM)***

Amongst numerous numerical methods, FEM has received special interests for metal cutting simulation. FEM was first introduced in the 1960s, and has been widely used to analyze the tools design and forming processes (Sartkulvanich, 2007). When using FEM, it becomes possible to investigate the effects of process parameters (see Figure 1.17) on machining responses that are not measurable or extremely difficult to measure; including contact stresses on the rake face and flank face of the tool, cutting temperature at the tool-chip and tool-workpiece interfaces, chip temperature field, and sliding velocities between the chip and the tool. An adequate knowledge of these process parameters provides a better understanding of the cutting physics and may enable simulation of the cutting forces, tool temperature, stresses, chip formation and burr formation (Sartkulvanich, 2007). A comprehensive overview of reported works on FE modeling of burr formation will be presented in the following passages.

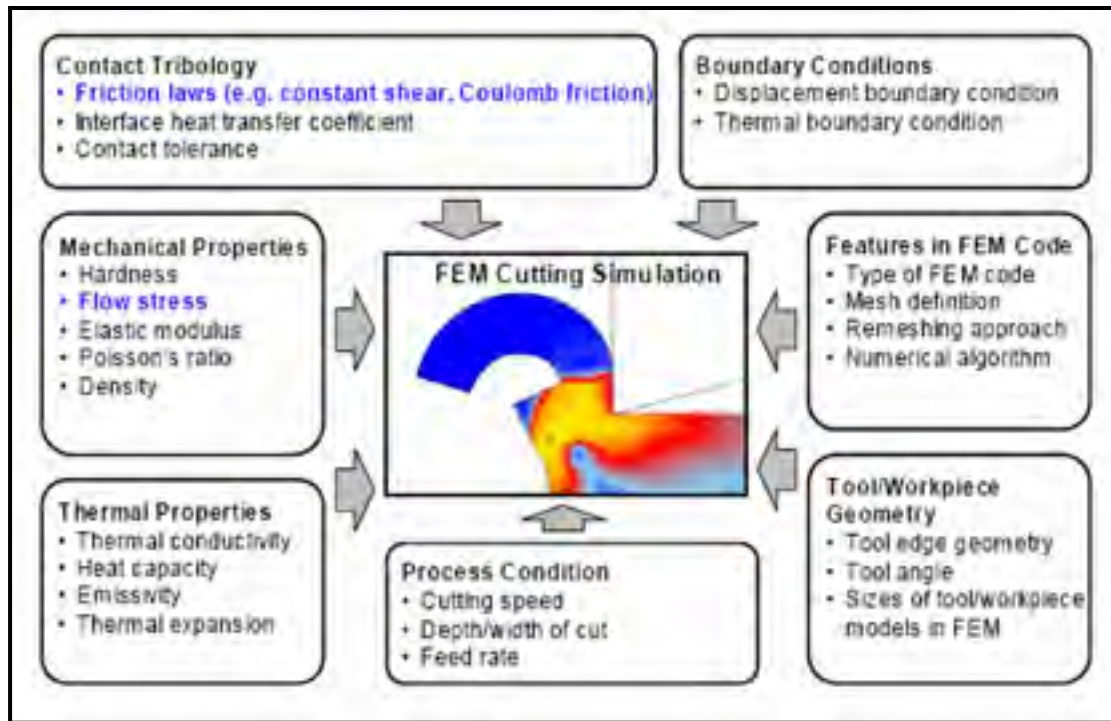


Figure 1.17 Major process parameters for FEM simulation of metal cutting (Sartkulvanich, 2007)

### ***FEM applications in milling burr formation modeling***

The main aim of numerical analysis (e.g. FEM simulation) of burr formation is burr minimization (Leopold and Wohlgemuth, 2010). According to (Chern, 1993), by introducing new models of material behavior under high strain rate, many aspects of FE models of metal cutting, including burr formation models have become more realistic (see Figure 1.18). Burr formation modeling using FEM was initiated in (Park, 2000a). The FEM code “*ABAQUS/Explicit*” and element-separation criterion were used for modeling approach. Furthermore, it was assumed that the tool and workpiece were rigid and plastic and the cutting tool is perfectly sharp. Park (2000a) then used FEM to determine the effects of exit angle, rake angle and backup materials on burr formation processes (Park, 2000b). Hashimura *et al.* (1999) developed a basic model of burr formation. It includes the influence of material properties in orthogonal cutting. The FEM-simulation confirmed experimental results using an elastic–plastic model with assumed plain strain condition.

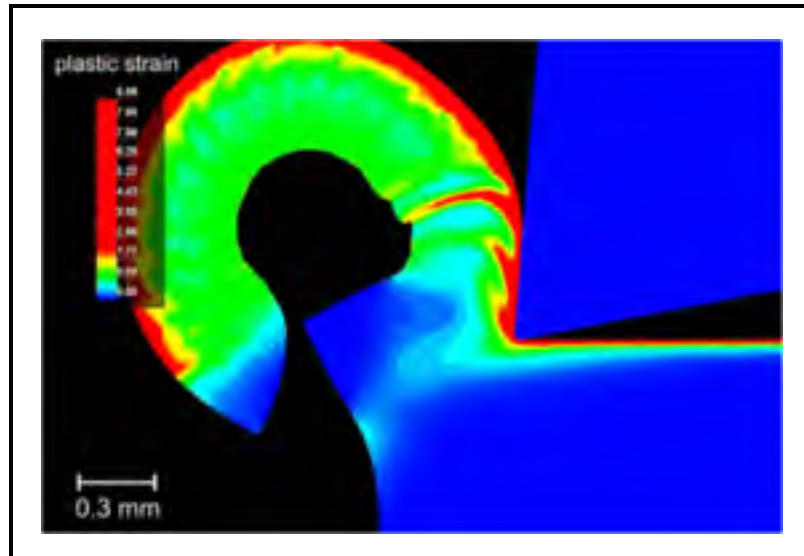


Figure 1.18 FEM simulation of burr formation in orthogonal cutting (Sartkulvanich, 2007)

A series of FEM simulation were performed to model the friction along the tool-chip interface and the interior of the cutting tool (Leopold and Wohlgemuth, 2010). It was found that the chip-tool contact length is influenced by friction coefficient and in comparison with previous investigations; the chip geometry is also influenced by friction. According to (Regel, Stoll and Leopold, 2009), a region of high negative hydrostatic pressure was observed in the transition from steady-state cutting operation to burr formation. Until now, the exact effects of hydrostatic pressure on burr formation are unknown. Chu *et al.* (2000) proposed a milling burr predicting system using burr control chart (burr predicting system). Klocke *et al.*(2004) presented 2D FE models of burr formation in orthogonal cutting using implicit Lagrangian codes. They found that the FE modeling of burr formation leads to satisfactory results and detailed information on distribution of stress, strain, strain rate and temperature. However, a part of simulation results did not correspond well with the experimental results. The modeled burrs size (thickness and height) are different as those measured experimentally. This was related to chip formation mechanism which largely influences experimental and modeling results.

One of the crucial inputs for FEM simulation of high speed machining processes is the availability of material plastic properties under that specific machining condition (*i.e.* flow stress as a function of strain, strain rate and temperature). Due to wide range of limitation imposed, except few reported works (Sartkulvanich, Sahlan and Altan, 2007; Soo, Aspinwall and Dewes, 2004a; 2004b), three-dimensional (3D) FE models of milling burr formation are rarely available (Leopold and Wohlgemuth, 2010). As described earlier, one of the main critics drawn against FEM is that the results obtained are relevant to the accuracy of input boundary conditions, which are not yet advanced and, therefore, are usually simplified. Previous FE models of burr formation in turning, drilling and non-traditional machining operations are listed in (Aurich *et al.*, 2009).

## **1.4 Optimization methods**

As mentioned earlier, amongst recent optimization methods, special interest has been paid to use of Taguchi method, RSM and desirability function. These optimization methods have been extensively studied and implemented in this thesis for simultaneous multiple response optimization in slot milling of aluminium alloys.

### **1.4.1 Taguchi method**

According to Taguchi's approach, quality is measured by deviation of a functional characteristic from its target value (Dhavamani and Alwarsamy, 2011). Noises (uncontrolled variables) can cause such deviations resulting in quality loss. The Taguchi method has been known as a powerful tool that differs from traditional practices (Phadke, 1989). It has been extensively employed in the optimization of milling parameters (Bagci and Aykut, 2006; Hou, Su and Liu, 2007; Moshat *et al.*, 2010; Nalbant, Gökkaya and Sur, 2007; Tsao, 2009; Zhang, Chen and Kirby, 2007). However, the original Taguchi method is designed to optimize a single performance characteristic (Gaitonde, Karnik and Davim, 2009), while except few works such as (Lee and Lee, 2003; Lin, 2002; Moshat *et al.*, 2010), optimization of multiple milling responses using Taguchi method has relatively received less attention,

particularly when dealing with burrs. This is due to several constraints that restrict the direct application of Taguchi method, as each performance characteristic may not have the same measurement unit. Hence, a limited number of modifications have been suggested so far (Kilickap, 2010). Therefore, proposing new modifications to application of Taguchi method for correct selection of optimum setting levels of process parameters and multiple responses optimization are truly recommended.

#### **1.4.2 Response surface methodology (RSM)**

Response surface methodology (RSM) is a collection of mathematical and statistical techniques for modeling and analyzing engineering problems. It has powerful applications in the design, development and formulation of new products (Myers, Montgomery and Anderson-Cook, 2009). In most of RSM problems, the relationship between the independent variables and the response(s) can not be formulated, thus it is approximated.

#### **1.4.3 Desirability function**

The desirability is one of the most frequently used technique for multiple responses optimization which was originally developed by Harrington (1965) and was later modified by Derringer (1980). It can be combined to form a composite desirability function, which converts a multiple responses problem into a single-response problem. The desirability lies between 0 and 1, and it represents the closeness of a response to its ideal value. If a response falls within the unacceptable intervals, the desirability is 0, and if a response falls within the ideal intervals, or the response reaches its ideal value, the desirability is 1. Meanwhile, when a response falls within the tolerance intervals but not the ideal interval, or when it fails to reach its ideal value, the desirability lies between 0 and 1. The more closely the response approaches the ideal intervals or ideal values, the closer the desirability is to 1.

Very limited studies reported the use of desirability function for multiple responses optimization in machining operations. A complete overview of desirability function will be presented in the chapter four.

## **1.5 Conclusion of literature review and refining of problematic**

In this chapter various aspects of machining burrs classifications and formation mechanisms were presented. The burr removal and measurement methods were analyzed. Furthermore, the milling burr formation mechanism, modeling approaches and factors governing burrs size were described.

This work has led us to conclude that:

- There is a substantial need to minimize, prevent and eliminate burrs. The main benefit is to reduce the needs of deburring operations. However, the use of deburring operations in some cases is mandatory.
- There is no general burr formation model that can be used for all machining operations. Amongst machining operations, milling process has a highly complex mechanism. Thus, more attention should be paid to understanding, control and optimization of milling burrs. Special concentration should be also paid to slot milling burrs which have a more complex mechanism than face milling burrs and have received less reported works.
- A few studies have focused on the influence of the cutting tool coating, dry high speed machining, and tool end nose radius ( $R_e$ ) on slot milling burr formation in oblique and orthogonal cutting schemes. In other words, it was revealed that the dominant cutting parameters on slot milling burr formation, size and location are still unclear. Therefore, extensive investigations to discover the factors governing slot milling burr formation are required to acquire a sufficient knowledge for burrs size minimization and eventually burr elimination.

- Very limited analytical models have been reported for burr size prediction. Most of existing analytical models are constructed based on experimentally measured parameters such as shear angle ( $\Phi$ ) and tool-chip contact length ( $L$ ). Furthermore, no analytical model was found to predict the slot milling burr size.
- FEM is the most prominent numerical method for burr formation modeling. However the FE results are relevant to the accuracy of applied input boundary conditions, which are not yet advanced and, therefore, are usually simplified. Further, the results are strongly influenced by the software applied; time-consuming and usually experimental data are required for model construction.
- Most of the existing research works in literature aim to measure and/or predict the burr height, while burr thickness could be used as a critical parameter for correct selection of desirable deburring techniques.
- No work has been reported in the literature to (1) solely present simultaneous optimization of burrs size of slot milled machined parts and (2) multiple responses optimization, including burrs size and other milling (face and slotting) performance characteristics, such as surface roughness and tool life.
- Amongst reported optimization techniques in literature, special attention has been paid to use of Taguchi method for correct selection of process parameters. However the original Taguchi method is designed to optimize a single response. Therefore, certain levels of modifications should be incorporated to Taguchi method for simultaneous multiple responses optimization.



## CHAPTER 2

### INVESTIGATION OF FACTORS GOVERNING SLOT MILLING BURR FORMATION

#### 2.1 Introduction

Burr formation and edge finishing are research topics with high relevance to industrial applications. To remove burrs, however, a secondary operation known as deburring is usually required. Until now more than 100 deburring methods have been developed (Gillespie, 1999), which their appropriate selection depends on many factors including, burr location and dimension. Among machining operations, milling burr formation has a more complex mechanism with multiple burrs formed at different locations with varying sizes. This yields to many difficulties during deburring process. Therefore, it is extremely beneficial to limit burr formation rather than deburring them in subsequent finishing operations. One approach is to develop analytical models of burr formation process. Since theoretical approaches are usually not available, more focus has been paid to experimental studies to identify the effects of cutting parameters on burr formation.

The effects of numerous process parameters on face milling burrs were reported in (Avila and Dornfeld, 2004; Chern, 1993; Hashimura, Hassamontr and Dornfeld, 1999; Kishimoto *et al.*, 1981; Kitajima *et al.*, 1990; Korkut and Donertas, 2007; Olvera and Barrow, 1996; Olvera and Barrow, 1998; Tsann-Rong, 2000). Furthermore, most of the existing research works in literature characterized the burr height, while from deburring perspective, the burr thickness is of interest, because it describes the time and method necessary for deburring a workpiece (Aurich *et al.*, 2009). In addition, only few studies have used statistical analysis to precisely determine the dominant process parameters on burrs size (Lekkala *et al.*, 2011; Mian, Driver and Mativenga, 2011a). As per author's knowledge, surprisingly except few works (Chen, Liu and Shen, 2006; Mian, Driver and Mativenga, 2011a; Tang *et al.*, 2011), very low volume of information is available about factors governing slot milling burrs.

In this chapter, the burrs formed on exit up milling side ( $B_1$ ), exit bottom ( $B_2$ ), top up/down milling sides ( $B_4, B_8$ ), and entrance down milling side ( $B_5$ ) will be investigated (see Figure 1.16). Statistical tools and experimental study in the form of multi-level full factorial design of experiment (see Table 2.1) are used to determine the dominant cutting parameters on burrs size (height and thickness) during slot milling of AA 2024-T351 and AA 6061-T6, which are commonly used materials in aeronautical and automotive industries.

The results presented in this chapter led to three scientific articles (two conferences and one journal), which their abstracts are shown in ANNEX (I-III). A complete overview of their contribution towards research objectives is discussed in chapter 5. The major contribution was accepted for publication in the *Institution of Mechanical Engineers (IMechE), Part B, Journal of Engineering Manufacture* in March 2013.

## **2.2 Experimental procedure**

### **2.2.1 Experimental plan**

A multi-level full factorial design of experiment ( $3^3 \times 2^2$ ) is selected in this study. The AA 6061-T6 and AA 2024-T351 with relatively similar mechanical properties are used for experiments (see Table 2.2). The experimental factors and their levels are shown in Table 2.1. Cutting tool and workpiece materials were treated as qualitative factors while other remaining factors were considered quantitative. In total, 108 experiments were performed under dry milling using a 3-axis CNC machine tool (Power: 50kW, Speed: 28000 rpm; Torque: 50 Nm), as shown in Figure 2.1(a). An Iscar coated end milling cutting tool (E90-A-D.75-W.75-M) with three flutes ( $Z=3$ ), and tool diameter ( $D$ ) 19.05mm was used (see Figure 2.1(b)). With respect to cutting conditions used, the suitable inserts were consequently used in cutting tests.

Table 2.1 Experimental process parameters and their levels

Experimental parameters		Level		
		1	2	3
A: Material		AA 6061-T6	-	AA 2024-T351
B: Tool	<i>Coating</i>	TiCN	TiAlN	TiCN+Al <sub>2</sub> O <sub>3</sub> +TiN
	<i>Insert nose radius, Rε (mm)</i>	0.5	0.83	0.5
C: Depth of cut (mm)		1	-	2
D: Feed per tooth (mm/z)		0.01	0.055	0.1
E: Cutting speed (m/min)		300	750	1200



Figure 2.1 Experimental devices: (a) 3-Axis CNC machine (b) Cutting tool used

Table 2.2 Mechanical properties of studied aluminium alloys  
(Committee and Knovel, 2004)

Material	Mechanical Properties		
	Brinell Hardness	Yield Strength	Elongation at Break
AA 6061- T6	95 HB	275 MPa	17 (%)
AA 2024- T351	120 HB	325 MPa	20 (%)

### 2.2.2 Experimental observations

#### Burr size

An optical microscope (see Figure 2.2) equipped with high resolution camera was used to take the burrs images. The burr size measurements were then conducted on captured images. To measure the burr height, the microscope was focused on the plane of the workpiece exit surface and then on the plane of the top surface of the burr. Focusing on the plane of the parent material, burr thickness image was captured. An average of four burr thickness ( $B_t$ ) readings and maximum value of burr height ( $B_h$ ) were taken as the burr size in the following sections.



Figure 2.2 Optical microscope used for burr size measurement

Surface roughness measurements were conducted on a profilometer Mitutoyo SJ 400 (see Figure 2.3), which was connected to a data acquisition system. The following setting parameters were used:

Measuring length: 204 mm, range: 800 microns, speed: 1 mm/s, number of points: 4800.

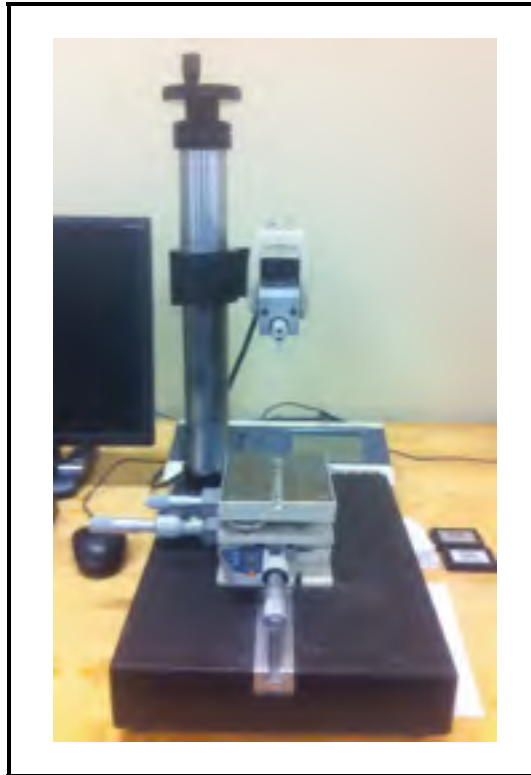


Figure 2.3 Profilometer used for surface roughness measurement

### **Cutting force**

A 3-axis dynamometer (Kistler-9255B) was used for cutting force signals acquisition. According to cutting conditions used, the directional cutting forces were analyzed and calculated using sampling frequencies of 10 KHz and 24 KHz. Cutting forces in normal ( $F_y$ ), feed ( $F_x$ ) and axial directions ( $F_z$ ) were then computed (see Figure 2.4). Tangential force ( $F_t$ ) was also measured through directional cutting forces.

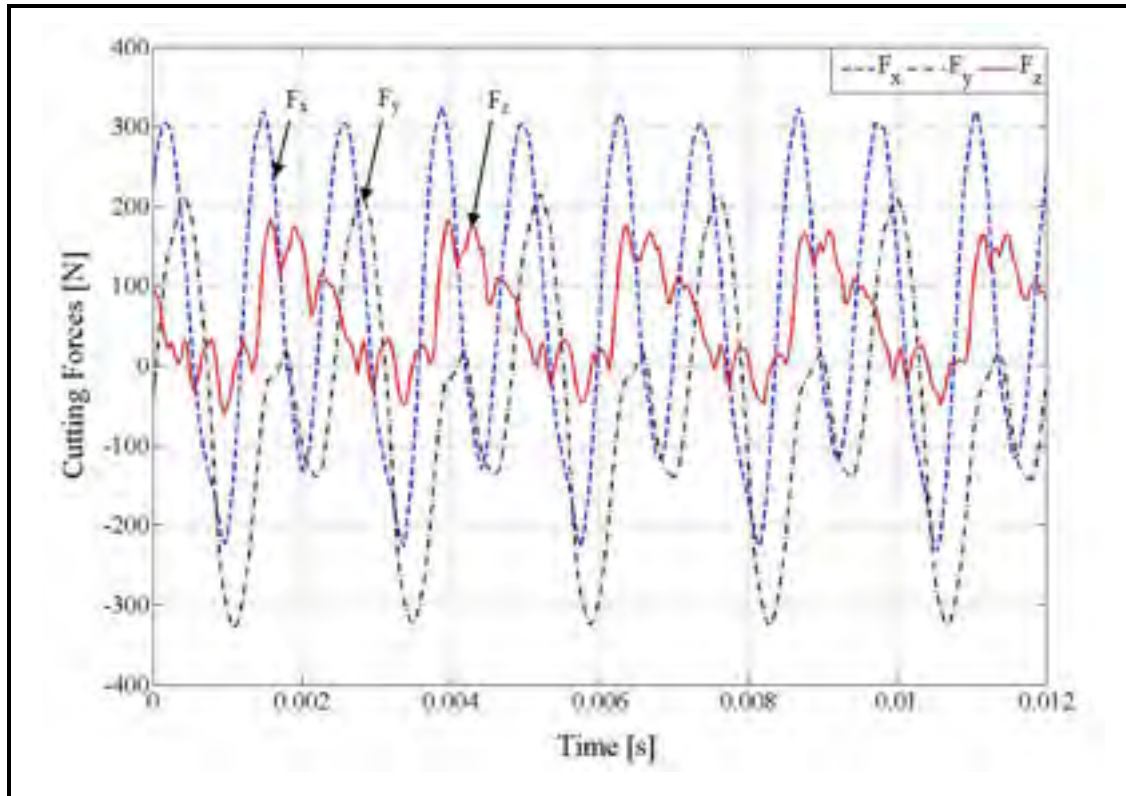


Figure 2.4 Cutting forces in normal, axial and feed directions

### 2.2.3 Assumptions

It must be noted that machining of aluminium alloys can not be carried out without a certain amount of difficulty. These materials tend to adhere to the tool surface, and burrs are formed inside the holes and at the top of machined part edges (Songmene V., Khettabi and Kouam, 2012). Therefore to develop the experimental set-up, the following assumptions are made:

- The slot milling operations are assumed chatter free. Vibrations, machine and tool dynamic behavior are not considered. This condition was fulfilled by carrying out preliminary tests and checking the stability of cutting process.
- The deflections of the tool and workpiece are assumed negligible. This condition was fulfilled using rigid tools and workpiece fixtures.
- After each cutting test, new inserts were used to avoid possible deviations in experimental results due to tool wear.

- It is to note that the similar assumptions were used in other sections of this thesis.

## 2.3 Results and discussion

### 2.3.1 Method of analysis

In analyzing the machined parts quality index (e.g. burr size, surface roughness), the use of statistical techniques plays a prominent role (Kilickap, 2010).

The following terms and techniques are used in this thesis for statistical analysis:

1. *ANOVA*: The analysis of variance (ANOVA) allows an examination of the main effects of independent variables and their interaction effects to determine their combined effects on the responses at 95% confidence interval (CI). The following statistical terms are used for results analysis:
  - ❖ *P-value*: The probability (ranging from zero to one) that the results observed in a study (or results more extreme) could have occurred by chance;
    - If  $P\text{-value} > 0.10$ , the parameter is insignificant
    - If  $0.05 \leq P\text{-value} \leq 0.10$ , the parameter is mildly significant
    - If  $P\text{-value} < 0.05$ , the parameter is significant
    - The coefficient of determination ( $R^2$ ) provides a measure of variability in the observed response values and can be explained by the controllable factors and their interactions. If  $R^2$  is greater than 75%, the predicted model is thought to be *sensitive* to variation of process variables. If not, the model is considered as *insignificant*.
    - $R^2_{\text{adj}}$  is more suitable for comparing models with different numbers of independent variables. Unlike  $R^2$ , the  $R^2_{\text{adj}}$  increases only if the new term improves the model more than would be expected.  $R^2_{\text{adj}}$  can be negative and is always smaller than or equal to  $R^2$ .

2. *Pareto analysis*: A Pareto chart compares the relative importance and statistical significance of the main and interaction effects between process parameters. This chart identifies influential factors in order of decreasing contribution.
3. *Main effect plot*: The analysis of means (ANOM) is used to determine the optimal cutting conditions by estimating the effect of each parameter on response, which is presented in the main effect plot diagram (Phadke, 1989).
4. *Interaction effects analysis*: Presents the interaction effects between process parameters.

The similar method of analysis is used in the following sections of this thesis.

### **2.3.2 Effects of process parameters on slot milling burrs**

Burrs can be excessively large and irregular (see Figure 2.5(a)) or very small in size, even not visible for naked eyes (see Figure 2.5(b)). Therefore, a proper understating of burr formation mechanism and correct selection of cutting parameters setting levels is recommended to reduce the incidence of burr formation and possibly surface quality and tool life improvement. In the following sections, burr formation over top, entrance and exit sides of slot milled parts will be extensively studied.

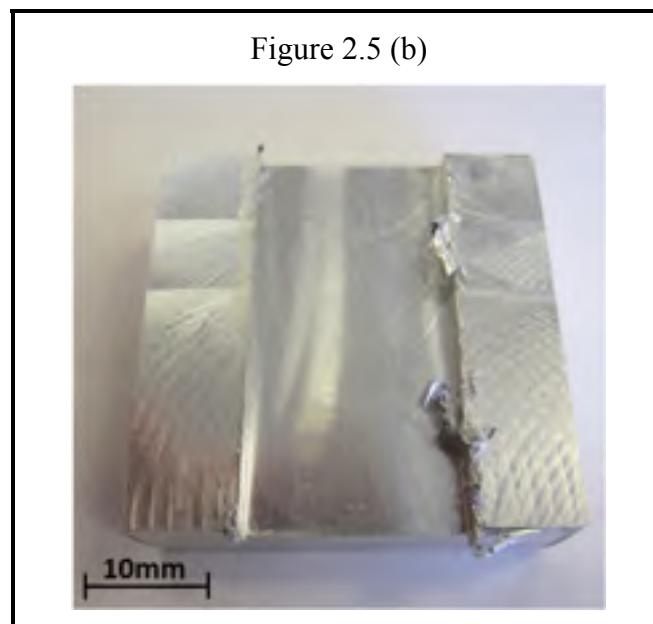
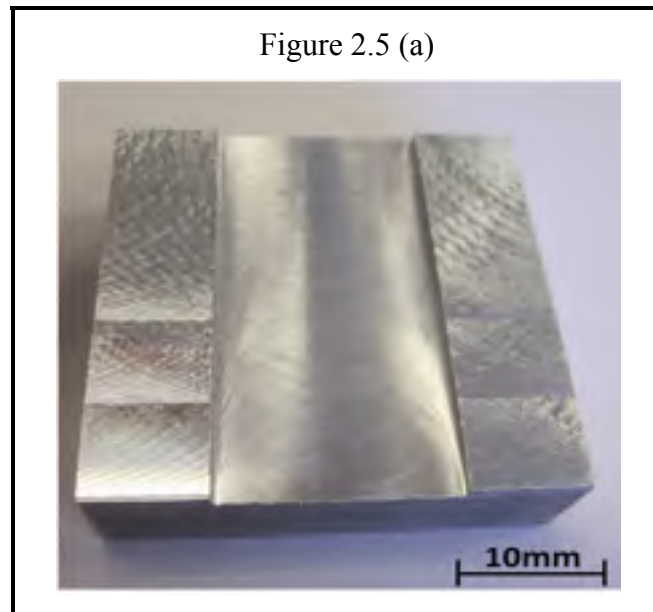


Figure 2.5 Slot milled machined parts with (a) burr formation with tiny scales; (b) large burr formation

### Exit burrs

Figures 2.6-2.7 present standardized Pareto charts of exit burrs. As can be seen in Figure 2.6(a),  $B_1$  height is influenced by interaction effects between cutting tool- depth of cut (BC),

depth of cut-feed per tooth (CD), feed per tooth-cutting speed (DE) and depth of cut-cutting speed (CE), followed by direct effects of feed per tooth (D), material properties (A) and depth of cut (C). According to (Lauderbaugh, 2009), yield strength ( $\sigma_e$ ) is the main material property with significant effects on exit burr formation. As presented in Figure 2.6(b), there are several direct and interaction effects between cutting parameters that affect the variation of  $B_1$  thickness. Amongst, direct effects of feed per tooth (D), depth of cut (C) and tool (B) are the most dominant factors. According to Figure 2.7(a), the  $B_2$  height is affected by direct effects of depth of cut (C), cutting speed (E) and tool (B), caused by tool coating and insert nose radius ( $R_e$ ). The interaction effects of depth of cut-cutting speed (CE) and cutting speeds (EE) are also significant parameters on variation of  $B_2$  height. Contrary, based on Figure 2.7(b), the governing factors on  $B_2$  thickness are direct effects of depth of cut (C) and tool (B), followed by interaction effects between depth of cut- cutting speed (CE). As illustrated in Figures 2.8-2.9, milling tests with higher levels of feed per tooth and depth of cut and smaller insert nose radius ( $R_e$ ) yield to longer and thicker  $B_1$  and shorter and thinner  $B_2$ . As it is evident from Figure 2.8, variation of cutting process parameters has similar influences on  $B_1$  height and thickness.

In metal cutting, feed per tooth, depth of cut, cutting speed and tool geometry are the main controlling parameters (Korkut and Donertas, 2007). In order to comfort deburring operation, milling burr size minimization can be conducted by facilitating the transition of primary burrs to secondary burrs. This phenomenon may occur when the burr leans towards the transition material and breaks off from the machined surface. In such a case, side burrs formed instead of exit bottom ( $B_2$ ) or entrance bottom ( $B_6$ ) burrs. According to face milling burr formation mechanism, exit bottom burr ( $B_2$ ) is formed by loss of material from the exit up milling side ( $B_1$ ) burr (AM De Souza *et al.*, 2003). Assuming similar burr formation mechanism in exit side of face milling and slot milling operations, transition from primary to secondary burr formation is observed on the exit burrs along up/down milling sides ( $B_1$  and  $B_3$ ). When Transition from primary to secondary burr formation is not correctly done, primary exit bottom burr ( $B_2$ ) appear in the exit side when tool leaves the machined part (see Figure 2.10(a)). When burr smoothly leans towards the transition material and breaks off from the

machined surface, then longer  $B_1$  and shorter  $B_2$  is resulted (see Figure 2.10(b)). According to slot milling burr formation mechanism and by considering a negligible  $B_3$  size, it can be stated that trials to reduce the  $B_2$  size led to longer  $B_1$  (see Figures 2.8-2.9).

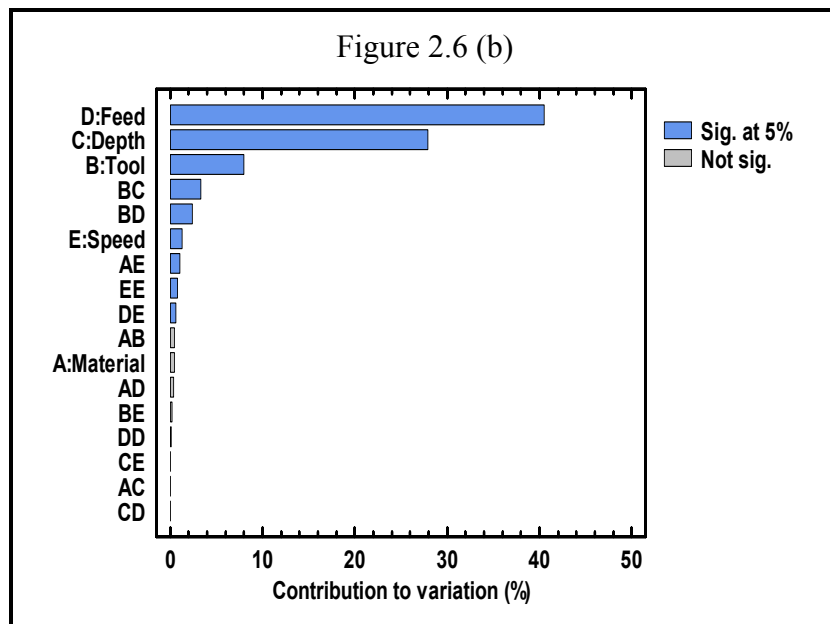
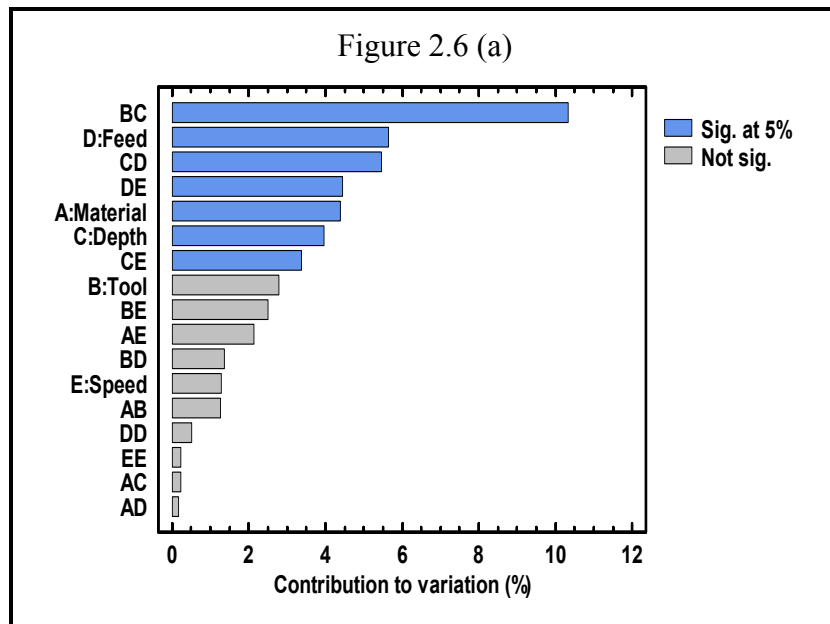


Figure 2.6 Pareto chart of (a)  $B_1$  height, (b)  $B_1$  thickness

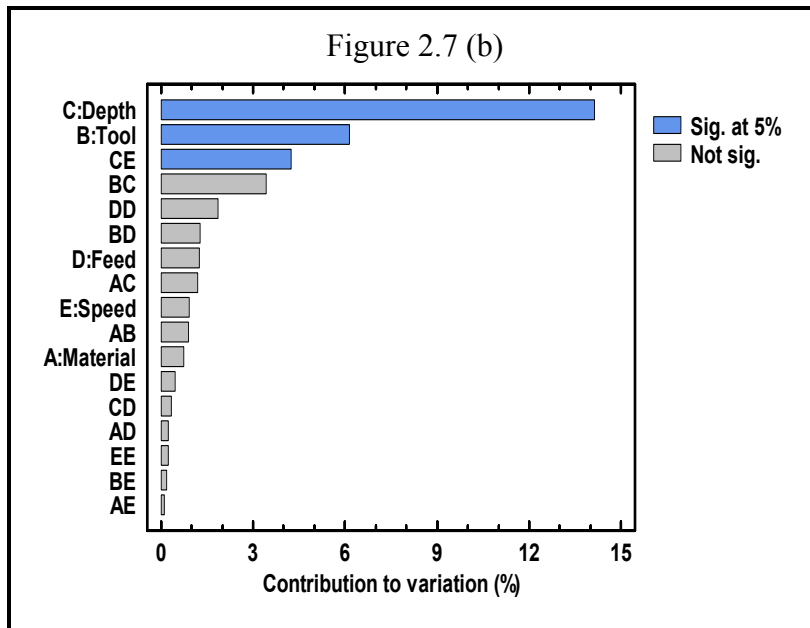
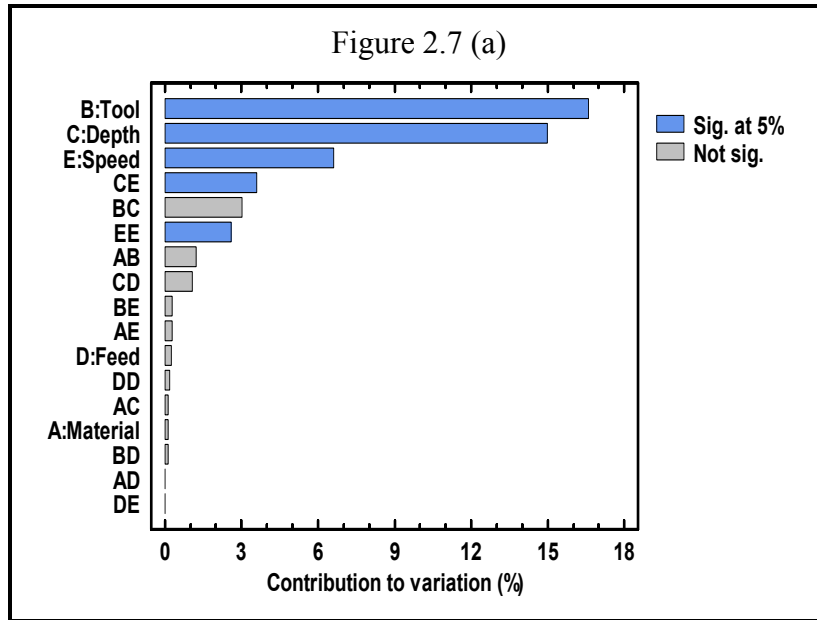


Figure 2.7 Pareto chart of (a) B<sub>2</sub> height, (b) B<sub>2</sub> thickness

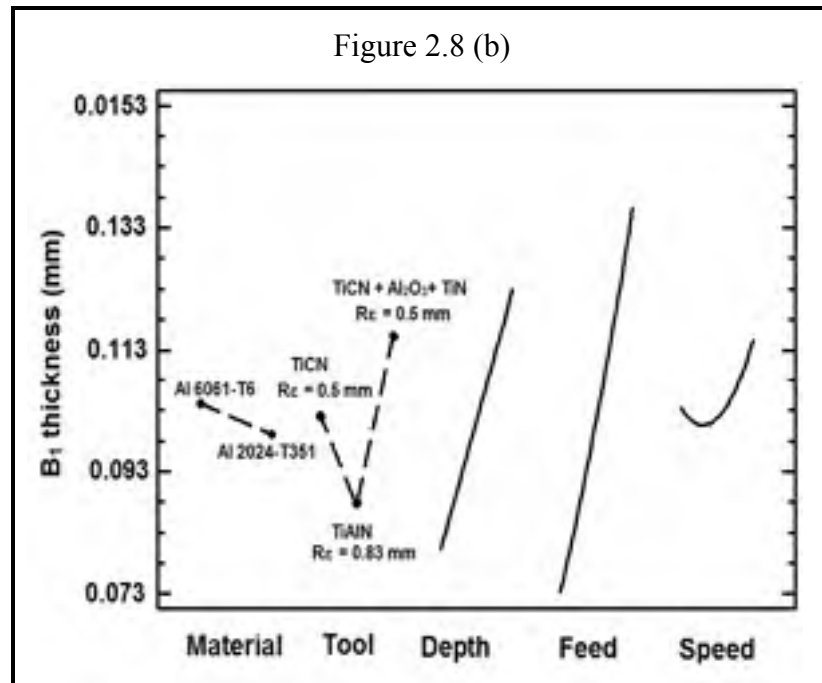
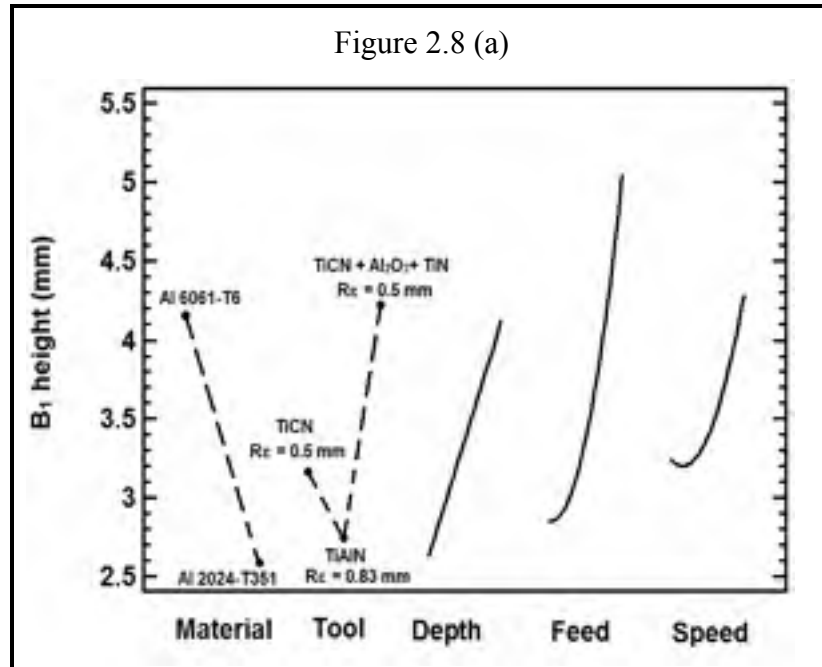


Figure 2.8 Direct effect plot of (a)  $B_1$  height, (b)  $B_1$  thickness

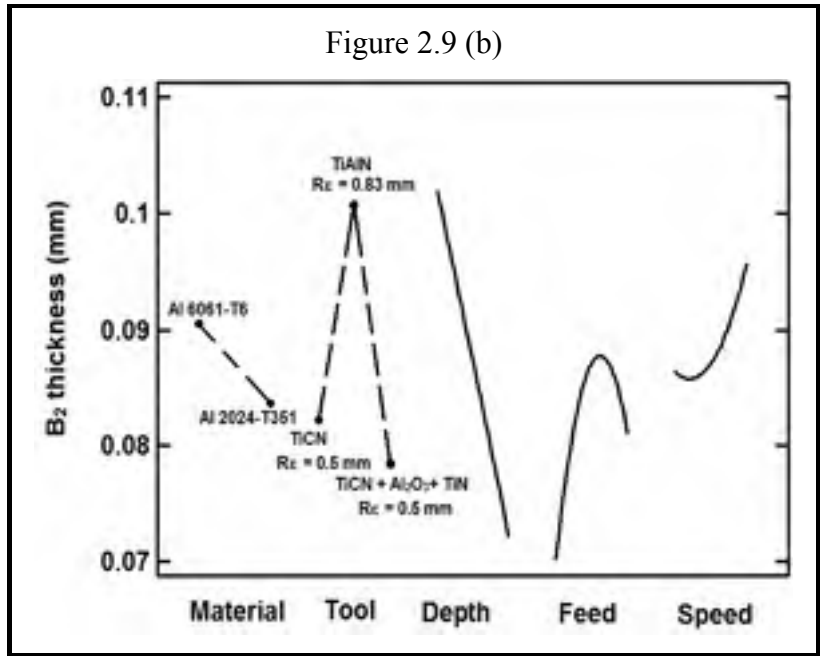
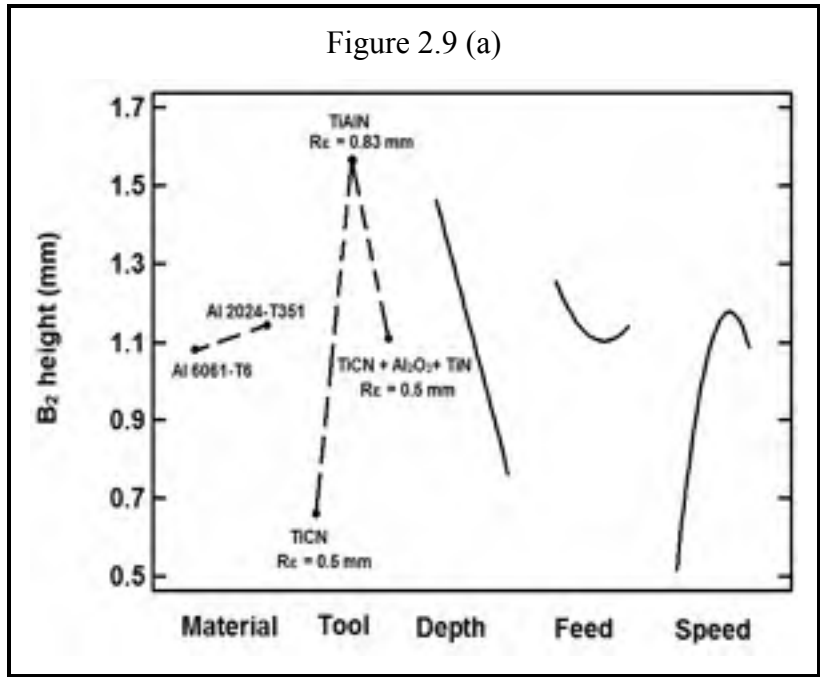


Figure 2.9 Direct effect plot of (a) B<sub>2</sub> height, (b) B<sub>2</sub> thickness

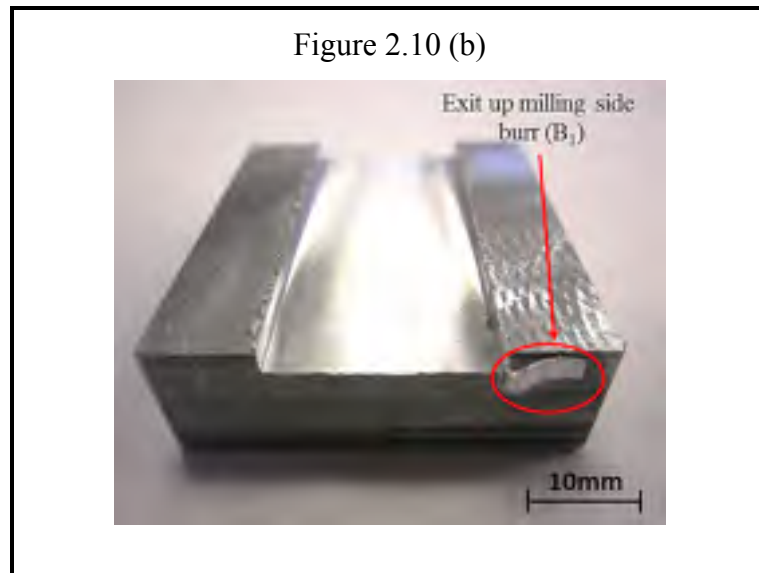
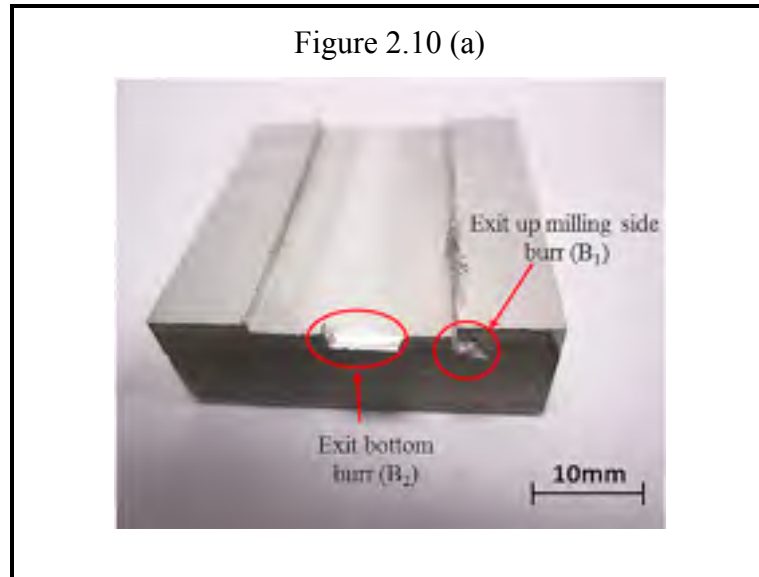


Figure 2.10 Slot milling exit burrs

The first considerations of burr formation in metal cutting came along with investigations about chip formation, as burr formation mechanism highly depends on chip formation mechanism. In milling operation, the chip thickness  $h(\varphi)$  varies periodically as a function of time-varying immersion angle ( $\varphi$ ) as:

$$h(\varphi) = f_z \times \sin(\varphi) \quad (2.1)$$

Where  $f_z$  is feed per tooth which can be presented as follows:

$$f_z = Z \times f_r \quad (2.2)$$

Where  $f_r$  is feed rate and  $Z$  is the tool teeth number.

Tangential force  $F_t(\varphi)$ , radial force  $F_r(\varphi)$  and axial force  $F_a(\varphi)$  can be represented by using the specific cutting force coefficients  $K$  in each direction as follows:

$$\begin{aligned} F_t(\varphi) &= K_{tc}ah(\varphi) + K_{te}a_p \\ F_r(\varphi) &= K_{rc}ah(\varphi) + K_{re}a_p \\ F_a(\varphi) &= K_{ac}ah(\varphi) + K_{ae}a_p \end{aligned} \quad (2.3)$$

Where  $a_p$  is depth of cut.

The coefficients  $K_{tc}$ ,  $K_{rc}$  and  $K_{ac}$  are the directional specific cutting force coefficients, respectively. The  $K_{te}$ ,  $K_{re}$  and  $K_{ae}$  are the specific edge cutting force coefficients. According to Eqs(2.1-2.3), increase in feed per tooth and depth of cut increases directional forces. However when tool leaves the workpiece in slot milling, the magnitude of tangential force  $F_t$  is greater than radial force  $F_r$ . In addition, a significant role is played by friction in milling burr formation in exit side, which is a function of  $F_t$  and  $F_r$ . The effects of friction can be divided to three basic mechanisms, one due to asperity deformation, one due to adhesion and one due to particle ploughing.

In orthogonal milling, friction coefficient ( $\mu$ ) can be approximated as (San-Juan, Martín and Santos, 2010):

$$\mu = \tan(\varphi) = F_r \times F_t^{-1} \quad (2.4)$$

According to Eq(2.4), when the friction at tool faces decreases, there is a corresponding increase in the shear angle ( $\Phi$ ) and accompanying decrease in the chip thickness  $h(\phi)$ . Thus, the plastic strain associated with chip formation is reduced. This results to longer and thicker  $B_2$  and shorter and thinner  $B_1$ .

Increase the cutting speed and insert nose radius ( $R\epsilon$ ) increase the  $F_r$  to a large extent, particularly where the depth of cut is smaller than the insert nose radius ( $R\epsilon$ ). In addition, materials with higher machinability generate larger  $F_r$ , which may lead to a reduction in friction occurred between the chip and tool (San-Juan, Martín and Santos, 2010). Furthermore, during milling operation, slight plastic deformation, serious rubbing and ploughing effects appear which therefore yield to heat generation and increase in the burr size, especially during high speed machining. When using tools with multiple teeth, some heat is produced, particularly during high speed machining. This yields to tearing off a part of the burr that accumulated on the top side of the workpiece. This part finally sticks to the side face of the machined part, and consequently turns to a burr. However, as depicted in Figures 2.6-2.7, cutting speed has statistically negligible influence on slot milling exit burrs. Because of yield strength, which is higher in AA 2024-T351 than in AA 6061-T6, a thinner and shorter exit up milling side burr ( $B_1$ ) is obtained for AA 6061-T6 under similar cutting conditions.

The interaction effects of cutting parameters on exit burrs dimensions are presented in Figures 2.11-2.12. As clearly shown in Figure 2.11(a), under lower levels of depth of cut, the longest and shortest  $B_1$  are obtained when using tool 3 and tool 2, respectively. In this cutting condition, a large difference between resulting values of  $B_1$  height is observable, when using different cutting tools. When changing the depth of cut to higher level (2mm), the longest  $B_1$  is obtained when using tool 2. In this case, the  $B_1$  height does not highly vary when using cutting tools with various insert nose radius and cutting tool coating. This exhibits strong interaction effects between tool and depth of cut. Similarly at higher level of depth of cut, similar  $B_1$  thickness could be obtained when using tools 1-2. However, at lower level of depth of cut (1 mm), a significant difference between resulting values of  $B_1$  thickness is

observed when using the same cutting tools (see Figure 2.11(b)). This exhibits that  $B_1$  size is highly influenced by interaction effects between tool and depth of cut (BC). As shown in Figures 2.8-2.9, larger and thicker  $B_1$  and shorter  $B_2$  are observed when changing the cutting tool 1 (TiCN,  $R\epsilon = 0.5$  mm) to tool 3 (TiCN+Al<sub>2</sub>O<sub>3</sub>+TiN,  $R\epsilon = 0.5$  mm). Considering the similar insert nose radius ( $R\epsilon$ ) in both tools, this difference corresponds to effect of tool coating on exit burrs size. This finding is in contrast with the conclusion made in (Olvera and Barrow, 1996), stating negligible influence of tool coating on face milling burrs.

According to Figure 2.12, milling tests at higher level of depth of cut and fixed cutting speed generate thinner and shorter  $B_2$ . In the fixed depth of cut 1mm, thinner  $B_2$  appears when using higher level of cutting speed. However, when changing the depth of cut to 2mm, the thinner  $B_2$  formed at higher cutting speed. This indicates strong interactions effects between cutting speed and depth of cut, which significantly influence the  $B_2$  dimension.

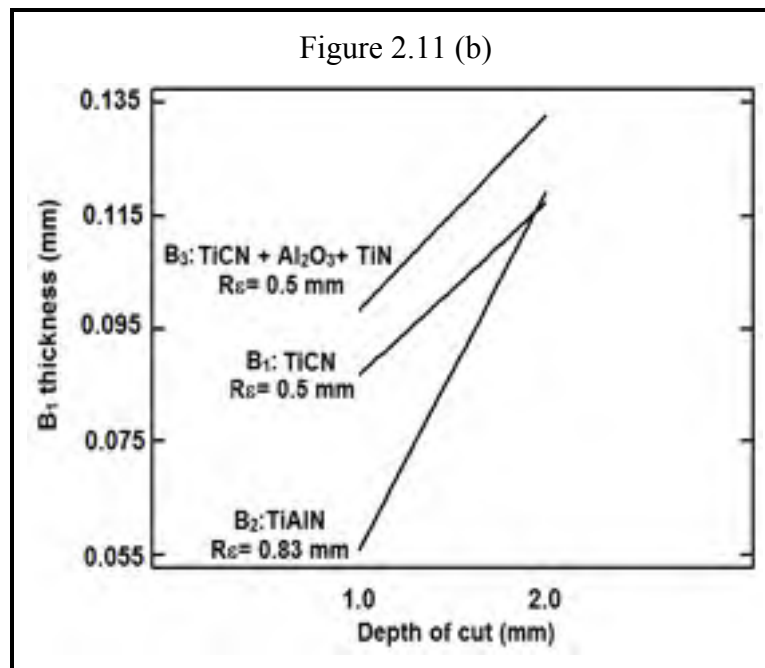
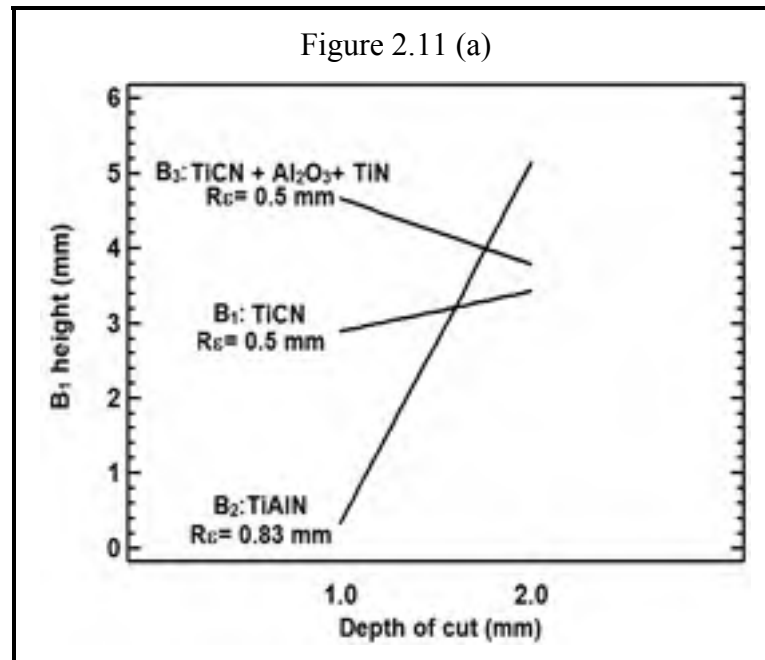


Figure 2.11 Interaction effect of tool - depth of cut (BC) on  
(a) B<sub>1</sub> height and (b) on B<sub>1</sub> thickness

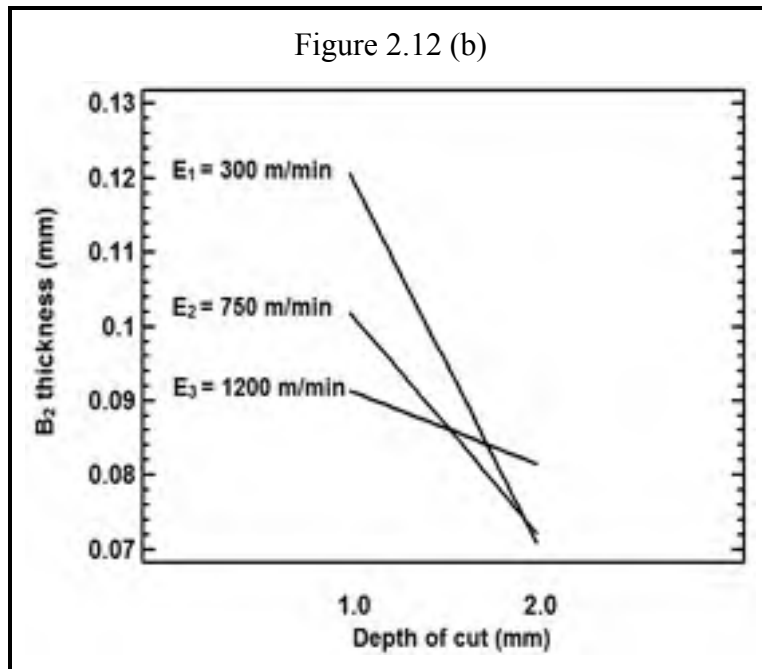
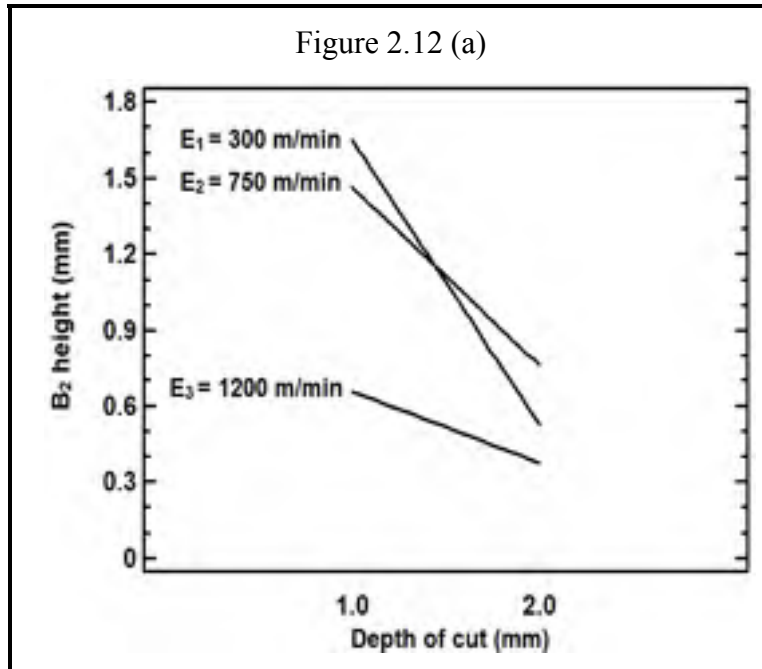


Figure 2.12 Interaction effect of depth of cut-cutting speed (CE) on  
(a) B<sub>2</sub> height and (b) B<sub>2</sub> thickness

### Entrance side burr

The entrance side burr along down milling ( $B_5$ ) is formed following a rollover process, when bending the chip is easier than cutting it or fracturing the workpiece edge. According to Figure 2.13(a),  $B_5$  height is dominated by direct effects of feed per tooth (D), material properties (A), depth of cut (C) and interaction effects between depth of cut-feed per tooth (CD), material properties-feed per tooth (AD) and cutting speeds (EE). The tool coating and insert nose radius ( $R\epsilon$ ) have negligible effects on  $B_5$  height. As can be seen in Figure 2.13(b), direct effects of tool (B) and feed per tooth (D) are dominant parameters on variation of  $B_5$  thickness. Figure 2.13 clearly shows that cutting speed (E) has insignificant influence on  $B_5$  size.

It is believed that during cutting operations with high engagements between cutting tool flutes and machined parts (e.g. milling), larger burr formation is anticipated. This is mainly caused by a change in the plastic zone size in the transition material ahead of the tool. In both milling and orthogonal cutting operations, tool exit creates forward flow of materials. Conversely, tool entrance induces the backward flow of material during orthogonal cutting. However during milling of ductile materials such as aluminium alloys, tool entrance induces the forward flow of material. As a result, generated entrance burrs are not necessarily smaller than exit burrs (Avila and Dornfeld, 2004).

As similar as exit burrs, in order to comfort deburring operation, entrance burrs minimization can be conducted by facilitating the transition of primary burrs to secondary burrs. In this case, entrance side burrs along up/down milling sides ( $B_5$  and  $B_7$ ) are formed instead of large entrance bottom burrs ( $B_6$ ). Increase in the depth of cut reduces the incidence of primary entrance bottom burr formation. Instead, longer and shorter entrance side burrs generated (Figure 2.14). However, the maximum depth of cut is limited to stock material left during the roughing or semi finishing process requirements and also minimum depth of cut demanded to suppress the chatter vibration. As can be seen in Figure 2.14, cutting tests on AA 2024-T351 (more ductile than AA 6601-T6) led to shorter and thinner  $B_5$  than those generated in AA

6061-T6. It is inferred that in ductile materials, larger primary entrance bottom burr ( $B_6$ ) and smaller entrance side burr ( $B_7$  and  $B_5$ ) are more likely to be formed. Furthermore, larger feed per tooth generates shorter and thicker  $B_5$

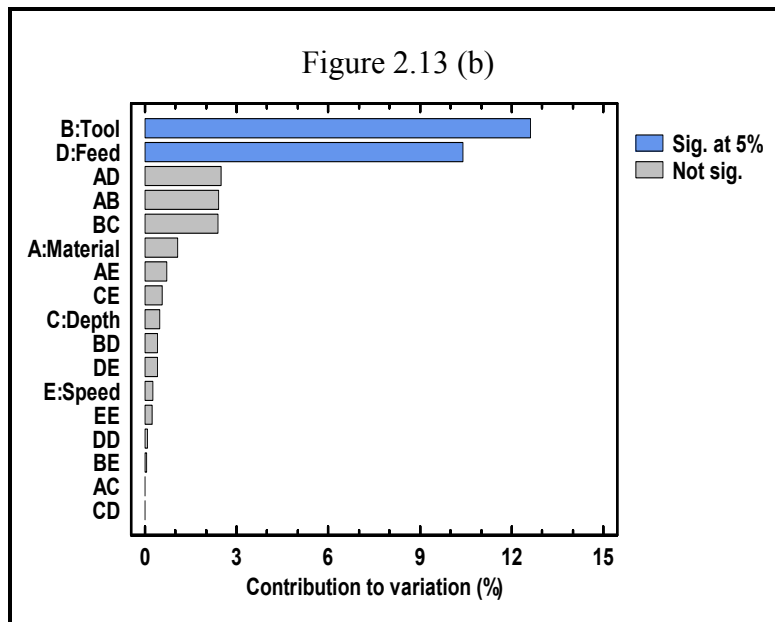
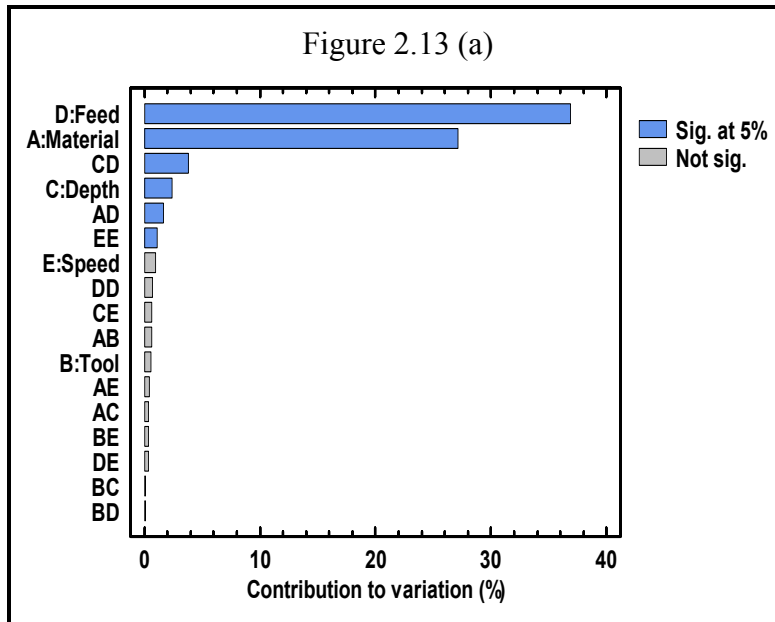


Figure 2.13 Pareto chart of (a)  $B_5$  height, (b)  $B_5$  thickness



which have a tendency to form through the longitudinal direction (see Figure 2.15). According to Figure 2.16(b), the most dominant parameters on  $B_4$  thickness are direct effects of feed per tooth (D), tool (B) and material properties (A). However based on Figure 2.16(a),  $B_4$  height can be controlled by direct effects of tool (B), material properties (A), depth of cut (C) and interaction effects AD, AE, EE, and DD. In addition, based on Figure 2.17,  $B_8$  height is mainly influenced by direct effects of feed per tooth (D) and material properties (A), while  $B_8$  thickness is influenced by interaction effects of tool-cutting speed (BE), material-tool (AB) and material-cutting speed (AE). It could be inferred that the dominant interaction effects on top burrs height are statistically insignificant parameters on top burrs thickness. In other words, top burrs thickness and height are dominated by different cutting parameters. In addition, the use of optimum setting levels of process parameters as shown in Figures 2.18-2.19 led to thicker top burrs in AA 2024-T351 and longer top burrs in AA 6061-T6.

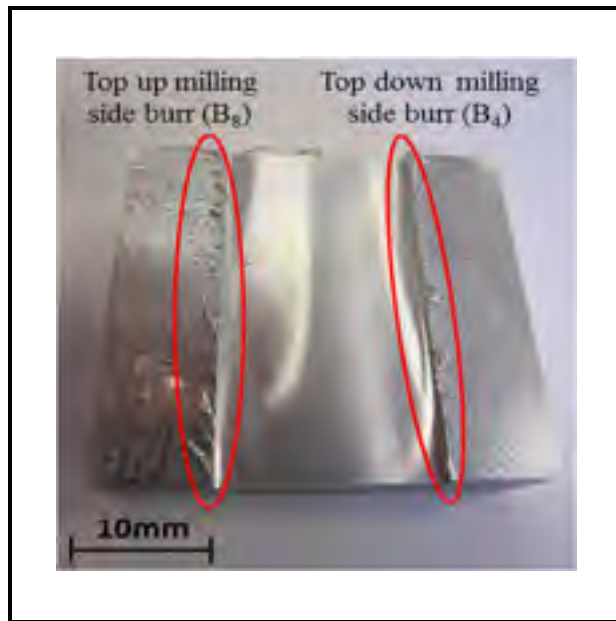


Figure 2.15 Slot milling top burrs

The cutting tests with tool 2 (TiAlN,  $R\epsilon = 0.83$  mm) led to thinner and shorter  $B_4$  and shorter  $B_8$ . According to Figures 2.18-2.19, changing the cutting tool 3 (TiCN+Al<sub>2</sub>O<sub>3</sub>+TiN,  $R\epsilon = 0.5$  mm) to cutting tool 1 (TiCN,  $R\epsilon = 0.5$  mm) generates shorter top burrs. This

exhibits the significant influence of tool coating on top burrs, as similar as exit burrs ( $B_1$  and  $B_2$ ) and entrance down milling burr ( $B_5$ ).

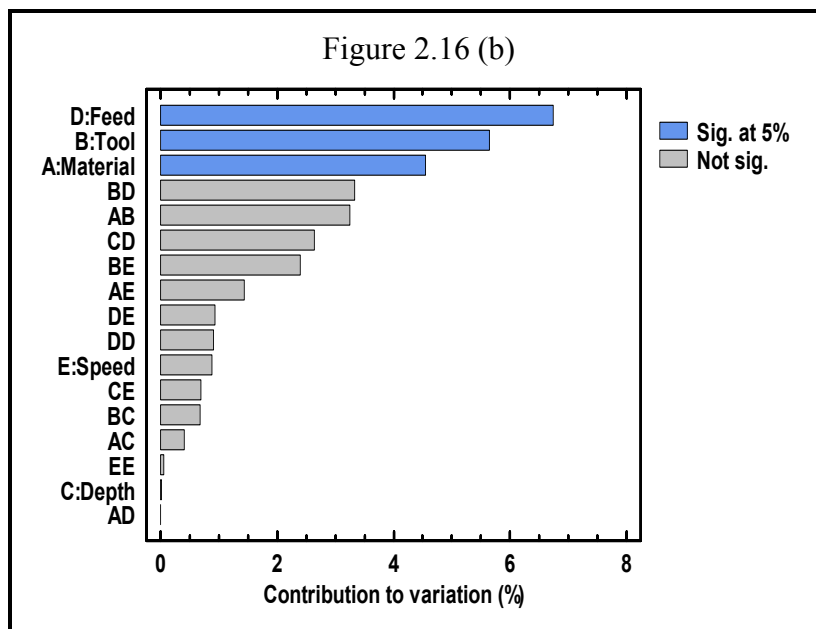
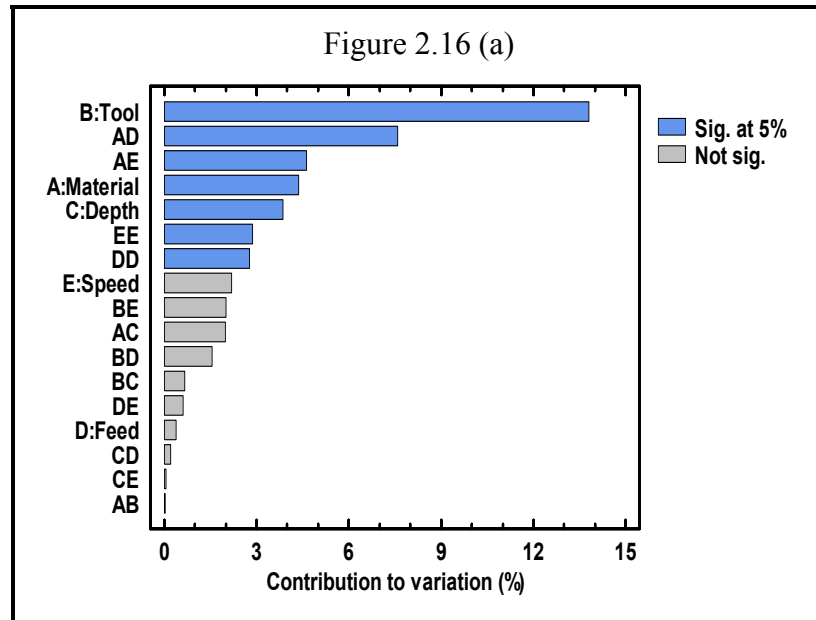


Figure 2.16 Pareto chart of (a)  $B_4$  height, (b)  $B_4$  thickness

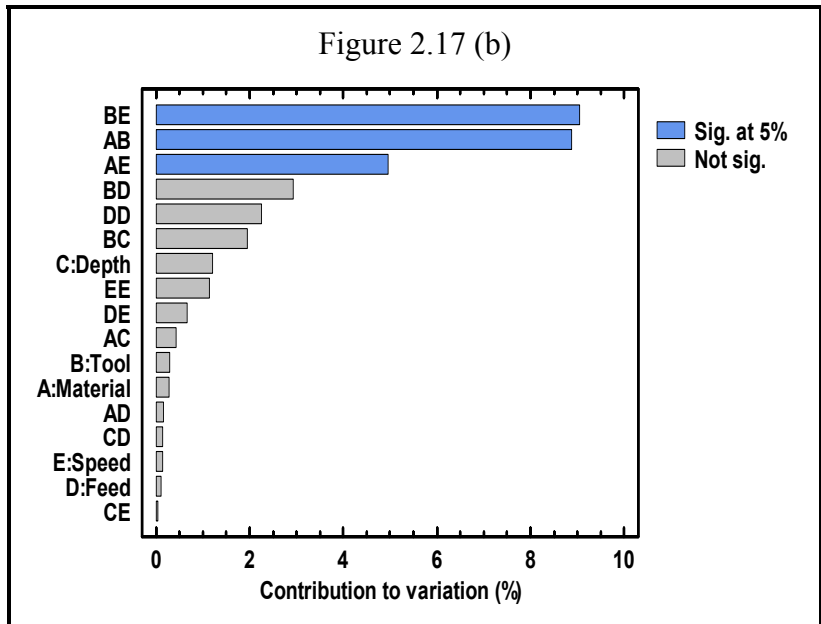
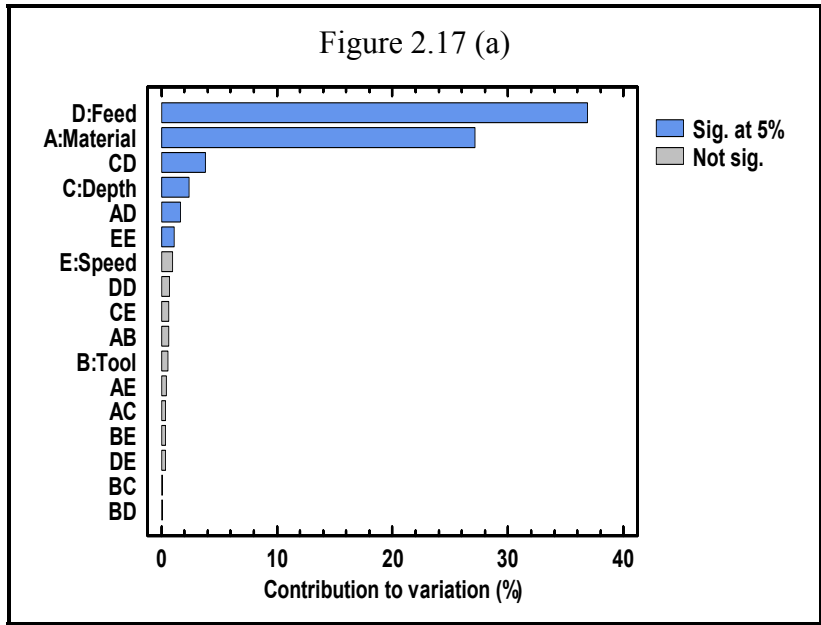


Figure 2.17 Pareto chart of (a) B<sub>8</sub> height, (b) B<sub>8</sub> thickness

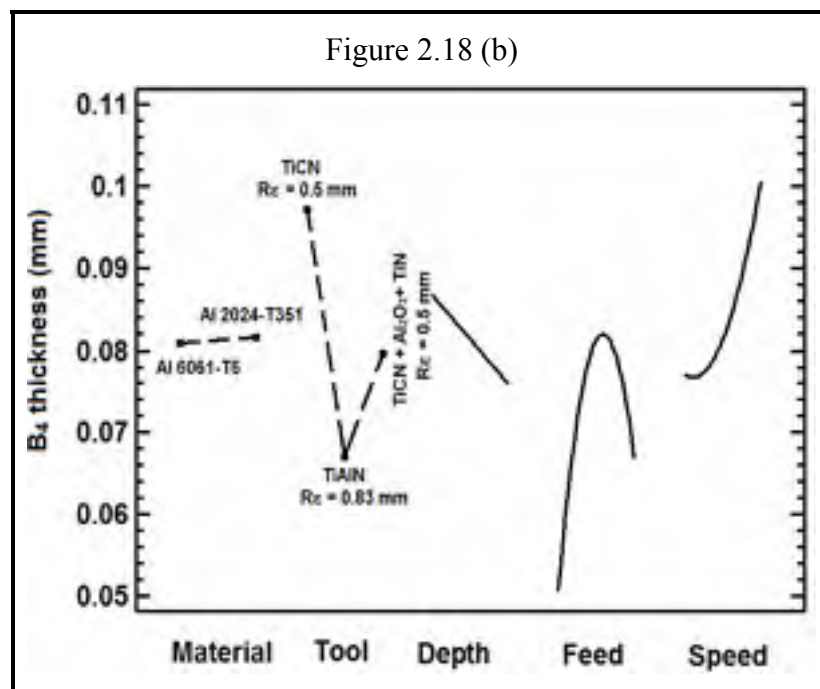
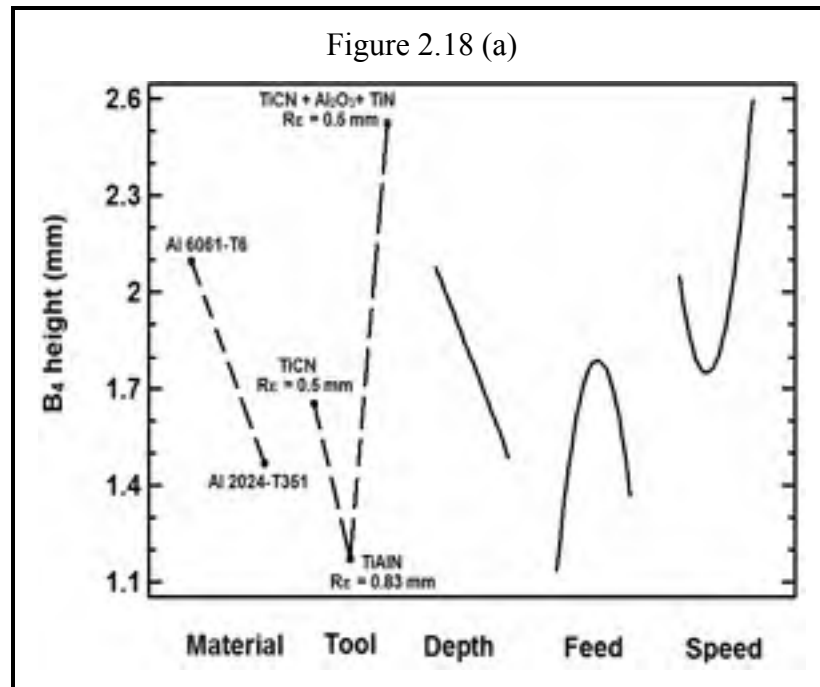


Figure 2.18 Direct effect plot of (a) B<sub>4</sub> height, (b) B<sub>4</sub> thickness

When using high speed machining, high temperature is generated on chip-tool contact area. As a result, when tool leaves the workpiece after each feeding motion, small chips

(fragments) stick to the machined surfaces and lateral machined face along down milling. This results to thicker and longer top down milling side burr ( $B_4$ ) as presented in Figure 2.18. According to Figure 2.19, considerable  $B_8$  height was first occurred when using low level of feed per tooth. During slot milling operation, the chip is often unable to be evacuated. Therefore, it sticks on the top side (along up milling) of the corresponding lateral machined face and it eventually leads to longer top burrs along up milling side ( $B_8$ ), in particular when using higher levels of cutting speed and depth of cut and lower level of feed per tooth (see Figure 2.19(a)). From Figure 2.20(a), it is evident that at lower feed per tooth, lower resulting value of  $B_4$  height is obtained for AA 2024-T351. When changing the feed per tooth to 0.1 mm/z, shorter  $B_4$  is obtained for AA 6061-T6. This exhibits that as presented in Figure 2.16(a), the interaction effects between material-feed per tooth (AD) has a significant effect on  $B_4$  height. Similarly, when lower level of feed per tooth is used, longer  $B_8$  is obtained for AA 6061-T6 (see Figure 2.20(b)). The difference between the  $B_8$  heights in both materials becomes smaller when changing the feed per tooth to upper level (0.1 mm/z).

The  $B_4$  and  $B_8$  thickness are highly influenced by cutting speed and tool coating. As presented in Figure 2.21, at lower level of cutting speed, when using cutting tools with similar insert nose radius ( $R_\epsilon$ ), lower resulting values of  $B_4$  and  $B_8$  thickness are obtained when using cutting tool 1 (TiCN,  $R_\epsilon = 0.5$  mm). Vice versa, under similar cutting conditions, when cutting speed increases to 1200 m/min, thinner  $B_4$  and  $B_8$  are obtained when using cutting tool 3 (TiCN+Al<sub>2</sub>O<sub>3</sub>+TiN,  $R_\epsilon = 0.5$  mm). This exhibits significant interactions between cutting speed and tool coating that largely affects both  $B_4$  and  $B_8$  thickness.

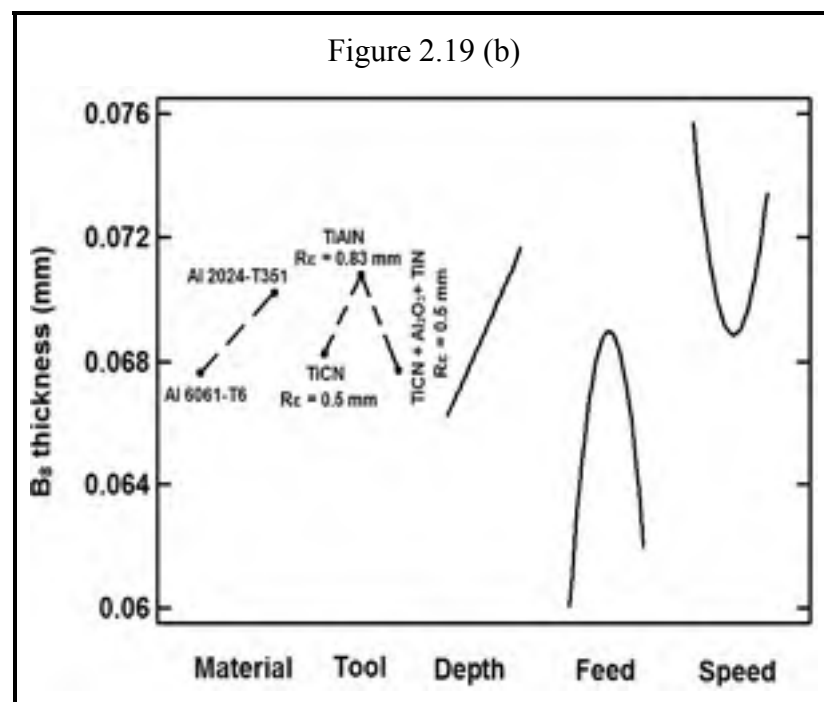
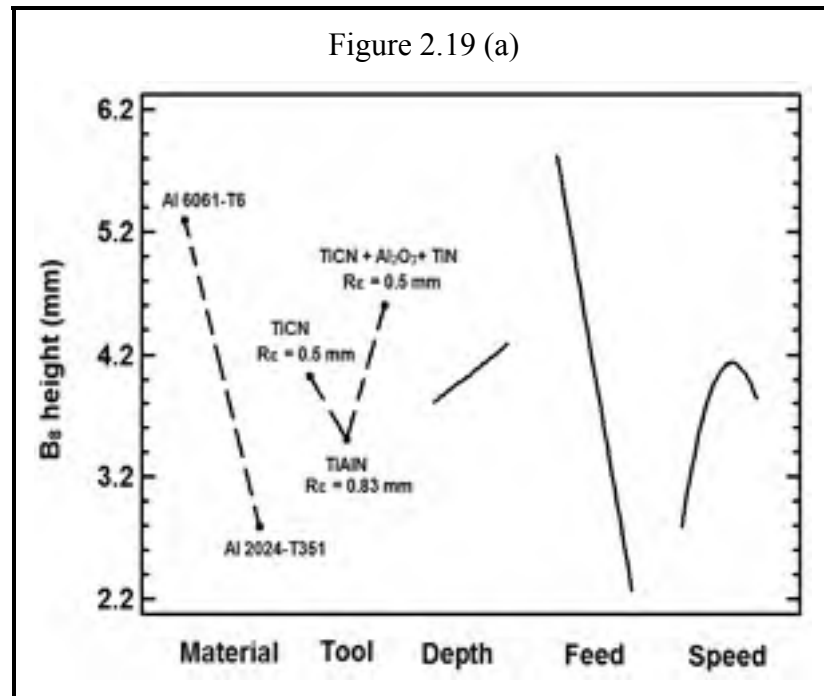


Figure 2.19 Direct effect plot of (a)  $B_8$  height, (b)  $B_8$  thickness

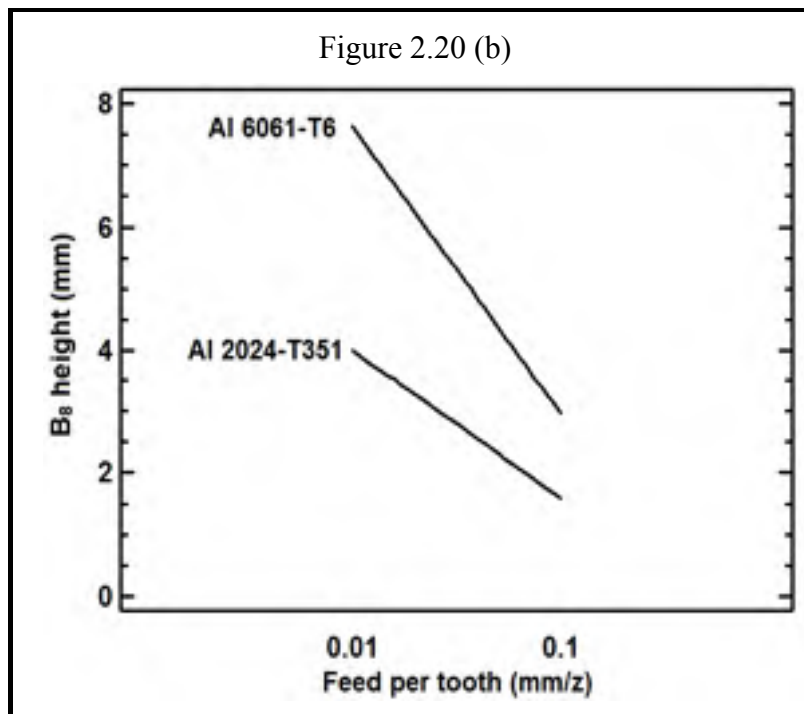
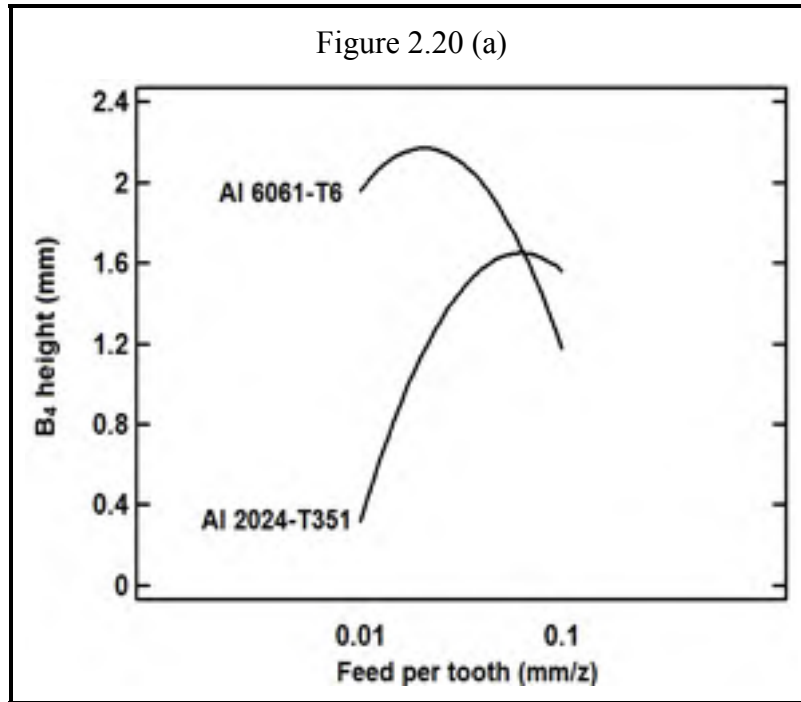


Figure 2.20 Interaction effect of material- feed per tooth (AD) on (a) B<sub>4</sub> height and (b) B<sub>8</sub> height

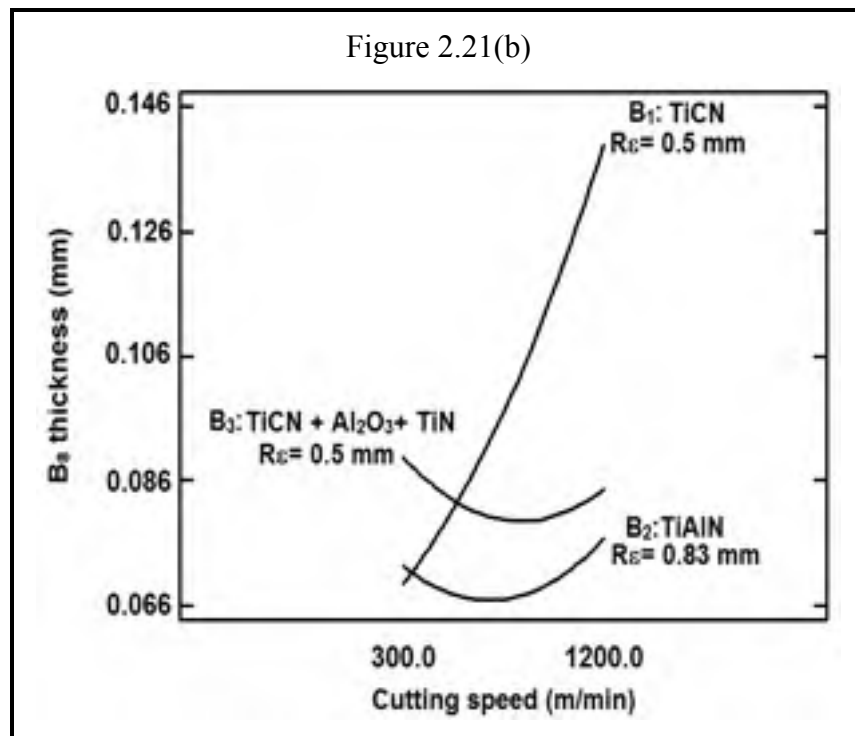
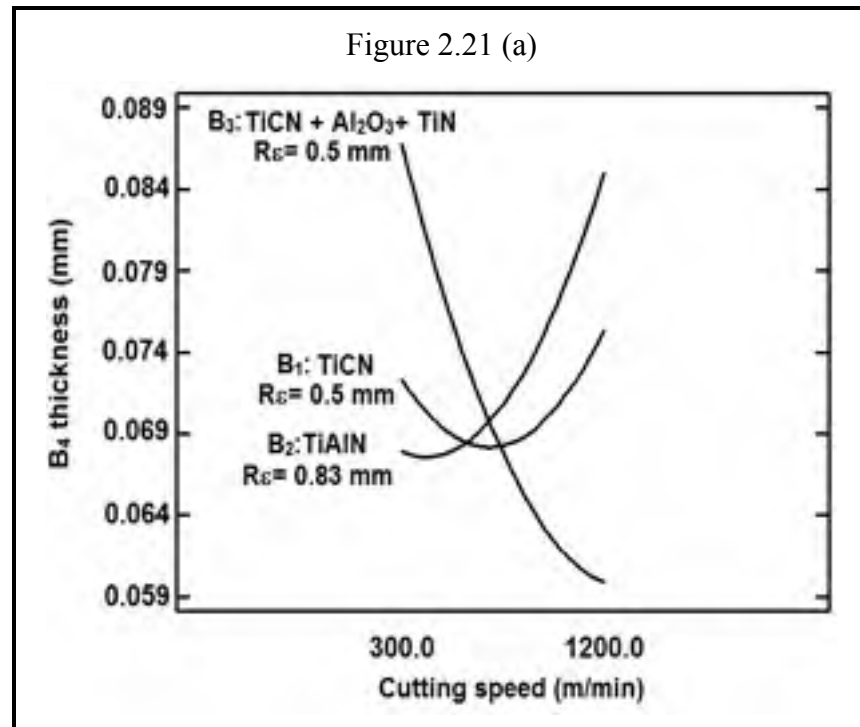


Figure 2.21 Interaction effect of tool-cutting speed (BE) on  
(a) B<sub>4</sub> thickness and (b) B<sub>8</sub> thickness

### 2.3.3 Response surface models

Table 2.3 summarizes the governing factors and interaction effects on each of the five burrs studied. The optimum cutting conditions to minimize slot milling burrs are also presented in Table 2.3. It appears that the optimum process parameters setting levels to minimize each burr are different (see Table 2.3). None of the two tested materials systematically have a higher size when a specific burr is considered. The 3D response surface models of the optimum cutting condition are presented in Figures 2.22-2.23. According to Figures 2.22-2.23, the B<sub>1</sub> is the longest and thickest burr amongst other burrs studied. From Figure 2.22, it appears that the height of B<sub>2</sub> and B<sub>5</sub> are negligible as compared to other burrs. According to Figures 2.22-2.23, in some of the burrs studied, no linear relationship can be formulated between the burrs sizes and cutting parameters. This becomes more apparent when studying the burr height. This can be due to strong interaction effects between process parameters that pose complexity for precise estimation and modeling of burr height.

Table 2.3 Statistical summary of results

List	Response characteristics	Dominant process parameters at 95% Confidence Interval		Optimum process parameters setting levels
		Direct effects	Interaction effects	
1	B <sub>1</sub> height	D, A, C	BC,CD,DE,CE	A <sub>2</sub> B <sub>2</sub> C <sub>1</sub> D <sub>1</sub> E <sub>2</sub>
2	B <sub>1</sub> thickness	D, C, B, E	BC,BD,AE,EE,DE	A <sub>2</sub> B <sub>2</sub> C <sub>1</sub> D <sub>1</sub> E <sub>2</sub>
3	B <sub>2</sub> height	B, C, E	CE,EE	A <sub>1</sub> B <sub>1</sub> C <sub>2</sub> D <sub>2</sub> E <sub>1</sub>
4	B <sub>2</sub> thickness	C,B	CE	A <sub>2</sub> B <sub>3</sub> C <sub>2</sub> D <sub>1</sub> E <sub>2</sub>
5	B <sub>4</sub> height	B,A,C	AD,AE, EE, DD	A <sub>2</sub> B <sub>2</sub> C <sub>2</sub> D <sub>1</sub> E <sub>2</sub>
6	B <sub>4</sub> thickness	D,B,A	-	A <sub>1</sub> B <sub>2</sub> C <sub>2</sub> D <sub>1</sub> E <sub>2</sub>
7	B <sub>5</sub> height	B, E, C	AD,AE,EE,DD	A <sub>2</sub> B <sub>2</sub> C <sub>1</sub> D <sub>3</sub> E <sub>1</sub>
8	B <sub>5</sub> thickness	B,D	-	A <sub>2</sub> B <sub>2</sub> C <sub>1</sub> D <sub>1</sub> E <sub>1</sub>
9	B <sub>8</sub> height	D, A	-	A <sub>2</sub> B <sub>2</sub> C <sub>1</sub> D <sub>3</sub> E <sub>1</sub>
10	B <sub>8</sub> thickness	-	BE,AB,AE	A <sub>1</sub> B <sub>3</sub> C <sub>1</sub> D <sub>1</sub> E <sub>2</sub>

A: Material; B: Tool; C: Depth of cut; D: Feed per tooth; E: Cutting speed

Figure 2.22 (a)

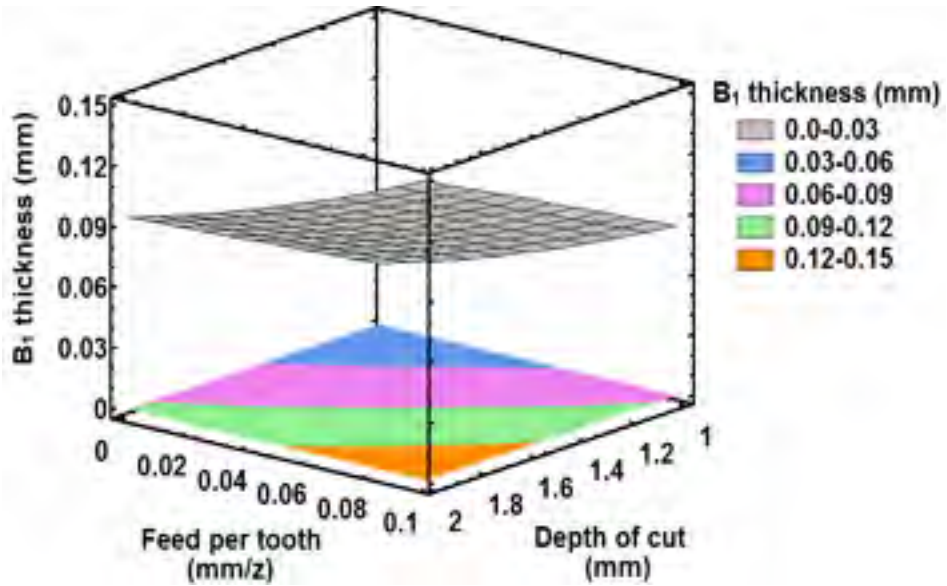


Figure 2.22 (b)

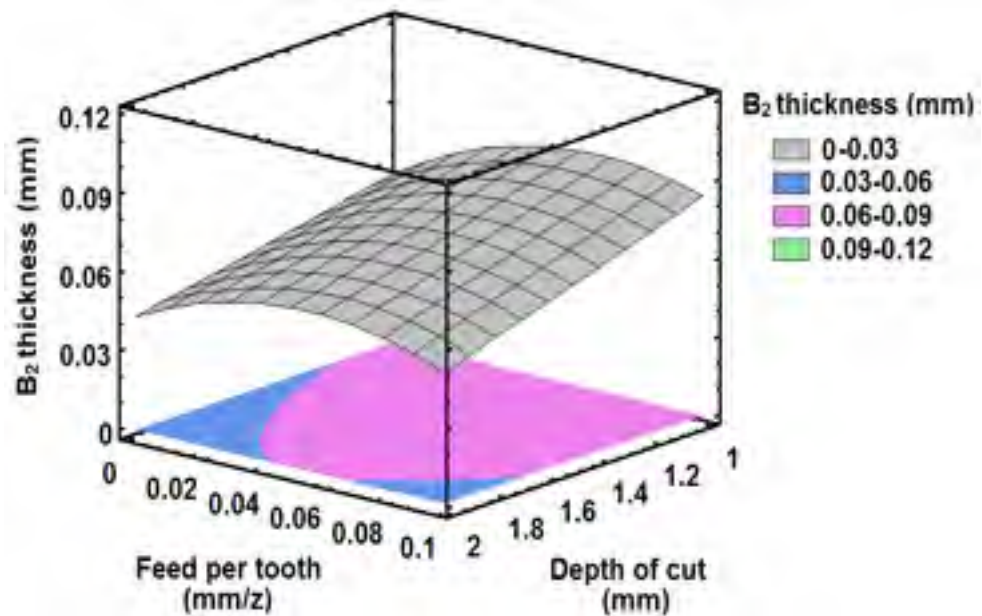


Figure 2.22 (c)

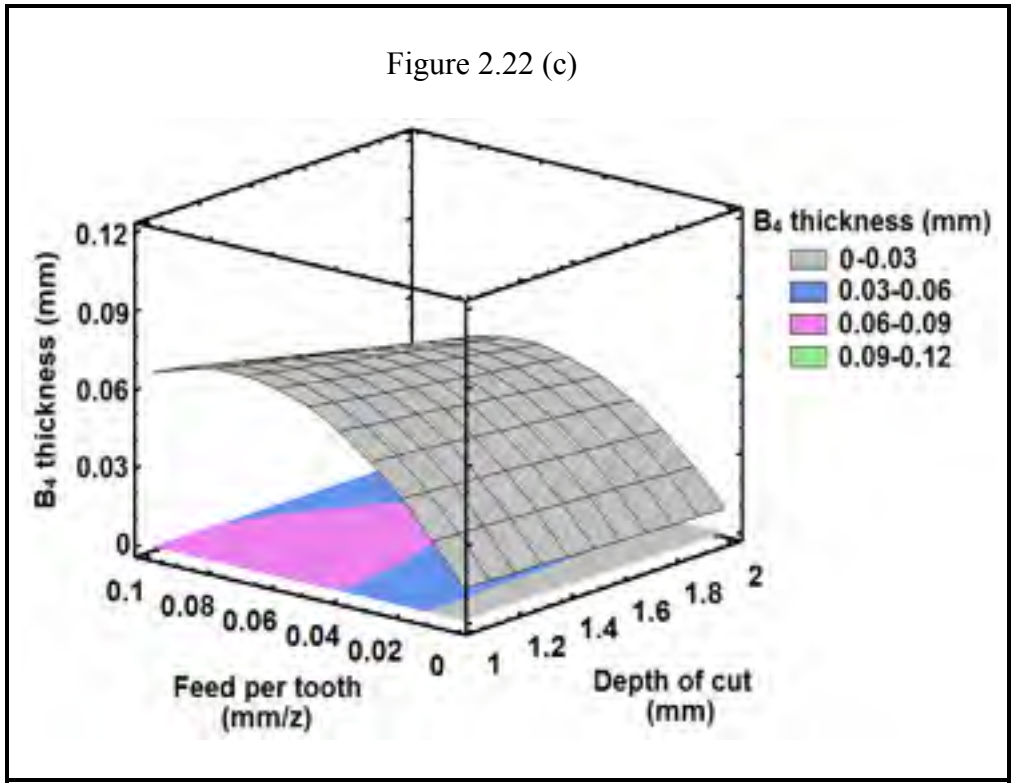
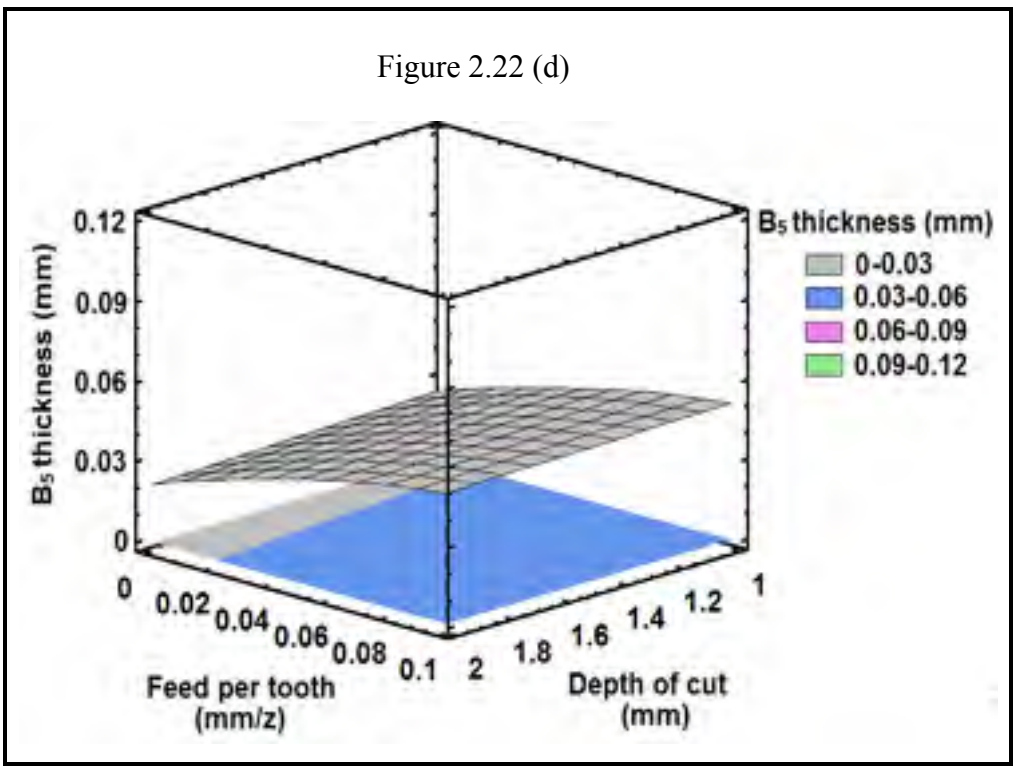


Figure 2.22 (d)



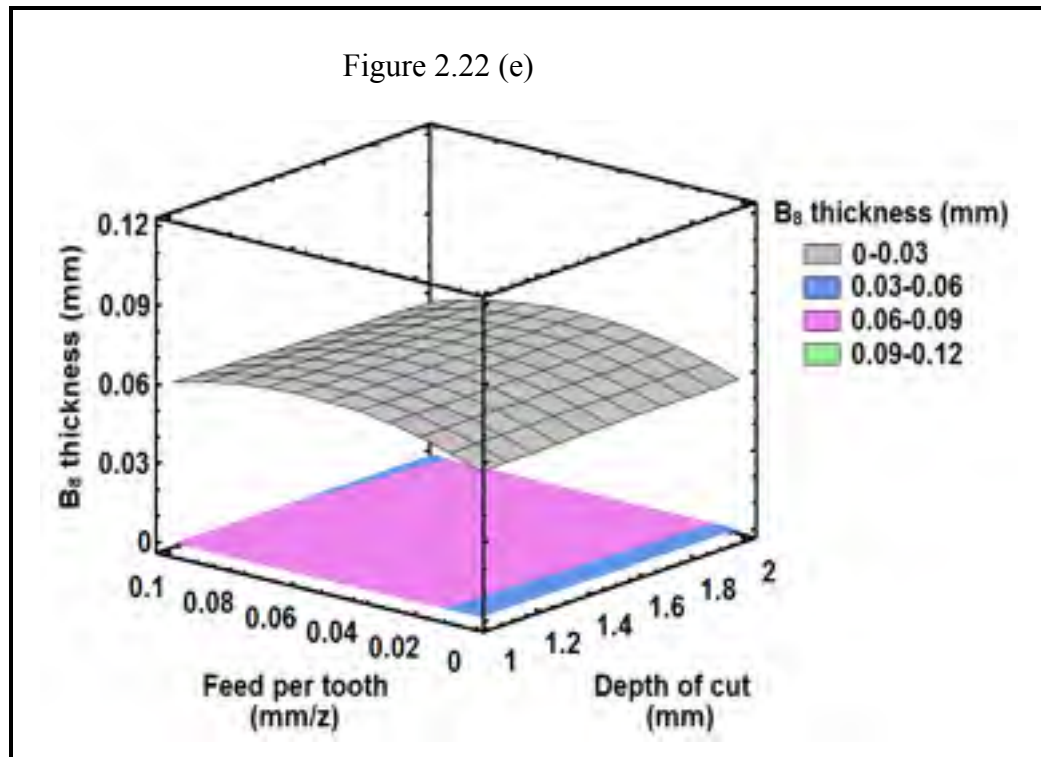


Figure 2.22 3D contour plot of burr thickness studied at optimum cutting conditions

Figure 2.23 (a)

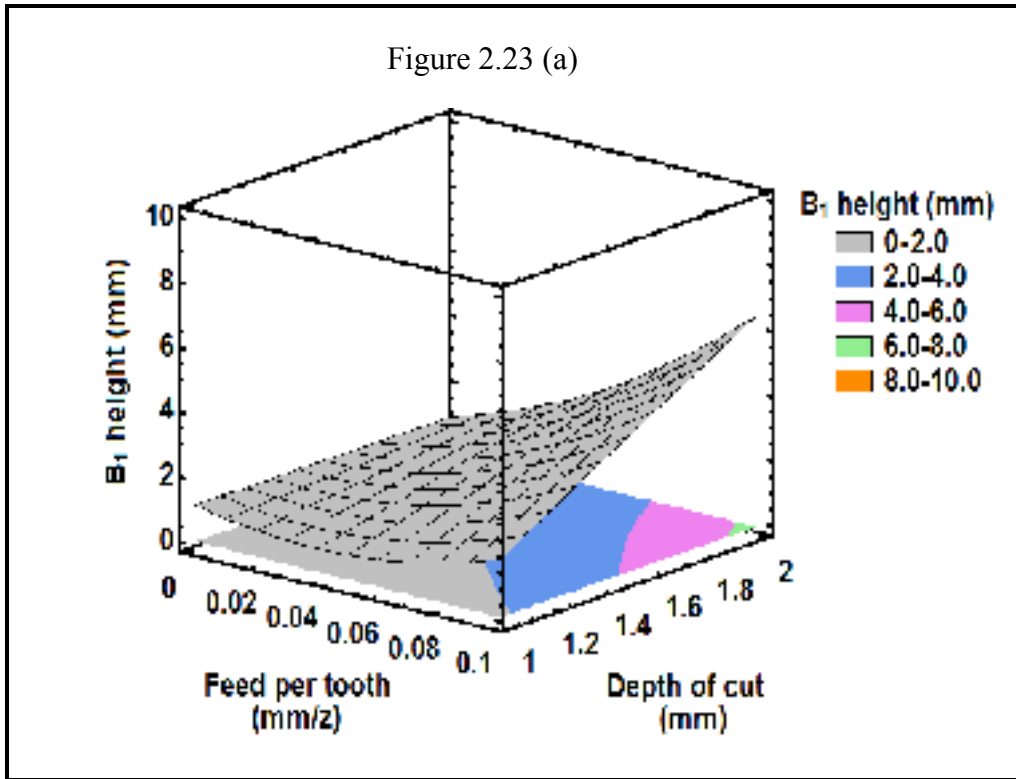


Figure 2.23 (b)

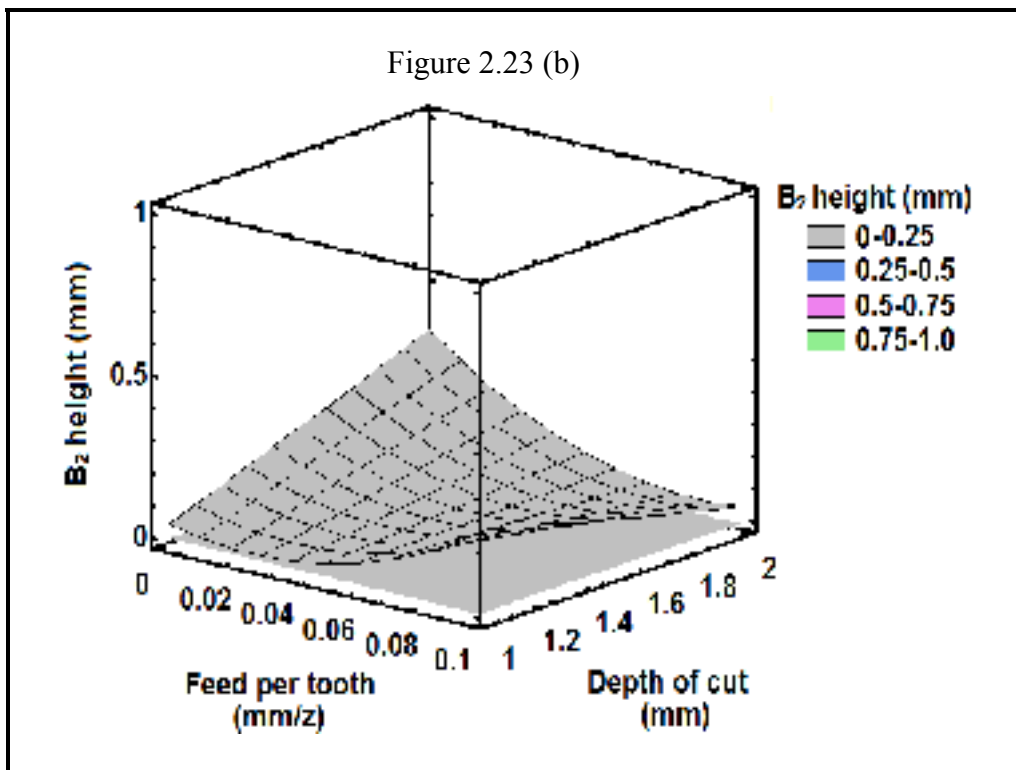


Figure 2.23 (c)

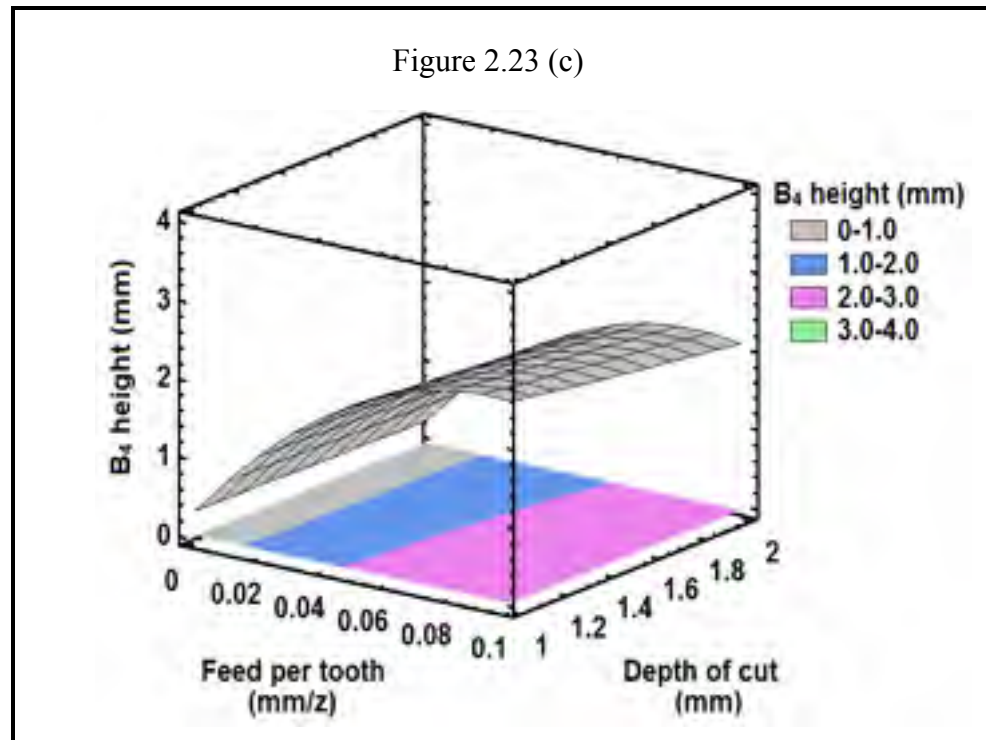
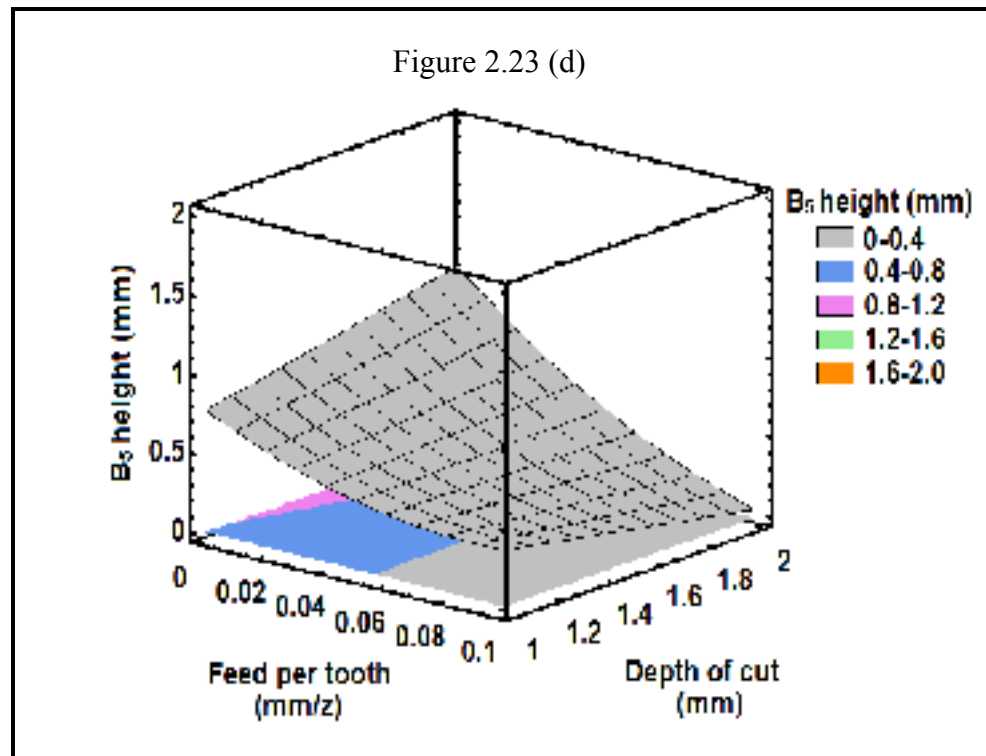


Figure 2.23 (d)



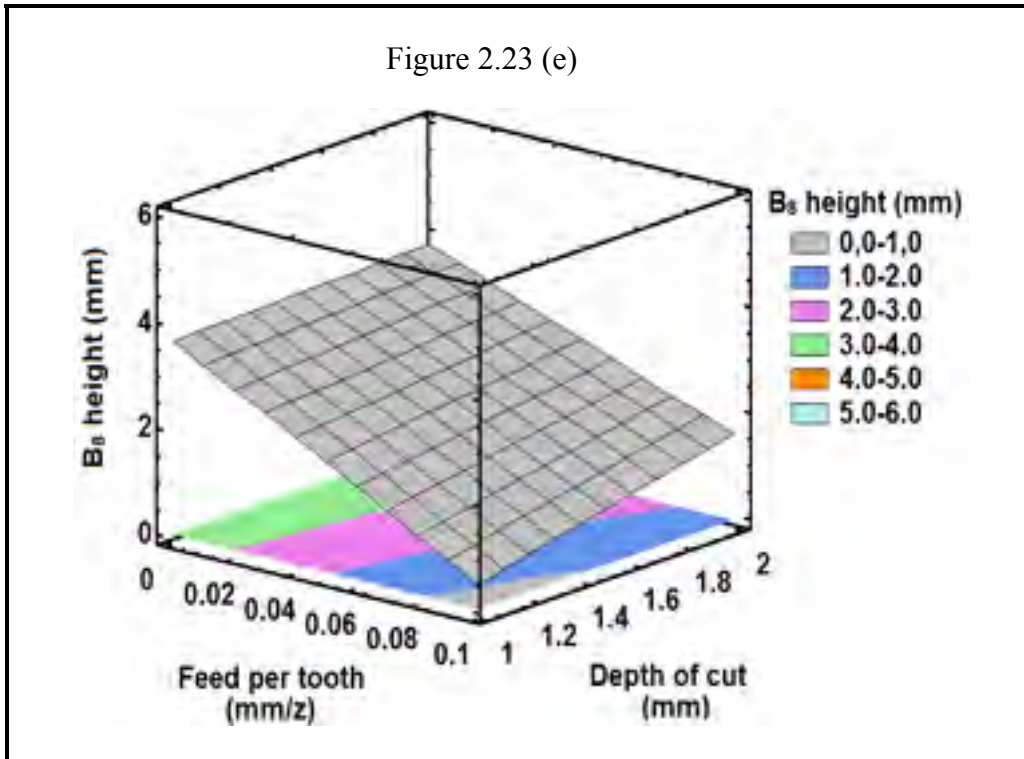


Figure 2.23 3D contour plot of burr height at optimum cutting conditions

### Analysis of Variance (ANOVA)

Three design models are used to statistically analyze the influence of process parameters on burrs size. By considering the statistical  $R^2$  and  $R^2_{adj}$  of design models for each burr (see Tables 2.4-2.5); it is evident that the variation of burr height in all studied burrs can not be statistically controlled by cutting parameters. Similarly, amongst studied burrs thickness, only  $B_1$  thickness could be controlled by cutting parameters. This means that except  $B_1$  thickness, no accurate relationship can be formulated between the burrs size and cutting parameters.

According to Table 2.5, the non-considerable difference between  $R^2$  and  $R^2_{adj}$  in linear and quadratic models of  $B_1$  thickness determines that the interaction effects between process parameters have an effect of 9.1% on variation of  $B_1$  thickness. In addition, a P-value of 0 in

each three models indicates that the models are adequate (see Table 2.5). Then linear model of  $B_1$  thickness will be used for further investigations.

Table 2.4 Statistical summary of burr height models

No.	Milling burr	Design Model	R <sup>2</sup> %	R <sup>2</sup> <sub>adj</sub> %	F ratio	P value	Remark
1	Exit up milling side burr ( $B_1$ )	Linear	14.2	5.3	1.59	0.18	Insignificant
		2-Factor Interactions	57.5	42.3	3.77	0	Insignificant
		Quadratic	57.8	39.6	3.19	0	Insignificant
2	Exit bottom burr ( $B_2$ )	Linear	40.3	34.1	6.49	0.001	Insignificant
		2-Factor Interactions	56.7	41.2	3.65	0.007	Insignificant
		Quadratic	58.1	39.9	3.26	0.001	Insignificant
3	Top Down milling burr ( $B_4$ )	Linear	59.5	55.3	14.1	0	Insignificant
		2-Factor Interactions	76.1	64.4	8.85	0	Insignificant
		Quadratic	77.6	67.9	8.03	0	Insignificant
4	Entrance down milling side ( $B_5$ )	Linear	39.9	33.7	6.39	0.001	Insignificant
		2-Factor Interactions	50.3	32.4	2.82	0.005	Insignificant
		Quadratic	51.1	29.8	2.41	0.013	Insignificant
5	Top up milling burr thickness ( $B_8$ )	Linear	26.5	18.8	3.45	0.009	Insignificant
		2-Factor Interactions	36.7	14.1	1.61	0.117	Insignificant
		Quadratic	50.6	29.2	2.36	0.015	Insignificant

Table 2.5 Statistical summary of burr thickness models

No.	Milling burr	Design Model	R <sup>2</sup> %	R <sup>2</sup> <sub>adj</sub> %	F ratio	P value	Remark
1	Exit up milling side burr (B <sub>1</sub> )	Linear	83.1	81.3	47.5	0	Significant
		2-Factor Interactions	90.3	86.8	25.9	0	Significant
		Quadratic	92.2	88.9	27.5	0	Significant
2	Exit bottom burr (B <sub>2</sub> )	Linear	22.9	14.9	2.85	0.024	Insignificant
		2-Factor Interactions	40.0	18.5	1.86	0.063	Insignificant
		Quadratic	46.1	22.8	1.97	0.043	Insignificant
3	Top Down milling burr (B <sub>4</sub> )	Linear	14.1	5.04	1.56	0.186	Insignificant
		2-Factor Interactions	26.1	0	0.99	0.482	Insignificant
		Quadratic	28.1	0	0.90	0.575	Insignificant
4	Entrance down milling side (B <sub>5</sub> )	Linear	35.8	29.1	5.35	0.005	Insignificant
		2-Factor Interactions	41.7	20.8	1.99	0.044	Insignificant
		Quadratic	42.1	17.2	1.68	0.094	Insignificant
5	Top up milling burr thickness (B <sub>8</sub> )	Linear	19.8	11.5	2.38	0.052	Insignificant
		2-Factor Interactions	39.6	17.9	1.82	0.069	Insignificant
		Quadratic	46.9	23.95	2.04	0.036	Insignificant

### 2.3.4 Controllable response

According to presented results, under similar experimental conditions, relatively thicker B<sub>1</sub> is obtained when studying AA 6061-T6. Therefore, the following sections only present the test results of AA 6061-T6. The relative contribution of milling parameters (Pareto chart) and main effect plot of B<sub>1</sub> thickness in linear design model are shown in Figure 2.24. Based on Figure 2.24(a), feed per tooth (B), depth of cut (B) and tool (A) are the cutting parameters with the most contribution to variation of B<sub>1</sub> thickness. According to Figure 2.24(b), at higher levels of feed per tooth and depth of cut, B<sub>1</sub> thickness increases. From Figure 2.25(a-c), it is observed that at higher levels of feed per tooth and depth of cut, B<sub>1</sub> thickness increases at fixed cutting speed 1200 m/min, when cutting tools 1-3 are used, respectively. By assessing these plots, it could be inferred that, regardless the effect of feed per tooth,

depth of cut and cutting speed,  $B_1$  thickness decreases when cutting tool 2 with insert nose radius ( $R\epsilon$ ) 0.83 mm is used.

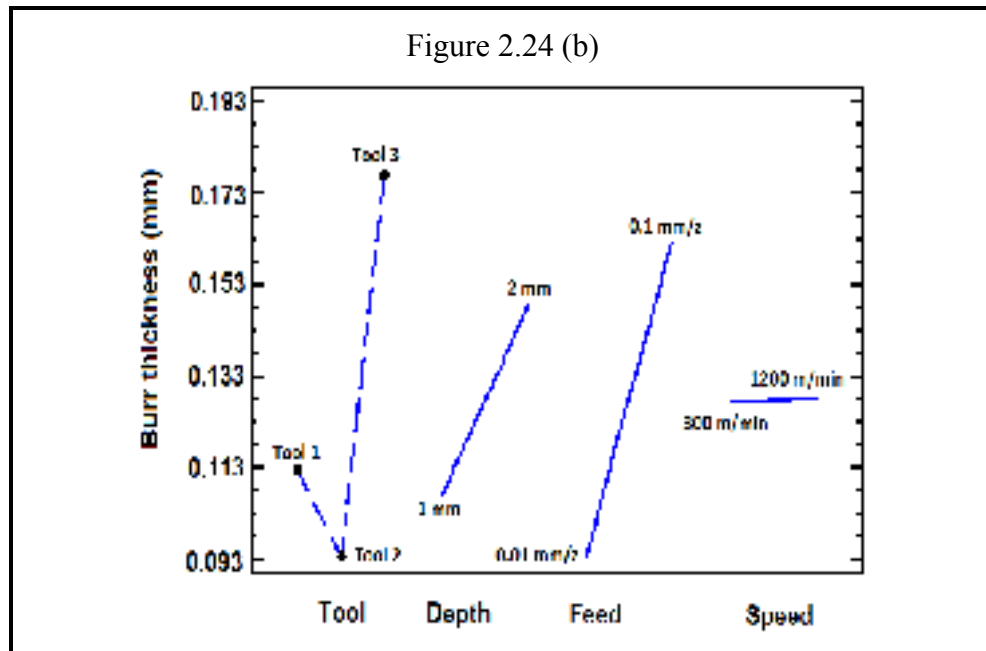
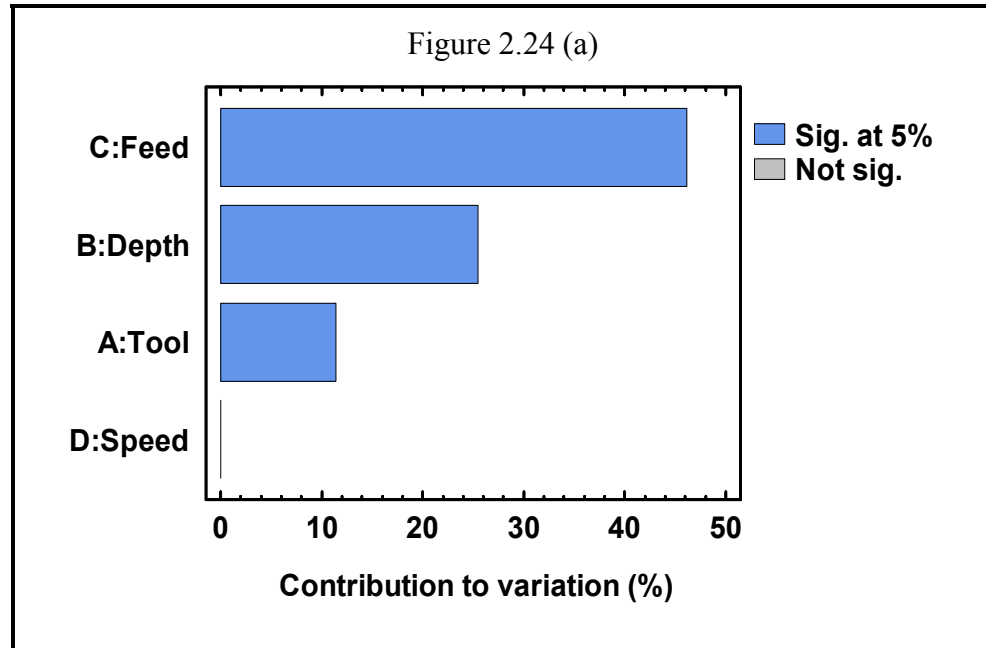
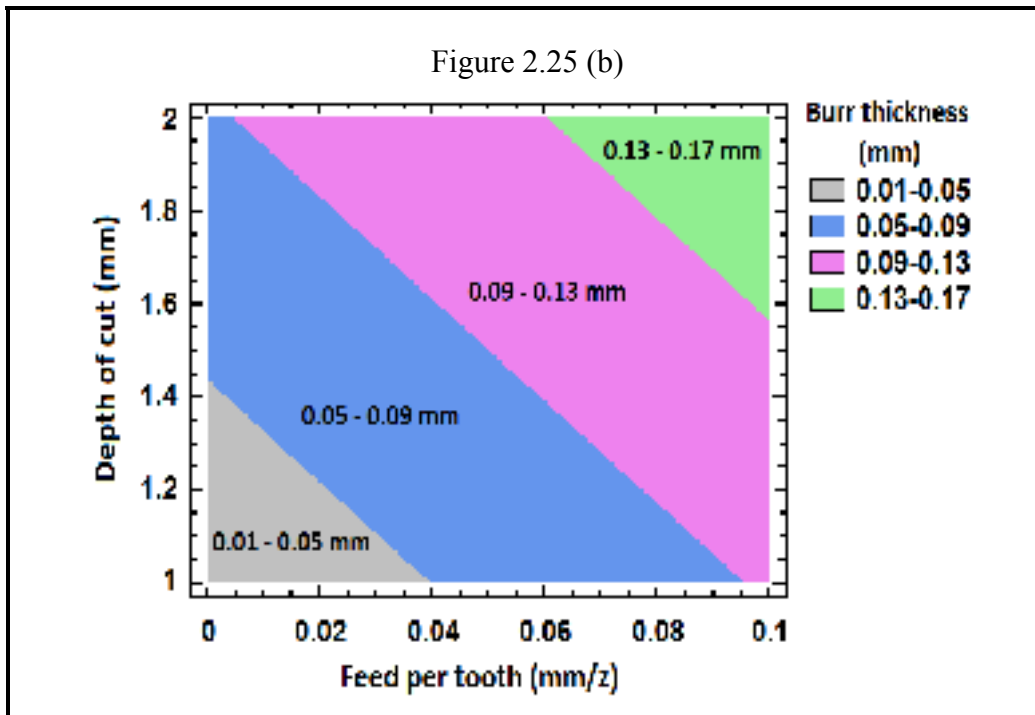
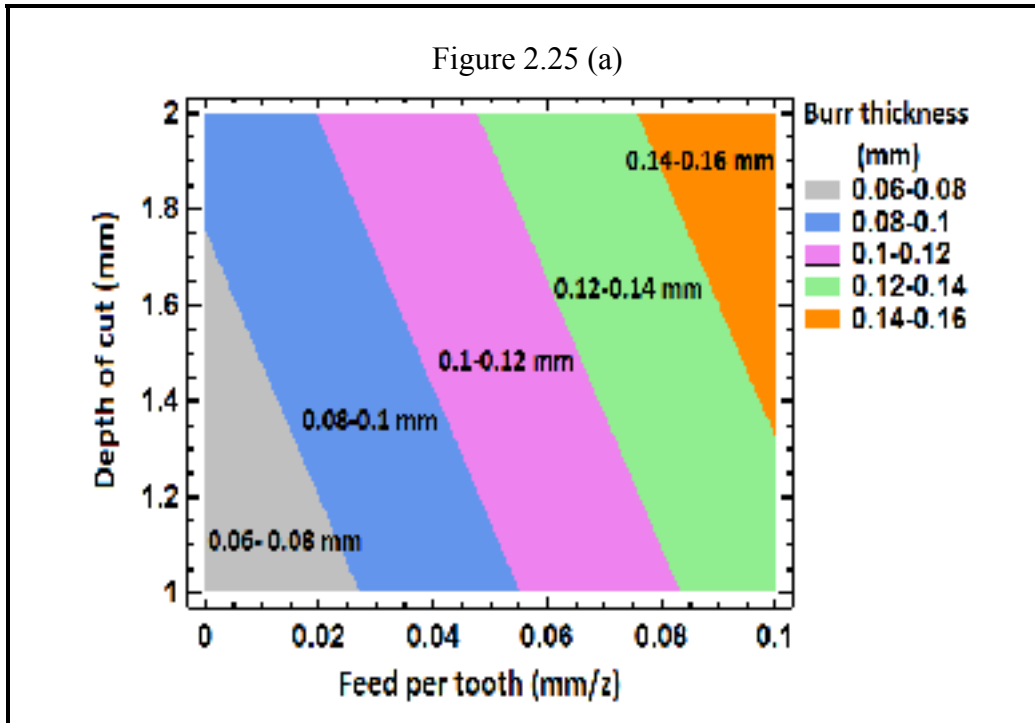


Figure 2.24 (a) Pareto chart of  $B_1$  thickness in linear design model, (b) Direct effect plot of  $B_1$  thickness



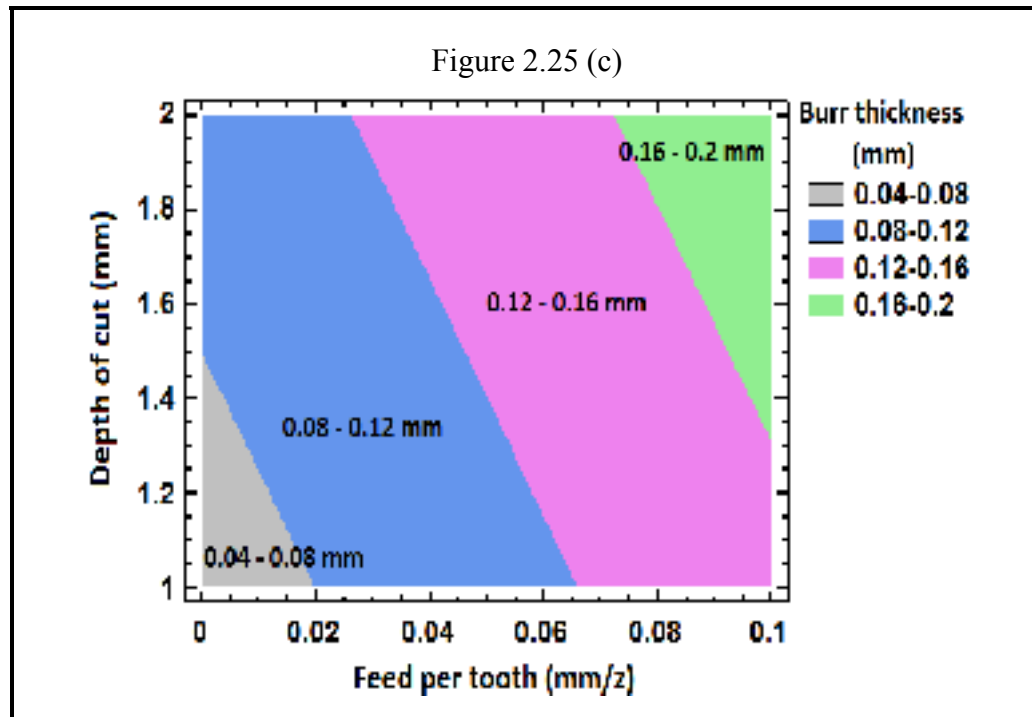


Figure 2.25 2D contour plot of  $B_1$  thickness:  
(a) Tool 1, (b) Tool 2, (c) Tool 3

### Tangential cutting force ( $F_t$ )

The ANOVA is applied to study the effects of cutting parameters on measured values of  $F_t$  in each trial. In order to have a better result analysis, three statistical design models as presented in Table 2.6 are used. According to Table 2.6, the difference between  $R^2$  and  $R^2_{adj}$  in linear and quadratic models of  $F_t$  is about 9%. Therefore, as similar as the case of  $B_1$  thickness, linear design model of  $F_t$  will be used for further investigations. The Pareto chart and direct effect plot of  $F_t$  in linear design model are shown in Figures 2.26-2.27, respectively.

From Figure 2.26, depth of cut and feed per tooth have a significant influence on  $F_t$ . Figure 2.27 shows that increase in the feed per tooth and depth of cut increases  $F_t$ . This is due to direct effects of these two cutting parameters on chip thickness, which largely affects directional cutting forces. The cutting speed and tool have the least significant effect on variation of  $F_t$  as compared to feed per tooth and depth of cut. Figures 2.24(b) and 2.27

reveal that the use of larger insert nose radius ( $R\epsilon$ ) led to lower  $F_t$  and  $B_1$  thickness. According to Figure 2.28, exponential model is found as the best regression model for  $F_t$  and  $B_1$  thickness with 86.26% correlation coefficient (see Figure 2.28), followed by multiplicative and linear models with correlation coefficients of 84.41% and 79.89%, respectively.

Table 2.6 Statistical summary of  $F_t$  design models

No.	Design models	$R^2$ %	$R^2_{adj}$ %	F-ratio	P value
1	Linear	89.43	88.34	81.29	0
2	2-Factor Interactions	97.39	96.45	104.04	0
3	Quadratic	97.83	96.89	104.34	0

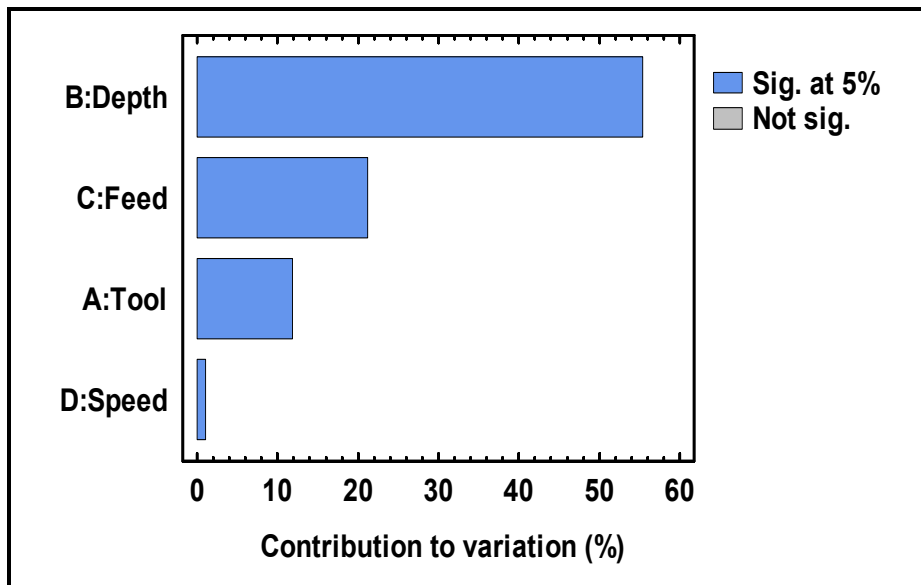


Figure 2.26 Pareto chart of  $F_t$  in linear design model

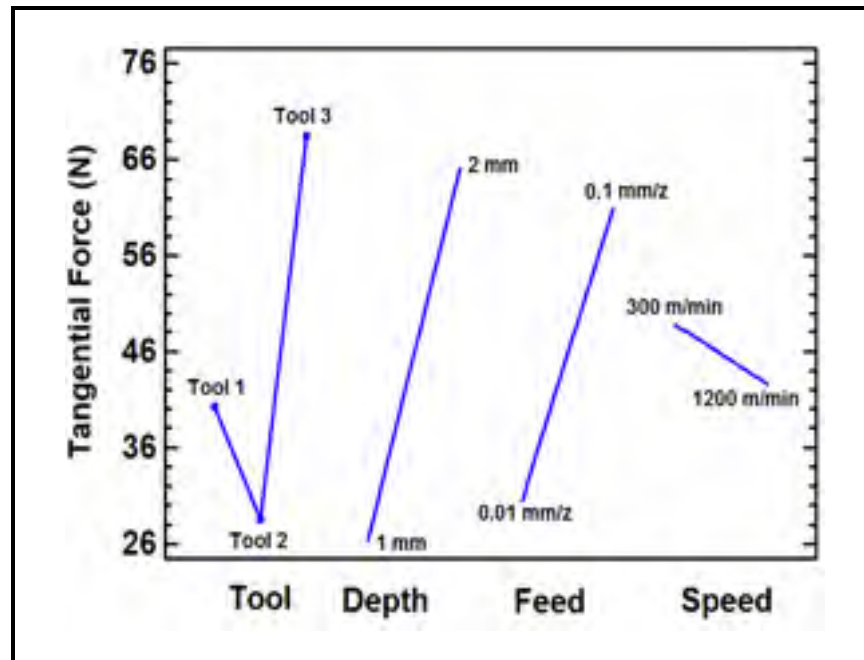


Figure 2.27 Direct effect plot of  $F_t$

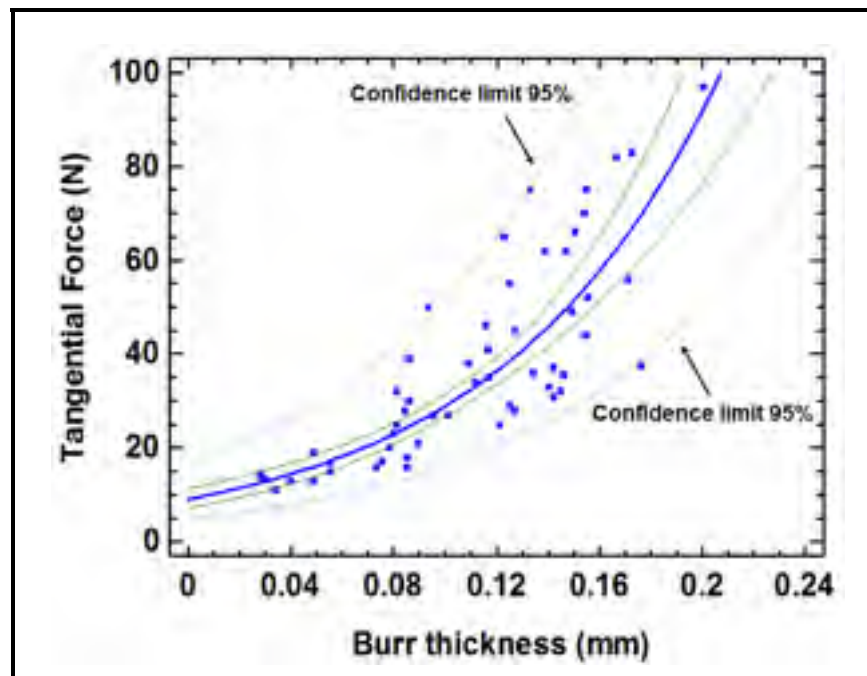


Figure 2.28 Exponential regression model between  $F_t$  and  $B_1$  thickness

## RSM based modeling

Linear first order mathematical models (Eqs 2.5-2.10) are developed to predict  $F_t$  and  $B_1$  thickness as a function depth of cut ( $a_c$ ) and feed per tooth ( $f_z$ ), when cutting tests were performed using various cutting tools:

### $B_1$ thickness

$$B_{t,1} (\text{Tool 1}) = -0.035 + 0.71 \times f_z + 0.025 \times a_c \quad R^2 = 91.73\% \quad (2.5)$$

$$B_{t,2} (\text{Tool 2}) = -0.043 + 0.71 \times f_z + 0.065 \times a_c \quad R^2 = 91.96\% \quad (2.6)$$

$$B_{t,3} (\text{Tool 3}) = 0.028 + 0.86 \times f_z + 0.034 \times a_c \quad R^2 = 85.95\% \quad (2.7)$$

### Tangential cutting force ( $F_t$ )

$$F_{t,1} (\text{Tool 1}) = -47.65 - 534.722 \times f_z + 50.33 \times a_c \quad R^2 = 93.42\% \quad (2.8)$$

$$F_{t,2} (\text{Tool 2}) = -15.16 + 156.5 \times f_z + 23.38 \times a_c \quad R^2 = 87.95\% \quad (2.9)$$

$$F_{t,3} (\text{Tool 3}) = -31.18 + 340.74 \times f_z + 38.77 \times a_c \quad R^2 = 91.58\% \quad (2.10)$$

According to Eqs(2.5-2.10),  $B_1$  thickness and cutting force  $F_t$  could be linearly formulated as a function of  $a_c$  and  $f_z$ .

## 2.4 Conclusion

The slot milling burrs in AA 6061-T6 and AA 2024-T351 were comprehensively studied. Their formation mechanism and factors governing their creation were investigated using a multi-level full factorial design of experiment. According to experimental results and statistical analysis, the following conclusions are drawn:

- Burr size can be reduced significantly by selecting appropriate cutting parameters and cutting tools. However, optimum setting levels of process parameters to minimize each burr are different.
- It was found that amongst the most of the burrs studied, the dominant process parameters on burr height have the opposite effect on burr thickness. Moreover, no mathematical relationship was formulated between burrs thickness and height.
- Depth of cut, feed per tooth and tool (insert nose radius and coating) were found as the dominant process parameters on most of the burrs.
- Exit burrs are highly affected by feed per tooth, depth of cut, insert end nose radius ( $R\epsilon$ ) and coating. Slot milling tests with higher levels of feed per tooth and depth of cut and smaller insert nose radius ( $R\epsilon$ ) led to longer and thicker  $B_1$  and shorter and thinner  $B_2$ . According to experimental results, trials to minimize the  $B_2$  size led to thicker  $B_1$ .
- The side burrs, whether entrance or exit side burrs ( $B_1$  and  $B_5$ ) are mainly dominated by the feed per tooth. The top burrs are mainly affected by variation of cutting condition, chip evacuation dynamic, insert nose radius ( $R\epsilon$ ) and tool coating.
- The significant effect of coating on slot milling burrs was observed in this study. This observation is in conflict with previous findings in the literature, stating minor influence of coating on face milling burr formation.
- High speed machining has no significant effect on the top burrs size. Furthermore, cutting tools with very similar insert nose radius ( $R\epsilon$ ) to depth of cut generate primary exit bottom ( $B_2$ ) burr, regardless of the cutting speed used.

- Amongst the burrs studied, only exit up milling side burr ( $B_1$ ) thickness could be controlled by variation of cutting process parameters. Considering that cutting tool and spindle vibrations were controlled, it could be stated that factors governing slot milling burrs are not yet fully identified. In addition, burrs are highly influenced by interaction effects between process parameters that consequently pose difficulties in their precise modeling. This can be considered as a complex nature of slot milling burr formation.
- It was also found that cutting force  $F_t$  has a very good correlation with  $B_1$  thickness. They both can be controlled by varying the feed per tooth and depth of cut. In addition, milling tests with larger insert nose radius ( $R\epsilon$ ) led to smaller  $F_t$  and thinner  $B_1$ .
- Increase the cutting speed led to decreased  $F_t$  and increased  $B_1$  thickness, respectively. However according to statistical analysis, cutting speed has the least significant effects on variation of  $F_t$  and  $B_1$  thickness than other cutting parameters. Therefore, linear mathematical models were presented to predict  $F_t$  and  $B_1$  thickness as a function of feed per tooth and depth of cut, when cutting tests were performed using various cutting tools.

## CHAPTER 3

### MODELING OF BURR THICKNESS IN MILLING OF DUCTILE MATERIALS

#### 3.1 Introduction

Among machining operations, analytical modeling of burr formation in milling is very challenging. Most of reported works in the literature aim to measure and/or predict the burr height, but this information is not very useful for deburring purposes. The thickness of the burr is much of interest because it describes the time and method necessary for deburring a workpiece (Aurich *et al.*, 2009). However burr thickness measurements are costly and non-value-added operations that in most of cases require the use of Scanning Electron Microscope (SEM) for accurate burr characterization. Therefore, to avoid such non-desirable expenses, the use of alternative methods for burr thickness prediction is strongly recommended.

According to experimental results in chapter 2, it was found that exit up milling side burr ( $B_1$ ) is the longest and thickest milling burr. In addition,  $B_1$  thickness can be controlled by feed per tooth and depth of cut. In this chapter, an analytical model is proposed to predict the  $B_1$  thickness ( $B_t$ ) in the exit up milling side burr (see Figure 3.1) during slot milling operation of ductile materials. The model is built on the geometry of burr formation and the principle of continuity of work at the transition from chip formation to burr formation that also considers the effect of cutting force on burr formation. For experimental validation, the  $B_t$  was recorded at four locations and the average of readings was taken as the burr size. We also anticipate proposing a procedure for computational modeling of  $B_t$  by assuming negligible effect of coated insert nose radius and cutting speed on  $B_t$ .

A scientific article on proposed models was published in *Journal of Advanced Manufacturing Technology* in September 2012 (see ANNEX IV).

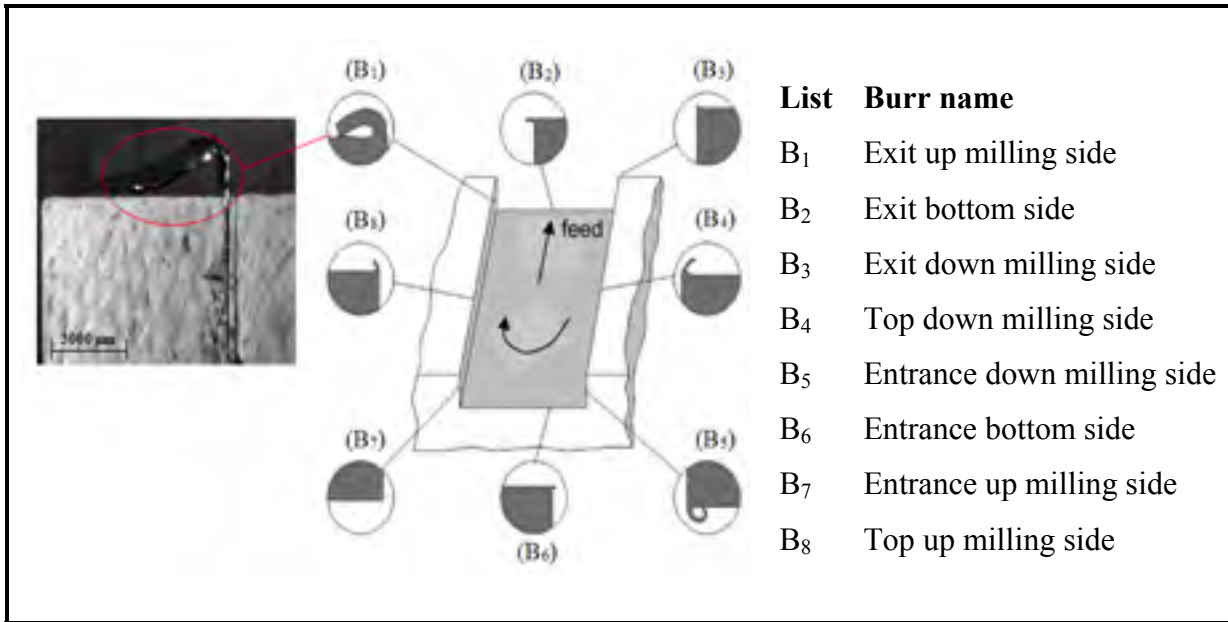


Figure 3.1 Slot milling burrs

### 3.2 Theoretical modeling of milling burr thickness

It is believed that when the cutting tool is about to exit the workpiece (see Figure 3.2), the positive shear angle,  $\Phi$ , may have a transition to a negative value,  $\beta_0$ . At a certain point, natural chip formation stops, and the sub-surface plastic deformation begins. This point is known as transition point (Ko and Dornfeld, 1991). It is believed that the work done for chip formation is equal to that done for burr formation at the transition point. Consequently, after this point, no further natural chip formation occurs (see Figure 3.2). The exit up milling side (B<sub>1</sub>) burr most likely forms when the cutting tool is about to leave the workpiece. The initial negative shear plane determines the location of the plastic hinge point, B. It is located where the initial negative shear plane crosses the end surface of the workpiece, and acts as a plastic hinge. It remains unchanged as burr is formed (Ko and Dornfeld, 1991).

The following assumptions were used to develop the theoretical model:

1. The model is based on the burr formation geometry. Burr formation in the exit zone is modeled as an orthogonal process, and consequently, the effect of the plunge depth and the cutter geometry is ignored.



According to (Ko and Dornfeld, 1991), in triangles APB and A'PB depicted in Figure 3.2(b),  $B_t$  is equal to  $PB$ , which can be expressed as:

$$PB = l' \sin \beta = \omega \tan \beta_0 \quad (3.1)$$

Where  $\beta_0$  is the initial negative shear angle and  $\omega$  is the tool distance to the end of the workpiece.

From Figure 3.2,  $d\theta$  and  $d\beta$  are small angle. Therefore, based on Figure 3.2 (a) and triangle AA'B in Figure 3.2(b):

$$AA' = R d\theta = l' d\beta \quad (3.2)$$

From Eq(3.1)

$$l' = \frac{\omega \tan \beta_0}{\sin \beta} \quad (3.3)$$

By considering that the maximum value of  $\beta$  may occur at  $90^\circ$ , Eq(3.3) becomes:

$$\int_{\beta_0}^{\frac{\pi}{2}} \frac{\omega \tan \beta_0}{\sin \beta} d\beta = \int_0^\theta R d\theta \quad (3.4)$$

$$-\omega \times \tan \beta_0 \times \log \left( \tan \frac{\beta_0}{2} \right) = R\theta \quad (3.5)$$

Rearranging Eq(3.5), the  $\omega$  can be formulated as:

$$\omega = - \frac{R\theta}{\tan \beta_0 \times \log \tan \left( \frac{\beta_0}{2} \right)} \quad (3.6)$$

Based on Eqs(3.1) and (3.6), the  $B_t$  is expressed using the following equation:

$$B_t = \omega \times \tan \beta_c = -\frac{R\theta}{\log \tan \left(\frac{\beta_c}{2}\right)} \quad (3.7)$$

According to (Ko and Dornfeld, 1991), by considering only a small advancement of the tool at the transition from chip formation to burr formation, the work done for cutting (chip formation) can be assumed as equal to the work carried out for burr formation by the continuity of energy.

$$\Delta W_c = \Delta W_b \quad (3.8)$$

Where  $W_c$  is work done for chip formation and  $W_b$  is work done for burr formation. It is assumed that the total work done in the chip formation zone,  $W_c$ , for exit up milling side burr formation, could be approximated by the work done by  $F_t$  (see Figure 3.3), which greatly affects the friction on the exit side of the machined part. The effects of friction can be divided to three basic mechanisms, one due to asperity deformation, one due to adhesion, and the last due to particle ploughing.

In orthogonal milling, friction coefficient ( $\mu$ ) can be approximated as (San-Juan, Martín and Santos, 2010):

$$\mu = \tan (\varphi) = F_r \times F_t^{-1} \quad (3.9)$$

Where,  $F_t$ : tangential force;  $F_r$ : radial force and  $\varphi$  is the instantaneous angle of immersion.

The  $F_t$  and  $F_r$  can be calculated from the cutting force in the normal direction ( $F_y$ ), feed direction ( $F_x$ ) and axial direction ( $F_z$ ) using the following transformation:

$$\begin{pmatrix} -\cos (\varphi) & -\sin (\varphi) & 0 \\ \sin (\varphi) & -\cos (\varphi) & 0 \\ 0 & 0 & 1 \end{pmatrix} \begin{pmatrix} F_x \\ F_y \\ F_z \end{pmatrix} = \begin{pmatrix} F_t \\ F_r \\ F_a \end{pmatrix} \quad (3.10)$$

According to (San-Juan, Martín and Santos, 2010), at the beginning of cutting operation, the friction coefficient ( $\mu$ ) achieves high values until cutting conditions become stable. At the end of the tool revolution, it drops to lower values and in the zone where  $h(\varphi)$  changes from increasing to decreasing, it becomes stable.

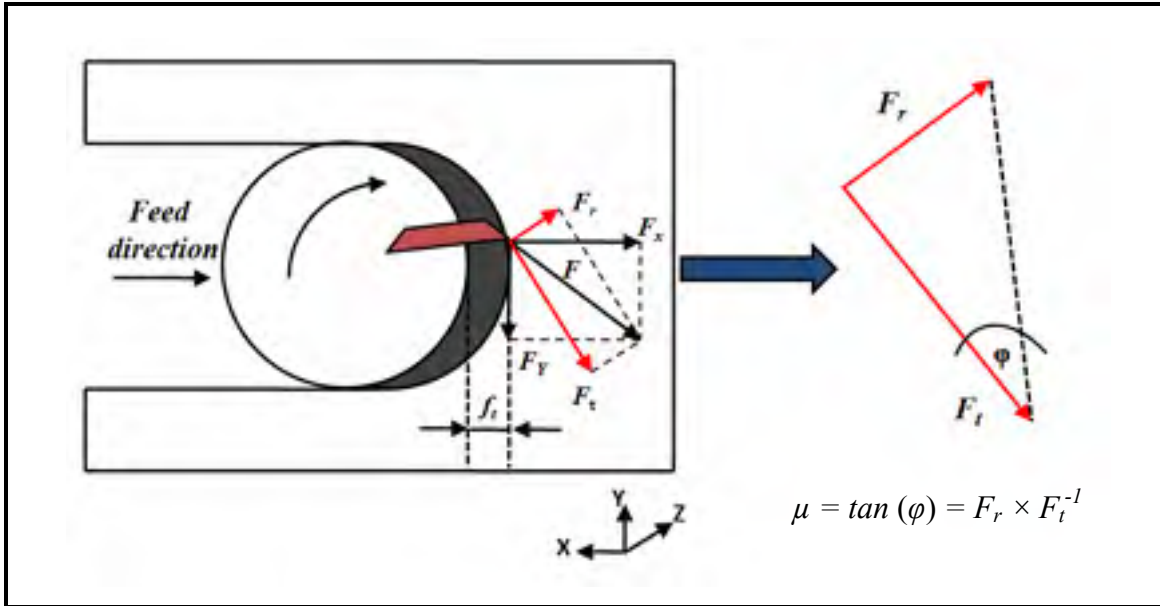


Figure 3.3 Slot milling under orthogonal cutting conditions  
(adapted from (San-Juan, Martín and Santos, 2010))

When  $F_t$  decreases, the tool face friction decreases, which leads to a corresponding increase in shear angle ( $\Phi$ ). The plastic strain associated with chip formation is thus reduced, which in turn decreases the exit up milling side ( $B_1$ ) burr size.

Based on Figure 3.2(a), the total incremental tool distance travelled is  $Rd\theta$ . Assuming that the burr formation occurs when tool is about to leave the workpiece, consequently, the total work done in the chip formation zone is:

$$\Delta W_C = \int_0^{\theta} F_t R d\theta = F_t R \theta \quad (3.11)$$

The energy required for burr formation in orthogonal machining has been estimated in (Ko and Dornfeld, 1991) as:

$$\delta W_b = \int_0^\theta \left( \frac{k_0}{2} \cos^2 \beta_0 + \frac{\sigma_e}{4} \tan \beta_0 \right) \omega R d\theta a_p \quad (3.12)$$

Where  $k_0$  is the yield shear strength,  $\sigma_e$  is the yield strength,  $Rd\theta$  is the tool movement distance since the onset of the plastic hinge  $B$  and  $a_p$  is the depth of cut. Extending Eq(3.12) to the transition point in the milling exit region, the work done for the exit up milling side burr formation can be expressed as:

$$\Delta W_b = \left( \frac{k_0}{2} \cos^2 \beta_0 + \frac{\sigma_e}{4} \tan \beta_0 \right) \omega R \theta a_p \quad (3.13)$$

According to the Von-Mises criterion for shear strength,  $\sigma_e = \sqrt{3k_0}$ , therefore, Eq(3.13) becomes:

$$\Delta W_b = \left( \frac{\sigma_e}{2\sqrt{3}} \cos^2 \beta_0 + \frac{\sigma_e}{4} \tan \beta_0 \right) \omega R \theta a_p \quad (3.14)$$

Substituting the  $B_t$  value in Eq(3.7) into Eq(3.14) yields to:

$$\Delta W_b = \frac{R\theta}{\tan \beta_0} \left( \frac{\sigma_e}{2\sqrt{3}} \cos^2 \beta_0 + \frac{\sigma_e}{4} \tan \beta_0 \right) B_t a_p \quad (3.15)$$

Based on Eqs(3.11) and (3.15):

$$F_t R \theta = \frac{R\theta}{\tan \beta_0} a_p \left( \frac{\sigma_e}{2\sqrt{3}} \cos^2 \beta_0 + \frac{\sigma_e}{4} \tan \beta_0 \right) B_t \quad (3.16)$$

Eq(3.16) simplified as:

$$F_t = \sigma_e a_p B_t \left[ \frac{\left( \frac{\sqrt{12}}{12} \cos^2 \beta_0 + \frac{1}{4} \tan \beta_0 \right)}{\tan \beta_0} \right] \quad (3.17)$$

Let us assume that:

$$A = \frac{\left( \frac{\sqrt{12}}{12} \cos^2 \beta_0 + \frac{1}{4} \tan \beta_0 \right)}{\tan \beta_0} \quad (3.18)$$

According to (Ko and Dornfeld, 1991), irrespective to workpiece material used,  $\beta_0 = 20^\circ$  under various cutting conditions. By assuming the constant value of  $A$  in Eq(3.18) as a function of  $\beta_0$ , Eq(3.17) will therefore become:

$$F_t = B_t \sigma_e a_p A \quad (3.19)$$

According to Eqs(3.7-3.8 and 3.19)  $B_t$  can therefore be expressed as:

$$B_t = \frac{F_t}{\sigma_e a_p A} \quad (3.20)$$

It is evident that the only unknown parameter in Eq(3.20) is  $F_t$ . In order to calculate the  $B_t$  and validate the model presented in Eq(3.20), the  $F_t$  can either be measured experimentally or estimated computationally. The next section fully describes the validation methods used in this study.

### 3.3 Experimental results and discussion

The model presented in this study was validated experimentally by measuring the  $F_t$ . Slot milling tests were carried out under orthogonal cutting conditions on specimens with length 38 mm; width 38 mm and thickness 12 mm. Table 3.1 summarizes the cutting parameters and their levels. The cutting tool and the workpiece materials were treated as qualitative factors, while the other remaining factors were quantitative. In total, 36 experiments were needed to complete the study, including 18 tests for each material. The experimental and modeling results obtained by using Eq(3.20) are shown in Table 3.2.

The main experimental stages were as follows:

1. Slot milling tests according to the process variables listed in Table 3.1, using a 3-axis CNC machine tool, as shown in Figure 2.1.
2. Cutting force measurement using a 3-axis dynamometer (Kistler-9255B) with a sampling frequency of 10,000 Hz.
3. Tangential force ( $F_t$ ) measurement through each output signal.
4. Burr thickness ( $B_t$ ) measurement using an optical microscope, equipped with high resolution camera to capture the burrs images (see Figure 2.2).

To develop the experimental set-up, the following assumptions were made:

- Machining tests were assumed chatter-free. This condition was fulfilled by carrying out preliminary tests and checking the stability of cutting process.
- The deflection of the tool and workpiece were assumed negligible. This condition was fulfilled using a rigid tool and workpiece fixtures.
- Figures 3.4-3.5 are plotted to present the experimental and modeled values of  $B_t$  in each material. Three fitting models were used to study the correlation between modeled and experimental values of  $B_t$  in both materials.

Table 3.1 Cutting parameters and their levels

Process Parameters	Level		
	1	2	3
A: Cutting speed (m/min)	300	750	1200
B: Feed per tooth (mm/z)	0.01	0.055	0.1
C: Depth of cut (mm)	1	-	2
D: Material	AA 2024-T351	-	AA 6061-T6
E: Tool	Z=3, R $\epsilon$ = 0.5 mm, Coating: TiCN+Al <sub>2</sub> O <sub>3</sub> +TiN		
Cutting fluid	None (Dry machining)		

According to the linear and exponential design models are the best fitting models for AA 2024-T351 and AA 6061-T6 with minimum correlation coefficients of 95.11% and 88.13%, respectively.

Table 3.2 Experimental and modeling results

No.	Process parameters			AA 2024-T351		AA 6061-T6	
	$v_c$ (m/min)	$f_z$ (mm/z)	$a_p$ (mm)	Experimental $B_t$ (mm)	Modeled $B_t$ (mm)	Experimental $B_t$ (mm)	Modeled $B_t$ (mm)
1	300	0.01	1	0.053	0.057	0.055	0.057
2	750	0.01	1	0.061	0.065	0.049	0.065
3	1200	0.01	1	0.059	0.055	0.075	0.069
4	300	0.055	1	0.089	0.123	0.125	0.096
5	750	0.055	1	0.092	0.097	0.121	0.096
6	1200	0.055	1	0.126	0.123	0.101	0.107
7	300	0.1	1	0.124	0.146	0.176	0.173
8	750	0.1	1	0.141	0.160	0.146	0.169
9	1200	0.1	1	0.144	0.149	0.145	0.131
10	300	0.01	2	0.064	0.081	0.116	0.088
11	750	0.01	2	0.093	0.081	0.128	0.086
12	1200	0.01	2	0.089	0.070	0.116	0.079
13	300	0.055	2	0.121	0.142	0.133	0.144
14	750	0.055	2	0.130	0.122	0.125	0.106
15	1200	0.055	2	0.150	0.151	0.147	0.119
16	300	0.1	2	0.166	0.186	0.200	0.187
17	750	0.1	2	0.191	0.192	0.166	0.158
18	1200	0.1	2	0.193	0.184	0.172	0.160

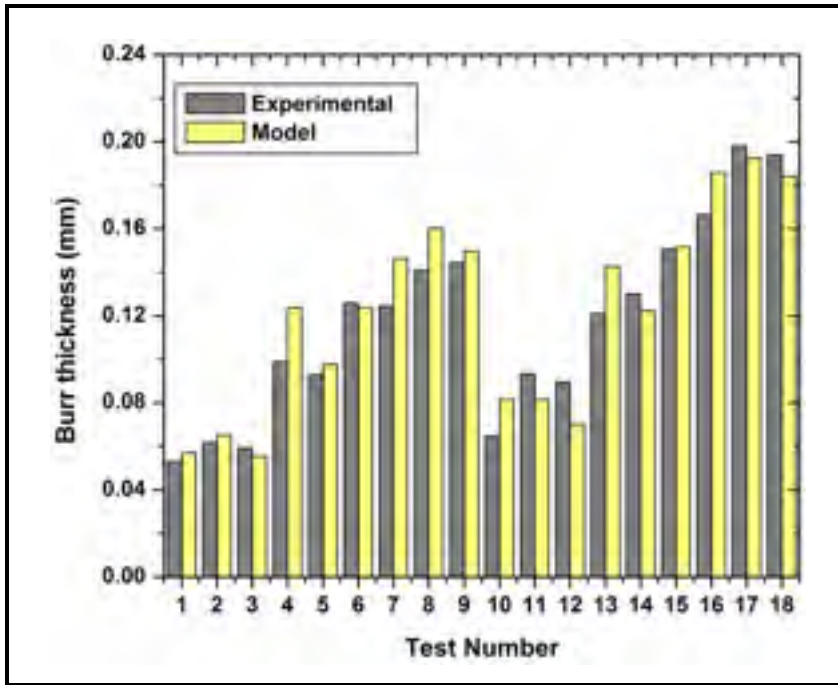


Figure 3.4 Experimental and modeled  $B_r$  for AA 2024-T351 (using Eq(3.20))

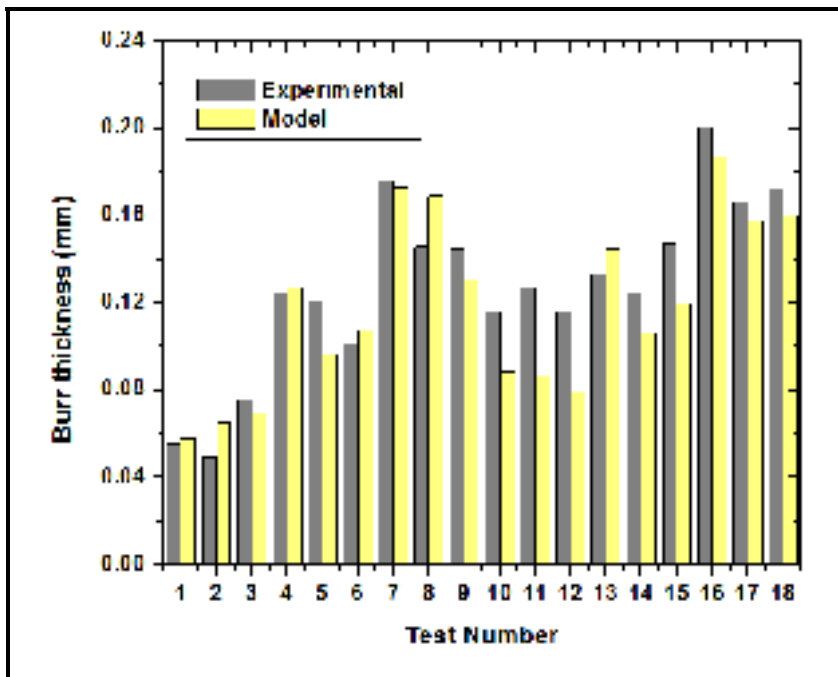


Figure 3.5 Experimental and modeled  $B_r$  for AA 6061-T6 (using (Eq(3.20))

Table 3.3 Statistical summary of regression models between experimental and modeled  $B_t$

List	Regression Model	AA 2024-T351				AA 6061-T6			
		CC (%)	R <sup>2</sup> (%)	F	P	CC (%)	R <sup>2</sup> (%)	F	P
1	Linear	<b>95.96</b>	<b>91.44</b>	<b>171.13</b>	<b>0</b>	89.66	80.39	65.61	0
2	Exponential	95.11	95.11	151.8	0	<b>91.68</b>	<b>84.05</b>	<b>84.33</b>	<b>0</b>
3	Multiplicative	95.37	90.96	161.12	0	88.13	77.68	55.69	0

### 3.4 Computational results and discussion

In milling operations, the instantaneous chip thickness  $h(\varphi)$  varies periodically as a function of a time-varying instantaneous immersion angle ( $\varphi$ ). The  $h(\varphi)$  can be approximated as:

$$h(\varphi) = f_z \times \sin(\varphi) \quad (3.21)$$

Where  $f_z$  is feed per tooth (mm/tooth).

It must be mentioned that cutting forces are generated only when the cutting tool is in cutting zone:

$$\varphi_{st} \leq \varphi \leq \varphi_{ex}$$

Where  $\varphi_{st}$  is entrance angle and  $\varphi_{ex}$  is the exit angle. For a full slotting operation,  $\varphi_{st}$  and  $\varphi_{ex}$  are 0 and  $\pi$ , respectively. It should be noted that there might be more than one tooth cutting simultaneously, depending on the number of teeth on the cutter and the radial width of cut. The tooth spacing angle or cutter pitch angle,  $\theta_p$ , is given as:

$$\theta_p = \frac{2\pi}{Z} \quad (3.22)$$

In this study, end mill tools with  $\beta = 30^\circ$ ,  $D = 19.05$  mm, and  $Z = 3$  were used. The effect of tool coating and Re on burr formation are not considered. In order to validate the model computationally, the tool was discretized to  $L$  elements of thickness  $da_p$  through axial depth of cut  $a_p$ . The bottom ends of the remaining flutes were at angles:

$$\theta_j(0) = \varphi + j.\theta_p \quad (3.23)$$

Where  $j = 0, 1, 2, \dots, N-1$ .

According to (Altintas, 2000), at an axial depth of cut  $a_p$ , the lag angle  $\gamma_0$ , is:

$$\gamma_0 = k_\beta \times a_p \quad (3.24)$$

Where:

$$k_\beta = \frac{2 \tan \beta}{D} \quad (3.25)$$

When the bottom point of a reference flute of the end mill is at an immersion angle ( $\varphi$ ), a cutting edge point that is axially above will have an immersion angle of ( $\varphi - \gamma_0$ ). The immersion angle for flute  $j$  at axial depth of cut  $a_p$  is:

$$\varphi_j(a_p) = j.\theta_p - \gamma_0 \quad (3.26)$$

The chip thickness in flute  $j$  at axial depth of cut,  $a_p$ , is:

$$h_j(\varphi_j(a_p)) = f_z \times \sin d\varphi_j(a_p) \quad (3.27)$$

The elementary cutting forces acting on the cutter in radial and tangential directions are expressed using the mechanistic equations as follows:

$$\begin{cases} dF_t = [K_{tc} \times h_j(\varphi_j(a_p)) + K_{te}] \times d(a_p) \\ dF_r = [K_{rc} \times h_j(\varphi_j(a_p)) + K_{re}] \times d(a_p) \end{cases} \quad (3.28)$$

Where,  $dF_t$  and  $dF_r$  are the differential tangential and radial forces. The two coefficients,  $K_{tc}$  and  $K_{rc}$  are specific cutting pressure coefficients provided by shearing actions in the tangential and radial directions, respectively, while  $K_{te}$  and  $K_{re}$  are the specific cutting pressure coefficients provided by the contact edge in the tangential and radial directions. The edge and shear coefficients can be extracted using orthogonal cutting tests, or average cutting forces. According to (Zaghbani *et al.*, 2012), many authors have mentioned the dependency of average cutting forces to feed rate and speed. It is evident that this technique is relatively time consuming, especially when certain levels of cutting speeds and tools are employed. In addition, according to (Lauderbaugh, 2009; Mian, Driver and Mativenga, 2011a) and experimental results presented in second chapter of this thesis, the effects of cutting speed on burr size is negligible. Therefore to computationally validate the model presented in Eq(3.20), the effect of cutting speed on  $B_t$  can be considered negligible. Furthermore, in order to avoid repeating the preliminary tests for cutting force coefficients measurements, an alternative method is proposed to approximate the cutting forces using specific cutting force coefficient,  $K_c$ , with respect to material properties that can be found in material handbooks (Davis, Mills and Lampman, 1990).

Differential tangential force ( $dF_{t,j}$ ) acting on a differential flute element with height  $da_p$  is then expressed as:

$$dF_{t,j}(\varphi_j(a_p)) = [K_c \times h_j(\varphi_j(a_p))] \times d(a_p) \quad (3.29)$$

According to (Davis, Mills and Lampman, 1990), in the case of milling, when  $h_m \neq 0.2$  mm, the  $K_c$  can be obtained using Eq(3.29):

$$K_c = K_s \left( \frac{0.2}{h_m} \right)^{0.29} \quad (3.30)$$

Where,  $h_a$  is the average chip thickness per revolution and  $K_s$  (N/mm<sup>2</sup>) is the specific cutting force coefficient when  $h_m \neq 0.2$  mm.

The  $h_m$  can be calculated from the swept zone as:

$$h_m = \frac{\int_{\varphi_{st}}^{\varphi_{ex}} f_z \times \sin \varphi (d\varphi)}{\varphi_{ex} - \varphi_{st}} = f_z \frac{\cos(\varphi_{ex}) - \cos(\varphi_{st})}{\varphi_{ex} - \varphi_{st}} \quad (3.31)$$

The  $K_s$  values for different materials when using various levels of feed rate ( $f_r$ ) can be found in (Davis, Mills and Lampman, 1990). By substituting obtained values of  $K_s$  and  $h_m$  in Eq(3.30), the corresponding values of  $K_c$  under specific cutting conditions is obtained. Table 3.4 presents  $h_m$ ,  $K_c$  and  $K_s$  values in each verification test performed on AA 6061-T6 and AA 2024-T351. Using the prescribed method, an algorithm was written to calculate the  $h(\varphi)$  under various cutting conditions. Tangential forces were then approximated based on Eq(3.29). Therefore, differential burr thickness with respect to immersion angle in flute j,  $dB_{t,j}(\varphi_j(a_p))$ , can be presented in Eq(3.32):

$$dB_{t,j}(\varphi_j(a_p)) = \frac{[K_c \times h_j(\varphi_j(a_p))] \times d(a_p)}{\sigma_e A a_p} \quad (3.32)$$

The following procedure (see Figure 3.6) is used to model the  $B_t$  in exit up milling side burr in MATLAB:

1. Set the input variables, such as cutting parameters ( $a_p$ ,  $f_z$ ,  $n$ ,  $\varphi_{st}$ ,  $\varphi_{ex}$ ), tool geometry ( $Z$ ,  $D$ ,  $\beta$ ), cutting constant ( $K_c$ ) and cutter pitch angle ( $\theta_p$ ).
2. Discretize the cutting tool into small elements of thickness  $da_p$ .

3. Calculate the immersion angle ( $\varphi$ ) for first flute  $j$  with respect to each flute's bottom edge using Eq(3.23).
4. Calculate the immersion angle due helix angle ( $\beta$ ) for flute  $j$  (if the tool cuts the edge) using Eqs(3.24-3.29).
5. Calculate the  $h(\varphi)$  in flute  $j$  at axial depth of cut  $a_p$  using Eq(3.27).
6. Calculate the  $K_c$  (Eq(3.30)) by using  $h_m$  value of the tested material obtained from Eq(3.31)).
7. Calculate differential tangential force ( $dF_{t,j}$ ) acting on a differential flute element with height  $da_p$  using Eq(3.29).
8. Use of assumption made in the model;  $\Delta W_c = \Delta W_b$  and  $\beta_0 = 20^\circ$ .
9. Calculate  $B_t$  according to Eq(3.32).

The computational model presented in Eq(3.20) was used to simulate the  $B_t$  according to the process parameters listed in Table 3.1. Simulated values of  $B_t$  as presented in Table 3.4 were then compared with those obtained through experimental measurements. Because of yield strength ( $\sigma_e$ ) which is higher in AA 2024-T351 than in AA 6061-T6 (see Table 2.2), larger resulting values of  $B_t$  is obtained for AA 6061-T6 (see Figures 3.7-3.8). Statistical summary of regression models in Table 3.5 exhibits a significant agreement between simulated and experimental values in both materials, despite of ignoring the effects of insert nose radius ( $R\epsilon$ ), tool coating and cutting speed on cutting force and burr formation. The correlation coefficient between simulated and experimental values of  $B_t$  exceeds 92% in AA 2024-T351 and 83% in AA 6061-T6 (see Table 3.5).

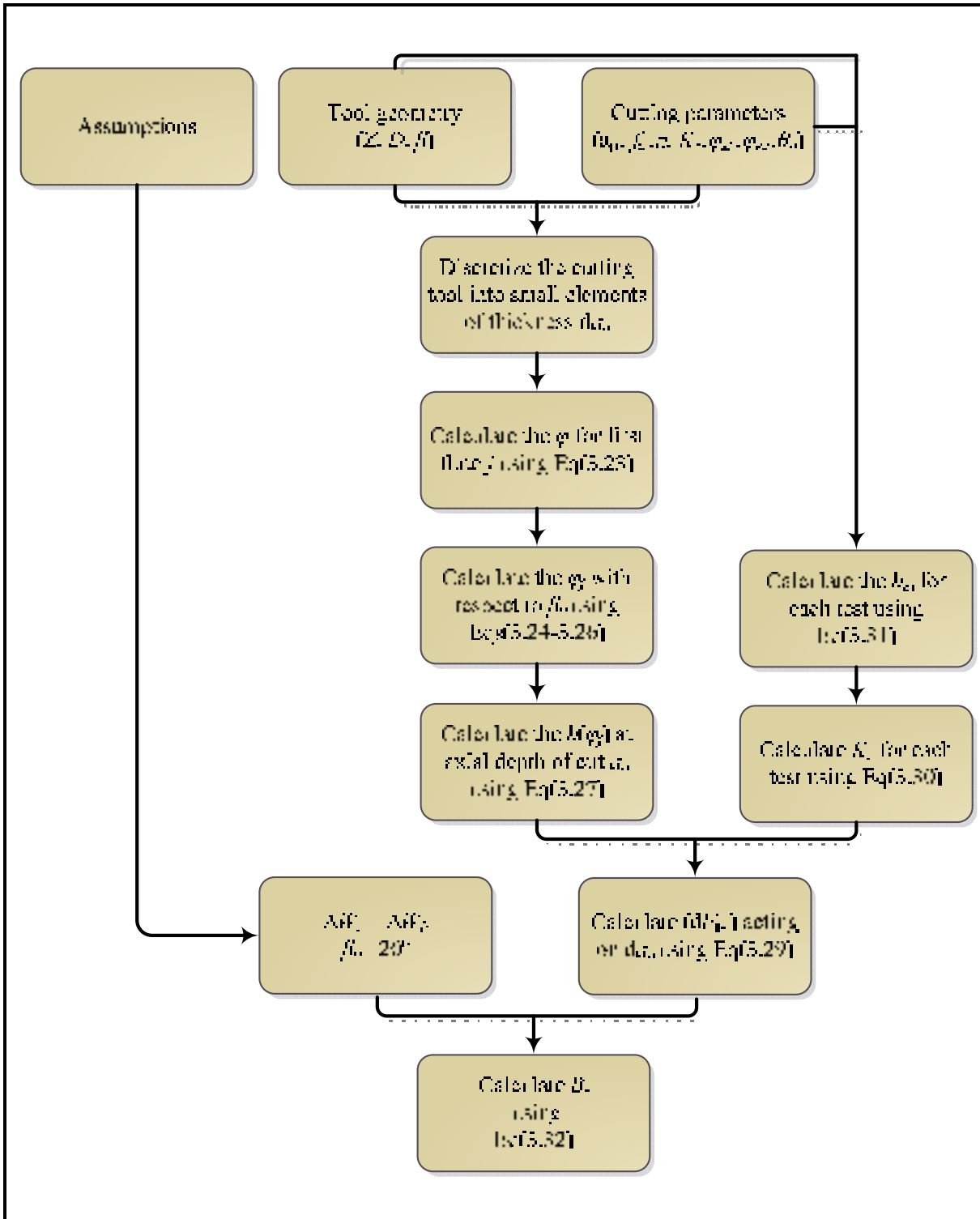


Figure 3.6 Scheme of the proposed theoretical model for  $B_1$  prediction

Table 3.4 Experimental and simulated results when  $Z=3$ ;  $D=19.05$  mm;  $\beta=30^\circ$  and  $v_c=300$ m/min

Test No.	Process parameters					AA 2024-T351		AA 6061-T6	
	$f_r$	$a_p$	$h_m$	$K_s$	$K_c$	$B_{Dexp}$ (mm) *	$B_{Dsim}$ (mm)**	$B_{Texp}$ (mm) *	$B_{Tsim}$ (mm)**
1	0.03	1	0.006	700	1908	0.053	0.055	0.055	0.065
2	0.165	1	0.035	480	798	0.099	0.128	0.125	0.151
3	0.3	1	0.063	400	559	0.124	0.162	0.176	0.191
4	0.03	2	0.006	700	1904	0.064	0.057	0.116	0.067
5	0.165	2	0.035	480	798	0.121	0.132	0.133	0.155
6	0.3	2	0.063	400	559	0.166	0.167	0.201	0.198

\*: Experimental burr thickness; \*\*: Simulated burr thickness

Table 3.5 Statistical summary of the regression models between experimental and simulated results

List	Regression model	AA 2024-T351				AA 6061-T6			
		CC (%)	R <sup>2</sup> (%)	F	P	CC (%)	R <sup>2</sup> (%)	F	P
1	Linear	94.03	88.42	30.54	0	<b>88.32</b>	<b>78.01</b>	<b>14.19</b>	<b>0.0196</b>
2	Exponential	92.06	84.75	22.23	0.0092	85.11	72.44	10.52	0.0316
3	Multiplicative	<b>96.10</b>	<b>92.36</b>	<b>48.36</b>	<b>0.0022</b>	83.69	70.04	9.35	0.0377

CC = Correlation Coefficient; F = F- ratio; P = P- value

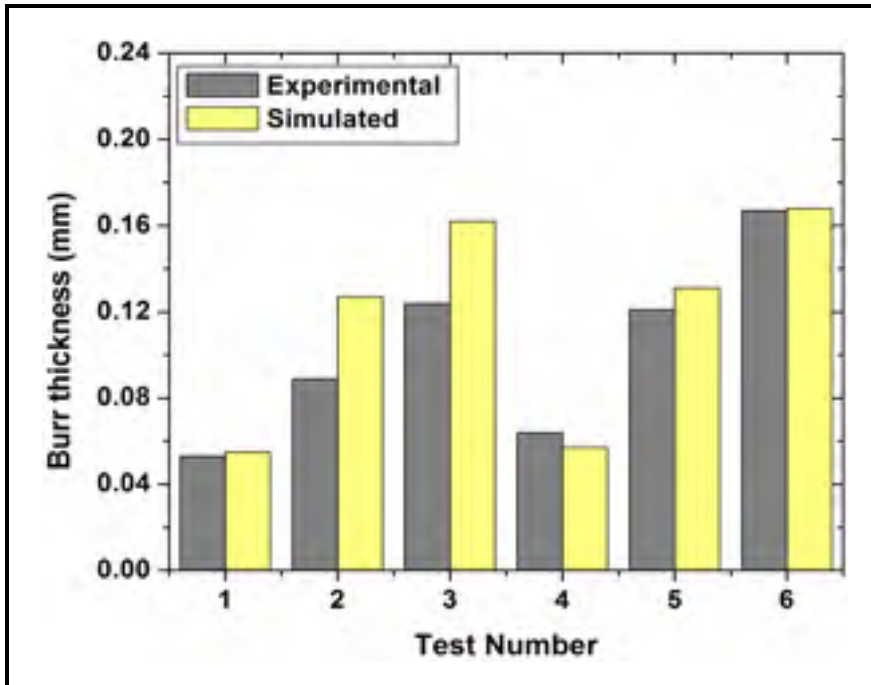


Figure 3.7 Experimental and simulated  $B_t$  for AA 2024-T351 (using Eq(3.32))

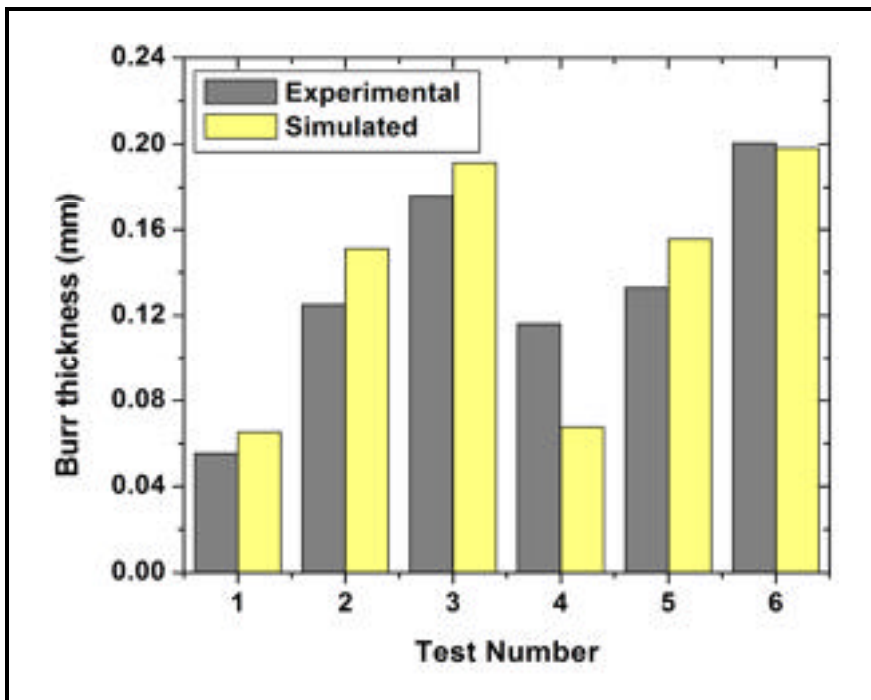


Figure 3.8 Experimental and simulated  $B_t$  for AA 6061-T6 (using Eq(3.32))

### 3.5 Conclusion

- The analytical and computational models are proposed to predict the exit up milling side burr thickness ( $B_t$ ). The main advantage of the proposed models is that they are both sensitive to material properties and cutting parameters. The only unknown parameter in models is  $F_t$ , which is also a function of cutting parameters and material properties, and it could be easily predicted.
- The proposed models do not require the experimental measurements of the shear angle ( $\Phi$ ), friction angle ( $\lambda$ ) and tool chip contact length ( $L$ ), unlike existing analytical burr size prediction models.
- Regardless of different levels of process parameters and assumptions employed, both models were verified experimentally. Very good correlations were found between the experimental and modeled values of  $B_t$  in both materials.
- It was found that the  $B_t$  in ductile materials is highly sensitive to material properties such as yield strength ( $\sigma_e$ ) and cutting force coefficient ( $K_e$ ).
- Because of yield strength which is higher in AA 2024-T351 than in AA 6061-T6, larger resulting values of  $B_t$  are obtained for AA 6061-T6 under similar cutting conditions.



## CHAPTER 4

### SIMULTANEOUS OPTIMIZATION OF BURR SIZE AND SURFACE FINISH DURING SLOT MILLING OPERATION

#### 4.1 Introduction

Nowadays due to growth of industrials competition, the use of suitable optimization methods for correct selection of process parameters is extremely necessary to avoid non- value added expenses. The optimization of process parameters requires a systematic methodological approach by using experimental methods and mathematical/statistical models (Gaitonde, Karnik and Davim, 2009). Fuzzy logic (FL), genetic algorithm (GA), Neural Network (NN), Taguchi method and response surface methodology (RSM) are the latest optimization techniques that are being applied successfully in industrial applications. Artificial neural network (ANN) is a computational learning system which attempts to simulate the human intuition in making decisions and drawing conclusions when presented with complex, irrelevant, and partial information (Karnik, Gaitonde and Davim, 2008). In the past, ANNs have been successfully employed to model several processes and also define the optimum conditions of process parameters (Tong, Kwong and Yu, 2004; Vafaeseefat, 2009).

On the other hand, RSM-based models can be developed with minimum process knowledge, thus, saving time and cost in experimentation is anticipated. RSM has been also widely used for modeling and optimization of machining operations (Lee, Chung and Lee, 2011; Mandal, Doloi and Mondal, 2012; Moola, Gorin and Hossein, 2012; Yang *et al.*, 2012). However the RSM models are only accurate for a narrow range of input process parameters, while developing higher order models requires a larger number of experiments (Karnik, Gaitonde and Davim, 2008). In order to perform GA optimization, developing an accurate model that describes the complex and nonlinear relationships between process parameters and performance characteristics (responses) is strongly required. Several methods such as desirability function were proposed for multiple responses optimization. In a recent study by (Niknam, Kamguem and Songmene, 2012), desirability function was employed to select the

optimum setting levels of process parameters for simultaneous minimization of surface roughness and exit burr size (thickness and height) during slot milling of AA 6061-T6. The obtained results were pretty close to optimum conditions.

Amongst described methods, the Taguchi-based optimization method has produced a unique and powerful discipline that differs from traditional practices. It has shown a wide range of industrial applications for making the product/process insensitive to any uncontrollable factors such as environmental variables (Luo, Liu and Chen, 2008; Phadke, 1989). In addition, Taguchi method can be used to optimize the performance characteristics, while it can economically satisfy the needs of problem solving and design optimization with less number of experiments without the need for process model developments. The original Taguchi method is designed to optimize a single response (Gaitonde, Karnik and Davim, 2009). However, most of the products have multiple responses, and hence, there is a need to obtain a single optimal setting level that can be used to produce products with optimum or near optimum characteristics as a whole.

Optimization of multiple responses in Taguchi style experiments has received little attention, because Taguchi method can not be applied directly, as each response may not have the same measurement unit. Hence, it is extremely necessary to apply modifications to Taguchi method. A limited number of modifications to original Taguchi method has been suggested until now (Kilickap, 2010). Therefore, the objective of this chapter is to propose new modifications to application of Taguchi method for correct selection of process parameters and multiple responses optimization. The proposed methodology will be verified by presenting the optimum cutting conditions for burrs size and surface roughness optimization during slot milling of AA 6061-T6.

The presented results in this chapter led to a journal article that was submitted to *Journal of Precision Engineering and Manufacture* in July 2012.

## 4.2 An overview of Taguchi Method

Robust design is recognized as the most significant contribution of Taguchi method for improving the product quality and system reliability. A robust design drawn by Taguchi aims to obtain the lowest cost solution to the product design specifications based on clients expectations. The optimization of a process or product design using Taguchi approach can be accomplished upon fulfillment of concept design, system design, parameter design and tolerance design. Taguchi method based on factorial design of experiment divides the independent variables into controllable and noise factors. Controllable factors are those that can be maintained to a desired value, while noise factors are those that may not be controlled. Inadequate selection of these factors can lead to false conclusion, thus experimentations must be repeated. After selecting the factors, their desired number of levels is determined. The third stage is performed after completion of the parameters design. A robust design drawn by Taguchi method aims to achieve a robust process or product design whose response values are less sensitive to noise factors. Considering signal to noise ratio (SNR), the aim can be fulfilled by reducing the variability around target value through the use of quality loss function.

The Taguchi method classifies quality characteristics to one of the following three types (Kilickap, 2010):

- Larger- the- better

$$\text{SNR} (\eta) = -10 \log_{10} \left( \frac{I}{N} \sum_{i=1}^N Y_i^{-2} \right) \quad (4.1)$$

Where  $N$  is number of replications and  $Y_i$  is response.

- Smaller- the- better

$$\text{SNR} (\eta) = -10 \log_{10} \left( \frac{I}{N} \sum_{i=1}^N Y_i^2 \right) \quad (4.2)$$

The larger-the-better and smaller-the-better terms are applied to maximize and minimize the quality characteristics, respectively.

- Nominal-the-better

$$\text{SNR} (\eta) = -10 \log_{10} \left( \frac{m^2}{\sigma^2} \right) \quad (4.3)$$

Where:

$m$  = mean of responses

$\sigma$  = standard deviation of responses

Upon successful implementation of the SNR to responses, it is then possible to reduce the mean values of responses while also minimizing their variances.

The main critics drawn against Taguchi method are (Kilickap, 2010):

1. The approach fails to adequately deal with situations where significant interactions between process parameters are present.
2. The logic behind SNR is unconvincing and usually misleading.

### 4.3 Proposed methodology

In order to optimize the multiple responses, Taguchi design is not applied directly, as each response may not have the same measurement unit. Hence, it is extremely necessary to apply appropriate modifications to Taguchi method to obtain an objective function. This can be accomplished by proposing fitness mapping function ( $\psi$ ) for each trial as:

$$\psi = M_p (Y_1, Y_2, \dots, Y_n) \quad (4.4)$$

Where,  $M_p$  is mapping function;  $\psi$  is fitness mapping function and  $Y_1, Y_2, \dots, Y_n$  are non-identical responses in each trial.

Each response has a range ( $R$ ) as follows:

$$Y_i : [0-R_i] \quad (4.5)$$

Where,  $R_i$  is the maximum value of  $Y_i$  that can be experimentally determined and/or can be maintained as a desired value followed by experience or modeling approaches.

If  $n$  responses in each trial are studied, then the following relationships exist:

$$\begin{aligned} 0 &\leq Y_1 \leq R_1 \\ 0 &\leq Y_2 \leq R_2 \\ &\vdots \\ 0 &\leq Y_n \leq R_n \end{aligned} \quad (4.6)$$

In order to construct the  $\psi$ , each response within the range of  $[0-R_i]$  must be mapped into a fixed fitness range of  $[M-0]$ , where  $M$  is the maximum value of fitness mapping range ( $M_R$ ). All objective functions may have the same contribution on the  $\psi$ . If not, weighting coefficients ( $\omega$ ) can be maintained for each response, which varies their level of importance on the  $\psi$ . When this level is equal to one, the  $\psi$  formed by combination of  $n$  objective functions in trial  $i$  can be presented as:

$$\psi_i = \frac{\psi_1 + \psi_2 + \dots + \psi_n}{n} \quad (4.7)$$

Where,  $\psi_1, \psi_2, \dots, \psi_n$  are fitness mapping function of responses. In order to map response  $Y_i$  with a range of  $[0, R_i]$  into  $\psi_i$  with a  $M_R = [M, 0]$ , a mapping coefficient must be used as follows:

$$\begin{aligned} \psi_1 &= M - (\mu_1 \times Y_1) \\ \psi_2 &= M - (\mu_2 \times Y_2) \\ &\vdots \\ \psi_n &= M - (\mu_n \times Y_n) \end{aligned} \quad (4.8)$$

Where  $\mu_1, \mu_2, \dots, \mu_n$  are mapping coefficients of  $n$  responses.

Thus, mapping coefficients can be rewritten as:

$$\begin{aligned}\mu_1 &= (R_1^{-1}) \times M \\ \mu_2 &= (R_2^{-1}) \times M \\ &\vdots \\ \mu_n &= (R_n^{-1}) \times M\end{aligned}\tag{4.9}$$

Combining Eqs(4.7) and (4.9) yields to Eq(4.10) as follows:

$$\psi_i = \frac{M - (\mu_1 \times Y_1) + \dots + M - (\mu_n \times Y_n)}{n}\tag{4.10}$$

The Eq(4.10) can be rewritten as:

$$\psi_i = M - \left[ \frac{1}{n} \sum_{j=1}^n \mu_j \times Y_j \right]\tag{4.11}$$

When there are  $N$  replications, Eqs(4.4-4.11) must be used to calculate the  $\psi_i, \dots, \psi_n$ .

Taguchi recommends analyzing the mean response for each run in the inner array using an appropriately chosen  $SNR(\eta)$  that can serve as an objective function for optimization (Phadke, 1989). The process parameters governing objective functions could be determined using ANOVA. To this end, the Taguchi method's category must be defined first (larger-the-better, nominal-the-better and smaller-the-better). Considering the case of "larger-the-better" category,  $SNR(\eta)$  is then applied on constructed  $\psi_i$  in trial  $i$  as:

$$\eta_{\psi_i} = -10 \log_{10} (\psi_i)^2\tag{4.12}$$

Overall mean ( $m$ ) of  $\eta_\psi$  is given by:

$$m_{\eta_\psi} = \frac{1}{N} \sum_{i=1}^N \eta_{\psi_i} \quad (4.13)$$

Effect of a factor level  $k$  for parameter  $P$  with total levels of  $L$  is:

$$\left(m_{\eta_\psi}\right)_{k,p} = \frac{1}{L} \sum_{i=1}^N (\eta_{\psi})_i \quad (4.14)$$

When Taguchi method in “larger-the-better” category is used, therefore, the optimum level of a factor  $P$  is the level with the highest SNR as follows:

$$(P)_{k,opt} = \left(m_{\eta_\psi}\right)_{k,p} \max \quad (4.15)$$

Where  $k=1, \dots, L$  is level of process parameter.

The  $(\eta_\psi)_{opt}$  under optimal condition can be determined as follows:

$$\left(\eta_\psi\right)_{k,opt} = \left(m_{\eta_\psi}\right)_{k,p} + \sum_{p=1}^T \left[ \left( \left(m_{\eta_\psi}\right)_{k,p} \right)_{\max} - \left(m_{\eta_\psi}\right)_{k,p} \right] \quad (4.16)$$

Where  $\left( \left(m_{\eta_\psi}\right)_{k,p} \right)_{\max}$  is maximum SNR of  $\eta_\psi$  in optimum level  $k$  of factor  $P$  and  $T$  is the total number of influencing process parameters on the responses.

After introducing the optimum process parameters, the predicted optimum responses can be determined as:

$$\left\langle \begin{matrix} (A_k, B_k, \dots, Z_k)_{opt} \\ k = 1, 2, \dots, L \end{matrix} \right\rangle (Y_1, Y_2, \dots, Y_n)_{opt} \quad (4.17)$$

Where:

$k=1, \dots, L$  is level of optimized process parameters;

$(A_k, B_k, \dots, Z_k)_{opt}$  are optimum process parameters setting levels;

$(Y_1, Y_2, \dots, Y_n)_{opt}$  are optimum responses;

The mean value of each identical response characteristic  $i$ , when implementing  $N$  trials is:

$$(m_Y)_a = \left( \frac{1}{N} \sum_{i=1}^N Y_i \right)_a \quad (4.18)$$

Where  $\alpha = 1, \dots, N$  are the responses obtained in  $N$  replications.

Suppose  $Y_i$  is within the range of  $(B, C)$ , where  $B$  and  $C$  are minimum and maximum values of measured/expected responses. Therefore the desirable range is when  $B \leq Y_i \leq C$ . In this case, desirability of each response ( $d_i$ ) can be defined as follows:

$$d_i = \left( \frac{Y_i - C}{B - C} \right)^t \quad (4.19)$$

Where  $t$  is a weight exponent value.

If the importance level of all responses is similar,  $t$  can be assigned as one. Therefore, the desirability of simultaneous objective function is a geometric mean of all transformed responses:

$$D_i = (d_1 \times d_2 \times \dots \times d_n)^{1/n} = \left( \prod_{i=1}^n d_i \right)^{1/n} \quad (4.20)$$

Where  $n$  is the number of responses planned for optimization.

According to Eq(4.19), if any of individual desirability index of proposed optimum response ( $d_1, \dots, d_n$ ) is 0, then  $D_i$  becomes 0. This means that the proposed optimum condition is completely undesirable for multiple responses optimization. Therefore the process parameters must be revised (see Figure 4.1).

The prediction error ( $\varepsilon$ ) is:

$$\varepsilon = \frac{m_{\eta_{\psi}} - (\eta_{\psi})_{opt}}{m_{\eta_{\psi}}} \times 100\% \quad (4.21)$$

The optimization rate ( $\kappa$ ) corresponding to each response is:

$$\kappa = \frac{(m_Y)_a - (Y_a)_{opt}}{(m_Y)_a} \times 100\% \quad (4.22)$$

The proposed procedure for multiple responses optimization using Taguchi method is presented in Figure 4.1

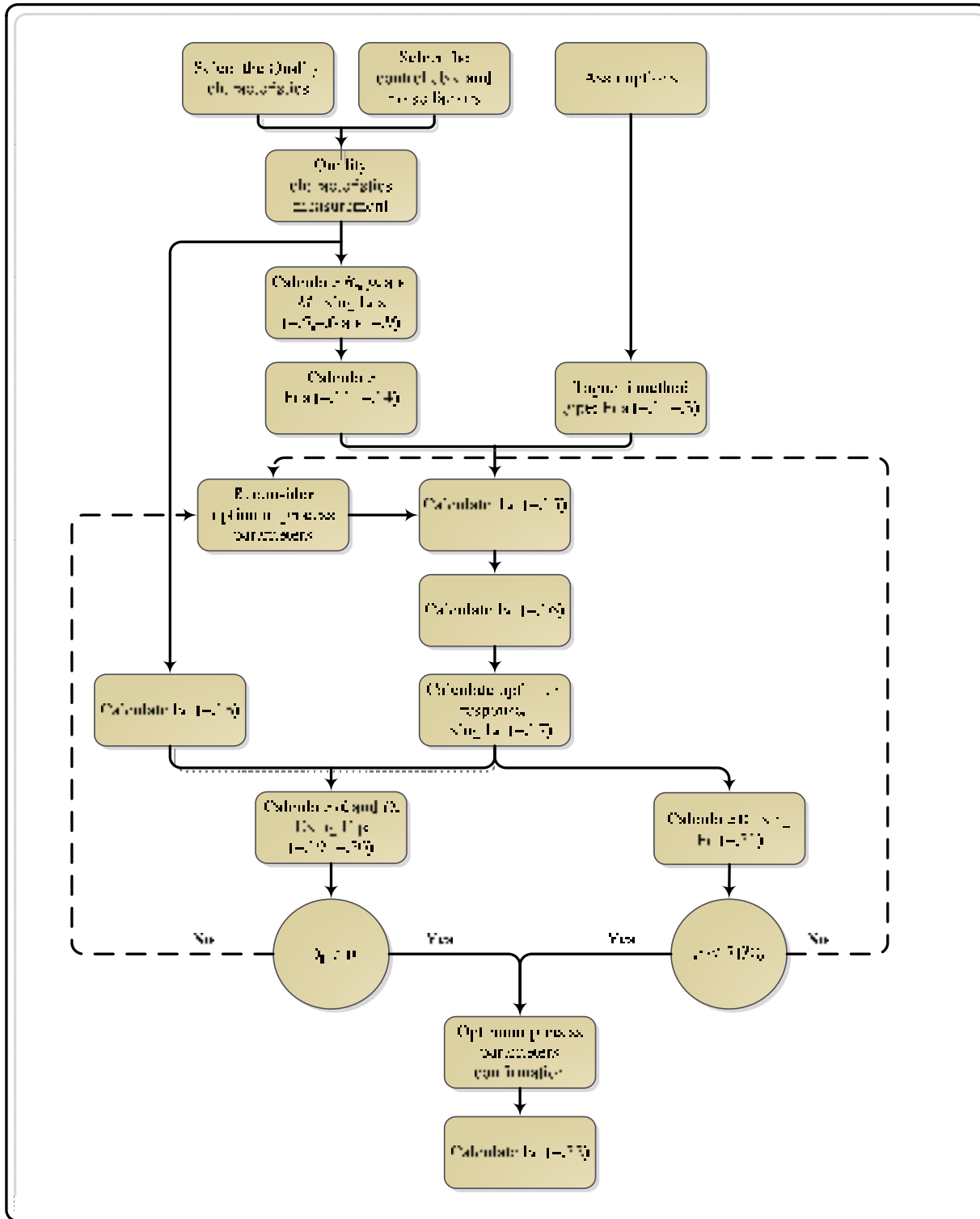


Figure 4.1 Procedure of multiple responses optimization using Taguchi method

## 4.4 Experimental results

### 4.4.1 Experimental procedure

Slot milling operations were performed on AA 6061-T6 specimens under the orthogonal dry cutting condition using a machine tool HURON - K2X10 (Power: 50kW, Speed: 28000 rpm Torque: 50 Nm). A multi-level full factorial design ( $3^3 \times 2$ ) with 54 trials was selected. The experimental factors and their levels are shown in Table 4.1. A coated end milling cutting tool with tool diameter ( $D$ ) 19.05 mm was used. As shown in Table 4.1, various levels of insert nose radius ( $R\epsilon$ ) and coating were used in experimental design plan. An optical microscope, equipped with high resolution camera was used to take the burrs images (see Figure 2.2). The burr size measurements were conducted on captured images. An average of minimum four burr thickness readings was taken as the burr size in this study (Table 4.2). Surface roughness measurements were conducted on a surface profilometer Mitutoyo SJ 400 (see Figure 2.3).

Table 4.1 Cutting parameters and their levels

Experimental parameters		Level		
		1	2	3
A: Tool	Coating	TiCN	TiAlN	TiCN+Al <sub>2</sub> O <sub>3</sub> +TiN
	Insert nose radius, $R\epsilon$ (mm)	0.5	0.83	0.5
B: Depth of cut (mm)		1	-	2
C: Feed per tooth (mm/z)		0.01	0.055	0.1
D: Cutting speed (m/min)		300	750	1200

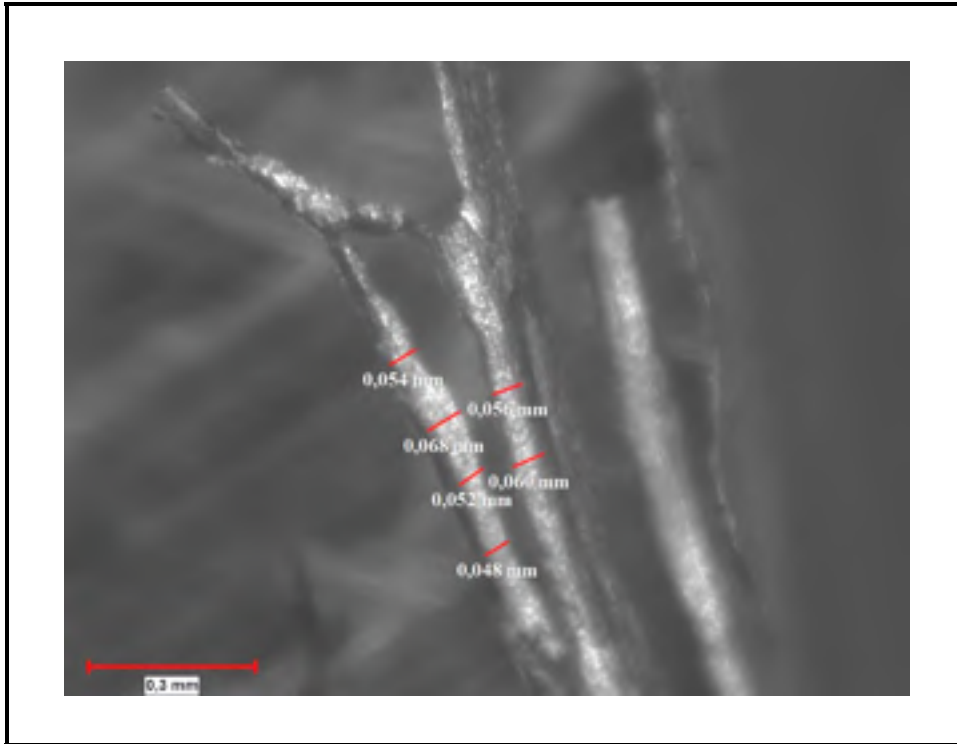


Figure 4.2 Measurement overview of exit up milling side burr ( $B_1$ )

#### 4.4.2 Analysis of responses

The measured responses alongside their mean, maximum and minimum values are presented in Table 4.2. In analyzing the quality index parameters of machined parts (e.g. burr thickness, surface roughness), statistical models play an important role (Kilickap, 2010).

Based on Figures 4.3- 4.8 and Table 4.3, it can be stated that:

- Trials with larger insert nose radius ( $R\epsilon$ ) led to thinner  $B_1$ ,  $B_4$  and  $B_5$ .
- According to Figure 4.8, a negligible difference on  $R_a$  values is observable when changing the cutting tool 2 to 1.
- Trials with higher levels of cutting speed led to thinner  $B_1$ ,  $B_4$ ,  $B_5$  and  $B_8$ , while maximized the size of  $B_2$  and  $R_a$ .
- Trials with lower level of depth of cut led to thinner  $B_1$ ,  $B_4$ ,  $B_5$  and smaller  $R_a$ .

Table 4.2 Experimental responses

Test No.	B <sub>1</sub> (mm)	B <sub>2</sub> (mm)	B <sub>4</sub> (mm)	B <sub>5</sub> (mm)	B <sub>8</sub> (mm)	Ra (μm)	ψ	η <sub>ψ</sub>
1	0.040	0.106	0.067	0.067	0.102	0.105	70.547	36.969
2	0.055	0.110	0.053	0.080	0.043	0.137	74.100	37.396
3	0.085	0.089	0.087	0.062	0.054	0.147	70.911	37.014
4	0.095	0.095	0.048	0.050	0.045	0.163	74.392	37.430
5	0.080	0.084	0.082	0.055	0.047	0.234	72.070	37.155
6	0.127	0.084	0.078	0.070	0.049	0.124	69.331	36.818
7	0.134	0.084	0.104	0.077	0.072	0.298	62.373	35.899
8	0.140	0.095	0.094	0.180	0.081	0.339	53.934	34.637
9	0.142	0.072	0.090	0.115	0.056	1.499	49.261	33.851
10	0.117	0.078	0.077	0.105	0.062	0.107	67.263	36.555
11	0.085	0.078	0.174	0.072	0.033	0.109	65.801	36.364
12	0.109	0.078	0.071	0.048	0.058	0.127	72.112	37.161
13	0.123	0.134	0.068	0.067	0.071	0.181	64.783	36.229
14	0.093	0.087	0.073	0.072	0.042	0.125	72.175	37.167
15	0.139	0.062	0.051	0.118	0.042	0.343	67.118	36.536
16	0.155	0.062	0.075	0.200	0.041	0.359	58.547	35.351
17	0.154	0.039	0.083	0.128	0.050	0.319	63.938	36.115
18	0.151	0.056	0.077	0.095	0.049	0.588	62.851	35.966
19	0.030	0.051	0.050	0.063	0.069	0.101	79.128	37.966
20	0.028	0.047	0.030	0.033	0.048	0.604	79.355	37.991
21	0.034	0.056	0.047	0.048	0.075	0.169	78.742	37.924
22	0.078	0.218	0.054	0.078	0.061	0.344	61.621	35.794
23	0.048	0.134	0.044	0.062	0.055	0.702	67.593	36.598
24	0.073	0.199	0.099	0.141	0.082	0.284	54.188	34.678
25	0.081	0.051	0.093	0.067	0.077	0.493	67.065	36.529
26	0.089	0.104	0.073	0.161	0.080	0.467	58.472	35.339
27	0.085	0.178	0.078	0.051	0.041	0.440	64.254	36.158
28	0.081	0.052	0.028	0.027	0.029	0.076	83.771	38.461
29	0.086	0.037	0.040	0.057	0.100	0.094	74.786	37.476
30	0.084	0.092	0.079	0.028	0.084	0.117	71.477	37.083
31	0.155	0.122	0.075	0.035	0.098	0.517	59.005	35.417
32	0.111	0.076	0.039	0.041	0.078	0.198	72.801	37.242
33	0.142	0.113	0.064	0.086	0.131	0.321	57.459	35.187
34	0.171	0.101	0.059	0.087	0.106	0.687	54.744	34.766
35	0.149	0.109	0.095	0.111	0.087	0.710	52.338	34.376
36	0.154	0.098	0.051	0.079	0.066	0.432	63.408	36.042
37	0.055	0.064	0.043	0.066	0.076	0.342	73.886	37.371

Table 4.2 Experimental responses (continued)

Test No.	B <sub>1</sub> (mm)	B <sub>2</sub> (mm)	B <sub>4</sub> (mm)	B <sub>5</sub> (mm)	B <sub>8</sub> (mm)	Ra (μm)	ψ	η <sub>ψ</sub>
38	0.048	0.101	0.042	0.076	0.063	0.295	72.881	37.252
39	0.075	0.110	0.045	0.051	0.042	0.262	74.073	37.393
40	0.125	0.065	0.133	0.079	0.135	0.432	55.011	34.808
41	0.121	0.067	0.057	0.103	0.047	0.209	69.495	36.839
42	0.101	0.042	0.061	0.076	0.064	0.512	69.306	36.815
43	0.176	0.064	0.089	0.158	0.067	1.331	45.751	33.207
44	0.146	0.104	0.045	0.069	0.051	0.918	60.595	35.648
45	0.145	0.119	0.057	0.089	0.066	1.305	51.650	34.262
46	0.116	0.050	0.044	0.059	0.064	0.292	72.644	37.224
47	0.127	0.042	0.047	0.061	0.051	0.333	72.820	37.245
48	0.116	0.051	0.040	0.069	0.035	0.273	75.015	37.503
49	0.133	0.056	0.121	0.189	0.133	0.481	48.333	33.684
50	0.125	0.063	0.063	0.088	0.062	0.257	68.376	36.698
51	0.147	0.050	0.151	0.111	0.063	0.484	56.349	35.017
52	0.205	0.080	0.074	0.060	0.080	1.250	50.736	34.106
53	0.166	0.068	0.087	0.149	0.050	1.452	47.087	33.458
54	0.172	0.092	0.051	0.134	0.044	1.494	49.197	33.838
<b>Max</b>	0.205	0.218	0.174	0.200	0.135	1.499	83.771	38.461
<b>Average</b>	0.111	0.085	0.070	0.085	0.066	0.444	64.906	36.148
<b>Min</b>	0.028	0.037	0.028	0.027	0.029	0.076	45.751	33.207

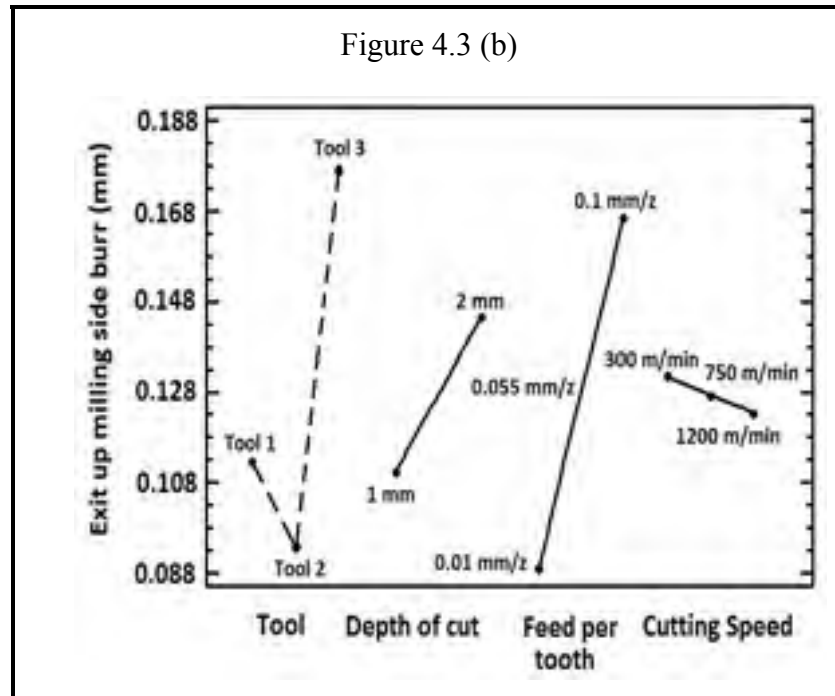
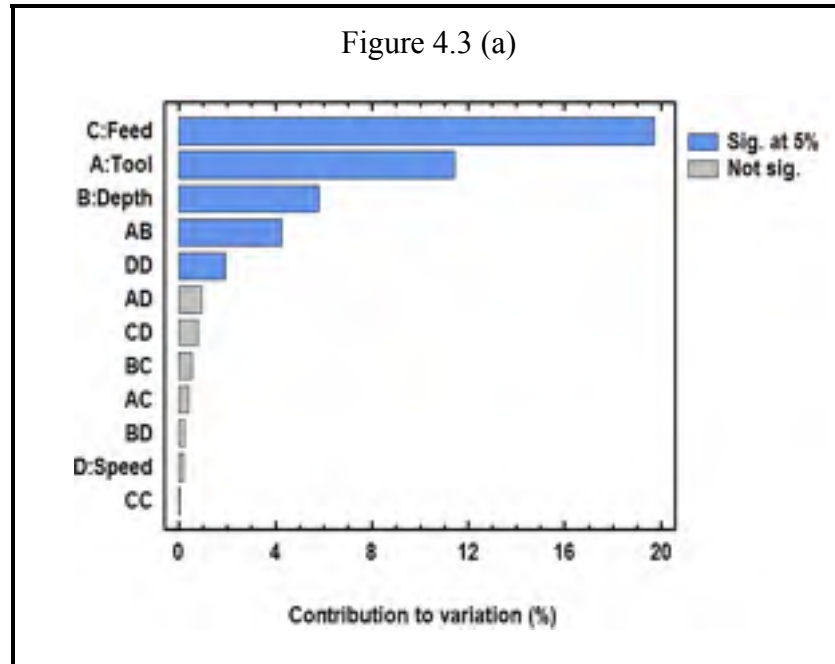


Figure 4.3 (a) Pareto chart and (b) main effect plot of B<sub>1</sub> burr thickness

Where

- Tool 1: TiCN, R<sub>e</sub> = 0.5 mm
- Tool 2: TiCN+Al<sub>2</sub>O<sub>3</sub>+TiN, R<sub>e</sub> = 0.83 mm

- Tool 3: TiAlN ,  $R_e = 0.5$  mm

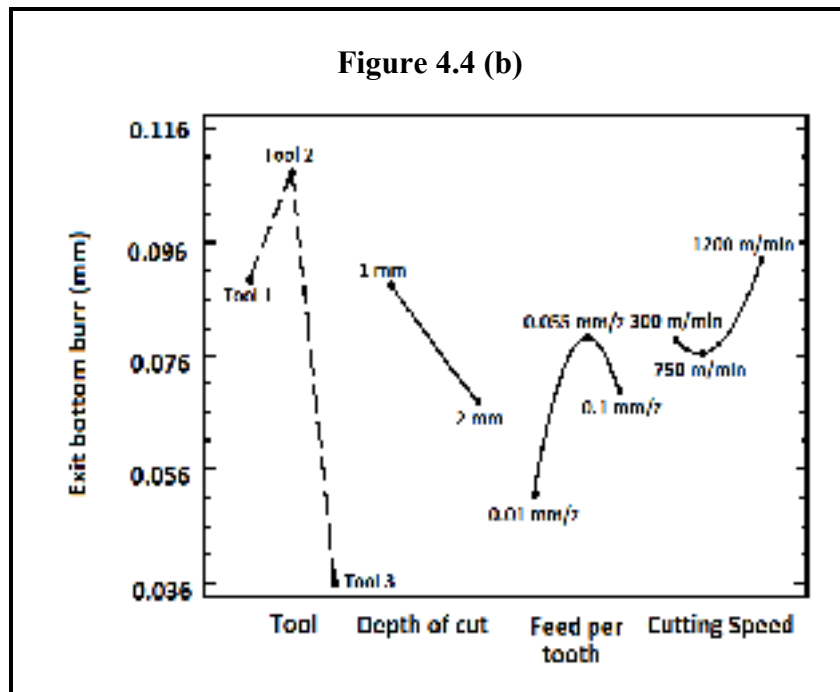
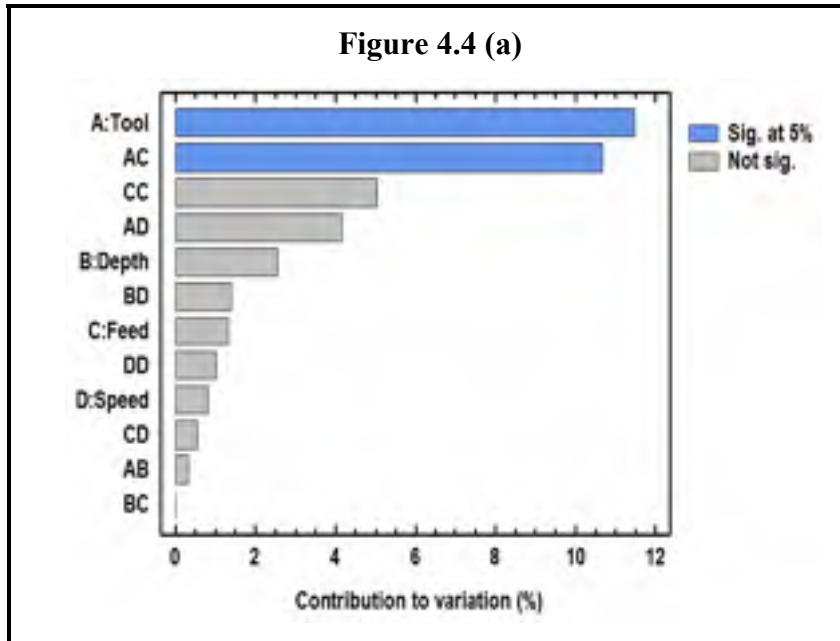


Figure 4.4 (a) Pareto chart and (b) main effect plot of B<sub>2</sub> burr thickness

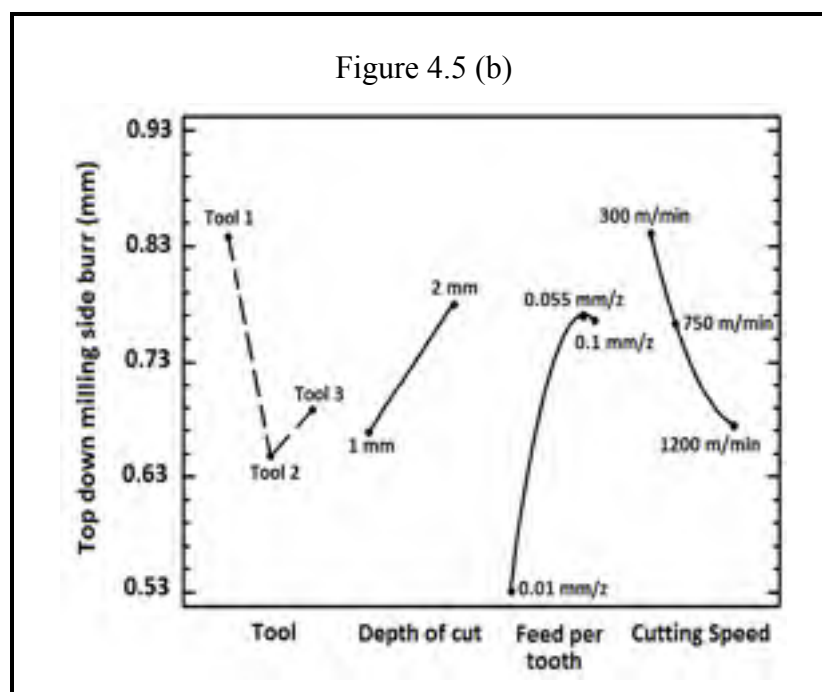
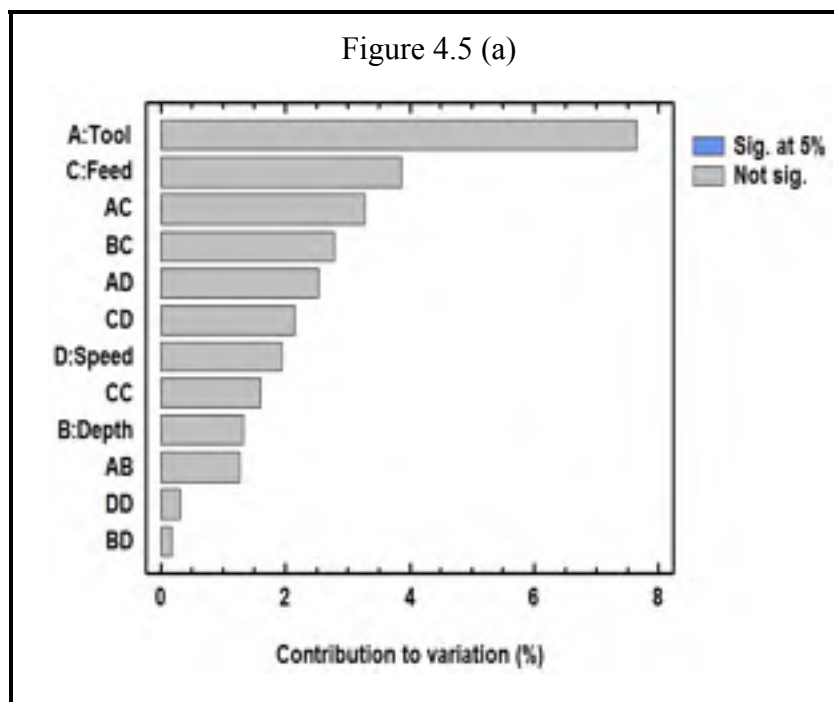


Figure 4.5 (a) Pareto chart and (b) main effect plot of B<sub>4</sub> burr thickness

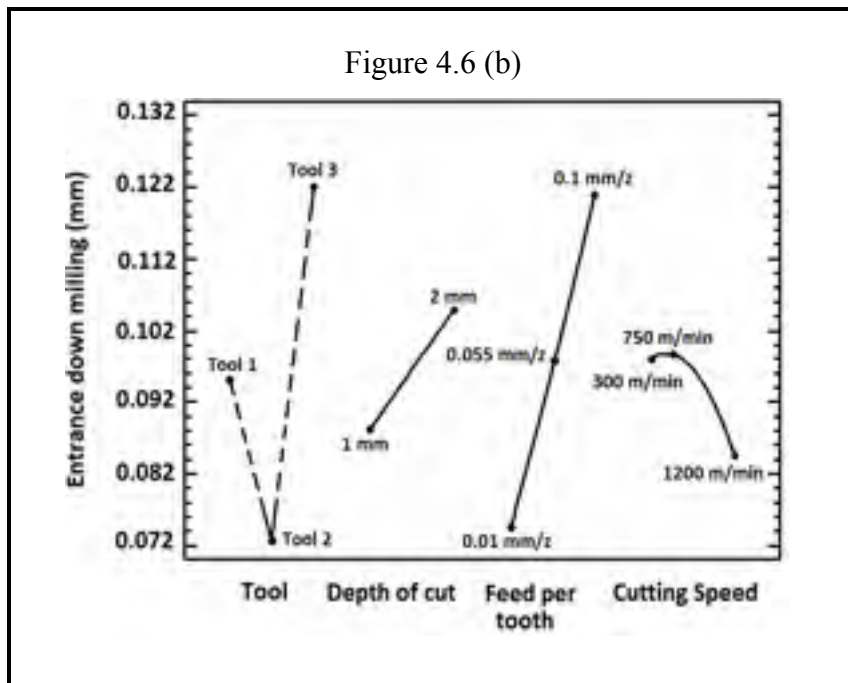
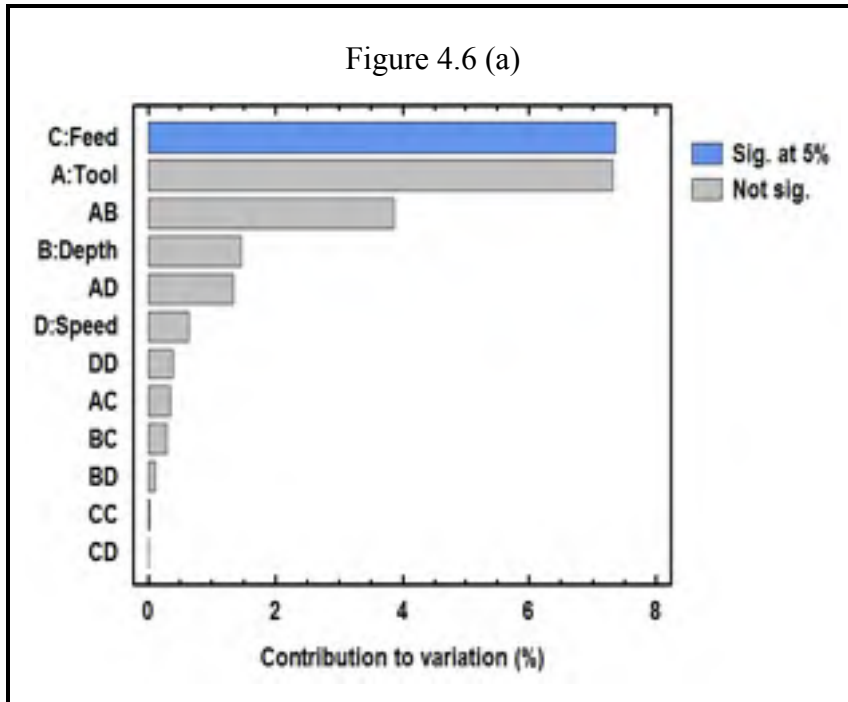


Figure 4.6 (a) Pareto chart and (b) main effect plot of B<sub>5</sub> burr thickness

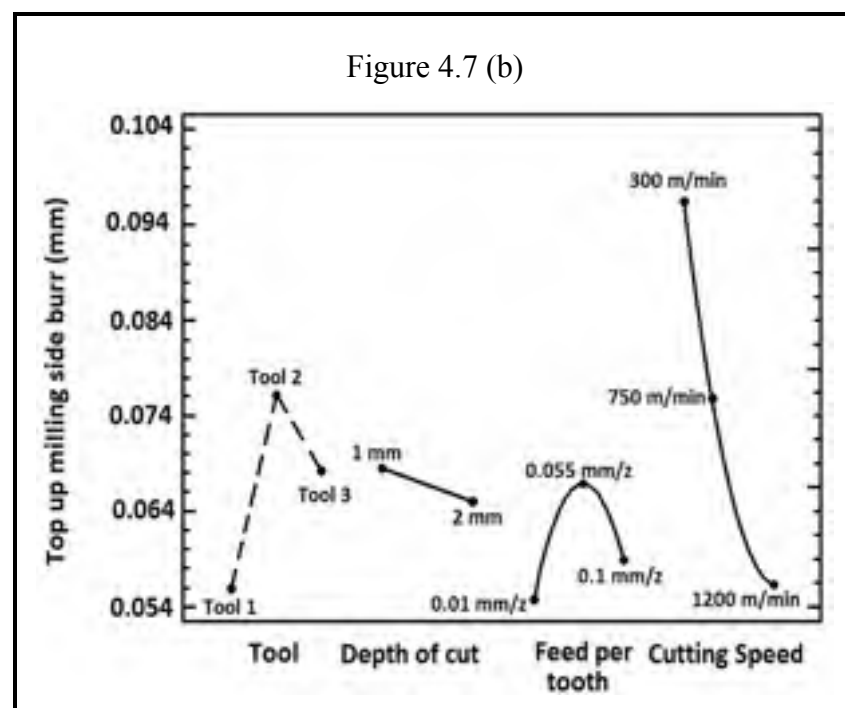
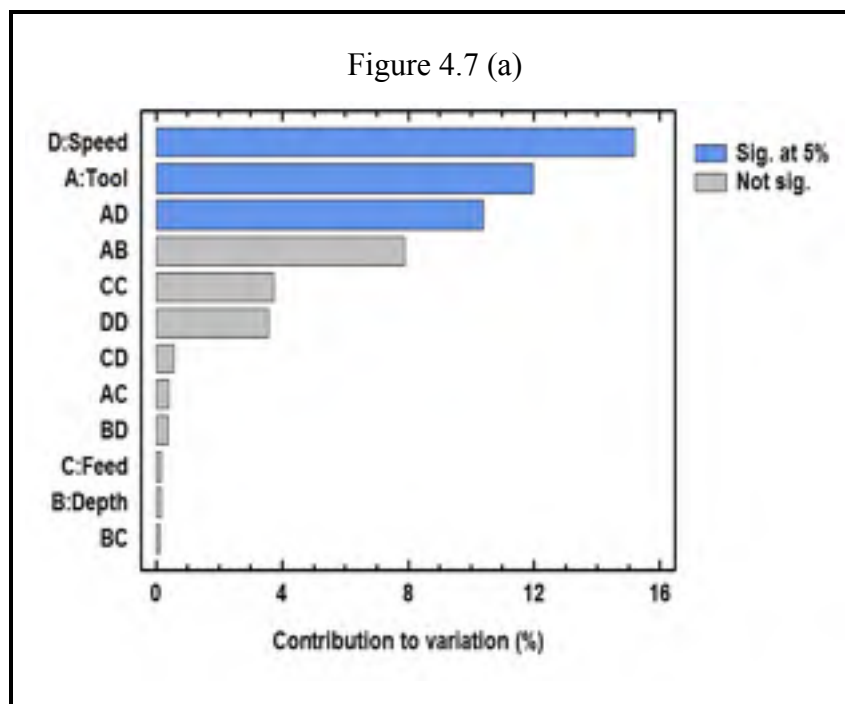


Figure 4.7 (a) Pareto chart and (b) main effect plot of  $B_8$  burr thickness

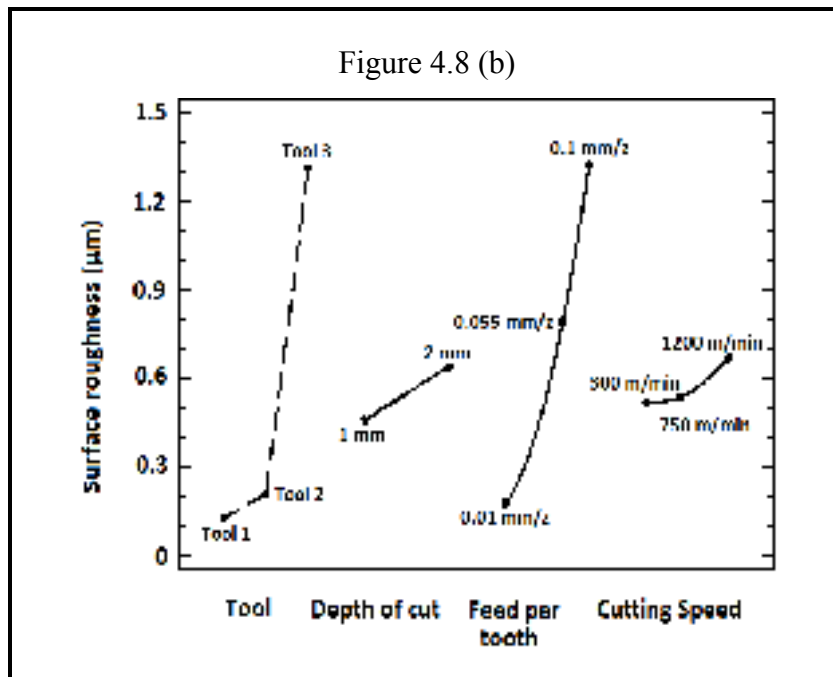
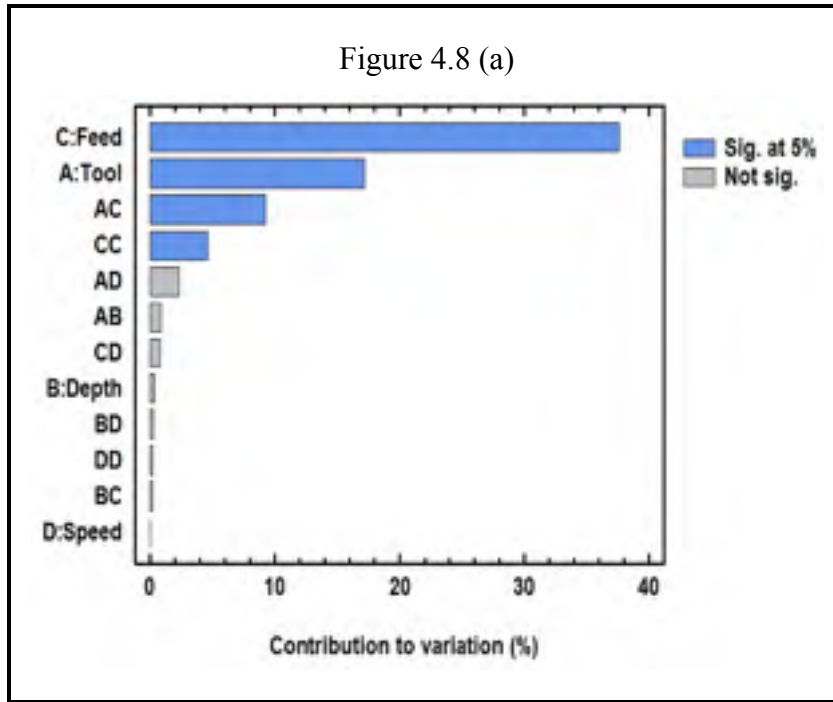


Figure 4.8 (a) Pareto chart and (b) main effect plot of surface roughness (Ra)

Table 4.3 Statistical results of responses

List	Responses	R <sup>2</sup> %	R <sup>2</sup> <sub>adj</sub> %	P value	F ratio	Dominant process parameters at 95% confidence interval	Optimum process parameters setting levels
1	B <sub>1</sub>	90.31	86.82	0	25.92	Feed per tooth, Tool, Depth of cut, AB, DD	A <sub>2</sub> B <sub>1</sub> C <sub>1</sub> D <sub>3</sub>
2	B <sub>2</sub>	46.11	22.79	0.043	1.97	Tool, AC	A <sub>3</sub> B <sub>2</sub> C <sub>1</sub> D <sub>2</sub>
3	B <sub>4</sub>	28.11	0	0.571	0.9	-	A <sub>2</sub> B <sub>1</sub> C <sub>1</sub> D <sub>3</sub>
4	B <sub>5</sub>	42.18	17.19	0.093	1.68	Feed per tooth	A <sub>2</sub> B <sub>1</sub> C <sub>1</sub> D <sub>3</sub>
5	B <sub>8</sub>	46.91	22.79	0.036	2.04	Tool, Speed, AD	A <sub>1</sub> B <sub>2</sub> C <sub>1</sub> D <sub>3</sub>
6	Ra	76.58	66.54	0	7.56	Feed per tooth, Tool, AC,CC	A <sub>1</sub> B <sub>1</sub> C <sub>1</sub> D <sub>1</sub>

#### 4.5 Multiple responses optimization

As can be seen in Table 4.3, the best setting levels of process parameters for each response are different. In addition, B<sub>2</sub>, B<sub>4</sub>, B<sub>5</sub> and B<sub>8</sub> are not statistically controlled by process parameters as their P-value > 0.05. Therefore, correct selection of process parameters setting levels for multiple responses optimization is a challenging issue. The burr thickness in exit up milling side (B<sub>1</sub>) of machined parts is found as the most sensitive response to variation of cutting parameters, as compared to other burrs which are statistically known as insignificant responses.

The Eqs(4.4 - 4.9) are used to calculate the terms required to construct the  $\psi$  as presented in Table 4.3. According to Eq(4.11), the fitness mapping function of trial  $i$  ( $\psi_i$ ) can be constructed as in Eq(4.23):

$$\psi_i = M - \frac{(\mu_1 \times Y_1) + \dots + (\mu_n \times Y_n)}{n} \quad (4.23)$$

Where  $i = 1, \dots, n$  are non-identical responses in trial  $i$ .

By knowing that  $n = 6$  and  $M = 100$ , by replacing the presented terms (see Table 4.2) into Eq(4.23), the  $\psi_i$  becomes:

$$\psi_i = 100 - \frac{(66.66 \times Y_1) + (400 \times Y_2) + (400 \times Y_3) + (500 \times Y_4) + (400 \times Y_5) + (500 \times Y_6)}{6} \quad (4.24)$$

Upon applying the same procedure and implementing Eq(4.23) into responses, the  $\psi_1, \dots, \psi_N$  were constructed as shown in Table 4.2. As it was mentioned before, Taguchi method in the category of “larger-the-better” is used in this work. Therefore, Eqs(4.11-4.14) are used to calculate  $\eta_\psi$ . The relative contribution of direct and interaction effects of process parameters on  $\eta_\psi$  are presented in ANOVA table (see Table 4.5) and Pareto chart in Figure 4.9(a). As can be seen in Figure 4.9(a), feed per tooth (C), cutting tool (A) and their interaction effects (AC) are the main significant process parameters on  $\eta_\psi$ . The  $R^2$  in Table 4.5 indicates that the model as fitted explains 83.06% of the variability in  $\eta_\psi$ . Neglecting the effects of non-significant parameters, the  $R^2_{adj}$  becomes 67.95%. Based on Table 4.5, P-value of 0 in model exhibits a significant model.

Table 4.4 Response characteristic terms ( $n = 6$  and  $N = 54$ )

List	Response Characteristic	Index	$R$	$R_i$	$M_R$	$\mu_i$	$m_Y$
1	Ra	$Y_1$	0-1.5 $\mu\text{m}$	1.5	[100:0]	66.66	0.44
2	$B_1$	$Y_2$	0-0.25 mm	0.25	[100:0]	400	0.111
3	$B_2$	$Y_3$	0-0.25 mm	0.25	[100:0]	400	0.085
4	$B_4$	$Y_4$	0-0.20 mm	0.20	[100:0]	500	0.0708
5	$B_5$	$Y_5$	0-0.25 mm	0.25	[100:0]	400	0.085
6	$B_8$	$Y_6$	0-0.20 mm	0.2	[100:0]	500	0.066

Table 4.5 ANOVA table for  $\eta_v$

List	Parameter	DOF	SS	MS	F	P	Remark
1	A	2	5.746	2.873	-0.413	0.013	<b>Significant</b>
2	B	1	1.034	1.034	-18.28	0.187	Insignificant
3	C	2	50.9	25.45	3.42	0	<b>Significant</b>
4	D	2	1.62	0.81	22.22	0.256	Insignificant
5	AB	2	0.737	0.368	-17.62	0.529	Insignificant
6	AC	4	9.442	2.36	21.51	0.009	<b>Significant</b>
7	AD	4	2.891	0.722	23.32	0.303	Insignificant
8	BC	2	0.146	0.073	-23.18	0.879	Insignificant
9	BD	2	0.365	0.182	-21.77	0.727	Insignificant
10	CD	4	4.933	1.233	22.91	0.097	<b>Mid-significant</b>
11	<b>Model</b>	<b>25</b>	<b>77.82</b>	<b>3.113</b>	<b>5.494</b>	<b>0</b>	<b>Significant</b>
12	R <sup>2</sup> = 83.06 %						
13	R <sup>2</sup> adj = 67.95%						

DOF: Degree of freedom; SS: Sum of square error; MS: Mean of square error; F: F ratio; P: P-value

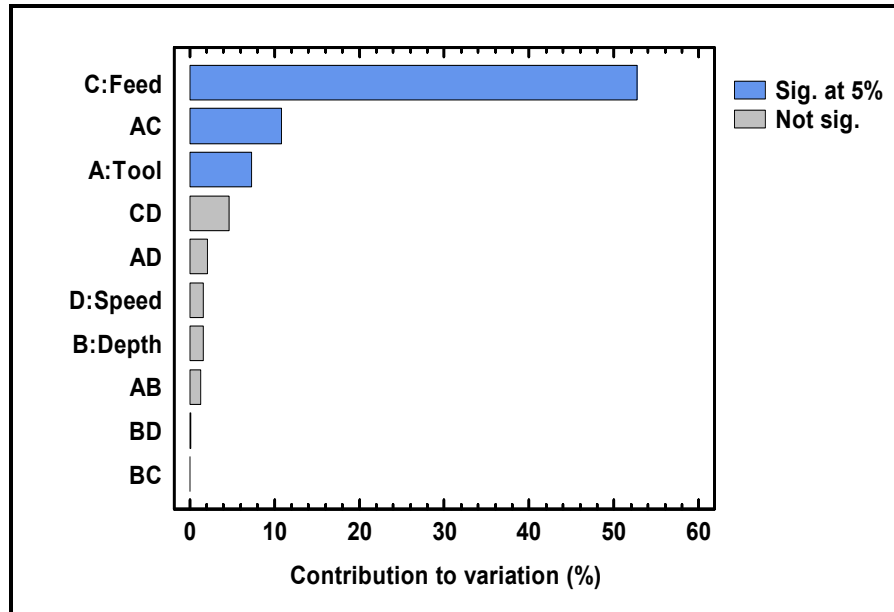


Figure 4.9 Pareto chart of  $\eta_v$

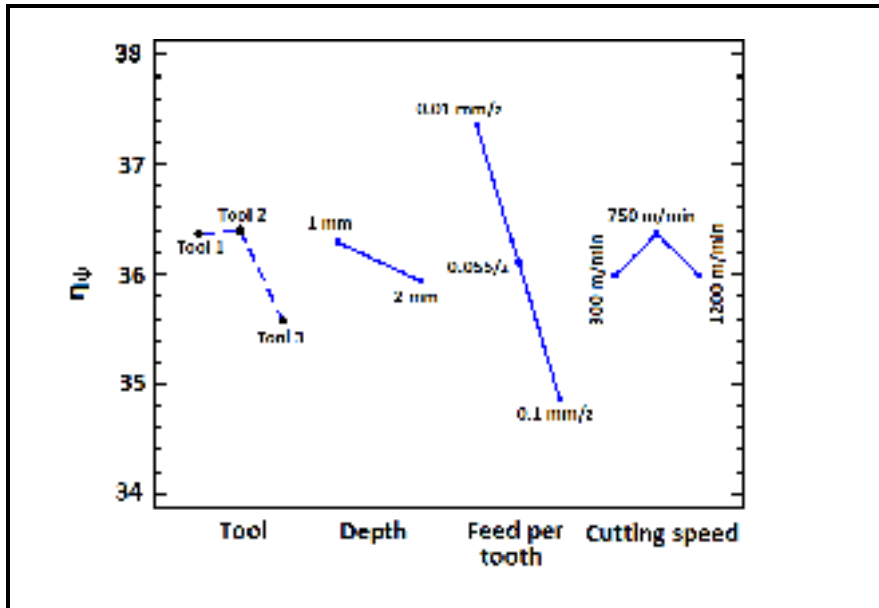


Figure 4.10 Main effect plot of  $\eta_\psi$

The ANOM is used as a tool to firstly determine the main effect of each parameter on  $\eta_\psi$  and secondly introduce the optimal setting levels of process parameters (see Figure 4.10). According to Eq(4.14) and Figure 4.10, the optimum condition to minimize the responses are cutting tool 2 ( $A_2$ ), depth of cut 1 mm ( $B_1$ ), feed per tooth 0.01 mm/z ( $C_1$ ) and cutting speed 750m/min ( $D_2$ ). As presented in Table 4.6, using the proposed cutting conditions, the optimum values of burrs size and surface response are obtained.

Eqs(4.19- 4.20) were then used to calculate the prediction error ( $\varepsilon$ ) and desirability of the individual and whole proposed predicted optimum values ( $Y_{opt}$ ). According to Table 4.6, using the proposed setting levels of process parameters, the minimum experimental value of  $B_1$  was obtained. In addition, the obtained values of  $B_2$ ,  $B_4$ ,  $B_5$  and  $B_8$  are much lower than mean values (see Tables 4.6-4.7), very near to their minimum values. The predicted value of optimum surface roughness  $(Y_1)_{opt}$  is higher than  $Y_{mean}$ . However while the surface roughness values vary widely when changing the cutting conditions (see Table 4.6), the obtained desirability level ( $d_i = 0.60$ ) is acceptable.

According to Eq(4.20), the desirability of proposed process parameters and responses is  $D_i = (0.434)^{0.166} = 0.87$  (see Table 4.6).

Table 4.6 Desirability of proposed setting levels of process parameters

List	Response Characteristic	Index	$Y_{opt}$ (mm)	$Y_{min}$ (mm)	$Y_{max}$ (mm)	$Y_{mean}$ (mm)	$\sigma_Y$	Desirability ( $d_i$ )	$\kappa$ %
1	Ra	Y <sub>1</sub>	0.64	0.076	1.499	0.44	0.385	$d_1 = 0.60$	-45
2	B <sub>1</sub>	Y <sub>2</sub>	0.028	0.028	0.205	0.111	0.041	$d_2 = 1$	74.7
3	B <sub>2</sub>	Y <sub>3</sub>	0.047	0.037	0.218	0.085	0.037	$d_3 = 0.94$	44.7
4	B <sub>4</sub>	Y <sub>4</sub>	0.033	0.028	0.174	0.071	0.028	$d_4 = 0.96$	53.3
5	B <sub>5</sub>	Y <sub>5</sub>	0.033	0.028	0.2	0.085	0.037	$d_5 = 0.97$	67
6	B <sub>8</sub>	Y <sub>6</sub>	0.048	0.028	0.135	0.066	0.024	$d_6 = 0.81$	79.2
<b><math>D_i = 0.87</math>, <math>\varepsilon = 1.3\%</math></b>									

Where  $\varepsilon$  is prediction error.

The 3D surface plots in Figures 4.11-4.13 show the relationship between  $\eta_\psi$  and feed per tooth and depth of cut, when using cutting tool 2 at constant levels of cutting speed. According to Figures 4.11-4.13, higher values of  $\eta_\psi$  were obtained when cutting tests with lower levels of feed per tooth (0.01 mm/z) and depth of cut (1mm) were used. According to the main effect plot in Figure 4.10, variation of cutting speeds has relatively similar effect on  $\eta_\psi$ . In addition, according to (Lauderbaugh, 2009; Mian, Driver and Mativenga, 2011a; Niknam, Kamguem and Songmene, 2012; Niknam and Songmene, 2012; 2013; Niknam, Zedan and Songmene, 2012), it has been statistically shown that the influence of cutting speed on milling and drilling burrs size is insignificant as compared to depth of cut and feed per tooth. Therefore to verify the adequacy of proposed process parameters, the new cutting tests were performed using cutting tool 2, lower level of the depth of cut, lower and center levels of feed per tooth and all tested levels of cutting speeds (see Table 4.7). Each test was repeated twice. The following passages present the experimental verifications.

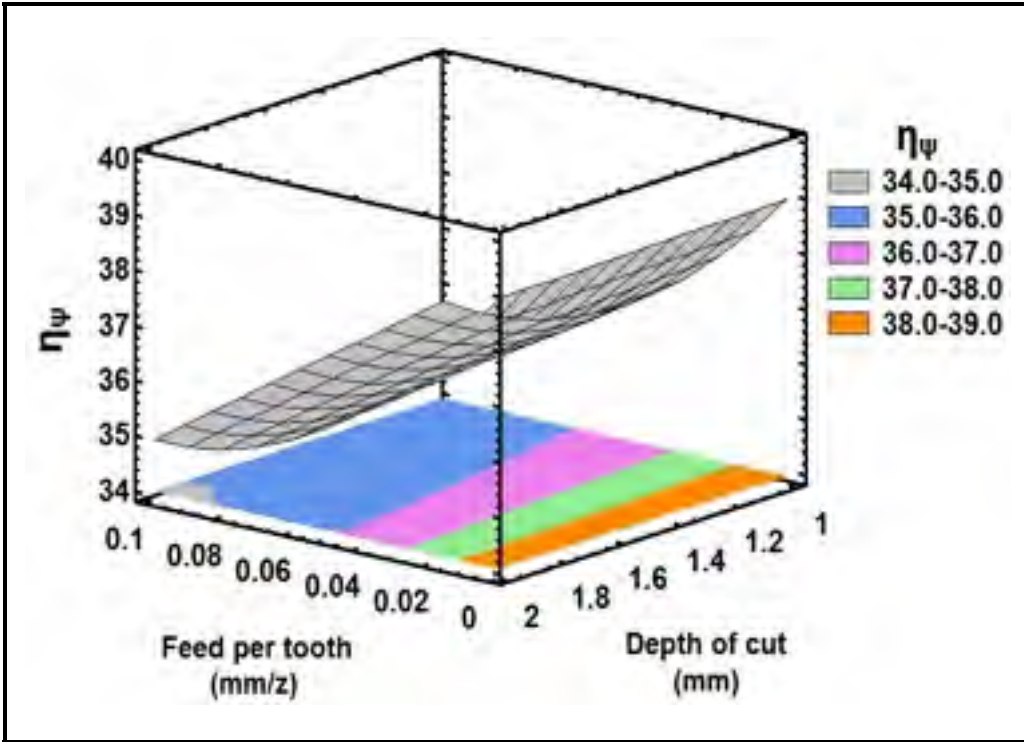


Figure 4.11 3D contour plot of  $\eta_\psi$  at cutting speed 300 m/min

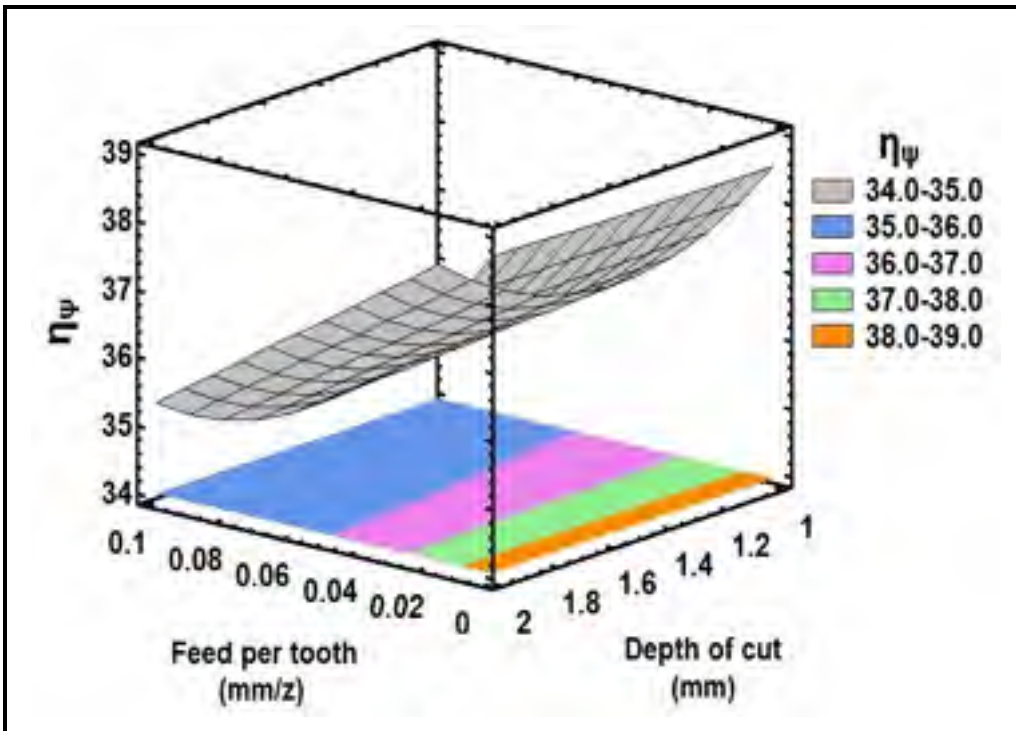


Figure 4.12 3D contour plot of  $\eta_\psi$  at cutting speed 750 m/min

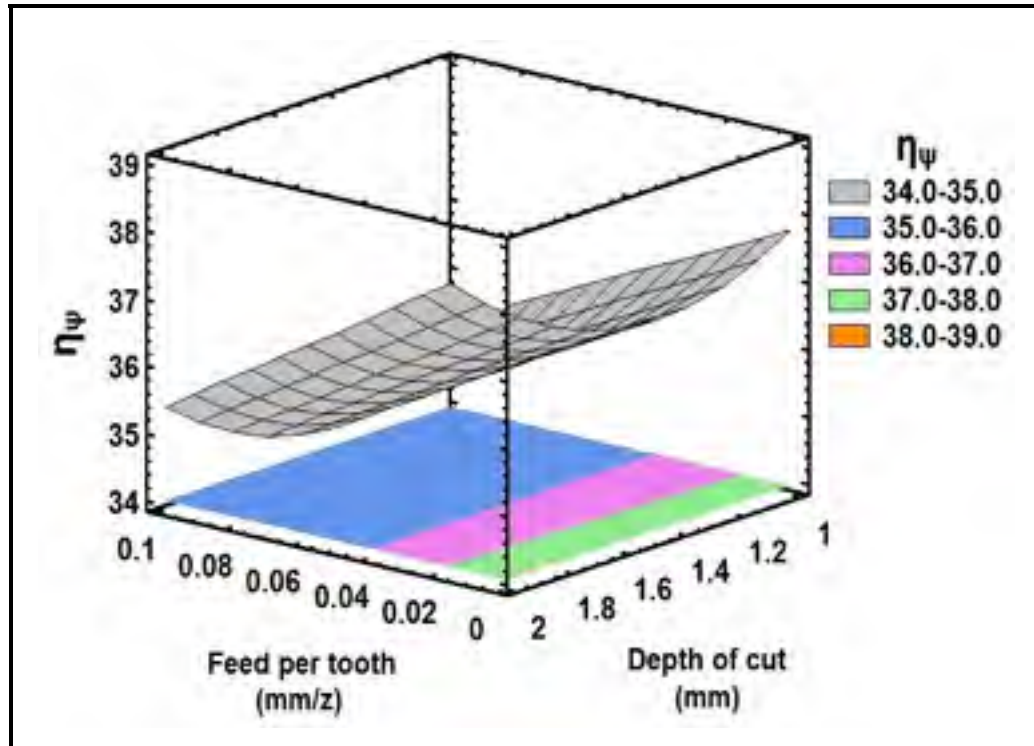


Figure 4.13 3D contour plot of  $\eta_\psi$  at cutting speed 1200 m/min

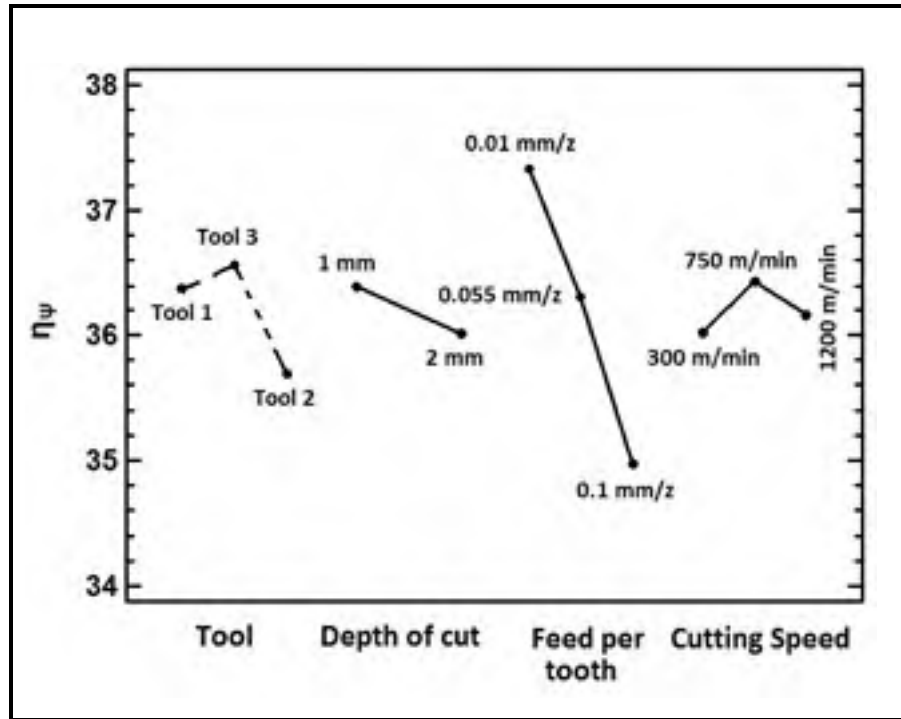
#### 4.6 Experimental validation

The following setting levels of process parameters as illustrated in Table 4.7 were used for verification tests. According to Table 4.7, six cutting conditions have been repeated three times. Having the verification results added to Table 4.2, the relative contribution and direct effects of process parameters on  $\eta_\psi$  are presented in the main effect plot in Figure 4.14. The  $R^2$  statistic indicates that the model as fitted explains 84.73% of the variability in  $\eta_\psi$ . The  $R^2_{adj}$  is 77.10%. The  $\psi$  and  $\eta_\psi$  when using the verification tests were also calculated (see Table 4.7). From Table 4.7, the highest values of  $\psi$  and  $\eta_\psi$  were obtained when using the cutting condition  $A_2B_1C_1D_2$ . This exhibits that the proposed optimum condition is verified under similar experimental conditions. The responses when using optimized condition are presented in Table 4.8. The Eqs(4.19-4.21) were then applied to the refined cutting condition

to calculate the  $D_i$ ,  $d_i$  and  $\varepsilon$  (see Table 4.8). From Table 4.8, using the proposed setting levels of process parameters, all responses are optimized 30-59%.

Table 4.7 Process parameters used for verification tests

Test No.	Cutting condition		Responses							
	$f_z$	$v_c$	$B_1$ (mm)	$B_2$ (mm)	$B_4$ (mm)	$B_5$ (mm)	$B_8$ (mm)	Ra ( $\mu\text{m}$ )	$\psi$	$\eta_\psi$
1	0.01	300	0.049	0.052	0.044	0.053	0.057	0.295	78.17	37.86
2		<b>750</b>	<b>0.040</b>	<b>0.049</b>	<b>0.050</b>	<b>0.040</b>	<b>0.056</b>	<b>0.195</b>	<b>80.49</b>	<b>38.12</b>
3		1200	0.059	0.047	0.052	0.049	0.069	0.317	76.20	37.64
4	0.055	300	0.122	0.171	0.057	0.074	0.062	0.45	60.73	35.67
5		750	0.063	0.112	0.061	0.057	0.052	0.458	70.06	36.91
6		1200	0.088	0.074	0.095	0.104	0.108	0.168	63.52	36.06
7	0.01	300	0.038	0.059	0.044	0.041	0.068	0.377	77.35	37.77
8		<b>750</b>	<b>0.076</b>	<b>0.052</b>	<b>0.061</b>	<b>0.017</b>	<b>0.041</b>	<b>0.326</b>	<b>78.36</b>	<b>37.88</b>
9		1200	0.040	0.031	0.036	0.044	0.076	0.32	79.44	38.01
10	0.055	300	0.087	0.084	0.037	0.035	0.057	0.434	73.65	37.34
11		750	0.072	0.082	0.051	0.057	0.050	0.208	75.29	37.53
12		1200	0.075	0.062	0.056	0.092	0.074	0.452	68.86	36.76
13	0.01	300	0.119	0.053	0.038	0.054	0.040	0.164	76.62	37.69
14		<b>750</b>	<b>0.070</b>	<b>0.051</b>	<b>0.037</b>	<b>0.047</b>	<b>0.040</b>	<b>0.151</b>	<b>80.81</b>	<b>38.15</b>
15		1200	0.060	0.104	0.052	0.040	0.082	0.214	72.90	37.25
16	0.055	300	0.100	0.136	0.052	0.071	0.034	0.433	67.67	36.61
17		750	0.060	0.104	0.052	0.040	0.082	0.214	76.16	37.63
18		1200	0.070	0.074	0.066	0.094	0.058	0.202	71.55	37.09

Figure 4.14 Main effect plot of optimized  $\eta_v$ Table 4.8 Desirability of verified process parameters ( $A_2B_1C_1D_2$ )

Responses		Measurement tests			$Y_{\text{mean}}$	Desirability ( $d_i$ )	$\kappa$ (%)
		Test 1	Test 2	Test 3			
1	$B_1$ (mm)	0.040	0.076	0.070	0.224	$d_1 = 0.897$	48.7
2	$B_2$ (mm)	0.049	0.052	0.051	0.062	$d_2 = 0.863$	45.4
3	$B_4$ (mm)	0.050	0.061	0.037	0.050	$d_3 = 0.908$	38.1
4	$B_5$ (mm)	0.040	0.017	0.047	0.049	$d_4 = 0.86$	30.2
5	$B_8$ (mm)	0.056	0.041	0.040	0.034	$d_5 = 0.965$	59.1
6	Ra ( $\mu\text{m}$ )	0.195	0.326	0.151	0.045	$d_6 = 0.841$	30.9
<b><math>D_i = 0.88</math> <math>\varepsilon = 1.1\%</math></b>							

The proposed method could be used for various design of experiment models, such as multi-level full factorial design and orthogonal array. It is to note that the use of Taguchi method for multiple responses optimization can become more accurate, if suitable modification techniques are adjusted to Taguchi method.

#### **4.7 Conclusion**

- This work has shown that surface roughness and burrs size are governed by different machining process parameters. According to experimental results, some burrs are governed by feed per tooth and cutting speed while others are controlled by tool geometry and feed per tooth.
- New modification to application of Taguchi method is proposed for simultaneous multiple responses optimization. The methodology was verified by simultaneous minimization of surface roughness and exit, entrance and top burrs thickness of slot milled parts of AA 6061-T6.
- The use of proposed approach has helped achieving better surface finish and acceptable burr size at the same time. The adequacy of proposed optimum cutting condition was reconfirmed through verification tests, achieving desirability level ( $D_i$ ) of 0.88 and a percentage error ( $\varepsilon$ ) of 1.1%.
- The findings in this work are in conflict with mentioned critics drawn against Taguchi method applications for multiple responses optimization.

## CHAPTER 5

### SUBSTANTIAL SUMMARY OF THE RESEARCH WORK

#### 5.1 Introduction

Burr formation is a common problem occurs in several industrial sectors, such as aerospace, ship construction, automobile, *etc.* It becomes an even more important issue when dealing with ductile materials, such as aluminium alloys. Any solution to prevent or at least minimizing burr formation starts by understanding the fundamentals of burr formation. Nevertheless, the burr formation minimization and prevention still require research and close attention. This therefore calls for a review of existing approaches.

The research work presented in this thesis consisted of three aspects which construct the main and specific objectives of this research work (see Figure 5.1). The first aspect of this study is devoted to experimental and statistical studies to determine the factors governing burrs size during slot milling of aluminium alloys. The second aspect focuses on theoretical work, including predictive (analytical and computational) modeling of slot milling burrs in ductile materials. The simultaneous multiple responses optimization during milling (slotting) operation is the subject of the last aspect of this thesis. As described in introduction, all these three aspects are related to others and were designed for burr size minimization which is the main research objective of this work (see Figure 5.1).

This chapter presents a discussion of the obtained results in each aspect and aims to link them with the proposed research objectives in this work.

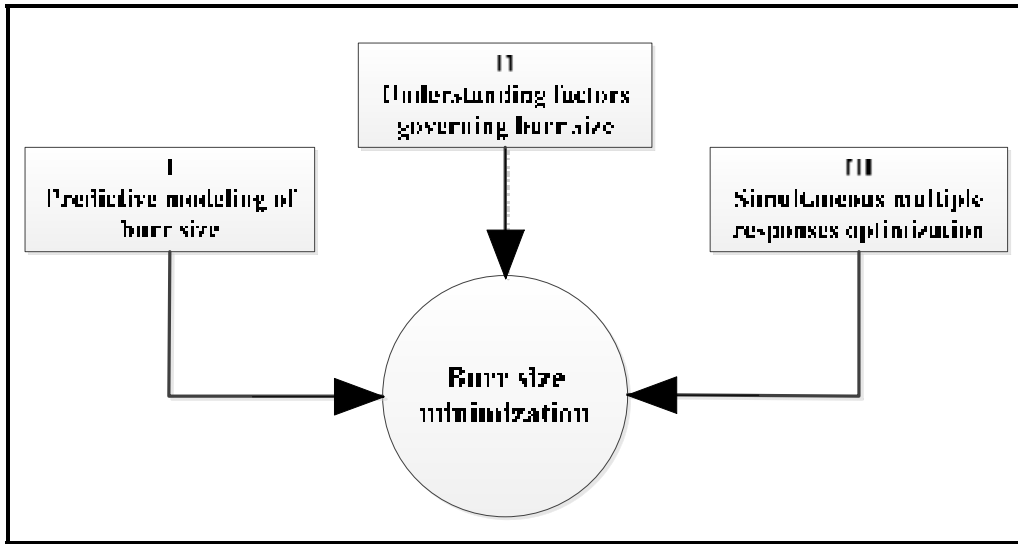


Figure 5.1 The main and specific research objectives

## 5.2 Dominant process parameters on slot milling burrs size

Numerous research works employed experimental studies to identify the main effective parameters in milling operations and to optimize the cutting process, which is an acute industrial requirement. Due to complex mechanisms of burr formation, direct and interaction effects between process parameters, a large number of experiments is required to evaluate the effects of process parameters on burr formation and size (Lauderbaugh, 2009). In addition to massive expenses, the dominant process parameters on burr formation during oblique and orthogonal milling operations are still unknown. Therefore, the outcomes of experimental studies are not always consistent. This can be due to temperature effects, machine tool conditions, stability of cutting process, material properties, *etc.* For instance, (AM De Souza *et al.*, 2003; Schäfer, 1978) showed that the low level of feed per tooth reduces the burr size, while (Jones and Furness, 1997; Kishimoto *et al.*, 1981; Wang and Zhang, 2003b) revealed that increase in the feed per tooth reduces burr size. Furthermore, according to (Jones and Furness, 1997), the exit angle of  $76^{\circ}$ - $118^{\circ}$  generate smaller burr, while, from (Luo, Liu and Chen, 2008), the largest burr size appears in exit angle of  $90^{\circ}$ . In addition, when dealing with dry high speed milling, limited information is available for adequate selection of cutting

parameters. According to (Klocke and Eisenblätter, 1997), dry cutting is a suitable approach for machining of aluminium alloys. However, except few works (Kim and Kang, 1997; Shefelbine and Dornfeld, 2004b; Songmene V., Khettabi and Kouam, 2012), very limited studies have considered the effects of high speed dry milling on burr formation.

The proper selection of cutting parameters by means of burr size minimization becomes even more complicated in slot milling, particularly when various levels of machining parameters such as cutting tools with various end nose radiuses and coatings are used. Therefore, in order to remedy these lacks, the combination of statistical and experimental approaches was used in this work to better understand the burr formation mechanism and to define the factors governing burrs size during slot milling of aluminium alloys. To this end, a broad range of cutting tool parameters (coating and geometry), machining strategy (dry high speed) and cutting parameters (cutting speed, feed per tooth, and depth of cut) were used in experimental study. In order to better understand the effects of material properties on burrs size, two aluminium alloys of the same family were employed. The non-significant effects of material properties on most of the burrs studied exhibit that burr formation control is a delicate subject that requires further investigations.

In order to minimize the exit and entrance burrs and facilitating deburring operations, the transition of primary to secondary burrs must be conducted. This can be done by correct selection of process parameters. Based on statistical analysis, the optimum process parameters setting levels to minimize each burr are different. Consequently, it is difficult to optimize all eight slot milling burrs. According to experimental results, feed per tooth, depth of cut, insert nose radius ( $R\epsilon$ ) and coating are dominant process parameters on most of the burrs studied. However their influence on each burr is dissimilar.

The side burrs, whether entrance ( $B_5$ ) or exit side ( $B_1$ ) burrs are dominated by the feed per tooth, material properties and depth of cut. The top burrs ( $B_4$  and  $B_8$ ) are mainly affected by variation of cutting condition, chip evacuation dynamic, insert nose radius ( $R\epsilon$ ) and coating. According to (Olvera and Barrow, 1996), tool coating has a negligible influence on face

milling burrs. However, a certain level of coating influence on slot milling burrs was observed in this work. Generally, a coated tool has a higher wear resistance and lower coefficient of friction than an uncoated one. The increased wear resistance has an influence on burr dimension. In addition, the coated inserts normally have a larger cutting edge radius than an uncoated one. This may cause ploughing effect and reduction in total deformation and friction, which consequently affects the burr size. This finding is in contrast with the conclusion made in (Olvera and Barrow, 1996), presenting a negligible influence of tool coating on face milling burrs dimension.

Burr size is also strongly affected by variation of chip thickness  $h(\varphi)$ . As mentioned before, in the milling operation, the  $h(\varphi)$  varies periodically as a function of time-varying immersion angle ( $\varphi$ ) and feed per tooth. Immersion angle ( $\varphi$ ) is directly affected in a large extent by depth of cut, pitch angle ( $\theta_p$ ) and tool geometry, including lag angle ( $\gamma_0$ ) and rake angle. Therefore, it could be inferred that the changes in cutting tool geometry and cutting parameters strongly affect the burr formation process. The presented outcomes were written as one conference and a journal article (see ANNEX I-II). The major contribution was accepted for publication in *Institution of Mechanical Engineers (IMechE), Part B, Journal of Engineering Manufacture*, in March 2013.

### 5.3 Controllable responses

The controllability of responses was evaluated using experimental and statistical analysis. Although most of the existing research works in literature aim to measure and/or predict the burr height, but in terms of deburring perspective, the burr thickness is the principle factor in burr removal. Therefore, no further studies by means of modeling and minimizing burr height were carried out in this thesis. Instead, more focus was paid to simultaneous optimization of burrs thickness and surface finish. This was extensively studied in chapter four. According to statistical results, a linear relationship was found between the thickest burr ( $B_1$ ) and  $F_t$ . As similar to  $B_1$  thickness, variation of  $F_t$  is mainly affected by cutting parameters. Linear first order mathematical models were developed to show that both  $F_t$  and

$B_1$  thickness are a function of depth of cut and feed per tooth. Having this in mind helped us to assume that  $B_1$  thickness is highly affected by direct effects of process parameters. Therefore, it could be most likely modeled analytically as a function of cutting parameters. This is the subject of the second aspect of this work. Further theoretical works on this issue is the subject of the next section.

A conference article on this topic was presented in *1<sup>st</sup> International Conference on Virtual Machining Process Technology* (CIRP Sponsored Conference), which was held in Montréal, Canada, in May 28 – June 1, 2012.

#### **5.4 Milling burr size modeling of ductile materials**

Investigations on milling burr formation were conducted using experimental studies, analytical modeling and numerical methods such as FEM. Amongst; milling burr formation modeling has received less attention. Due to complexity of milling burr formation modeling, most of the previous studies were based on orthogonal cutting scheme (Toropov, Ko and Lee, 2006). Burr formation in orthogonal cutting was studied as the plastic bending of non-cut parts of materials using minimum energy principles, the incompressibility assumption and FE modeling. However the FE models are strongly relevant to the accuracy of input boundary conditions, which are not yet advanced, and therefore are usually simplified. Furthermore, the results are strongly influenced by the software applied; time-consuming and generally experimental data are required for model construction. Moreover, only limited studies have proposed analytical models of milling burrs, which were only focused on exit burrs (Chern and Dornfeld, 1996; Ko and Dornfeld, 1996; Ko and Dornfeld, 1991). Ko and Dornfeld (1991) proposed a quantitative model of burr formation for ductile materials that does not include fracture during orthogonal cutting. They later improved their model by presenting an analytical model of material exhibiting fracture during burr formation (Ko and Dornfeld, 1996). The burr size estimations were found accurate for less ductile materials (i.e. AA 6061-T6 and AA 2024-T4), while the results of ductile materials were not consistent. In their model, the undeformed chip thickness was assumed uniform. This is not however the case in

most of milling processes that use the cutting tools with multiple flutes. Furthermore, their models require the use of experimental measurement and/or approximation of shear angle ( $\Phi$ ), friction angle ( $\lambda$ ) and the tool chip contact length ( $L$ ), when studying the cutting tools with multiple flutes. Therefore, to propose more accurate milling burr size models, these lacks should be remedied.

### **Analytical modeling**

In this thesis, as similar as the method proposed by (Ko and Dornfeld, 1991), certain levels of assumptions were used, and the burr formation mechanism in ductile materials was divided into three parts including; initiation, development, and burr formation. The experimental results showed that the exit up milling side burr ( $B_1$ ) is the longest and thickest burr amongst those burrs studied. Therefore, the burr formation in the exit zone was modeled as an orthogonal process, and consequently, the effects of the plunge depth, cutter geometry and cutting speed were ignored. In order to consider the tool rotation angle and non-uniform chip thickness on burr formation process, a set of mathematical operations was applied on milling burr formation at the end of a cut. By considering only a small advancement of the tool at the transition from chip formation to burr formation, and according to principles of energy conservation theory, the work done for chip formation was assumed as equal to the work carried out for burr formation. Extending the theory, a mathematical model was proposed (Eq 3.17) for burr thickness estimation. The validation results of analytical model correlate very well with experimental values. Further verification tests as shown in Figures 5.2-5.3 show that the variation of cutting speed has no significant effects on resultant force at different levels of feed per tooth.

### **Computational modeling**

According to Eq(3.17), the only unknown parameter required to predict the burr thickness ( $B_i$ ) is tangential cutting force ( $F_t$ ), which could either be measured experimentally or estimated computationally. However, in order to simplify the model, computational

modeling approach was also established which enabled simulating the  $B_t$  with even no need of experimental measurement of  $F_t$ . In fact, by considering that the instantaneous chip thickness  $h(\varphi)$  varies periodically as a function of time-varying instantaneous immersion angle ( $\varphi$ ), it was assumed that for a full slotting operation, the entrance angle ( $\varphi_{st}$ ) and exit angle ( $\varphi_{ex}$ ) are 0 and  $\pi$ , respectively. In order to simulate the  $F_t$  in a full slot milling operation and consequently  $B_t$  simulation, an algorithm was established by discretizing the cutting tool into L elements of thickness ( $da_p$ ) through axial depth of cut ( $a_p$ ). The effects of lag angle ( $\gamma\phi$ ), helix angle ( $\beta$ ) and tool diameter ( $D$ ) on immersion angle ( $\varphi$ ) were also considered.

The elementary cutting forces acting on the cutter in radial and tangential directions were expressed using the mechanistic force model. According to previous studies (Zaghbani *et al.*, 2012) and experimental results presented in this thesis, it could be inferred that  $F_t$  is mainly affected by feed per tooth and depth of cut, not cutting speed. Therefore, the effects of cutting speed on  $F_t$  and consequently burr formation was assumed negligible. In addition, to avoid repeating the preliminary tests for cutting force coefficients measurements, an alternative method was proposed to approximate the  $F_t$  using specific cutting force coefficient,  $K_c$ . The  $K_c$  values with respect to material properties can be found in (Davis, Mills and Lampman, 1990) and many material handbooks. The  $K_c$  was formulated as a function of average chip thickness per revolution ( $h_m$ ), when  $h_m \neq 0.2$  mm. Differential tangential force ( $dF_{t,j}$ ) acting on a differential flute elements with the height of  $da_p$  was formulated (see Eq 3.29). Therefore, differential burr thickness with respect to immersion angle in flute j,  $dB_{t,j}(\varphi_j(a_p))$ , could be calculated from Eq(3.32). The correlation rates between the simulated values of  $B_t$  and those obtained through experimental measurements exceed 92% in AA 2024-T351 and 83% in AA 6061-T6, respectively.

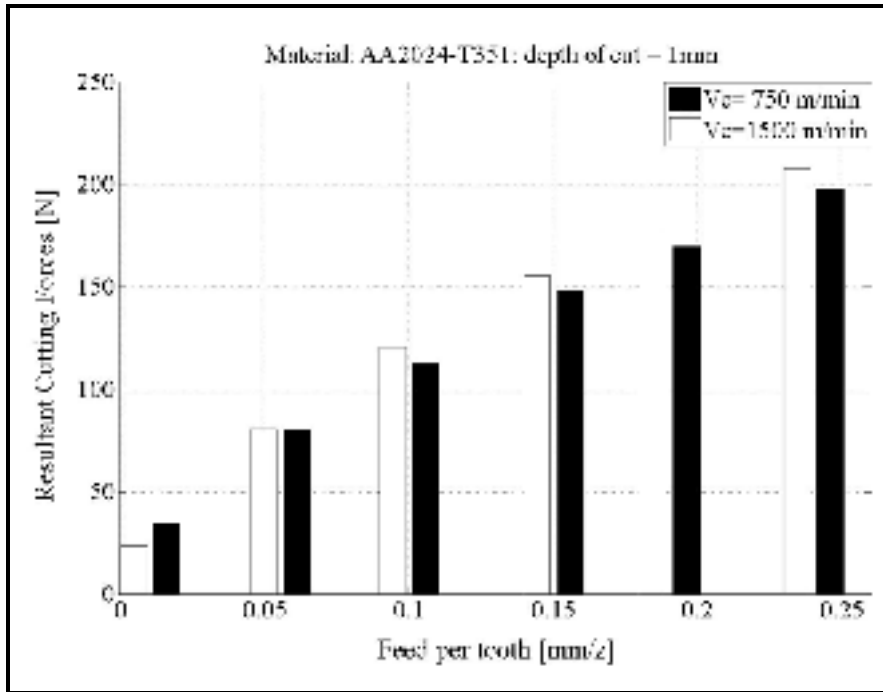


Figure 5.2 Variation of resultant cutting force during slot milling of AA 2024-T351

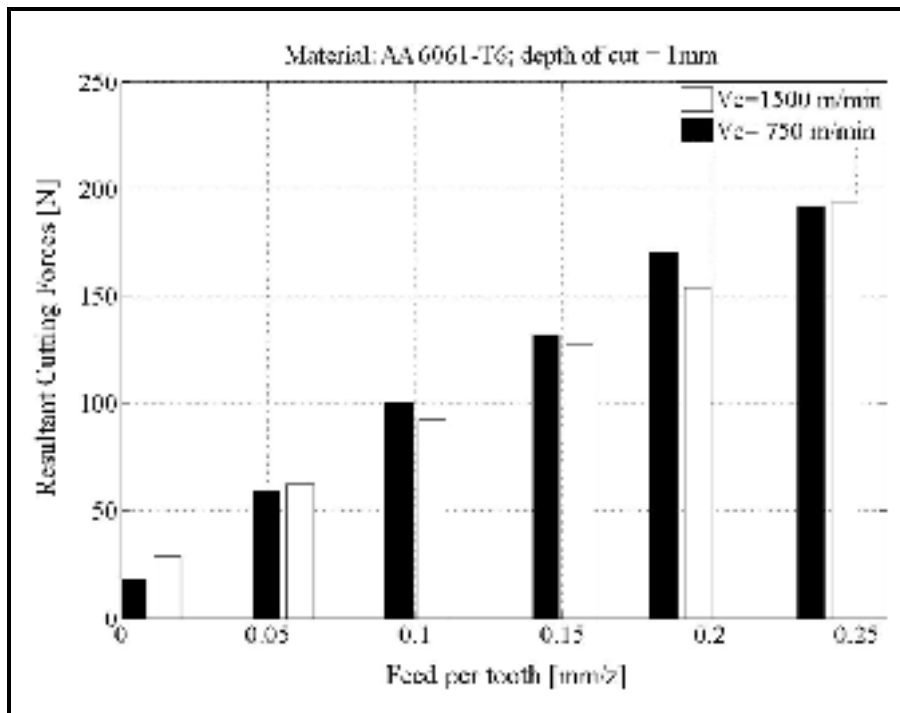


Figure 5.3 Variation of resultant cutting force during slot milling of AA 6061-T6

It must be however noted that slot milling burr size prediction is extremely challenging due to effects of factors that are very difficult to model explicitly. In the presented models, a number of simplifying assumptions were used, including orthogonal cutting that ignores the flute geometry and the yield stress that was assumed uniform irrespective to cutting conditions used. Furthermore, micro structural effects, such as grain size and boundary effects were all ignored. The errors related to the effects of specific cutting pressures and coated tool on burr formation were also neglected. In addition, before cutting force measurements, the stability of machine and cutting tool were controlled in preliminary tests.

A full overview of mathematical formulations performed for burr size modeling, analytical and computational burr thickness ( $B_t$ ) models and statistical analysis were written as a journal article which was published in *International Journal of Advanced Manufacturing Technology* in September 2012 (see ANNEX IV). Furthermore, a summary of factors governing burrs during slot milling of aluminium alloys, alongside with computational model of the burr thickness ( $B_t$ ) were presented in a conference article that was accepted for presentation in ASME 2013 International Manufacturing Science and Engineering Conference (MSEC2013), Madison, Wisconsin, USA June 10-14, 2013 (see ANNEX V).

## **5.5 Multiple responses optimization in slot milling**

Knowing that the best setting levels of process parameters to minimize each response are not similar, the question drawn is how to obtain the best setting levels of process parameters to reach the optimum or near optimum burrs size. This issue becomes more complex considering that for a given machined part; cutting parameter optimization for only burr size minimization may frequently deteriorate other machining performances, such as tool life and surface roughness. Therefore, in this study, surface finish was also investigated.

The main optimization concerns considered in this work are as follows: (1) simultaneous optimization of slot milling responses such as burrs and surface roughness, (2) optimization

of multiple responses using Taguchi method has received little attention; hence the importance of applying new modifications to the original Taguchi method is necessary.

We conducted a study to use desirability function for simultaneous minimization of surface roughness and exit burr size (thickness and height) during slot milling of AA 6061-T6 (Niknam, Kamguem and Songmene, 2012). In most of the responses, the proposed setting levels were pretty close to optimum conditions. Due to complex mathematical formulations, this approach cannot be easily and rapidly understood. The use of this method becomes even more complicated when dealing with non-statistically significant responses (e.g. burr height). In such cases, it is necessary to simultaneously define the best setting levels of process parameters and evaluate their desirability with respect to existing or proposed optimum responses using a predefined scale values. Therefore, in this work, new modifications to the original Taguchi method were suggested and verified for simultaneous multiple responses optimization. Upon selecting the optimum cutting conditions, prediction error ( $\varepsilon$ ) and optimization rate ( $\kappa$ ) corresponding to each response were defined. The new modifications can remedy the lacks mentioned. Nevertheless, the use of Taguchi method for multiple responses optimization may become more accurate when suitable modifications are adjusted to it.

This part of the work has led to a conference article that was presented in ASME IMECE 2012 (Niknam, Kamguem and Songmene, 2012), and a journal article which was submitted to *Journal of Precision Engineering and Manufacture* in July 2012 (see ANNEX VI-VII).

## **5.6 Key contributions and outcomes of the thesis**

The key contribution of this thesis can be summarized to the following main points:

1. By considering the complex burr formation mechanism in slot milling operation, a lack of information on factors governing burrs size (thickness and height) was observed. This shortcoming was intended to be unified by understanding the effects of cutting tool

- conditions (coating and geometry), machining strategy (dry high speed) and cutting parameters (cutting speed, feed per tooth, depth of cut) on burrs size (thickness and height) during slot milling of aluminium alloys. In total five visible burrs were studied. The statistical techniques were then used in this work to better interpret the results. The factors governing burrs size (thickness and height) were clearly addressed. The controllability of each burr with respect to variation of process parameters was investigated using statistical analysis. The thickest burr ( $B_1$ ) was found sensitive to variation of process parameters and its linear first order mathematical models were developed as a function of depth of cut and feed per tooth. A very good correlation was found between  $F_t$  and  $B_1$  thickness. It was found that tangential cutting force  $F_t$  is highly controlled by process parameters. According to obtained results, it was intended to propose an analytical model of the thickest burr ( $B_1$ ) as a function of cutting parameters. This is the subject of the third chapter of this thesis. The experimental studies and results analysis could generate effective recommendations for burrs size minimization during slot milling of aluminium alloys.
2. The burr formation in the exit zone was modeled. An analytical model was proposed to predict the thickest burr ( $B_1$ ). Certain levels of assumptions, mathematical modeling of burr formation and theory of energy conservation were used in modeling approach. The only model's unknown parameter is cutting force  $F_t$ , which itself is directly affected by cutting parameters. A computational model was then proposed to approximate the  $F_t$  and consequently simulate the burr thickness ( $B_t$ ). To this end, a computational algorithm was developed by discretizing the cutting tool into  $L$  elements of thickness  $da_p$  through axial depth of cut, ( $a_p$ ). Using the cutting parameters, the instantaneous immersion angle ( $\phi$ ) and undeformed chip thickness could be calculated. The specific cutting force coefficient ( $K_c$ ) with respect to material properties were used alongside with instantaneous immersion angle ( $\phi$ ) and undeformed chip thickness values to calculate the cutting force  $F_t$  and consequently simulate the  $B_t$ . The presented computational model is sensitive to material properties, cutting parameters (feed per tooth, depth of cut) and cutting tool geometry, such as lag angle ( $\gamma_0$ ), helix angle ( $\beta$ ), tool diameter ( $D$ ) and tool flutes ( $Z$ ). In

addition both analytical and computational models in their present forms have capabilities for successful prediction and minimization of exit up milling burr thickness ( $B_1$ ). Unlike existing analytical models, the proposed models in this thesis do not need experimental measurements of shear angle ( $\Phi$ ), friction angle ( $\lambda$ ) and tool chip contact length ( $L$ ) for burr size measurement.

3. Considering that the factors governing burrs and other machining performance characteristics such as surface roughness are different, a significant demand arises for multiple responses optimization. Using desirability function in a simultaneous optimization approach, it was proven that one could obtain better surface finish and burr size, if proper cutting parameters are used (Niknam, Kamguem and Songmene, 2012). New modifications to Taguchi method were proposed and verified by simultaneous minimization of surface roughness and thickness of five burrs during slot milling of AA 6061-T6. The optimization results demonstrate the potential and capability of the proposed approach.

According to experimental works in this thesis, an active process control to address the slot milling burrs characterization and minimization in aluminium alloys could be implemented. The obtained results can be later used for industrial implementations and in subsequent studies dealing with burr formation modeling in precision milling of aluminium alloys and other light metals. Furthermore, they can be used to find the optimum conditions and develop analytical and numerical models of burr formation. It could be inferred that the first objective of this thesis could be responded well according to presented results in second chapter. Knowing that the largest and thickest slot milling burr can be formulated as function of cutting parameters such as feed per tooth and depth of cut (see Figure 5.4), such understanding greatly helped us to propose and validate analytical and computational models of exit up milling burr ( $B_1$ ) thickness, which was extensively studied in the third chapter of this thesis. In other words, a direct relationship between the first and second specific objectives can be established. The outcomes are considered as a great achievement of this work, which also responded well to the second research objective in this work.

According to presented results in chapter 2, factors governing burr size are dissimilar. Therefore the use of simultaneous multiple responses optimization methods has been evolved. This subject was comprehensively studied in chapter four. Through the presenting results, we were able to determine the process setting levels that give us the optimum and/or near optimum results for all studied responses, using the modified approach of Taguchi method. Therefore, it could be stated that the third specific objective of this work was also responded well. We may anticipate using the proposed optimization approach for multiple responses optimization of other machining operations, such as drilling and turning. Furthermore the obtained results in second and fourth chapters are highly related to others. Therefore, a direct relationship between first and third specific objective can be observed (see Figure 5.4).

It is to note that a clear understating and approximation of burr size from predictive models (analytical and numerical) as presented in third chapter could be also applied as a guideline for better selection of deburring methods and it could be also used as a process window to better define the optimization conditions. Therefore a direct relationship between the second and third specific objectives can be also observed (see Figure 5.4).

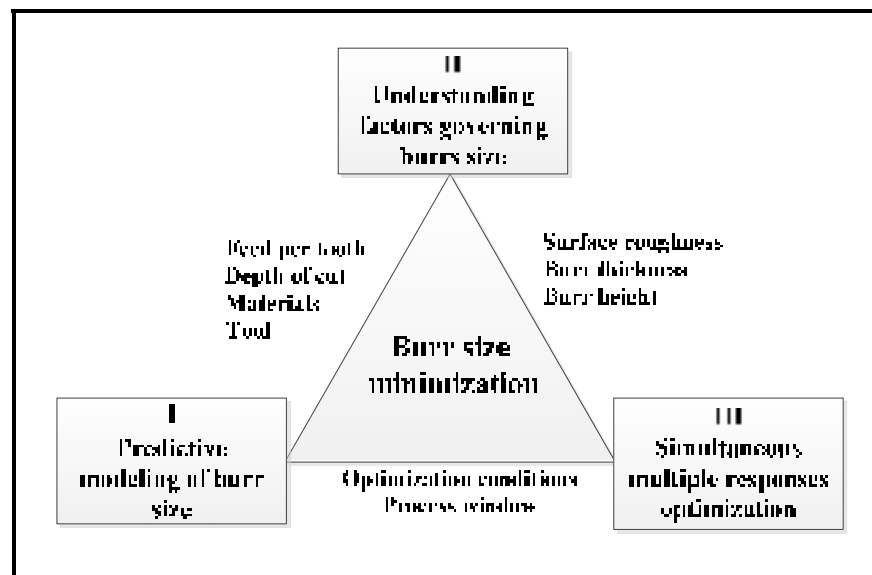


Figure 5.4 The links between main objective and specific research objectives



## CONCLUSION

Burr formation mechanism and patterns in slot milling of aluminium alloys were investigated in this work. Factors governing burrs size (thickness and height) were identified. Analytical and computational models were proposed to predict the longest and thickest burr. Considering that parameters optimization for only minimizing burr formation could frequently deteriorate other machining quality index, surface roughness and cutting forces were also investigated with burr formation. Multiple responses optimization during slot milling of aluminium alloys is presented. From analysis and discussion of results, the following conclusions are drawn:

- I. According to experimental results, feed per tooth controls most of burrs followed by depth of cut and tool geometry, depending on the burr considered. However factors governing each burr does not similarly identical for others. The side burrs, whether entrance ( $B_5$ ) or exit side burrs ( $B_1$ ) are dominated by feed per tooth, workpiece material and insert nose radius ( $R\epsilon$ ). The top burrs are mainly affected by variation of cutting conditions; insert nose radius ( $R\epsilon$ ) and tool coating.
- II. Factors governing slot milling burrs height and thickness were found dissimilar. Therefore no relationship could be formulated between the burr height and thickness at different edges of the machined part. One reason could be due to presence of strong interaction effects between process parameters which are difficult to observe and cannot be predicted by simple regression models. As a result, except few cases, empirical modeling of burrs size (height and thickness) was unsuccessful, particularly for slot milling, it does not serve a very good purpose.
- III. The milling burr formation in exit zone was modeled. The thickest burr ( $B_1$ ) was modeled analytically and computationally. Both models do not require the experimental measurements of shear angle ( $\Phi$ ), friction angle ( $\lambda$ ) and tool chip contact length ( $L$ ) for burr size measurement. The only unknown parameter in analytical model is cutting

force  $F_t$ , which could either be measured experimentally or simulated computationally. The use of specific cutting force coefficient ( $K_c$ ), instantaneous immersion angle ( $\phi$ ) and undeformed chip thickness in computational model has shown a successful performance for consequently cutting force ( $F_t$ ) and burr size prediction. The presented computational model is sensitive to material properties, cutting parameters and cutting tool geometry.

- IV. For simultaneous multiple responses optimization, application of a modified Taguchi method consisting of fitness mapping function ( $\psi$ ) and desirability index ( $D_i$ ) was proposed. The proposed approach was used for simultaneous optimization of worked part surface finish and five burrs thickness during slot milling of AA 6061-T6. The adequacy of the individual and set of proposed setting levels of process parameters was evaluated. It was found that feed per tooth has the most significant effect on simultaneous minimization of slot milling burrs size and surface finish.

## RECOMMENDATIONS

As mentioned earlier in the introduction, the main purpose of this study was to propose new strategies for understanding, modeling and optimizing burrs during slot milling of aluminium alloys. To complete the study, it is suggested that investigations being extended to cover the following aspects:

1. The temperature involved in the cutting process and the applications of cutting fluid have effects on burr size. The analytical and computational models could be improved by coupling with advanced cutting force and temperature modeling algorithms, which require only work-material properties and cutting conditions to predict the cutting forces and temperature during cutting operations.
2. This work could be expanded in wider scopes by developing databases describing cutting conditions for optimal edge quality, and design rules for burr prevention as well as standard terminology for describing edge features and burrs.
3. Attempting to present a strategy for real time estimation of burrs size using sensory information. This can be accompanied with strong signal processing algorithms, feature selection/extraction methods, advanced classification techniques and powerful data mining tools. The proposed setup can be also used for machine tool condition and health diagnosis.
4. Expanding experimental works to more materials, cutting parameters and tool geometries to discover the effect of other parameters on the burr size (e.g. energy level, lubrication mode) using theoretical and/or experimental studies followed by statistical approaches. A link between the burr size and the deburring difficulty will also be welcomed.



## ANNEX I

### CONFERENCE ARTICLE 1: BURR FORMATION DURING DRY MILLING OF WROUGHT ALUMINUM ALLOYS

20<sup>th</sup> Annual International Conference on Mechanical Engineering-ISME2012

16-18 May, 2012, Shiraz, Iran

Article No: ISME2012-3476

**Seyed Ali Niknam, Yasser Zedan and Victor Songmene**

Department of Mechanical Engineering, École de Technologie Supérieure (ÉTS)

1100 Notre-Dame West street, Montréal, Québec, H3C 1K3, Canada

Seyed-ali.niknam.1@ens.etsmtl.ca; Yasser.zedan.1@ens.etsmtl.ca; victor.songmene@etsmtl.ca

#### ABSTRACT

In this article, a multi-level experimental study on dry milling of 2024-T351 and 6061-T6 aluminum alloys is used to prescribe an operational window to control and minimize burr height ( $B_h$ ) in milling. Maximum height of exit burr and exit up milling side burr were measured. Statistical tools were then used to define the dominant process parameters on  $B_h$ . The effects of feed per tooth, depth of cut, friction, tool coating, insert nose radius ( $R_\epsilon$ ) and material properties on milling burrs profiles are discussed. The experimental results show that machining with larger  $R_\epsilon$  leads to bigger exit bottom burr and smaller exit up milling side burr. In addition, coated tools significantly affect  $B_h$  in slot milling operations.

**Key words:** dry milling, burr height, cutting parameters, cutting tool, aluminum alloys.



## ANNEX II

### **JOURNAL ARTICLE 1: FACTORS GOVERNING BURR FORMATION DURING HIGH-SPEED SLOT MILLING OF WROUGHT ALUMINUM ALLOYS**

The manuscript is accepted for publication in *Institution of Mechanical Engineers (IMechE), Part B, Journal of Engineering manufacture* in March 3 2012, JEM-12-0098.

**Seyed Ali Niknam and Victor Songmene**

Department of Mechanical Engineering, École de Technologie Supérieure (ÉTS)  
1100, Notre-Dame West street, Montreal, QC, H3C 1K3, Canada

#### **ABSTRACT**

Burr formation and edge finishing are research topics with high relevance to industrial applications. To remove burrs, however, a secondary operation known as deburring is usually required. Deburring is more complex and costly when dealing with milled parts, because multiple burrs form at different locations with various sizes. Therefore, proper selection of process parameters to minimize the burr size is strongly recommended. Therefore, this requires an understanding of milling burr formation mechanism and the governing cutting parameters on milling burrs. In this article, a multilevel experimental study is arranged to investigate the effects of machining conditions, tooling and workpiece materials on burr size (height and thickness). Statistical tools are then used to determine the dominant cutting parameters on burr size and to effectively prescribe an operational window to control and minimize burr formation. It was found that optimum setting levels of process parameters to minimize each burr are different. The analysis of results shows the significant effects of cutting tool, feed per tooth and depth of cut on slot milling burrs.

**Key words:** Slot milling, aluminum alloy, burr formation, machining conditions, statistical analysis.



## ANNEX III

### CONFERENCE ARTICLE 2: STATISTICAL INVESTIGATION ON BURR THICKNESS DURING MILLING OF 6061-T6 ALUMINIUM ALLOYS

1<sup>st</sup> International Conference on Virtual Machining Process Technology, CIRP Sponsored Conference, École Polytechnique, Montréal, Canada, May 28 – June 1, 2012

**Seyed Ali Niknam and Victor Songmene**

Department of Mechanical Engineering, École de Technologie Supérieure (ÉTS)  
1100, Notre-Dame West street, Montreal, QC, H3C 1K3, Canada

#### ABSTRACT

Burr formation is a research topic with high relevance to industrial applications. According to deburring perspective, the thickness of the burr is of interest as it describes the time and method necessary for deburring of the machined part. Burr thickness ( $B_t$ ) measurements are costly and non-value-added operations which in most of the cases require the use of Scanning Electron Microscope (SEM) for accurate burr characterization. This study presents an experimental study to evaluate parameters affecting the burr thickness and to search for correlation between the cutting parameters and the burr thickness. Amongst investigated burrs, exit up milling side burr is found to be highly controlled with machining parameters. It has shown a high correlation rate with tangential force ( $F_t$ ). Linear first order mathematical models are developed to predict exit up milling side burr thickness and  $F_t$  as a function of feed per tooth and depth of cut.

**Key words:** dry milling, burr formation, burr thickness, cutting parameters, aluminum.



## ANNEX IV

### JOURNAL ARTICLE 2: MODELING OF BURR THICKNESS IN MILLING OF DUCTILE MATERIALS

Int J Adv Manuf Technol (2013) 66:2029-2039  
DOI 10.1007/s00170-012-4479-3

Received: 5 April 2012 / Accepted: 21 August 2012 / Published online: 11 September 2012  
© Springer-Verlag London Limited 2012

**Seyed Ali Niknam and Victor Songmene**

Department of Mechanical Engineering, École de Technologie Supérieure (ÉTS)  
1100, Notre-Dame West street, Montreal, QC, H3C 1K3, Canada

#### ABSTRACT

Accuracy and surface finish play an important role in modern industry. The presence of undesired projections of materials, known as burrs, negatively affect the part quality and assembly process. To remove burrs, a secondary operation known as deburring is required for the post-processing and edge finishing of machined parts. The thickness of the burr is of interest as it describes the time and method necessary for deburring of the machined part. Burr thickness ( $B_t$ ) measurements are costly and non-value-added operations that in most cases require the use of a scanning electron microscope for accurate burr characterization. Therefore, to avoid such expenses, the implementation of alternative methods for predicting the burr thickness is strongly recommended. In this research work, an analytical model for predicting the burr thickness in end milling of ductile materials is presented. The model is built on the geometry of burr formation and the principle of continuity of work at the transition from chip formation to burr formation that also takes into account the cutting force influence on burr formation. A very good correlation was found between the modeled and experimental  $B_t$  values. The model has shown a great sensitivity to material properties such as yield strength and specific cutting force coefficient ( $K_c$ ). In addition, the sensitivity of the proposed model to the feed per tooth ( $f_t$ ) and depth of cut ( $a_p$ ) was considerably high. The proposed model allows the prediction of the thickness of the exit up milling side burr, without the need for experimental measurement and/or approximation of shear angle ( $\Phi$ ), friction angle ( $\lambda$ ), and the tool chip contact length ( $L$ ), unlike existing analytical burr size prediction models. Besides analytical modeling, statistical analysis is performed on experimental results in order to distinguish dominant process parameters on  $B_t$ . It is observed that the depth of cut and feed per tooth are the main parameters which significantly affect the  $B_t$ , while the speed has only a negligible effect on it.

**Key words:** milling, aluminum alloys, modeling, burr thickness.



## ANNEX V

### CONFERENCE ARTICLE 3: EXPERIMENTAL INVESTIGATION AND MODELING OF MILLING BURRS

Proceeding of the ASME 2013 International Manufacturing Science and Engineering Conference  
June 10-14, 2013, Madison, Wisconsin, USA

**Article No: MSEC2013-1176**

**Seyed Ali Niknam and Victor Songmene**

Department of Mechanical Engineering, École de Technologie Supérieure (ÉTS)  
1100, Notre-Dame West street, Montreal, QC, H3C 1K3, Canada

#### ABSTRACT

The burr formation is one of the most common and undesirable phenomenon occurring in machining operations which reduces assembly and machined part quality. Therefore, it is desired to eliminate the burrs or reduce the effort required to remove them. This paper presents the results of an experimental study and describe the influence of cutting parameters on slot milling burrs, namely top burrs and exit burrs. Statistical methods are also used to determine the controllability of each burr. A computational model is then proposed to predict the exit up milling side burr thickness based on cutting parameters and material properties such as yield strength and specific cutting force coefficient that are the only unknown variables in the model. The proposed computational model is validated using experimental results obtained during slot milling of 2024-T351 and 6061-T6 aluminium alloys.

**Key words:** Milling, Burr, Modeling, Aluminium alloys.



## ANNEX VI

### **JOURNAL ARTICLE 3: SIMULTANEOUS OPTIMIZATION OF BURRS SIZE AND SURFACE FINISH WHEN SLOT MILLING 6061-T6 ALUMINIUM ALLOYS**

The manuscript is submitted to *International Journal of Precision Engineering and Manufacturing* 18 July 2012; JPEM-D-12-00286, revised version sent on Dec 12, 2012

**Seyed Ali Niknam and Victor Songmene**

Department of Mechanical Engineering, École de Technologie Supérieure (ÉTS)  
1100, Notre-Dame West street, Montreal, QC, H3C 1K3, Canada

#### **ABSTRACT**

Taguchi-based optimization has been successfully applied in industrial applications. Some of these applications have more than one response to study. Most of reported applications of Taguchi method deal with single objective optimization, while multiple responses optimization has received relatively less attentions. The main objective of this article is to propose new modifications to application of Taguchi method by proposing fitness mapping function ( $\psi$ ) and Desirability index ( $D_i$ ) for correct selection of process parameters setting levels that can be used for multiple responses optimization. The proposed approach is verified by simultaneous minimization of surface roughness and burr thickness during milling of 6061-T6 aluminium alloy. It was found that surface roughness and burrs size can be optimized by selecting appropriate setting levels of process parameters. According to experimental results, feed per tooth has the major influence on variation of burr size and surface roughness, while cutting speed has shown less significant effect as compared to other cutting parameters used.

**Key words:** Slot milling, Aluminum alloys, Burr size, Surface finish, Taguchi method, Optimization.



## ANNEX VII

### CONFERENCE ARTICLE 4: ANALYSIS AND OPTIMIZATION OF EXIT BURR SIZE AND SURFACE ROUGHNESS IN MILLING USING DESIRABILITY FUNCTION

Proceeding of the ASME 2012 International Mechanical Engineering Congress & Exposition  
IMECE 2012, November 9-15, 2012. Huston, TX, USA

**Article No: IMECE-86201**

**Seyed Ali Niknam and Victor Songmene**

Department of Mechanical Engineering, École de Technologie Supérieure (ÉTS)  
1100, Notre-Dame West street, Montreal, QC, H3C 1K3, Canada

#### ABSTRACT

The burr formation mechanism and surface quality highly depend on machining conditions. Improper selection of cutting parameters may cause tremendous manufacturing cost and low product quality. Proper selection of cutting parameters which simultaneously minimize burr size and surface roughness is therefore very important, as that would reduce the part finishing cost. This article aims to present an experimental study to evaluate parameters affecting the exit burr size (thickness and height) and surface roughness during milling of 6601-T6 aluminum alloy. Desirability function,  $D_i(x)$ , is then proposed for multiple response optimization. Optimum setting levels of process parameters are determined for simultaneous minimization of surface roughness and exit burr thickness and height. It was found that the changes in feed per tooth and tool geometry and coating have significant effects on variation of  $D_i(x)$ .

**Key words:** milling, burr size, aluminum alloys, optimization, desirability function, surface roughness.

## BIBLIOGRAPHY

- Altintas, Y. 1992. « Prediction of cutting forces and tool breakage in milling from feed drive current measurements ». *Journal of Engineering for Industry (Transaction of the ASME)*, vol. 114, n° 4, p. 386-392.
- Altintas, Y. 2000. *Manufacturing automation*. Cambridge Univ. Pr.
- AM De Souza, J., WF Sales, EO Ezugwu, J. Bonney and AR Machado. 2003. « Burr formation in face milling of cast iron with different milling cutter systems ». *Proceedings of the Institution of Mechanical Engineers, Part B: Journal of Engineering Manufacture*, vol. 217, n° 11, p. 1589-1596.
- Anzai, M., H. Otaki, E. Kawashima and T. Nakagawa. 1993. « Application for deburring of mechanical parts using magnetic abrasive finishing ». *Int. J. Jpn. Soc. Precis. Eng.(Japan)*, vol. 27, n° 3, p. 223-224.
- Asakawa, N., K. Toda and Y. Takeuchi. 2002. « Automation of chamfering by an industrial robot; for the case of hole on free-curved surface ». *Robotics and Computer-Integrated Manufacturing*, vol. 18, n° 5, p. 379-385.
- Aurich, J. C., D. Dornfeld, P. J. Arrazola, V. Franke, L. Leitz and S. Min. 2009. « Burrs-Analysis, control and removal ». *CIRP Annals - Manufacturing Technology*, vol. 58, n° 2, p. 519-542.
- Aurich, JC, and F Publica. 2006. « SpanSauber. Ergebnisbericht der Untersuchung zur Beherrschung der Sauberkeit von zerspanend hergestellten Bauteilen: Forschung für die Produktion von morgen, Förderkennzeichen 02PB2500 ».
- Aurich, JC, H. Sudermann and H. Bil. 2005. « Characterisation of burr formation in grinding and prospects for modelling ». *CIRP Annals-Manufacturing Technology*, vol. 54, n° 1, p. 313-316.
- Avila, M.C., J. Choi, D.A. Dornfeld, M. Kapgan and R. Kosarchuk. 2004. « Deburring of cross-drilled hole intersections by mechanized cutting ». *LMA. Annual Reports 2003–2004, UC Berkeley*, p. 10-20.
- Avila, M.C., and D.A. Dornfeld. 2004. « On The Face Milling Burr Formation Mechanisms and Minimization Strategies at High Tool Engagement ». In *Intl. Conf. on Deburring and Edge Finishing*. (University of California at Berkeley), p. 191-200

- Bagci, E., and Ş. Aykut. 2006. « A study of Taguchi optimization method for identifying optimum surface roughness in CNC face milling of cobalt-based alloy (stellite 6) ». *The International Journal of Advanced Manufacturing Technology*, vol. 29, n° 9, p. 940-947.
- Bansal, A. 2001. *Comprehensive approach to Burr Prediction*. Coll. « 2001-2002 LMA Annual Reports »: University of California at Berkeley, USA.
- Bansal, AK. 2002. « Burr prediction system for face milling operation. ». Masters Thesis, University of California at Berkeley, USA.
- Beier, H.M. 1999. *Handbuch Entgrattechnik: Wegweiser zur Gratminimierung und Gratbeseitigung für Konstruktion und Fertigung*. Hanser.
- Beier, HM, and R. Nothnagel. 2004. « Development of a high-speed-deburring tool ». In *Proceedings of the 7th International Conference on Deburring and Surface Finishing*. (University of California, Berkeley), p. 271-279.
- Biermann, D., and M. Heilmann. 2010. « Burr Minimization Strategies in Machining Operations ». *Burrs-Analysis, Control and Removal*, p. 13-20.
- Chen, L., R.J. Stango and V. Cariapa. 1991. « Automated Prototype Deburring with Compliant Brushing Tool ». In *Annual Meeting of the American Society of Mechanical Engineers (ASME): Intelligent design and manufacturing for prototyping*. (December 1-6, 1991). Atlanta, Georgia, USA.
- Chen, M., G. Liu and Z. Shen. 2006. « Study on Active Process Control of Burr Formation in Al-Alloy Milling Process ». In *Proceeding of the IEEE, International Conference on Automation Science and Engineering*. (Shanghai, China, , 8-10 Oct. 2006), p. 431-436.
- Chern, G.L. 1993. « Analysis of Burr Formation and Breakout in Metal Cutting ». PhD Thesis, University of California at Berkeley, USA.
- Chern, G.L. 2006. « Experimental observation and analysis of burr formation mechanisms in face milling of aluminum alloys ». *International Journal of Machine Tools and Manufacture*, vol. 46, n° 12-13, p. 1517-1525.
- Chern, G.L., and D.A. Dornfeld. 1996. « Burr/breakout model development and experimental verification ». *Journal of Engineering materials and technology*, vol. 118, p. 201-206.
- Chu, C.H., DA Dornfeld and C. Brennum. 2000. *Prediction and simulation of milling burr formation for edge-precision process planning*. Coll. « 1999-2000 LMA Annual report »: University of California at Berkeley, USA.

- Chu, CH, and D. Dornfeld. 2004. « Linking tool paths generated with different offset distances for edge quality enhancement in planar milling ». *Proceedings of the Institution of Mechanical Engineers, Part B: Journal of Engineering Manufacture*, vol. 218, n° 7, p. 721-730.
- Committee, ASM International. Handbook, and Knovel. 2004. *ASM Handbook: Metallography and Microstructures*. ASM International.
- Dasch, J.M., C.C. Ang, C.A. Wong, Y.T. Cheng, A.M. Weiner, L.C. Lev and E. Konca. 2006. « A comparison of five categories of carbon-based tool coatings for dry drilling of aluminum ». *Surface and Coatings Technology*, vol. 200, n° 9, p. 2970-2977.
- Davis, J.R., KM Mills and SR Lampman. 1990. « Metals Handbook. Vol. 1. Properties and Selection: Irons, Steels, and High-Performance Alloys ». *ASM International, Materials Park, Ohio 44073, USA, 1990. 1063*.
- De Lacalle, L.N.L., A. Lamikiz, JA Sanchez and I. Cabanes. 2001. « Cutting conditions and tool optimization in the high-speed milling of aluminium alloys ». *Proceedings of the Institution of Mechanical Engineers, Part B: Journal of Engineering Manufacture*, vol. 215, n° 9, p. 1257-1270.
- Derringer, G. 1980. « Simultaneous optimization of several response variables ». *J. Quality Technol.*, vol. 12, n° 4, p. 214-219.
- Dhavamani, C., and T. Alwarsamy. 2011. « Review on optimization of machining operation ». *Int J Acad Res*, vol. 3, p. 476-485.
- Gaitonde, V. N., S. R. Karnik and J. Davim. 2009. « Multiperformance Optimization in Turning of Free-Machining Steel Using Taguchi Method and Utility Concept ». *Journal of materials engineering and performance*, vol. 18, n° 3, p. 231-236.
- Gillespie, L.R.K. 1981. *Deburring technology for improved manufacturing*. Dearborn, MI, USA: Society of Manufacturing Engineers (SME).
- Gillespie, LK. 1976. *Burrs produced by end milling*. BDX-613-1503, Bendix Corp., Kansas City, Mo.(USA).
- Gillespie, LK. 1996. « The battle of the burr: new strategies and new tricks ». *Manufacturing Engineering(USA)*, vol. 116, n° 2, p. 69-70.
- Gillespie, LK, and PT Blotter. 1976. « Formation and properties of machining burrs ». *J. Eng. Ind.(Trans. ASME, B)*, vol. 98, n° 1, p. 66-74.
- Gillespie, LRK. 1999. *Deburring and edge finishing handbook*. SME.

- Harrington, EC. 1965. « The desirability function ». *Industrial quality control*, vol. 21, n° 10, p. 494-498.
- Hashimura, M, J Hassamontr and DA Dornfeld. 1999. « Effect of in-plane exit angle and rake angles on burr height and thickness in face milling operation ». *Journal of Manufacturing Science and Engineering*, vol. 121, n° 1, p. 13-19.
- Hashimura, M.,and DA Dornfeld. 1995. « Analysis of burr formation mechanism in machining process ». *Technical Paper, Society of Manufacturing Engineering (SME)-All series*.
- Hirabayashi, H., S. Ohwada, I. Yoshida and M. Miki. 1987. *Force-Control Deburring Robots*. Coll. « Society of Manufacturing Engineers (SME) », p.1-12.
- Hou, T.H., C.H. Su and W.L. Liu. 2007. « Parameters optimization of a nano-particle wet milling process using the Taguchi method, response surface method and genetic algorithm ». *Powder Technology*, vol. 173, n° 3, p. 153-162.
- Ioi, T., M. Matsunaga and H. Kobayashi. 1981. « Computer Aided Selection of Deburring Methods, SME Tech ». *Paper, MR*, p. 81-389.
- Iwata, K., K. Osakada and Y. Terasaka. 1984. « Process modeling of orthogonal cutting by the rigid-plastic finite element method ». *Journal of Engineering materials and technology*, vol. 106, p. 132-138.
- Jagiella, M.,and S. Fericean. 2004. « Inductive sensor system for evaluation of burrs and edges in industrial application ». In. (7th International Conference on Deburring and Surface Finishing ), p. 89–102.
- Jones, SD, and RJ Furness. 1997. « An Experimental Study of Burr Formation for Face Milling 356 Aluminum ». *Transaction -North American Manufacturing Research Institution of SME*, p. 183-188.
- Karnik, S., V. Gaitonde and J. Davim. 2008. « A comparative study of the ANN and RSM modeling approaches for predicting burr size in drilling ». *The International Journal of Advanced Manufacturing Technology*, vol. 38, n° 9, p. 868-883.
- Kilickap, Erol. 2010. « Modeling and optimization of burr height in drilling of Al-7075 using Taguchi method and response surface methodology ». *The International Journal of Advanced Manufacturing Technology*, vol. 49, n° 9, p. 911-923.
- Kim, J.,and D.A. Dornfeld. 2002. « Development of an analytical model for drilling burr formation in ductile materials ». *Journal of Engineering materials and technology*, vol. 124, n° 2, p. 192-198.

- Kim, J.D.,and Y.H. Kang. 1997. « High-speed machining of aluminium using diamond endmills ». *International Journal of Machine Tools and Manufacture*, vol. 37, n° 8, p. 1155-1165.
- Kishimoto, W., T. Miyake, A. Yamamoto, K. Yamanaka and K. Takano. 1981. « Study of Burr Formation in Face Milling. Conditions for the Secondary Burr Formation ». *Bull. Jpn. Soc. Precis. Eng.*, vol. 15, n° 1, p. 51-52.
- Kitajima, K., T. Miyake, A. Yamamoto, Y. Tanaka and K. Takazawa. 1990. « Study on mechanism and similarity of burr formation in face milling and drilling ». *Technology Reports of Kansai University*, vol. 31, n° 1, p. 1-33.
- Klocke, F.,and G. Eisenblätter. 1997. « Dry cutting ». *CIRP Annals-Manufacturing Technology*, vol. 46, n° 2, p. 519-526.
- Klocke, F., S. Hoppe and R. Fritsch. 2004. « FE-modeling of burr formation in orthogonal cutting ». In *Proceeding of 7th Int. Conference on Deburring and Surface Finishing*. (University of California, Berkeley, USA.).
- Ko, S.L.,and D.A. Dornfeld. 1996. « Analysis of fracture in burr formation at the exit stage of metal cutting ». *Journal of Materials Processing Technology*, vol. 58, n° 2-3, p. 189-200.
- Ko, SL,and DA Dornfeld. 1991. « A study on burr formation mechanism ». *Journal of Engineering materials and technology*, vol. 113, p. 75-87.
- Ko, SL,and SW Park. 2006. « Development of an effective measurement system for burr geometry ». *Proceedings of the Institution of Mechanical Engineers, Part B: Journal of Engineering Manufacture*, vol. 220, n° 4, p. 507-512.
- Korkut, I.,and MA Donertas. 2007. « The influence of feed rate and cutting speed on the cutting forces, surface roughness and tool-chip contact length during face milling ». *Materials & design*, vol. 28, n° 1, p. 308-312.
- Kumar, S.,and D. Dornfeld. 2003. « Basic approach to a prediction system for burr formation in face milling ». *Journal of Manufacturing Processes*, vol. 5, n° 2, p. 127-142.
- Lauderbaugh, L. 2009. « Analysis of the effects of process parameters on exit burrs in drilling using a combined simulation and experimental approach ». *Journal of Materials Processing Technology*, vol. 209, n° 4, p. 1909-1919.
- Lee, K 2004. « Integration Precision Machining and Burr Minimization in Metals ». PhD Thesis, University of California at Berkeley, USA.

- Lee, K.C., H.P. Huang and S.S. Lu. 1993. « Burr detection by using vision image ». *The International Journal of Advanced Manufacturing Technology*, vol. 8, n° 5, p. 275-284.
- Lee, KC., HP. Huang and SS. Lu 2001. « Adaptive Hybrid Impedance Force Control of Robotic Deburring Processes ». In *Proceedings of the 32nd International Symposium on Robotics*. Vol. TC 5-3, p. 1-6.
- Lee, PH, H. Chung and SW Lee. 2011. « Optimization of micro-grinding process with compressed air using response surface methodology ». *Proceedings of the Institution of Mechanical Engineers, Part B: Journal of Engineering Manufacture*, vol. 225, n° 11, p. 2040-2050.
- Lee, Seoung Hwan, and Sang-Heon Lee. 2003. « Optimisation of cutting parameters for burr minimization in face-milling operations ». *International Journal of Production Research*, vol. 41, n° 3, p. 497-511.
- Lee, SH, and DA Dornfeld. 2001. « Precision laser deburring ». *Journal of manufacturing science and engineering*, vol. 123, p. 601-608.
- Lee, SH, DS Park and DA Dornfeld. 1996. « Burr Size Measurement Using a Capacitance Sensor ». In., p. 31–36.
- Lee, SW, HZ Choi, GH Kim, YJ Choi and S.L. Ko. 2004. « Micro Deburring Technology Using Ultrasonic Vibration with Abrasive ». In *Proceedings of the ISAAT, International Symposium on Advances in Abrasive Technology*. Vol. 3, p. 477-482.
- Lekkala, Ravi, Vivek Bajpai, Ramesh K. Singh and Suhas S. Joshi. 2011. « Characterization and modeling of burr formation in micro-end milling ». *Precision Engineering*, vol. 35, n° 4, p. 625-637.
- Leopold, J., and R. Wohlgemuth. 2010. « Modeling and Simulation of Burr Formation: State-of-the-Art and Future Trends ». *Burrs-Analysis, Control and Removal*, p. 79-86.
- Lin, T. R. 2002. « Optimisation Technique for Face Milling Stainless Steel with Multiple Performance Characteristics ». *The International Journal of Advanced Manufacturing Technology*, vol. 19, n° 5, p. 330-335.
- Luo, M, G Liu and M Chen. 2008. « Mechanism of burr formation in slot milling Al-alloy ». *International Journal of Materials and Product Technology*, vol. 31, n° 1, p. 63-71.
- Mandal, N., B. Doloi and B. Mondal. 2012. « Force prediction model of Zirconia Toughened Alumina (ZTA) inserts in hard turning of AISI 4340 steel using response surface methodology ». *International Journal of Precision Engineering and Manufacturing*, vol. 13, n° 9, p. 1589-1599.

- Mchugh, B. 1988. *Flexible Finishing with Dry Blast Deburring*. Technical report. 517. Society of Manufacturing Engineers (SME), 1-24 p.
- Means, M.. 1986. « Deburring—Part 2 ». *Tooling and Production* vol. 51, n° 10, p. 47–51.
- Mian, A J, N Driver and P T Mativenga. 2011a. « Estimation of minimum chip thickness in micro-milling using acoustic emission ». *Proceedings of the Institution of Mechanical Engineers, Part B: Journal of Engineering Manufacture*, vol. 225, n° 9, p. 1535-1551.
- Mian, Aamer, Nicholas Driver and Paul Mativenga. 2011b. « Chip formation in microscale milling and correlation with acoustic emission signal ». *The International Journal of Advanced Manufacturing Technology*, vol. 56, n° 1, p. 63-78.
- Moola, M.R., A. Gorin and K.A. Hossein. 2012. « Optimization of various cutting parameters on the surface roughness of the machinable glass ceramic with two flute square end mills of micro grain solid carbide ». *International Journal of Precision Engineering and Manufacturing*, vol. 13, n° 9, p. 1549-1554.
- Moshat, S., S. Datta, A. Bandyopadhyay and P. Pal. 2010. « Optimization of CNC end milling process parameters using PCA-based Taguchi method ». *International Journal of Engineering, Science and Technology*, vol. 2, n° 1, p. 95-102.
- Myers, R.H., D.C. Montgomery and C.M. Anderson-Cook. 2009. *Response surface methodology: process and product optimization using designed experiments*, 705. John Wiley & Sons.
- Nakayama, K, and M Arai. 1987. « Burr formation in metal cutting ». *CIRP Annals-Manufacturing Technology*, vol. 36, n° 1, p. 33-36.
- Nalbant, M., H. Gökkaya and G. Sur. 2007. « Application of Taguchi method in the optimization of cutting parameters for surface roughness in turning ». *Materials & design*, vol. 28, n° 4, p. 1379-1385.
- Narayanaswami, R., and D. Dornfeld. 1994. « Design and process planning strategies for burr minimization and deburring ». *Transactions of the North American Manufacturing Research Institute of SME 1994.*, vol. 22, p. 313-322.
- Niknam, S.A., R. Kamguem and V. Songmene. 2012. « Analysis and optimization of exit burr size and surface roughness in milling using desirability function ». In *ASME 2012 International Mechanical Engineering Congress & Exposition IMECE2012*. (Huston, TX, USA, 9-15 November 2012). ASME.
- Niknam, S.A., and V. Songmene. 2012. « Statistical investigation on burrs thickness during milling of 6061-T6 aluminium alloy ». In *CIRP 1st International Conference on*

*Virtual Machining Process Technology*. (Montreal, QC, Canada, 28 May-1 June 2012).

- Niknam, S.A., and V. Songmene. 2013. « Modeling of burr thickness in milling of ductile materials ». *The International Journal of Advanced Manufacturing Technology*, vol. 66, n° 9, p. 2029-2039.
- Niknam, S.A., Y. Zedan and V. Songmene. 2012. « Burr formation during milling of wrought aluminum alloys ». In *20th ISME Annual International Conference on Mechanical Engineering*. (Shiraz, Iran, 16-18 May 2012).
- Nisbet, T.S., and GW Mullet. 1978. *Rolling Bearings in Service: Interpretation of Types of Damage*. Hutchinson.
- Oliveira, J.F.G., and C.M.O. Valente. 2004. « Monitoring and Control in Abrasive Robotic Deburring Operations, AC ». In. Vol. 7, p. 1-8.
- Olvera, O., and G Barrow. 1996. « An experimental study of burr formation in square shoulder face milling ». *International Journal of Machine Tools and Manufacture*, vol. 36, n° 9, p. 1005-1020.
- Olvera, O., and G. Barrow. 1998. « Influence of exit angle and tool nose geometry on burr formation in face milling operations ». *Proceedings of the Institution of Mechanical Engineers, Part B: Journal of Engineering Manufacture*, vol. 212, n° 1, p. 59-72.
- Park, IW. 2000a. « A study of burr formation processes using the finite element method: Part I ». *Journal of Engineering materials and technology*, vol. 122, n° 1, p. 221-228.
- Park, IW. 2000b. « A study of burr formation processes using the finite element method: part II—the influences of exit angle, rake angle, and backup material on burr formation processes ». *Journal of Engineering materials and technology*, vol. 122, n° 1, p. 229-237.
- Pekelharing, AJ. 1978. « The exit failure in interrupted cutting ». *Annals of the CIRP*, vol. 27, n° 1, p. 5-10.
- Phadke, M.S. 1989. *Quality engineering using robust design*. Prentice Hall Englewood Cliffs, NJ.
- Przyklenk, K. 1986. « Abrasive flow machining—a process for surface finishing and deburring of work pieces with a complicated shape by means of abrasive laden media ». *Advances in Non-traditional Machining, ASME, PED*, vol. 22, p. 101-110.
- Przyklenk, K., and M. Schlatter. 1987. « Deburring of Aluminum Workpieces. XII ». *Aluminium*, vol. 63, n° 1, p. 70-74.

- Rahman, M., A. Senthil Kumar and M. U. Salam. 2002. « Experimental evaluation on the effect of minimal quantities of lubricant in milling ». *International Journal of Machine Tools and Manufacture*, vol. 42, n° 5, p. 539-547.
- Rangarajan, A., C.H. Chu and DA Dornfeld. 2000. « Avoiding tool exit in planar milling by adjusting width of cut ». *ASME MFG Eng Div*, vol. 11, p. 1017–1027.
- Rangarajan, A.,and D.A. Dornfeld. 2004. « Back Cutting and Tool Wear Influence on Burrs in Face Milling-Analysis and Solutions ». *Consortium on Deburring and Edge Finishing, Laboratory for Manufacturing and Sustainability, UC Berkeley*, p. 63-70.
- Rangarjan, A. 2005. « Optimization of face milling process- Tool path and process planning techniques ». Ph.D Thesis, University of California at Brekeley, USA.
- Regel, J, A Stoll and J Leopold. 2009. « Numerical analysis of crack propagation during the burr formation process of metals ». *International Journal of Machining and Machinability of Materials*, vol. 6, n° 1, p. 54-68.
- San-Juan, Manuel, Óscar Martín and Francisco Santos. 2010. « Experimental study of friction from cutting forces in orthogonal milling ». *International Journal of Machine Tools and Manufacture*, vol. 50, n° 7, p. 591-600.
- Sartkulvanich, P. 2007. « Determination of material properties for use in FEM simulations of machining and roller burnishing ». Ph.D Thesis, The Ohio State University, USA.
- Sartkulvanich, Partchapol, Hakan Sahlan and Taylan Altan. 2007. « A finite element analysis of burr formation in face milling of a cast aluminum alloy ». *Machining science and technology*, vol. 11, n° 2, p. 157-181.
- Schäfer, F. 1975. *Entgraten*. Krausskopf.
- Schäfer, F. 1978. « Gratbildung und Entgraten beim Umfangsstirnfräsen ». *VDI-Zeitschrift*, vol. 120, n° 1-2, p. 47-55.
- Shaw, MC. 1984. *Metal Cutting Principles*. Oxford University Press.
- Shelfbine, W.,and D. Dornfeld. 2004a. « Influences on Burr Size During Face-Milling of Aluminum Alloys and Cast Iron ». In *Consortium on Deburring and Edge Finishing, Laboratory for Manufacturing and Sustainability*. University of California at Berkeley, USA.
- Shelfbine, W.,and D.A. Dornfeld. 2004b. « The Effect of Dry Machining on Burr Size ». In *Consortium on Deburring and Edge Finishing, Laboratory for Manufacturing and Sustainability*. University of California at Berkeley, USA.

- Sofronas, A.S. 1975. « The formation and control of drilling burrs ». PhD Thesis, University of Detroit, USA.
- Songmene V., R. Khettabi and J Kouam. 2012. « High Speed Machining: A Cost Effective & Green Process ». *Int. J. Manufacturing Research (IJMR)*, vol. 7, n° 3, p. 229-256.
- Soo, SL, DK Aspinwall and RC Dewes. 2004a. « 3D FE modelling of the cutting of Inconel 718 ». *Journal of Materials Processing Technology*, vol. 150, n° 1, p. 116-123.
- Soo, SL, DK Aspinwall and RC Dewes. 2004b. « Three-dimensional finite element modelling of high-speed milling of Inconel 718 ». *Proceedings of the Institution of Mechanical Engineers, Part B: Journal of Engineering Manufacture*, vol. 218, n° 11, p. 1555-1561.
- Tang, Y., Z. He, L. Lu, H. Wang and M. Pan. 2011. « Burr formation in milling cross-connected microchannels with a thin slotting cutter ». *Precision Engineering*, vol. 35, n° 1, p. 108-115.
- Thilow, A.P. 2008. *Entgrattechnik: Entwicklungsstand und Problemlösungen*, 392. expert verlag.
- Tiabi, A. 2010. « Formation des bavures d'usinage et finition de pieces ». M.Sc Thesis, École de technologie supérieure, Canada.
- Tong, KW, CK Kwong and KM Yu. 2004. « Process optimisation of transfer moulding for electronic packages using artificial neural networks and multiobjective optimisation techniques ». *The International Journal of Advanced Manufacturing Technology*, vol. 24, n° 9, p. 675-685.
- Toropov, A.,and S.L. Ko. 2006. « A model of burr formation in the feed direction in turning ». *International Journal of Machine Tools and Manufacture*, vol. 46, n° 15, p. 1913-1920.
- Toropov, AA, SL Ko and JM Lee. 2006. « A new burr formation model for orthogonal cutting of ductile materials ». *CIRP Annals-Manufacturing Technology*, vol. 55, n° 1, p. 55-58.
- Tripathi, S.,and D.A. Dornfeld. 2006. « Review of geometric solutions for milling burr prediction and minimization ». *Proceedings of the Institution of Mechanical Engineers, Part B: Journal of Engineering Manufacture*, vol. 220, n° 4, p. 459-466.
- Tsai†, D.M.,and W.J. Lu. 1996. « Detecting and locating burrs of industrial parts ». *International Journal of Production Research*, vol. 34, n° 11, p. 3187-3205.

- Tsann-Rong, Lin. 2000. « Experimental study of burr formation and tool chipping in the face milling of stainless steel ». *Journal of Materials Processing Technology*, vol. 108, n° 1, p. 12-20.
- Tsao, CC. 2009. « Grey–Taguchi method to optimize the milling parameters of aluminum alloy ». *The International Journal of Advanced Manufacturing Technology*, vol. 40, n° 1, p. 41-48.
- Tseng, P.C.,and I.C. Chiou. 2003. « The burrs formation prediction and minimization based on the optimal cutting parameters design method ». *JSME International Journal Series C*, vol. 46, n° 2, p. 779-787.
- Vafaeseefat, A. 2009. « Optimum creep feed grinding process conditions for Rene 80 super alloy using neural network ». *International Journal of Precision Engineering and Manufacturing*, vol. 10, n° 3, p. 5-11.
- Wang, G.C.,and C.Y. Zhang. 2003a. « Mechanism of Burr Formation in Milling ». *Key Engineering Materials*, vol. 259, p. 278-281.
- Wang, G.C.,and C.Y. Zhang. 2003b. « Study on the Forming Mechanism of the Cutting-Direction Burr in Metal Cutting ». *Key Engineering Materials*, vol. 259, p. 868-871.
- Weinert, K., I. Inasaki, J. W. Sutherland and T. Wakabayashi. 2004. « Dry Machining and Minimum Quantity Lubrication ». *CIRP Annals - Manufacturing Technology*, vol. 53, n° 2, p. 511-537.
- Wulf, C.,and M. Hayk. 2007. « Automatic residual burr detection on steel slabs by a thermographic system ». *Metallurgical Plant and Technology International* vol. 30, n° 2, p. 36-37.
- Yang, R.T., H.T. Liao, Y.K. Yang and S.S. Lin. 2012. « Modeling and optimization in precise boring processes for aluminum alloy 6061T6 components ». *International Journal of Precision Engineering and Manufacturing*, vol. 13, n° 1, p. 11-16.
- Zaghbani, I., JF. Chatelain, V. Songmene, S Bérubé, . and A. Atarsia. 2012. « A comprehensive analysis of cutting forces during routing of carbon fiber-reinforced polymer laminates ». *Journal of Composite Materials* vol. 46, n° 16, p. 1955-1971.
- Zedan, Y. 2011. « Machinability aspects of heat-treated Al-(6-11)% Si cast alloys: Role of intermetallics and free-cutting elements ». Ph.D Thesis, Université du Québec à Chicoutimi, Canada.
- Zhang, J.Z., J.C. Chen and E.D. Kirby. 2007. « Surface roughness optimization in an end-milling operation using the Taguchi design method ». *Journal of Materials Processing Technology*, vol. 184, n° 1, p. 233-239.

Zhang, Tao, Zhanqiang Liu and Chonghai Xu. 2013. « Influence of size effect on burr formation in micro cutting ». *The International Journal of Advanced Manufacturing Technology*, p. 1-7.